ZITTELIANA

95 2021

PENSOFT

SNSB Bayerische Staatssammlung für Paläontologie und Geologie

Zitteliana

Editor-in-Chief

Gert Wörheide
Ludwig-Maximilians-Universität München
Paläontologie & Geobiologie
Staatliche Naturwissenschaftliche Sammlungen Bayerns
Bayerische Staatssammlung für Paläontologie und Geologie
Munich, Germany
e-mail: bspg@snsb.de

Deputy Editor-in-Chief

Michael Krings
Staatliche Naturwissenschaftliche Sammlungen Bayerns
Bayerische Staatssammlung für Paläontologie und Geologie
Ludwig-Maximilians-Universität München
Paläontologie & Geobiologie
Munich, Germany
e-mail: krings@snsb.de

Deputy Editor-in-Chief

Alexander Nützel
Staatliche Naturwissenschaftliche Sammlungen Bayerns
Bayerische Staatssammlung für Paläontologie und Geologie
Ludwig-Maximilians-Universität München
Paläontologie & Geobiologie
Munich, Germany
e-mail: nuetzel@snsb.de

Editorial Secretary

Boryana Ovcharova
Pensoft Publishers
Sofia, Bulgaria
Prof. Georgi Zlatarski Street 12
1700 Sofia, Bulgaria
Tel.: +359-2-8704281
Fax: +359-2-8704282
e-mail: zitteliana@pensoft.net

Subject Editors

Gernot Arp, Göttingen, Germany
Dirk Erpenbeck, Munich, Germany
Peter Frenzel, Jena, Germany
Marc Gottschling, Munich, Germany
Stefan Hölzl, Nördlingen, Germany
William Orsi, Munich, Germany
Oliver Rauhut, Munich, Germany
Mike Reich, Braunschweig, Germany
Bettina Reichenbacher, Munich, Germany
Oliver Voigt, Munich, Germany

Zitteliana

2021. Volume 95

ISSN: 2512-5338 (print), 2747-8106 (online)

PENSOFT

Zitteliana

Content of volume **95** 2021

Norbert Wannenmacher, Volker Dietze, Matthias Franz, Günter Schweigert
New records of ostracods and ammonites from the Aalenian (mainly Concavum Zone) of the Zollernalb (Swabian Alb, SW Germany) 1

Gernot Arp, Sebastian Gropengießer, Christian Schulbert, Dietmar Jung, Andreas Reimer
Biostratigraphy and sequence stratigraphy of the Toarcian Ludwigskanal section (Franconian Alb, Southern Germany) 57

Steven L. Wick
Paleontological inventory of Paleozoic, Late Mesozoic, and Cenozoic plant, invertebrate, and vertebrate fossil species from Big Bend National Park, Texas, USA – over a century of paleontological discovery 95

Thilo C. Fischer
In search for the unlikely: Leaf-mining caterpillars (Gracillariidae, Lepidoptera) from Upper Cretaceous and Eocene ambers 135

Zitteliana 95, 2021, 1–55 | DOI 10.3897/zitteliana.95.56296

SNSB Bayerische Staatssammlung für Paläontologie und Geologie

ZITTELIANA
An International Journal of Paleontology and Geobiology

New records of ostracods and ammonites from the Aalenian (mainly Concavum Zone) of the Zollernalb (Swabian Alb, SW Germany)

Norbert Wannenmacher†, Volker Dietze[1], Matthias Franz[2], Günter Schweigert[3]

1 *Meraner Str. 61, 86720 Nördlingen, Germany*
2 *Regierungspräsidium Freiburg, Landesamt für Geologie, Rohstoffe und Bergbau, Albertstr. 5, 79104 Freiburg i. Br. Germany*
3 *Staatliches Museum für Naturkunde, Rosenstein 1, 70191 Stuttgart, Germany*

http://zoobank.org/F894DD92-D76C-42E1-A4A2-852E4D2ADD48

Corresponding author: Volker Dietze (dietze.v@t-online.de)

Academic editor: Alexander Nützel ♦ **Received** 15 July 2020 ♦ **Accepted** 29 December 2020 ♦ **Published** 17 June 2021

Abstract

The lithostratigraphy and ammonite/ostracod biostratigraphy and the accompanying fauna of several sections and outcrops around the Hohenzollern (Zollernalb, SW Germany), ranging from the topmost Opalinuston Formation (uppermost Lower Aalenian) to the basal Wedelsandstein Formation (lowermost Lower Bajocian) are described and analyzed. The study of ostracods from 41 samples from the Aalenian and Lower Bajocian of the Heiligenbach, Hausterberg and Roschbach sections has yielded approximately 4,100 specimens. Significant changes in the ostracod assemblage occur at the base of the Lower Aalenian "Comptum" Subzone, at the Bradfordensis/Gigantea subzonal boundary, at the Bradfordensis/Concavum zonal boundary and at the Aalenian/Bajocian boundary (Concavum/Discites zones). A minor change occurs above the Calceola-Bank within the Concavum Zone. The following new ostracod species are described: *Cytheropterina crassicostata* **sp. nov.**, *Eucytherura eberti* **sp. nov.** and *Eucytherura foveolata* **sp. nov.** In addition, 15 presumably new species are briefly described; 10 'incertae sedis' taxa are figured, but left in open nomenclature. The ammonite faunas of the Inopernabank and Konglomeratbank beds (Upper Aalenian, Bradfordensis Zone, Gigantea Subzone) as well as the ammonite faunas from the Calceolabank and Rostrote Kalkbank beds (Upper Aalenian, Concavum Zone, Concavum Subzone, *cavatum* biohorizon) are described and correlated with those of other areas.

Zusammenfassung

Die Lithostratigraphie und die Ammoniten-/Ostracoden-Biostratigraphie sowie die Begleitfauna mehrerer Profile und Aufschlüsse in der Umgebung des Hohenzollern (Zollernalb, SW-Deutschland), von der obersten Opalinuston-Formation (oberstes Unter-Aalenium) bis zum basalen Wedelsandstein (unterstes Unter-Bajocium), werden beschrieben. Die Auswertung von 41 Proben (aus dem Aalenium bis zum Unter-Bajocium) vom Heiligenbach, Hausterberg und Roschbach hat ca. 4100 Ostracoden erbracht. Signifikante Änderungen in der Ostracoden-Gemeinschaft gibt es an der Basis der "Comptum"-Subzone (Unter-Aalenium), den Grenzen der Bradfordensis-/Gigantea-Subzone, der Bradfordensis-/Concavum-Zone sowie an der Aalenium/Bajocium Grenze (Concavum-/Discites-Zone). Eine weniger stark ausgeprägte Änderung der Ostracoden-Gemeinschaft erfolgt innerhalb der Concavum-Zone, oberhalb der Calceola-Bank. Folgende neue Arten werden beschrieben: *Cytheropterina crassicostata* **sp. nov.**, *Eucytherura eberti* **sp. nov.** und *Eucytherura foveolata* **sp. nov.** Darüber hinaus werden 15 wahrscheinlich neue Arten kurz beschrieben; 10 "incertae sedis"-Taxa werden in offener Nomenklatur abgebildet. Die Ammonitenfaunen der Inopernabank und der Konglomeratbank (Ober-Aalenium, Bradfordensis-Zone, Gigantea Subzone) werden ebenso wie diejenige der Calceolabank und der Rostroten Kalkbank (Ober-Aalenium, Concavum-Zone, Concavum-Subzone, *cavatum*-Horizont) beschrieben und mit Ammonitenfaunen anderer Gebiete korreliert.

† deceased

Copyright *Norbert Wannenmacher et al.* This is an open access article distributed under the terms of the Creative Commons Attribution License (CC BY 4.0), which permits unrestricted use, distribution, and reproduction in any medium, provided the original author and source are credited.

PENSOFT®

Keywords

Upper Aalenian, Achdorf Formation, ammonites, ostracods, Zollernalb, SW Germany

Schlüsselworte

Ober-Aalenium, Achdorf-Formation, Ammoniten, Ostracoden, Zollernalb, SW-Deutschland

Table of content

1. Introduction and previous studies 2
2. Description of the sections 2
3. Description of the ostracod assemblages (M. Franz) 10
4. Description of the ammonite fauna 22
5. Bio-/Chronostratigraphy 23
6. Correlation 46
7. Additional macrofauna of the Upper Aalenian in the Zollernalb 47
8. Conclusions 48
References 49
Appendices 53

1. Introduction and previous studies

In the context of the field works on the occasion of the investigation of the lithostratigraphy as well as the ammonite and ostracod biostratigraphy of the "Unterer Wedelsandstein" and "Sowerbyi-Oolith" members (Wedelsandstein Formation; Lower Bajocian) of the Zollernalb (Dietze et al. 2019), the survey of the sections was expanded to the underlying beds of the Achdorf Formation (uppermost Lower and Upper Aalenian). Surprisingly, some of these beds yielded a rich ammonite fauna. This was quite unexpected, since Hahn (1975) mentioned that ammonites are very rare in the Upper Aalenian of this area. The microfauna samples are very rich in ostracods. Therefore, we decided to publish the lithostratigraphical and biostratigraphical results regarding the Achdorf Formation and parts of the Opalinuston Formation in a separate publication, which is presented here.

Our knowledge on the Aalenian ostracod fauna from Germany is mainly based on studies from the 1930's to 1960's as summarized by Dietze et al. (2019). Ernst (1989), Ohmert (1996, 2004), Brand and Mönnig (2009), Franz et al. (2009, 2014), and Dietze et al. (2017a, 2019), provided more recent data. Publications on Aalenian ostracods from other European areas include Bate (1963a, b, 1968, 1978, 2009), Sheppard (1981), Morris (1983), Ainsworth (1986, 1990, 1991), Ainsworth et al. (1989), Whittaker and Hart (2009) [Great Britain, Ireland], Dépêche (1985), Bodergat (1997) [France], Arias et al. (2009) [Spain], Tröster (1987), Reisdorf et al. (2016), and Tesakova (2017) [Switzerland]. Aalenian ostracods have also been described from Argentina (Ballent 1991; Boomer and Ballent 1996; Ballent and Whatley 2000, 2009) and Iran (Kochhann et al. 2015).

There is only little information available on the ammonites of the uppermost Aalenian (Concavum Zone) in SW Germany. Stratigraphic data and numerous local details were provided by Beisswenger (1920), Rieber (1922), Schmierer (1925, 1926), Stahlecker (1926, 1934), Schmidt (1933), Erb (1938), Lörcher (1939), Boomgaard (1948), Rieber (1961), Hahn (1975f), and Hiller and Kunze (1979). Rieber (1963) described and figured well-preserved ammonites from the Concavum Zone of the "Hofwald" section near Metzingen (Middle Swabian Alb). The so-called "Concava-Bank" of the Zollernalb in Rieber (1963: 16) corresponds to our "Konglomeratbank" (see also Rieber 1922: 46). Bayer (1969) described some hammatoceratid ammonites from the Concavum Zone of the Wutach area and the "Hofwald" section. Ohmert (1981) dealt as well with the outcrops in the "Hofwald". Sanns and Schweizer (1987), among others, investigated the lithology and formation of the "*concava*-Bank" bed. Finally, Franz and Nitsch (2009) revised the lithostratigraphy of the Aalenian in Baden-Württemberg.

2. Description of the sections

All sections are described bottom-up.

2.1 Balingen-Zillhausen (Roschbach)

Opalinuston Formation (Zillhausen Member)
Bed no.

1. [**Zopfplatten**] (ca. 1.0 m [Rieber 1963]).

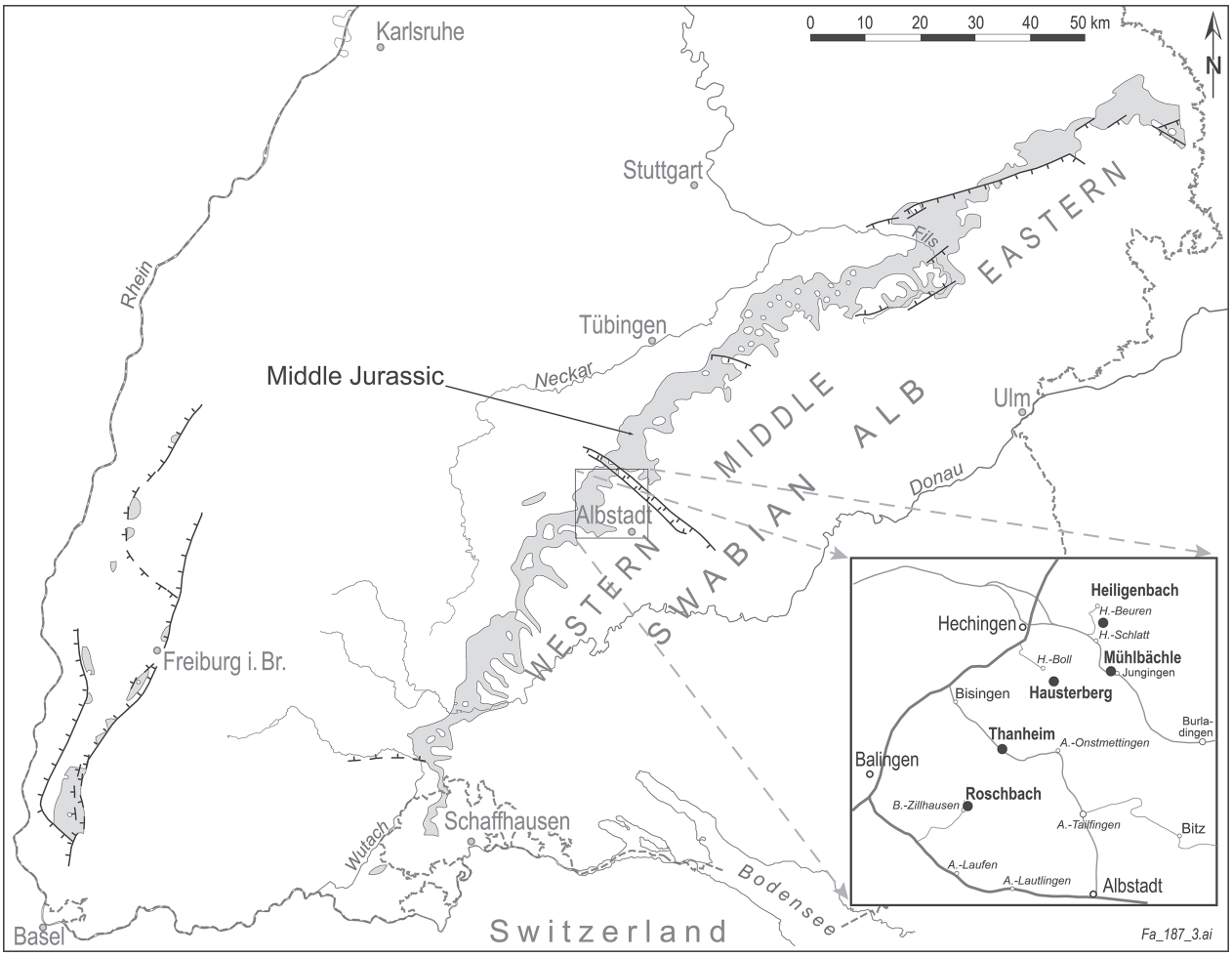

Figure 1. Location map of the sections studied in the Zollernalb (enlarged square).

2. (ca. 8.0 m [Rieber 1963]): claystone with layers of siderite concretions (only the uppermost 2 m are exposed) at 0.4 m, 0.9 m and 1.5 m below the top.

Achdorf Formation

3. (0.15–0.2 m): grey, hard marly limestone, with bivalves and *Leioceras crassicostatum*.
4. (0.15 m): grey carbonaceous marlstone; in the upper part gritty, with siderite concretions.
5. (0.03 m): grey, very hard marly limestone nodules.
6. (0.2 m): grey marlstone with compressed *Leioceras crassicostatum*.
7. (0.05 m): light grey, pyritic marly limestone nodules with dark grey *Chondrites* burrows. Mainly small specimens of *Leioceras* "*comptum*", irregularly embedded and partly accumulated.
8. (0.4 m): carbonaceous marlstone with higher clay content than in beds 4 and 6.
9. (0.03 m): grey marly limestone nodules.
10. (0.2 m): clay marlstone.
11. (0.18 m): marly limestone, partially splitting in the lower third. At the base with hazelnut-sized pebbles. Above very hard marly limestone concretions with shrinkage cracks (septaria) and fine shell debris.
12. (ca. 2.0 m): claystone, badly exposed.
13. (0.05 m): grey, hard marly limestone.
14. (ca. 5.5 m): claystone with layers of septaria und siderite concretions (section is divided by a wooden bridge at the "Geopfad" into a lower and an upper part) below: ca. 4.0 m claystone with a layer of septaria (0.05 m) ca. 1.8 m above the base above: ca. 1.5 m claystone (with layers of siderite concretions at 1.1 m, 0.8 m, 0.7 m and 0.4 m below the top; ca. 0.85 m below the top, a hard, sandy, micaceous marly limestone with ichnofossils; 0.25 m below the top another septaria layer).
15. (0.05 m): hard carbonaceous marlstone.
16. (0.2 m): greyish brown marly limestone with *Ludwigia murchisonae* (see Rieber 1963).
17. (0.4–0.45 m): grey carbonaceous marlstone.
18. (0.25 m): greyish brown, marly limestone.
19. (0.15 m): carbonaceous claystone.
20. (0.25 m): grey, hard marly limestone; with *Staufenia staufensis* and *Brasilia bradfordensis* (Rieber 1963). This is the top layer of the small waterfall.
21. (0–0.12 m): grey, very hard, loaf-shaped marly limestone nodules with *Staufenia staufensis* (SMNS 70519/1 [microconch]). From a corresponding nodule layer of the nearby Bezighofenbach section (Rieber 1963), a large *S.* cf. *staufensis* (SMNS 70519/55) with a relatively wide umbilicus was recorded.

22. (ca. 1.7 m): grey marlstone, mostly not exposed. (Rieber (1963) described 4 harder beds up to 1.65 m above bed 20, the uppermost one as an oolitic nodule layer with *Staufenia staufensis*).
23. (ca. 6 m): claystone, not exposed; only the uppermost 0.3 m are visible.
24. (0.05–0.15 m): **[Inopernabank]** spotty-grey, tough, marly limestone with greyish brown bark and isolated small, rounded pebbles. At the base larger *Thalassinoides* burrows, in the lower part of the bed small, flattened marlstone pebbles (0.03–0.05 m). Few fossils: *Gryphaea* sp., *Pinna* sp., belemnites.
25. (6.0 m): dark claystone with several layers of siderite concretions in the upper 0.5 m.
26. (0.05–0.1 m) **[Konglomeratbank** (= bed 3 in Dietze et al. 2019)**]**: grey marly limestone with abundant pebbles. *Ludwigella arcitenens* (Fig. 16: 3a, b).
27. (ca. 0.3 m): dark grey, laminated carbonaceous claystone, with fine shell debris and small nodules (up to 5 mm). Rare, compressed *Graphoceras* sp., a fragmentary *Graphoceras* sp. (SMNS 70519/2) at the top sample Ro19-1: 0–0.05 m above the Konglomeratbank sample Ro19-2. 0.25–0.3 m above the Konglomeratbank
28. (max. 0.1 m) **[Calceolabank** (= bed 5 in Dietze et al. 2019)**]**: grey, marly limestone with many *Gryphaea calceola* in its lower part, in clay-rich parts predominantly in "convex upward" position. Some of the shells are stacked into each other. The layer is nodular in some places and then wedges out. At one point many large *Trigonia alemanica* and compressed ammonites (?*Graphoceras*) occur. At another place nearby well-preserved *Graphoceras* cf. *concavum* (Fig. 16: 1, 4) and *Brasilia* cf. *decipiformis* (Fig. 21: 2a, b, 5a, b).
29. (0.15 m): carbonaceous claystone with few small gryphaeids.
30. (0.1–0.15 m): carbonaceous claystone with masses of small gryphaeids (*Gryphaea calceola*) up to 2 cm in diameter and small phosphorite concretions. Sample Ro19-3
31. (0.15 m): grey calcoolitic marlstone (reddish brown in weathered state), with single hard marly limestone nodules. Few bivalves and belemnites.
32. (0.15 m) **[Rostrote Kalkbank** (= bed 9 in Dietze et al. 2019)]: hard limestone, rusty red crust, inside greenish grey and brown-red marbled.
33. (0.95 m; see Ohmert 2004): carbonaceous claystone. Sample Ro19-4: 0–0.05 m above the Rostrote Kalkbank Sample Ro19-5: 0.05–0.15 m above the Rostrote Kalkbank

Wedelsandstein Formation

34–36. [**Sowerbyi-Oolith** (= beds 11–13 in Dietze et al. 2019)**]** (see Franz 1986, Dietze et al. 2019).
34. (0.05–0.07 m): limestone nodules, calcitic ooids only in *Chondrites* burrows.
35. (0.06–0.1 m): dark grey, muscovite-bearing, laminated oolitic claystone with belemnites and *Hyperlioceras*.
36. (0.04–0.13 m): grey elongated limestone nodules with irregular surfaces, hard, calcitic oolites (0.1–0.2 mm diameter), with small pebbles, in places densely packed. Bivalves (*Gryphaea*, *Entolium*), belemnites, serpulids; strongly bioturbated (*Chondrites*). Ammonites: *Hyperlioceras* sp. and *Euhoploceras* sp. (see Dietze et al. 2019).

Higher up **Unterer Wedelsandstein** (see Dietze et al. 2019).

2.2 Hechingen-Boll (Hausterberg)

Landslide above the former Friedrichstal castle near Hechingen-Boll

Achdorf Formation
Bed no. / sample no.

1. (min. 1.5 m): claystone, thickness unknown. Only uppermost part exposed.
2. (0–01.15 m): nodular bed of grey marly limestone, with small light grey, phosphoritic pebbles (0.2–1 cm) and marly limestone pebbles up to 3 cm, partly compressed. *Graphoceras* sp.
3. (1.5 m): dark grey claystone
4. (0.15 m): nodular bed, like bed 2, but continuously developed.
5. (ca. 4 m): grey claystone
   - not exposed
   - Slipped blocks from the **Rostrote Kalkbank** (0.15 m) and the **Calceolabank** (0.15 m) with *Gryphaea calceola*, *Graphoceras* sp. (SMNS 70519/3), *Euaptetoceras* sp. (SMNS 70519/4).
6. (ca 7–8 m): claystone, mostly badly exposed. The upper 3 m excavated for sampling. Layers of siderite concretions at 0.15 m, 0.2 m, 0.5 m and 1.5 m below top. 1.6 m below top 0.10–0.15 cm long and 0.03–0.04 m thick lenses of light grey, lenticularly bedded, fine-sandy limestones.
   - Ha19-1 (3.05–2.55 m below bed 7)
   - Ha19-2 (2.05–1.55 m below bed 7)
   - Ha19-3 (1.05–0.25 m below bed 7)
   - Ha19-4 (0.15–0.25 m below bed 7)
7. (0.15 m) [**Sowerbyi-Oolith**]: claystone, with occasional irregular-shaped, often flat nodules (up to 0.10 m long and 0.04 m thick) of greyish limestone with borings, the sediment infill of which is calcoolitic. The nodules are settled on all sides with bryozoans, oysters and serpulids and show in places a fine, dark brown coating. Small phosphoritic pebbles (up to 0.05 m) are not rare. Some of them show parallel scratch-like traces. In the pebbles occasionally casts of endobenthic bivalves occur. In the claystone fragments of *Actinostreon*, *Ctenostreon* and fragments of abraded belemnites

with borings occur. One fragmentary *Hyperlioceras* from the "Weinhalde" section, 700 m SE of the Haustberg section.
   - Ha19-5 / (above bed 7)
8. (0.15 m): sandy marly limestone with separation joints. Large *Thalassinoides* burrows at the base; *Zoophycos*.
9. (0.3 m): marly claystone; at the base sandy, at the top silty.
   - Ha19-6

2.3 Jungingen (Mühlbächle and Starzel)

2.3.1 Mühlbächle

Achdorf-Formation:
Bed no. / sample no.

1. (min. 0.5 m): claystone
2. (0.1–0.12 m): pyrite-bearing grey, weathered rusty, hard marly limestone. Many tiny gryphaeids, rare belemnites and bivalves. Few, mostly very small ammonites. *Brasilia bradfordensis* (Fig. 19: 1a, b)
3. (0.45 m): claystone. In the upper part a single carbonaceous burrow (diameter up to 0.04 m) was observed.
4. (0.05–0.1 m): hard, grey marly limestone with many pebbles of different size and burrows at the base.
5. (1.8–2.0 m): claystone; only partly exposed.
6. (0.05–0.08 m): grey marly limestone with pebbles; accumulations of very small gryphaeids.
7. (1.6 m): claystone with several layers of siderite concretions (0.4, 0.6, 0.8, 0.9, 1.0, 1.15 and 1.3 m above base).
8. (0.05–0.08 m) flat to nodular, hard, grey marly limestone with occasional pebbles.
9. (0.01–0.05 m): marlstone.
10. (0.15–0.18 m): **[Inopernabank]** greyish brown, hard marly limestone, easily splitting in weathered state. Numerous larger pebbles, especially in the lower part, where they can be flattened. Small, light grey pebbles give the rock a speckled appearance. Large burrows at the base. Bivalves are characteristic for the Inopernabank (big *Pholadomya*, *Inoperna sowerbyana*, *Gryphaea calceola* [smaller ones than those in the Calceolabank]). Some of the endobenthic bivalves are still in life position (see Quenstedt 1857: 357).
11. (ca. 3.5–4.0 m) claystone, not exposed.
12. (0.1–0.12 m) **[Konglomeratbank]**: hard, greyish brown marly limestone, with big pebbles. Large *Pholadomya* in life position.
13. (0.35 m): grey marl with abundant *Gryphaea calceola* (up to 0.03 m).
14. (0.15–0.18 m) **[Calceolabank]** (= bed 12 in Dietze et al. 2019): Hard, grey, pyrite-bearing marly limestone. Partly easily splitting. Weathered brown and decomposing. At the base abundant *Gryphaea calceola* (up to 0.06 m large), only very rarely with right valves. The gryphaeids are embedded individually or in accumulations. Well-preserved ammonites are relatively common, predominantly in the lower third of the bed: *Brasilia* cf. *decipiens* (Fig. 19: 5a, b), *B*. aff. *decipiens* (Fig. 20: 3a, b), *Graphoceras* aff. *magnum* (Fig. 20: 1a, b), *G. cavatum* (Fig. 21: 2a, b), *G*. cf. *cavatum* (Fig. 20: 2a, b; Fig. 21: 1a, b), *G. pulchrum* (Fig. 22: 3a, b), *G. decorum* (Fig. 22: 1a, b), *G. formosum* (Fig. 22: 2a, b, 5a, b), *G. fallax* (Fig. 22: 4), *Ludwigella cornu* (Fig. 19: 2), *L. attracta* (Fig. 19: 3), *L. micra* (Fig. 19: 4), *Euaptetoceras* cf. *euaptetum* (Fig. 23: 1a–c), *E.* cf. *kochi* (Prinz) (The ammonite figured in Fig. 24 comes from an excavation pit in Jungingen 500 m west of the Mühlbächle stream).
15. (0.20 m): grey carbonaceous claystone.
16. (0.05 m): single hard marly limestone nodules (up to 0.05 m).
17. (0.20 m): grey carbonaceous claystone with small phosphoritic nodules. Masses of small gryphaeids (*Gryphaea calceola*).
18. (0.10 m): rough, phacoidal, reddish marlstone with occasional hard marly limestone nodules; pholadomyids. *Graphoceras concavum* is recorded from the Bachenau section (Rieber 1922, 1963), which is situated about 50 m east of the Mühlbächle.
19. (0.08–0.1 m): light grey, very hard limestone with numerous dark grey burrows (*Chondrites* and cylindrical burrows up to 4 mm in diameter). Occasional compressed ammonites. Thin marly joint with bed 20.
20. (0.1–0.12 m) **[Rostrote Kalkbank]** (= bed 15 in Dietze et al. 2019): On the outer surface weathered with a typical rusty red margin. In fresh state a hard, light grey, reddish and greenish grey marbled limestone. *Graphoceras* sp.
21. (8.0 m) (= bed 16 in Dietze et al. 2019): claystone (thickness according to A. Rieber 1922). Poorly exposed.
   - Mue19-1

Wedelsandstein-Formation:

22. (0.15–0.2 m) **[Sowerbyi-Oolith]** (= bed 17 in Dietze et al. 2019): grey carbonaceous claystone with marly limestone nodules. Some nodules show concentric growth structures. Club-shaped borings are filled with calcitic oolites. The surface of rounded to flat nodules is densely covered on all sides with bryozoans, serpulids and sessile foraminifers. Some other nodules are grey inside, calcoolitic, with scattered very small light grey pebbles. Rare serpulids, belemnites, bivalves and pebbles occur in the matrix. The very irregular-shaped, calcoolitic limestone nodules are overgrown as well. In the claystone between the nodules occasional belemnites and endobenthic bivalves, *Entolium*.

Higher up follows the **Unterer Wedelsandstein** (see Dietze et. al. 2019).

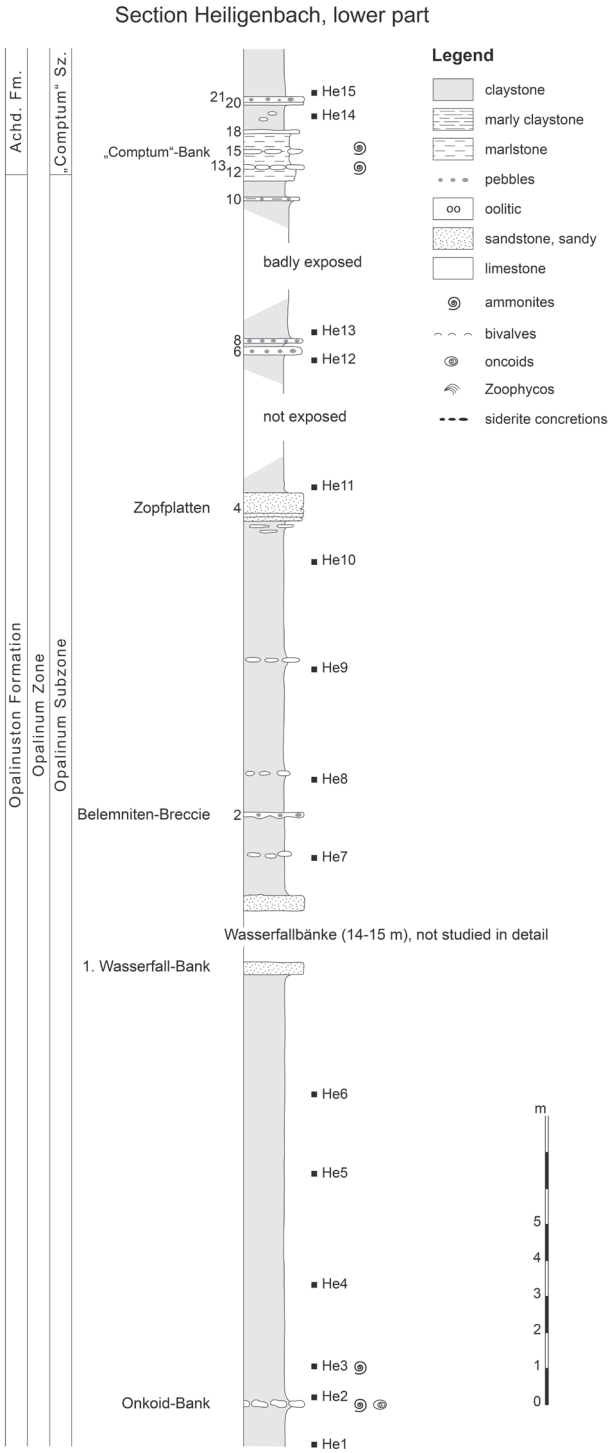

Figure 2. Section Heiligenbach, lower part. Achd. Fm = Achdorf Formation; Sz. = Subzone.

2.3.2 Starzel (river bed near the road Jungingen–Killer, see Lörcher (1939: 224):

Achdorf-Formation:
bed no.

1. (min. 0.4 m): claystone
2. (0.05 m): grey, flat nodular marly limestone.
3. (0.01–0.05 m): marly joint.
4. (0.15–0.2 m) **[Inopernabank]**: hard, grey limestone, in places speckled with small, light grey pebbles and large burrows at the base. Larger, mostly flattened pebbles occur predominantly in the lower part of the bed. The bed varies greatly in thickness and compactness. Large *Pholadomya lirata*, *Inoperna sowerbyana*, *Goniomya literata*, *Gryphaea calceola* (up to 0.03 m), *Entolium* sp., *Propeamussium pumilum*, and *Oxytoma inaequivalvis*. Small gastropods, belemnites and ammonites. *Graphoceras cavatum* (Fig. 13: 2a, b, 9a, b), *G.* aff. *fallax* (Fig. 13: 3), *Brasilia decipiens* (Fig. 13: 1a, b), *Ludwigella attracta* (Fig. 13: 7, 8), *L. tenuis* (Fig. 13: 4), *L.* aff. *tenuis* (Fig. 13: 5), *L. attenuata* (Fig. 13: 6), *Planammatoceras* sp. (Fig. 14: 1a–c). Lörcher (1939: 224) misidentified this bed as Calceolabank).
5. (min. 0.5 m): claystone.
6. Higher parts of the section are not exposed, except of the Rostrote Kalkbank bed above the railway bridge near the village Killer.

2.4 Hechingen-Beuren (Heiligenbach, Sießenwald, Hanneswiesle)

2.4.1 Heiligenbach

(the strata below bed 1 were not studied in detail)

Bed no. / sample no.

“Ob -1m“ He19-1 1.0 m below Onkoidbank.

“Ob“ (0.15–0.2 m) **[Onkoidbank]**: *L. opalinum* [m], about 11 m below “Wasserfallschichten”. In its upper part a marly limestone, dark grey, upper and lower surface very irregular, with shrinkage cracks and oncoids (Fig. 3).

“x” (about 11 m): sandy, carbonaceous claystone, a single *Lytoceras dilucidum*.

- He19-2 0–0.1 m above Onkoidbank: numerous crinoids and bivalves.
- He19-3 1 m above Onkoidbank, numerous crinoids, *Leioceras opaliniforme* (body chamber).
- He19-4 2 m above Onkoidbank.
- He19-5 5 m below “Wasserfallschichten”: Isolated lenticular, thin-layered, sandy-calcareous layers, micaceous, with crinoid debris (Pentacrinitenplatte with *Chariocrinus wuerttembergicus*), ichnofossils (*Gyrochorte*, *Palaeophycus* and others).
- He19-6 3 m below “Wasserfallschichten”

“WS” (about 14–15 m) **[Wasserfallschichten]**: with several cascades in the river bed (Rieber 1922; Lörcher 1939; Kobler 1972: 14, pl. 2 [left column]).

1. (2.0 m): claystone, dark grey (at approx. 1.0 ca. 0.04 m irregular carbonaceous marlstone pebbles.
   - He19-7 (middle)
2. (0.08–0.1 m) **[Belemnitenbreccie]**: hard, bluish-grey marly limestone, base very irregular; with a coquina of bivalves/echinoderms and grey pebbles, partially

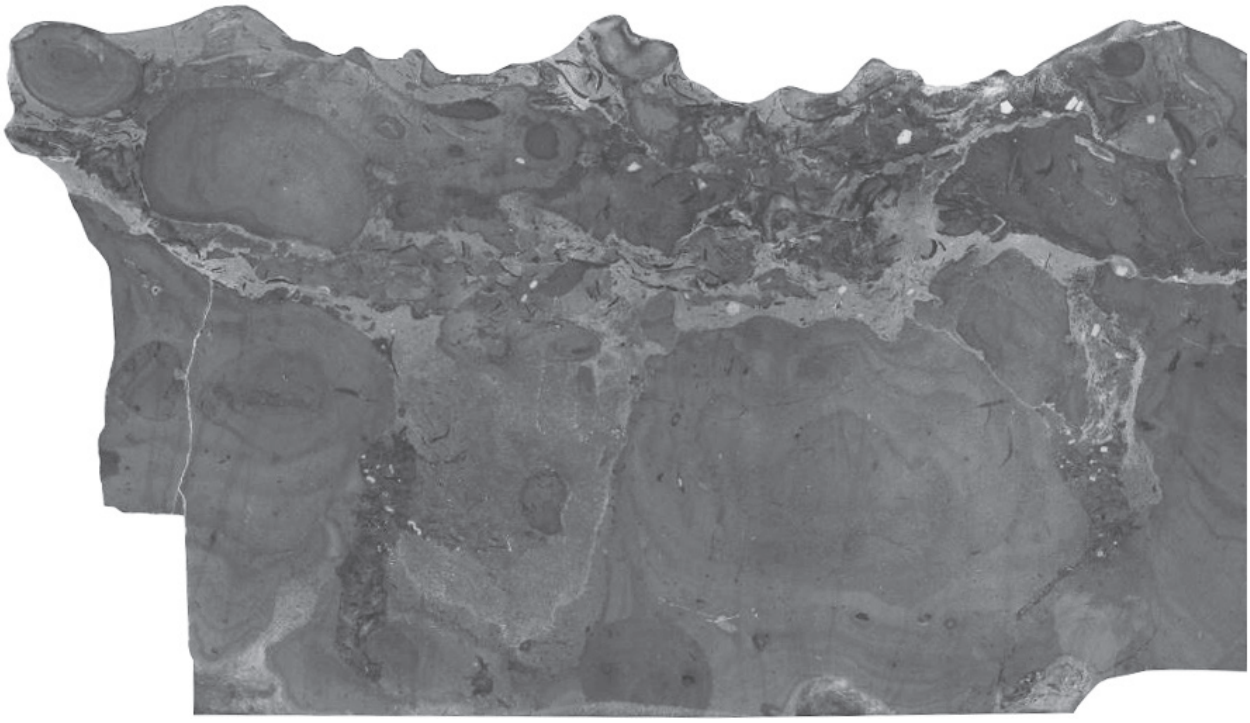

Figure 3. Obere Onkoidbank, polished section; the lower half of dark grey limestone bed consists of redeposited, marginally eroded, micritic oncoids up to 7 × 8 cm in size. This part is overlain by silty, fine sandy, fossil-bearing (crinoids, bivalve shells, rare belemnites) marly limestone, in which up to 4 cm large oncoids with borings and thin pyritized microbial crusts are embedded. This sediment also fills the interspaces between the oncoids. Opalinuston Formation, Heiligenbach. Width of the photo: 20 cm.

with bivalve borings, irregularly bedded. Abundant belemnites, *Gryphaea calceola*, *Chlamys textoria*.

3. (7–8 m): claystone with layers of siderite concretions; only partly exposed.
   - **3a**: 1.0 m above bed 2: layer of nodules (carbonaceous marlstone/siderite)
     - He19-8
     - He19-9 (3.0 m above bed 2): rare bivalves, *Bactryllium*, cylindrical burrows.
   - **3b**: ca. 4.0 m above bed 2: noticeable nodule layer (brown marly limestone)
     - He19-10 (1.0 m below top): burrows

   In the upper 0.25 m single mica-bearing fine sandy limestone plates (up to approx. 0.03 m thick) with a rich ichnofauna, *Gyrochorte comosa*.
4. (0.7 m) **[Zopfplatten]**: fine sandy limestone, mica-bearing, splitting into thin plates; *Gyrochorte comosa*.
5. (ca. 3.5 m): very poorly exposed
   - 1.5 m above bed 4: claystone with siderite nodules.
     - He19-11 small gastropods.
     - He19-12 (directly below bed 6): very numerous agglutinating foraminifera.
6. (0.15–0.2 m): grey, marly limestone, small pebbles (up to nut-size). Lörcher (1939) described ammonites probably coming from this bed (or from bed 10).
7. (ca. 0.1 m): dark grey claystone.
8. (0.05 m): grey marly limestone, few small pebbles.
9. (ca. 3–4 m): dark grey claystone, very badly exposed
   - He19-13 (middle)
10. (0.01 m): grey carbonaceous marl with a layer of pebbles.
11. (0.4 m): dark grey claystone.
12. (0.3 m): grey marlstone.
13. 0–10 cm grey, lenticular to nodular marly limestone; accumulations of remarkably small sized ammonites: *Leioceras* "*comptum*", *L. evolutum*, *L. striatum*, *L. paucicostatum* (from the corresponding layer of the Steinlach creek north of Mössingen-Talheim: *L. crassicostatum*, *L.* "*comptum*", *L. striatum*, *L. paucicostatum*, *L. evolutum*, *L.* sp. (with broad whorls)), occasional bivalves; shrinkage cracks.
14. (0.03 m) dark grey marly claystone.
15. (0–0.1 m): carbonaceous marl nodules, in places a continuous, very hard carbonaceous marlstone bed with calcite-filled shrinkage cracks (Septarienbank). Occasional small ammonites (*Leioceras* "*comptum*").
16. (0.02 m) (directly on top of bed 15): sandy carbonaceous marl tiles, trace fossils (not continuously present).
17. (0.35 m): dark grey marly claystone.
18. (0.08 m): grey sandy carbonaceous marlstone.
19. (0.65 m): dark grey claystone with siderite nodules.
    - He19-14
20. (0.05–0.08 m): dark grey carbonaceous marl with small pebbles; thin marly claystone layer.
21. (0.1–0.12 m): grey carbonaceous marl with small pebbles **[**20 + 21: "Doppelbank"**]**
22. (ca. 2 m): dark grey claystone with grey limestone lenses.

- He19-15 agglutinating foraminifera

23. (0.05–0.07 m): grey carbonaceous marl, irregular surface; abundant pyrite, pebbles up to 0.03 m.
24. (ca. 1 m): dark grey claystone, approx. 0.7 m above bed 23 with a layer of siderite nodules.
25. (0.05 m): grey marly limestone with small pebbles.
26. (1.3 m): dark grey claystone, layers of siderite nodules at 0.15, 0.65, and 1.15 m above bed 25.
    - He19-16 (0.01 m above bed 25): crinoids
27. (0.08 –0.1 m): brown, coarsely conglomeratic marly limestone; bivalves and belemnites.
28. (3.5–4 m): dark grey claystone, only partly exposed.
    - He19-17(0.25 m below bed 29)
29. (0.15 m): grey lenticular splitting carbonaceous marl.
30. (0.15 m): light grey marly limestone with dark grey spots.
31. (0.03 m): brownish grey carbonaceous marlstone with masses of small pebbles.
32. (0.15 m): brown marly limestone with bivalves **[**29–32: **Staufensisbank]**
33. (ca. 6 m): claystone, not exposed; according to Lörcher (1939) with several carbonaceous beds.
    - He19-18 (0.5 m above bed 32)
    - He19-19 (0.2 m below bed 34)
34. (0.1–0.15 m): grey marly limestone, thin bivalve shells; single small pebbles.
35. (2 m): claystone.
    - He19-20 (0.4 m below bed 36)
36. (0.01 m): grey marly limestone, small pebbles up to 3 cm; shell debris. Belemnite, nautiloid (*Cenoceras*), *Graphoceras*.
37. (ca. 0.7 m): dark grey claystone.
38. (0.05 m): irregularly shaped bed of grey marly limestone.
39. (0.7 m): claystone; 0.4 m above bed 38 a layer of siderite nodules. Arthropod burrows at the top.
    - He19-21 (0.4 m above bed 38)
40. (0.1 m) **[Inopernabank]**: grey, coarse conglomeratic limestone, with phosphoritic spots; *Pholadomya lirata*, *Gryphaea calceola*, *Inoperna sowerbyana*, ammonites: *Graphoceras* cf. *caduciferum* (Fig. 17: 1a, b), ?*Brasilia* sp. (SMNS 70519/54).
41. (4 m) (= bed 1 in Dietze et al. 2019): dark grey claystone, occasional flat siderite nodules at 0.6 m below top.
    - He19-22 (41 middle)
    - He19-23 (41, 0.5 m below bed 42)
42. (0.08–0.1 m) **[Konglomeratbank]** (= bed 2 in Dietze et al. 2019; starting from here this section had already been sampled in 1988): blueish grey limestone with pebbles. A fragment of *Graphoceras* sp. (Fig. 17: 2).
43. (0.02 m): calcoolitic marl.
    - He19-24
44. (0.15–0.17 m): grey to brownish marly claystone.
    - He19-25
45. (0.17 m) **[Calceolabank]**: (= bed 5 in Dietze et al. 2019) grey marly limestone, lenticular splitting, on top 0.02 m oolitic marl. Thin-shelled bivalves, at the base (in places in marl lenses) abundant *Gryphaea calceola*. Ammonites: *Brasilia decipiens* (Fig. 18: 1), *B.* aff.

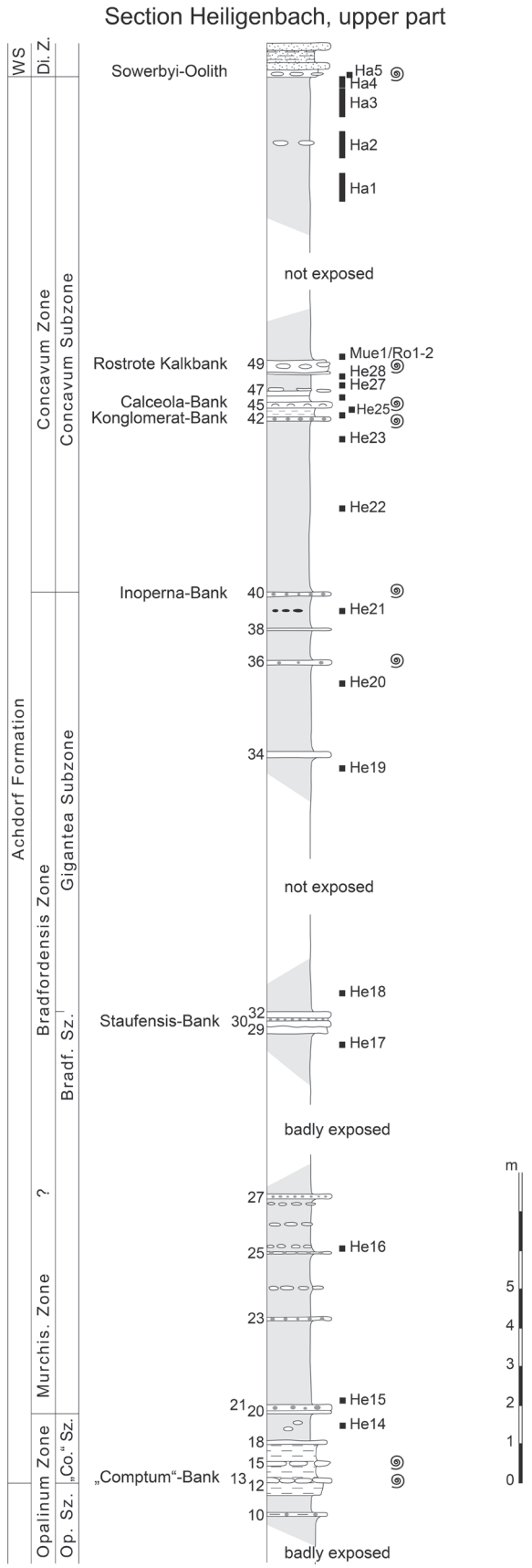

Figure 4. Section Heiligenbach, upper part, above the Rostrote Kalkbank, combined with the Mühlbächle, Roschbach and Hausterberg sections. WS = Wedelsandstein Formation; Murchis. = Murchisonae; Di. = Discites Zone; Op. Sz. = Opalinum Subzone; "Co. Sz. = "Comptum" Subzone; Bradf. Sz. = Bradfordensis Subzone.

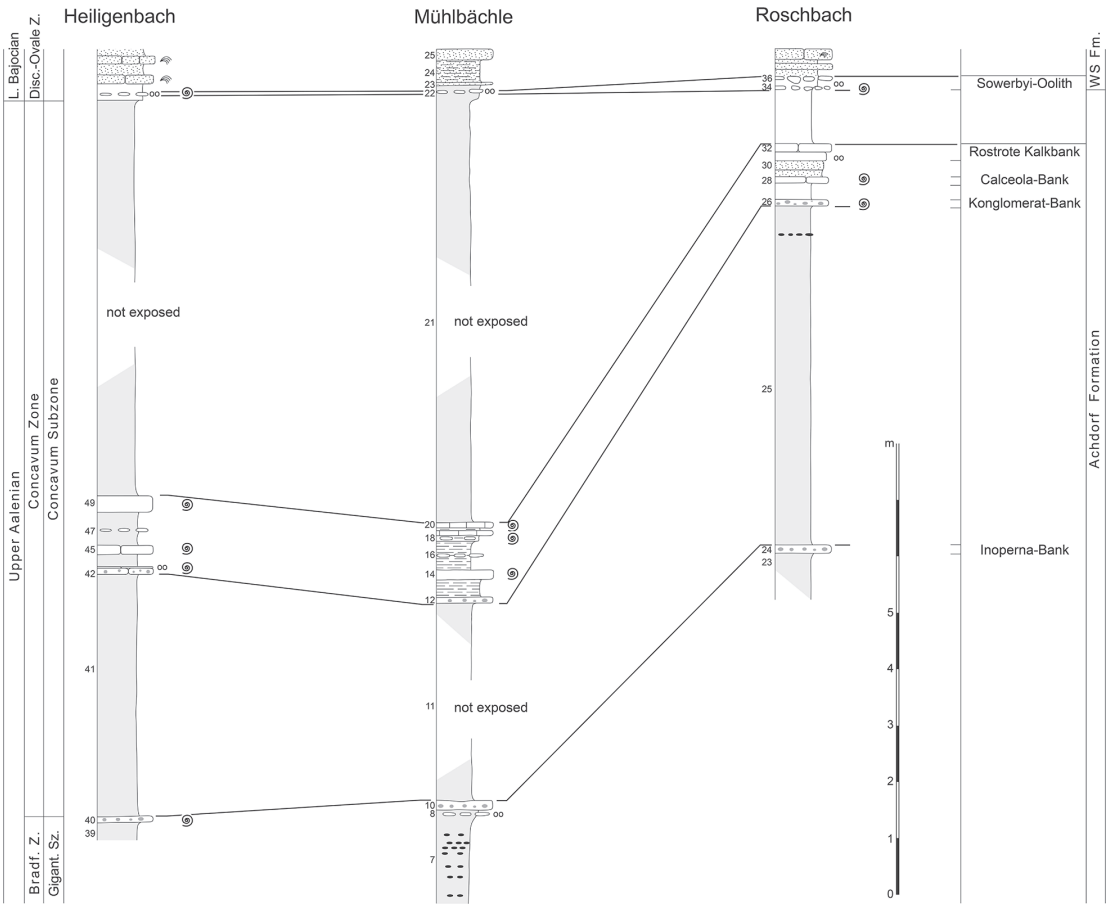

Figure 5. Sections Heiligenbach (above bed 49 combined with the Hausterberg section), Mühlbächle and Roschbach, detail of the Concavum Zone. L. Bajocian = Lower Bajocian, Bradf. Z. = Bradfordensis Zone; Disc.-Ovale Z. = Discites – Ovale zones; Gigant. Sz. = Gigantea Subzone.

decipiens (Fig. 18: 4a, b). *Graphoceras fallax* (Fig. 18: 5), *G. cavatum* (Fig. 18: 2), *G.* cf. *v-scriptum* (Fig. 18: 3), *Ludwigella arcitenens* (Fig. 17: 3), *L.* sp. (Fig. 17: 5), *Euaptetoceras infernense* sensu Buckman (Fig. 17: 4).

46. (0.02 m): greyish beige claystone.
    - He19-26
47. (0.05 m): single grey limestone nodules up to 5 cm, partly with numerous small *Gryphaea* and serpulids.
48. (0.33 m): grey laminated claystone, with abundant small gryphaeids, single belemnite.
    - He19-27 (at the base)
    - He19-28 (0.1 m above bed 47)
49. (0.25–0.35 m) **[Rostrote Kalkbank]** (= bed 9 in Dietze et al. 2019): reddish brown carbonaceous marl with marly limestone nodules; 2 or 3 layers of flat siderite nodules. At the base 0.05 m greenish brown marly limestone.
    This outcrop is covered by terrace gravel of the Heiligenbach.

2.4.2 Eastern tributary of the Heiligenbach coming from the Sießenwald, approx. 30 m east of the "Hunnengrab"

In the river bed there is a light grey, hard limestone bed (0.15 m) with a rust-coloured rim and many burrows. Its lithology resembles the lower bed of the Rostrote Kalkbank from the Mühlbächle section at Jungingen. An indeterminable ammonite fragment. A larger *Euaptetoceras* sp. (SMNS 70519/5) comes from a loose block of the Rostrote Kalkbank.

2.4.3 Hanneswiesle

This outcrop is located on a forest path in the Hanneswiesle district west of Beuren.

Bed no.

1. (0.08–0.1 m) **[Konglomeratbank]**.
2. (0.2 m): carbonaceous claystone.
3. (0.03 m): firm marlstone with many *Gryphaea calceola*.
4. (0.15–0.2 m) **[Calceolabank]**: brownish marly limestone, splitting into plates in places, but in places solid grey marly limestone with a reddish brown rim also in weathered state. Small gryphaeids are firmly fixed in clusters on the bed surface (see Erb 1938). Ammonites (*Graphoceras pulchrum* (Fig. 15: 5a, b), *G.* cf. *pulchrum* (Fig. 15: 4a, b), *G.* cf. *concavum* (Fig. 15: 1a, b), *G. decorum* (Fig. 15: 2), *G.* aff. *apertum* (Fig. 15: 3a, b), *Ludwigella arcitenens* (Fig. 15: 6a, b), *Euaptetoceras infernense* sensu Buckman (Fig. 14: 2a, b)) are mainly found in the lower part of the bed.

2.5 Bisingen-Thanheim (Heiligenkopf)

Since we did not find Aalenian ammonites in this outcrop, we here refer to Dietze et al. (2019) for the description of the section.

3. Description of the ostracod assemblages (M. Franz)

3.1 Methods

For the present study, a total of 41 samples were taken in September 2018 and September 2019. Individual samples, which were already taken in 1988 at the Heiligenbach, were included in the investigation.

Microfossils have been extracted by first drying the samples (0.5–1 kg), breaking them down with the aid of hydrogen peroxide (3% solution of H_2O_2) and then sieving them under water. The residues were then cleaned by boiling them for 15 minutes in a moderately concentrated sodium chloride solution (3 teaspoons NaCl / 0.25 l water). From the fractions > 0.5 mm and > 0.315 mm of the residues, 3–5 trays were examined. From the fractions > 0.2 mm and > 0.15 mm we examined 3 trays.

Photographs were taken using SEM in Stuttgart (SMNS).

3.2 Results

Introductionary remark:

The investigation of the Geisingen clay pit (Franz et al. 2018) has considerably increased the knowledge about the ostracod fauna of the Aalenian of SW Germany. The present investigation of approximately the same part of the section showed very good agreement in the Opalinum zone. However, several species are much rarer in the sections studied herein. In addition, strong changes in thicknesses and facies are noticeable. The vertical distribution of the species first described in Franz et al. (2018) – *Balowella catena*, *Cardobairdia tesakovae*, *Cytheropterina alacostata*, *Eucytherura eberti*, *Euc. foveolata*, *Euc*. sp. 3, *Euc*. sp. 5, *Pleurocythere ohmerti*, *Progonocythere scutula* – is consistent in both sections.

The 41 samples yielded a total of 4,149 specimens, ranging from 0 to > 700 specimens per sample. For a semi-quantitative analysis of the composition of the ostracod assemblages the greater numbers of single (right or left) valves were counted as 1, resulting in a total of 2.758 individuals.

A total of 108 species were identified, 329 specimens remained undetermined. From 34 species of the Upper Opalinuston Formation, 22 do not cross the boundary to the overlying Achdorf Formation. The Achdorf Formation yielded a total of 82 species including the 12 already known from the Opalinuston Formation. In the Lower Wedelsandstein Formation 4 new species appear, 11 persist from the Aalenian.

At zone or subzone level, two relative maxima in the total number of species are recorded in the Opalinum Subzone and Concavum Zone (Table 4). The highest number of species in the Concavum Zone correlates with the highest number of newly reported species as well as the total number of genera and families.

Short descriptions of new species of cytherurids (*Eucytherura* sp. 3–11, *Procytherura* sp. 2, P. sp. 5, *Procytheropteron* sp. 1) in our material are excluded. Ten presumably new species were found only in numbers of one to five specimens and could not be assigned to any known genus. For this reason, these taxa were left in open nomenclature. In the samples of the fine sandy layers, the ostracods are partly covered by remnants of sediment (mainly quartz grains) and/or fragmentarily preserved.

Abbreviations:

LGRB	Landesamt für Geologie, Rohstoffe und Bergbau im Regierungspräsidium Freiburg, Germany;
SMNS	Staatliches Museum für Naturkunde Stuttgart, Germany;
C	carapace;
RV	right valve;
LV	left valve;
HT	Holotype.

3.2.1 Systematic descriptions

In the following, the ostracod taxa that were found in the studied sections are listed in systematic order with information on their known occurrence. For detailed lists of synonyms, reference is made to Franz et al. (2018). Three new ostracod species are described. In addition, 15 presumably new species are briefly described in open nomenclature.

Order Myodocopida Sars, 1866
Family Polycopidae Sars, 1866
Genus *Polycope* Sars, 1866

***Polycope pelta* Fischer, 1961**

Material. 2 V in sample He19-9 and Mü I.

Distribution. Upper Toarcian to Upper Bathonian.

***Polycope* cf. *riegrafi* Brand, 1990**

Fig. 10: 1

Material. 2 C in sample He19-27

Distribution. Upper Aalenian, Concavum Zone; SW Germany.

***Polycope* sp.**

Material. 1 C, 4 V in samples He19-15–21.

Occurrence. Upper Aalenian, Murchisonae Zone – Concavum Zone; SW Germany.

Remarks: The material comprises predominantly very small, smooth carapaces and valves with no visible ornamentation and therefore it is not determinable to species level under the microscope. It cannot be excluded that they belong to different species.

Order Podocopida Müller, 1894
Family Cytherellidae Sars, 1866
Genus *Cytherella* Jones, 1849

***Cytherella apostolescui* Ainsworth, 1986**
Fig. 8: 1

Material. 30 C, 585 RV, 517 LV in samples He19-14–28, Mue19-1, Ha19-2–5 and Ro19-1–2.

Distribution. Upper Toarcian to Lower Oxfordian; SW Germany, Ireland.

***Cytherella apostolescui* ? ssp.**

Material. 12 RV in samples He19-24 and Ro19-1–2.

Distribution. Upper Aalenian, Concavum Zone; SW Germany.

Remarks. This ?subspecies was first described and figured from Thanheim (Dietze et al. 2019).

***Cytherella* cf. *fullonica* Jones & Sherborn, 1888**

Material. 1 C, 2 RV, 4 LV in samples He19-26 and Ro19-1–5.

Distribution. Upper Aalenian, Concavum Zone; SW Germany.

Genus *Cytherelloidea* Alexander, 1929

Cytherelloidea* cf. *cadomensis* (Bizon, 1960*)

Material. 11 C, 18 RV, 28 LV in samples Ha19-4–6 and Ro19-1.

Distribution. Upper Aalenian to Lower Bajocian; England, France, SW Germany.

***Cytherelloidea* cf. *catenulata* (Jones & Sherborn, 1888)**
Fig. 8: 2

Material. 2 RV, 1 LV in samples He19-17–18.

Distribution. Upper Aalenian to Bathonian; England, France, SW Germany.

***Cytherelloidea lordi* Ainsworth, 1986**
Fig. 9: 1

Material. 1 C, 1 RV, in samples He19-18–19.

Distribution. Toarcian to Lower Bajocian; SW Germany, Great Britain.

Family Pontocyprididae Müller, 1894
Genus *Liasina* Gramann, 1963

? *Liasina cylindrica* Ainsworth, 1986
Fig. 10: 2

Material. 2 RV, 1 LV in samples Ha19-2–4 and Lin18-1.

Distribution. Toarcian to Aalenian; SW Germany, Ireland.

Family Healdiidae Harlton, 1933
Genus *Cardobairdia* van den Bold, 1960

***Cardobairdia tesakovae* Franz et al., 2018**
Fig. 6: 1

Material. 4 RV and 2 LV in samples He19-3–8.

Distribution. Lower Aalenian, Opalinum Zone; SW Germany, N Switzerland.

***Cardobairdia toarcensis* Ainsworth, 1986**
Fig. 10: 3

Material. 1 LV in sample He19-26.

Distribution. Toarcian to Aalenian; SW Germany, Ireland.

Family Bairdiidae Sars, 1888
Genus *Bairdiacypris* Bradfield, 1935

***Bairdiacypris triangularis* Ainsworth, 1986**
Fig. 9: 2

Material. 1 C, 1 RV in samples He19-19 and He19-22.

Distribution. Toarcian to Aalenian; SW Germany, Ireland.

Family Paracyprididae Sars, 1923
Genus *Paracypris* Sars, 1866

***Paracypris* cf. *goodlandensis* Howe & Laurencich, 1958**

Material. 1 RV, 2 LV in sample He19-12.

Occurrence. Lower Aalenian, Opalinum Zone; SW Germany.

***Paracypris* sp.**

Material. 1 C in sample He19-1.

Occurrence. Lower Aalenian, Opalinum Zone; SW Germany.

Remark. The specimen is very small and preserved in pyrite and could therefore not be assigned with certainty to any species.

Family Macrocyprididae Müller, 1912
Genus *Macrocypris* Brady, 1868

***Macrocypris aequabilis* Oertli, 1959**
Fig. 9: 3

Material. 4 C samples in He19-19–21.

Distribution. Lower Aalenian to Lower Oxfordian; Germany, Scotland, N Switzerland, Russia.

***Macrocypris* ? *liassica* Bate & Coleman, 1975**
Fig. 10: 4

Material. 4 C, 3 RV, 1 LV in sample He19-27 and Ro19-3.

Distribution. Toarcian to Upper Aalenian; England, SW Germany; Upper Bathonian; N Germany.

***Macrocypris* sp.**

Material. 1 C, 1 R in samples He19-1 and He19-7.

Occurrence. Lower Aalenian, Opalinum Zone; SW Germany.

Family Bythocytheridae Sars, 1926
Genus *Bythoceratina* Hornibrook, 1952

***Bythoceratina* (*Praebythoceratina*) sp. 1**
Fig. 8: 3

Material. 1 C, 8 RV, 9 LV in samples He19-16–27 and Ro19-4–5.

Occurrence. Upper Aalenian, Murchisonae to Concavum zones; SW Germany.

Description. A species of *Praebythoceratina* which is distinguished by the combination of the following features: an U-shaped lobe with an irregularly reticulate spine in the ventro-central area. Its anterior branch is strongly convex and irregularly reticulate, with dominant subvertical ridges. The posterior branch is broad and gently arched and covered with irregular pores. Along the anterior margin there is a pronounced bulge, which is also irregularly reticulate.

Genus *Patellacythere* Gründel & Kozur, 1971

***Patellacythere paravulsa* cf. *tenuis* Brand, 1990**
Fig. 10: 5

Material. 2 C, 6 RV, 7 LV in samples He19-21–27 and Ro19-1–3.

Occurrence. Upper Aalenian, Concavum Zone; SW Germany.

***Patellacythere* cf. *vulsa* (Jones & Sherborn, 1888)**
Fig. 6: 2

Material. 1 LV in sample He19-9.

Occurrence. Lower Aalenian, Opalinum Zone; SW Germany.

***Patellacythere ungulina* (Triebel & Bartenstein, 1938)**
Fig. 10: 6

Material. 3 RV, 1 LV in sample Mue19-1.

Occurrence. Upper Aalenian, Concavum Zone; Germany.

Genus "*Monoceratina*" Roth, 1928

Remarks. This genus is in need of a revision and currently of unclear composition (Brand 1990.

***"Monoceratina"* aff. *posterocarinata* Brand, 1990**
Fig. 10: 7

Material. 2 C in sample He19-21 and Ro19-1.

Occurrence. Upper Aalenian, Concavum Zone; SW Germany.

Genus *Tanycythere* Cabral et al., 2014

***Tanycythere posteroelongata* Cabral et al., 2014**
Fig. 10: 8

Material. 1 C in sample He19-27.

Distribution. Upper Toarcian to Upper Aalenian; SW Germany, Portugal.

Family Cytheruridae Müller, 1894
Genus *Cytheropterina* Mandelstam, 1956

***Cytheropterina alacostata* Franz et al., 2018**
Fig. 10: 9

Material. 4 RV, 14 LV in samples He19-27, Mue19-1, Ha19-2 and Ro19-4–5.

Distribution. Upper Aalenian, Bradfordensis Zone (Gigantea Subzone) to Concavum Zone; SW Germany.

***Cytheropterina bicuneata* (Braun) in Franz et al., 2018**

Material. 53 RV, 50 LV in samples He19-16–27, Mue19-1, Ro19-1–5, Ha19-2.

Distribution. Lower Aalenian to Lower Bajocian; SW Germany.

***Cytheropterina crassicostata* sp. nov.**
http://zoobank.org/6732D1E8-29AD-472F-B6F9-BCC64C020053
Fig. 10: 10–13

Etymology. *crassus* (lat.) = coarse, fat; costatus (lat.) = ribbed; referring to the broad rounded ribs.

Holotype. Right valve, figured on Fig. 10: 10, SMNS 70521/71.

Paratypes. two left valves, one right valve, figured on Fig. 10: 11–13, SMNS 70521/72–74.

Type locality. Heiligenbach valley near Hechingen-Beuren (SW Germany).

Type horizon. Achdorf Formation, claystone above the Calceolabank, bed no. 46 in Fig. 4; Concavum Zone.

Material. 11 RV, 11 LV in samples He19-26–27, Mue19-1 and Ro19-4–5.

Diagnosis. Medium size. Subtriangular outline, with broad, rounded irregular ribs; the underside of the alate extension being smooth except for its posterior part.

Description. Carapace medium-sized, subtriangular. Right and left valve (identical in outline and ornamentation): Anterior margin symmetrically rounded. The dorsal margin is straight, medianly slightly concave. The ventral margin converges, partly straight or in a slight curve, to the acuminate posterior end. The ventral margin is obscured by a broad triangular wing. The anterior and posterior marginal zones are covered with roundish pits. The anterior marginal zone is offset with a small, asymmetrically rounded step against the lateral surface. A broadly rounded, mediodorsally-anteroventrally running rib forms a second step running diagonally over the anterior half of the valve. From this rib another broad rib branches off slightly below the middle, running subvertically towards the edge of the wing. The adjoining surface, which ends in the symmetrically rounded tip of the broad wing, is characterised by three wide, flat, bulbous elevations separated by wide furrows and pits. The furrows and pits as well as the ribs and depressions are covered with roundish secondary pits. Posteriorly, this area is bounded by a slightly curved, subvertical, rounded rib that tapers from dorsal to ventral. The posterior marginal zone is offset with a further, almost straight, subvertical step. Marginal zone wide anteriorly (Fig. 10: 13). The underside of the wing, which in ventral view forms a rectangular triangle, is smooth, except for its posterior third. A triangular area is covered by small grooves which are most prominent along the posterior margin of the wing. Hinge and other internal details are not observed.

Comparisons. *Cytheropterina crassicostata* resembles in outline *Cytheropterina bicuneata* (Braun) as reported by Franz et al. (2018) from the Aalenian and Lower Bajocian of SW Germany, and *Cytheropterina cribra* Fischer, 1962 (p. 339, Fig. 25: 8–11) from the Toarcian to Bajocian. The main differences are the coarse, softly rounded ornamentation, the smooth underside of the wing and the bigger size.

Occurrence. Upper Aalenian, Bradfordensis Zone (Gigantea Subzone) to Concavum Zone; SW Germany.

Table 1. Dimensions of *Cytheropterina crassicostata* sp. nov.

	Length	Height	Width
Holotype	0.516 mm	0.338 mm	
Paratype	0.556 mm	0.364 mm	
Paratype	0.557 mm		0.222 mm
Paratype	0.555 mm	0.363 mm	

***Cytheropterina cribra* (Fischer, 1962)**

Material. 1 C, 4 LV in samples He19-7–12.

Distribution. Lower Toarcian to Upper Bajocian; France, Germany, Ireland, Spain, N Switzerland.

***Procytherura celtica* Ainsworth, 1986**
Fig. 6: 3

Material. 2 RV in samples He19-12 and from the Geisingen clay pit.

Distribution. Upper Toarcian to Lower Bajocian; Germany, Ireland.

***Procytherura euglyphea* Ainsworth, 1986**
Fig. 6: 4, 5

Material. 2 RV, 1 ? LV in samples He19-1 and He19-12.

Distribution. Upper Toarcian to Lower Bajocian; Germany, Ireland.

***Procytherura multicostata* Ainsworth, 1986**
Fig. 6: 6, 7

Material. 3 C, 4 RV, 6 LV in samples He19-5–26.

Distribution. Upper Toarcian to Lower Bajocian; SW Germany, Ireland.

***Procytherura* aff. *serangodes* Ballent & Whatley, 2000**
Fig. 8: 4

Material. 1 C in sample He19-15.

Distribution. Lower Aalenian to Lower Bajocian; SW Germany; mid-Callovian; Argentina.

***Procytherura* sp. 2 Franz et al., 2018**
Fig. 6: 8

Material. 1 RV in sample He19-8, 1 C in the Geisingen clay pit.

Occurrence. Lower Aalenian, Opalinum Zone; SW Germany.

Description. Very small, subovoidal outline in lateral view. Lateral surface with five broadly rounded ribs, subhorizontal in the midventral to posteromedian area; in the anterior half of the valve bent anteroventrally. Roughly reticulated in the region of these ribs by subvertical transverse ribs.

***Procytherura* sp. 5**

Fig. 10: 14

Material. 1C, 1 RV in samples He19-24–25.

Occurrence. Upper Aalenian, Concavum Zone; SW Germany.

Description. Very small, subtriangular outline in lateral view. Lateral surface weakly ornamented by two fine longitudinal ribs delimiting a spindle-shaped field, posteriorly rounded and anteriorly pointed. Parallel to the anterior margin there is a third, also very fine rib. Another middorsal-midanterior rib halves the acute-angled triangular field between the frontal rib and the upper longitudinal rib.

Genus *Tethysia* Donze, 1975

***? Tethysia* sp.**

Material. 1 LV in sample He19-8.

Occurrence. Lower Aalenian, Opalinum Zone; SW Germany.

Genus *Eucytherura* Müller, 1894

***Eucytherura eberti* sp. nov.**

http://zoobank.org/12B4883C-8F55-481A-A41E-B2665DB8069F

Fig. 6: 9–11

2018 *Eucytherura* aff. *scottia* (Whatley, 1970). – Franz et al., p. 72, plate 3: 17.

2019 *Eucytherura* aff. *scottia* (Whatley). – Dietze et al., fig. 11.

Etymology. In honour of the German palaeontologist Martin Ebert, who initiated the investigation of the Geisingen clay pit with his extensive preliminary work.

Holotype. carapace, figured on Fig. 6: 9, SMNS 70521/9.

Paratypes. two carapaces, figured on Fig. 6: 10, 11, SMNS 70521/10–11.

Type locality. Heiligenbach valley near Hechingen-Beuren (SW Germany).

Type horizon. Achdorf Formation, claystone below the Inopernabank, bed no. 39 in Fig. 4; Bradfordensis Zone.

Material. 10 C, 28 RV, 34 LV from the Heiligenbach, Thanheim and Roschbach sections and the Geisingen clay pit.

Diagnosis. A new species of *Eucytherura* with broad, smooth posterodorsal, frontal and ventral ribs. Intercostate areas weakly reticulate.

Description. Very small, subrectangular. Left valve slightly larger than right with anterodorsal and posterodorsal overlap. Anterior margin weakly rounded with extremity below mid-height; posterior margin pointed in right and bluntly rounded in left valve, apex above mid-height. Posterior cardinal angle pronounced in both valves; anterior cardinal angle more rounded in right than in left valve. Dorsal margin slightly convex to straight; ventral margin medianly slightly convex. Greatest height at anterior cardinal angle; greatest width antero-ventrally; greatest length above mid-height. Ornament consists of a series of broad longitudinal ribs and swellings, and with weakly reticulate intervening areas. A broad, posteriorly weakly alate rib extends from a postero-ventral position across the ventro-lateral surface of the valve, terminating antero-ventrally. A similar broad rib extends mid-posteriorly to mid-dorsally. The eye tubercule is well developed and is connected to a narrower frontal rib, which parallels the anterodorsal margin. A less prominent second rib or elongate swelling parallels the latter mid-anteriorly. Intercostate areas are weakly reticulate, with a characteristic row of small elongate pits above the muscle-scar field. 3–4 small marginal denticles occur anteriorly. Normal pores few and wide-spaced. Internal details not observed.

Table 2. Dimensions of *Eucytherura eberti* sp. nov.

	Length	Height	Width
Holotype	0.306 mm	0.164 mm	
Paratype	0.292 mm	0.155 mm	
Paratype	0.318 mm		0.135 mm

Comparisons. *Euytherura eberti* closely resembles *Eucytherura scottia* Whatley, 1970 from the Callovian and Oxfordian of Scotland. It differs mainly in the length of the dorsal rib, the absence of the anterior tubercles, being replaced by two parallel ribs and the pits above the musclescar-field.

Distribution. Lower Aalenian to Upper Aalenian, Opalinum to Bradfordensis zones (Gigantea Subzone); SW Germany.

***Eucytherura foveolata* sp. nov.**

Fig. 6: 12–14

http://zoobank.org/7D6E8E7E-FA22-4597-837D-3E25EBF70FD7

2018 *Eucytherura* sp. 4. – Franz et al., p. 72, plate 3: 22

Etymology. From *fovea* (lat.) = pit; referring to the characteristic pits on the lateral surface.

Holotype. One carapace, figured in Fig. 6: 12, SMNS 70521/12.

Paratypes. Two carapaces, figured in Fig. 6: 13, 14, SMNS 70521/13–14.

Type locality. Drillcore KB 1/93 Geisingen (SW Germany).

Type horizon. Opalinuston Formation, Zillhausen Subformation, sample G08Fr, Lower Aalenian.

Material. 19 C, 2 RV, 2 LV from samples He 19-3–12 and from the Geisingen clay pit.

Diagnosis. A small-sized species of the genus *Eucytherura* with the following characteristics: pitted lateral surface with a fine median rib.

Description. Very small, subrectangular. Left valve slightly larger than right with dorsal overlap. Anterior margin rounded with extremity slightly below mid-height; posterior margin pointed in right and bluntly rounded in left valve, apex above mid-height. Posteri-

Table 3. Dimensions of *Eucytherura foveolata* sp. nov.

	Length	Height
Holotype	0.327 mm	0.158 mm
Paratype	0.318 mm	0.162 mm

or cardinal angle rounded; anterior cardinal angle pronounced in both valves. Dorsal margin straight in left, slightly convex in right valve; ventral margin straight or slightly concave. Greatest height at anterior cardinal angle; greatest length above mid-height. Ornament consists of a fine median, horizontal or subdiagonal rib, accompanied on both sides by shallow, about 15 µm wide, round or subangular pits with a rough surface. A third row of such pits running antero-medianly – postero-ventrally; further pits in variable numbers and positions scattered on the lateral surface. Particularly striking are 4 rhomboidally grouped pits (Fig. 6: 12) in the mid-dorsal area. Eye-tubercle only weakly developed. Internal details not observed.

Comparisons. All other previously known species of *Eucytherura* have a well-developed ornamentation with sharp or broad ribs and/or reticulate surfaces.

Occurrence. Lower Aalenian, Opalinum Zone; SW Germany.

***Eucytherura liassica* Bate & Coleman, 1975**
Fig. 6: 15

Material. 2C, 1 RV, 8 LV in samples He19-3–26 and Ro19-2.

Distribution. Toarcian to Upper Aalenian; England, SW Germany.

***Eucytherura michelseni* (Finger, 1983)**
Fig. 6: 16

Material. 2 C, 2 RV, 8 LV in samples He19-3–18 and Ro19-4–5.

Distribution. Upper Pliensbachian to Lower Bajocian; Denmark, England, Sweden, Germany, Argentina, ? Australia.

***Eucytherura* cf. *parairregularis* Brand, 1990**
Fig. 9: 4

Material. 5 C, 2 LV in samples He19-19–25, Ha19-4–5.

Distribution. Upper Aalenian, Bradfordensis Zone (Gigantea Subzone) to Concavum Zone; SW Germany.

***Eucytherura plumhoffi* Tesakova, 2017**
Fig. 7: 1

Material. 1 C, 3 RV, in samples He19-1–7.

Distribution. Lower Aalenian, Opalinum Zone; SW Germany, N Switzerland.

***Eucytherura transversiplicata* (Bate & Coleman, 1975)**
Fig. 7: 2

Material. 13 C, 9 RV, 7 LV in samples He19-3–28, Ha19-4–5 and Ro19-3–5.

Distribution. Pliensbachian to Bajocian; Argentina, Egypt, England, Germany, Ireland, North Africa, Wales.

***Eucytherura* cf. *yunga* Ballent & Whatley, 2009**
Fig. 9: 5

2018 *Tethysia* sp. 1 Tesakova. – Franz et al., p. 71, plate 3: 12.
2019 ? *Eucytherura* sp. 10. – Dietze et al., plate 7: 21.

Material. 1C, 10 RV, 6 LV in samples He19-19–27, Ro19-1, and from the Thanheim section and the Geisingen clay pit.

Distribution. Upper Aalenian to Lower Bajocian; Argentina, SW Germany.

***Eucytherura* aff. *yunga* Ballent & Whatley, 2009**
Fig. 10: 15

Material. 1 LV in sample He19-27.

Distribution. Upper Aalenian to Lower Bajocian; Argentina, SW Germany.

Remark. This specimen closely resembles plate 1: 7 in Ballent and Whatley (2009).

***Eucytherura* aff. sp. B Boomer & Ballent, 1996**
Fig. 10: 16

Material. 1 LV in sample He19-25.

Occurrence. Lower Aalenian, Opalinum Zone; SW Germany, N Switzerland.

Eucytherura sp. 1, *Euc*. sp. 3 and *Euc*. sp. 5 were first named and figured by Franz et al. (2018) but without descriptions; in the following we add their descriptions:

***Eucytherura* sp. 1 Franz et al., 2018**
Fig. 7: 3

Material. 5 RV, 1 LV in samples He19-2–12; 17 C, 1 RV from the Geisingen clay pit; 1 C from the Benken borehole (Switzerland).

Occurrence. Lower Aalenian, Opalinum Zone; SW Germany, N Switzerland.

Description. Very small, subrectangular. Left valve slightly larger than right with dorsal overlap. Anterior margin rounded with extremity slightly below mid-height; posterior margin pointed in right and bluntly rounded in left valve, apex above mid-height. Posterior cardinal angle rounded; anterior cardinal angle pronounced in both valves, slightly more rounded in right valve. Dorsal and ventral margins slightly convex in both valves. Greatest height at

anterior cardinal angle; greatest length above mid-height. Shell ornamentation reduced to a regular reticulation with rounded meshes of uniform size. Hemispherical eye-tubercle well developed. Internal details not observed.

***Eucytherura* sp. 3 Franz et al., 2018**
Fig. 7: 4

Material. 25 C, 4 RV, 4 LV in samples He19-6–18 and from the Geisingen clay pit.

Occurrence. Lower to Upper Aalenian, Opalinum to Bradfordensis zones; SW Germany.

Description. Very small, subrectangular. Left valve slightly larger than right with dorsal overlap. Anterior margin rounded with extremity slightly below mid-height; posterior margin pointed in right and bluntly rounded in left valve, apex above mid-height. Posterior cardinal angle rounded; anterior cardinal angle pronounced in both valves, slightly more rounded in right valve. Dorsal margin straight in right valve and slightly convex in left valve. Greatest height at anterior cardinal angle; greatest length above mid-height. Shell surface regularly reticulate with rounded meshes of uniform size. Hemispherical eye-tubercle well developed. Starting from the eye-tubercle, a fine frontal rib, straight in the left valve, convex in the right valve, runs parallel to the anterodorsal margin. A second rib runs subvertically from the eye-tubercle and then bends mid-anteriorly to the anterior margin. A ventral rib starts posteroventrally and ends midventrally with its anterior end slightly ascending towards the ventromedian side. A short subvertical ridge is located at the posterior cardinal angle. Internal details not observed.

***Eucytherura* sp. 5 Franz et al., 2018**
Fig. 9: 6

Material. 1 C in sample He19-19; 5 RV, 1 LV from the Geisingen clay pit.

Occurrence. Lower to Upper Aalenian, Opalinum to Bradfordensis zones; SW Germany.

Description. Very small, subovoidal. Anterior margin asymmetrically rounded with extremity below mid-height; posterior margin pointed, apex above mid-height. Posterior cardinal angle rounded; anterior cardinal angle pronounced in both valves. Dorsal margin slightly convex, ventral margin convex. Greatest height at anterior cardinal angle; greatest length above mid-height. Shell surface irregularly and coarsely reticulated. The most striking feature is the gently undulating surface with slight anterodorsal, middorsal and anteroventral depressions. The eye-tubercle is fused with a short, indistinct frontal rib. A short bulge-like rib is located at the posterior cardinal angle. Internal details not observed.

***Eucytherura* sp. 10**
Fig. 10: 17, 18

Material. 1 RV, 1 LV in samples He19-24–25.

Occurrence. Upper Aalenian, Bradfordensis Zone (Gigantea Subzone) to Concavum Zone; SW Germany.

Description. Very small, subovoidal. Anterior margin asymmetrically rounded with extremity below mid-height; posterior margin rounded, apex above mid-height. Anterior and posterior cardinal angles rounded; both slightly more pronounced in right valve. Dorsal margin slightly concave in ther right valve, slightly convex in the left one. Greatest height at anterior cardinal angle; greatest length above mid-height. Shell surface reticulate, with wide rectangular to polygonal meshes. Eye-tubercle absent.

***Right valve*:** A long, well-defined frontal rib runs from the anterior cardinal angle to the anteroventral margin. The lateral surface is characterized by three fine ribs, the first of which starts in the median region, runs a short distance towards the anterior cardinal angle, then bends perpendicularly towards the anterior margin and after a second 45° bend towards the anteroventral margin. The median rib starts mid-posteriorly above mid-height and ends anteromedianly below mid-height. A long, upwardly curved ventral rib runs from the posteroventral margin to the anteroventral region. One (or two) ribs parallel the ventral rib on the ventral side of the valve.

***Left valve*:** The frontal rib is slightly curved (preservation?) and only weakly developed. The (dorso) median – mid-anterior rib meets the ventral rib at an 60° angle. The median rib starts mid-posteriorly above mid-height and ends anteromedianly at mid-height. Two ribs parallel the ventral rib on the ventral side of the valve. Further, especially internal details were not observed, partly for preservation reasons.

***Eucytherura* sp. 11**
Fig. 9: 7

Material. 1 RV, 2 LV in samples He19-18 and He19-24–25.

Occurrence. Upper Aalenian, Bradfordensis Zone; SW Germany.

Description. Very small, subrectangular to subtriangular. Anterior margin rounded with extremity slightly below mid-height; posterior margin pointed, apex above mid-height. Posterior cardinal angle rounded; anterior cardinal angle pronounced in both valves, slightly more rounded in left valve. Dorsal straight to slightly concave, ventral margin straight to slightly convex. Greatest height at anterior cardinal angle; greatest length above mid-height. Shell surface strongly reticulate, including the anterior and posterior margins. The coarse-meshed, very prominent reticulation is divided by three ribs, which in the median area delimit an approximately circular area. A middorsal – anteromedian rib, a second middorsal – posteromedian rib, and a ventral rib that is strongly curved up in the anterior midventral section towards the anteromedian region. Another rib starting at the anterior cardinal angle parallels the anterior edge of that circular area approximately halfway to the anterior margin. Eye-tubercle absent; internal details not observed.

Genus *Balowella* Wienholz, 1967

***Balowella catena* (Franz et al., 2018)**
Fig. 9: 8, Fig. 11: 1

2018 *Procytheropteron catena* sp. nov. – Franz et al., p. 73, plate 4: 4–6.

Material. 3 C, 22 RV, 26 LV in sample He19-18–28.
Distribution. Upper Aalenian, Bradfordensis Zone (Gigantea Subzone) to Concavum Zone; SW Germany.

? *Balowella* sp.

Material. 1 RV in sample He19-18.
Distribution. Upper Aalenian, Bradfordensis Zone (Gigantea Subzone); SW Germany.
Remark. The single (juvenile ?) specimen is only tentatively placed in this genus due to its small size and poor preservation.

Genus *Cytheropteron* Sars, 1866

? *Cytheropteron* sp. 1
Fig. 11: 2, 3

Material. 3 RV, 4 LV in samples He19-25 – Ha19-3.
Occurrence. Upper Aalenian, Bradfordensis Zone (Gigantea Subzone) to Concavum Zone; SW Germany.
Description. Very small, triangular. Anterior margin rounded with extremity slightly below mid-height; posterior margin pointed, apex below mid-height. Cardinal angles rounded in left valve, cardinal angles pronounced in right valve.
***Right valve*:** Dorsal margin straight, medianly slightly convex, ventral margin slightly convex, medianly partly obscured by a median overhang of the lateral curvature. The punctate shell surface is longitudinally and vertically strongly curved with a ventral overhang. The curvature is concavely recessed in the uppermost area along a sharp oval bend, ending in a weak anteromedian lobe. A narrow anterodorsal depression parallel to the anterior margin is limited by a short, slightly curved frontal rib, ending above mid-height.
***Left valve*:** Dorsal margin strongly convex, otherwise identical to the right valve.
Hinge due to poor preservation not clearly visible, possibly merodont; other internal details not observed.

Genus *Procytheropteron* Ljubimova, 1955

***Procytheropteron* aff. *gramanni* Brand, 1990**
Fig. 11: 4, 5

Material. 3 RV, 2 LV in samples He19-22–24 and Ro19-1.
Occurrence. Upper Aalenian, Concavum Zone; SW Germany.
Remarks. Our specimens resemble *Procytheropteron gramanni* Brand, 1990 (plate 9: 10) from the Upper Bathonian of NW Germany; they differ in age and in the coarser ornamentation and reticulation.

***Procytheropteron* sp. 1 Franz et al., 2018**
Fig. 11: 6

Material. 2 LV in sample He19–24 and from the Geisingen clay pit.
Distribution. Upper Aalenian, Bradfordensis Zone; SW Germany.
Description. Very small, ovoidal. Anterior margin almost symmetrically rounded; posterior margin pointed, apex at mid-height. Cardinal angles rounded in the left valve.
Dorsal margin straight to slightly convex, ventral margin convex, medianly partly obscured by a median overhang of the lateral curvature. The complete lateral surface is decorated with vertical, broadly rounded ribs. The ribs in the median part of the valve are irregular, interrupted at about mid-height, and offset laterally against each other. The vertical ribs are framed by a curved ventral rib, which is also rounded, and a similar dorsal rib, which almost touch each-other mid-posteriorly.
Internal details not observed.

Genus *Metacytheropteron* Oertli, 1957

***Metacytheropteron opalinum* Plumhoff, 1963**

Material. 3 C, 5 RV, 3 LV in samples He19-5–12.
Distribution. Upper Toarcian to Upper Aalenian; Germany.

Genus *Aphelocythere* Triebel & Klingler, 1959

***Aphelocythere dilgeri* Franz et al., 2018**
Fig. 7: 5

Material. 2 RV, 3 LV in samples He19-1–22.
Distribution. Lower Aalenian to Lower Bajocian; SW Germany.

***Aphelocythere pygmaea* Plumhoff, 1963**
Fig. 7: 6

Material. 7 C, 10 RV, 9 LV in samples He19-1–13.
Distribution. Lower to Upper Aalenian, Opalinum to Murchisonae zones; Germany, Switzerland.

***Aphelocythere* ? *pygmaea* Plumhoff, 1963**

Material. 1 C in sample He19-15.
Occurrence. Upper Aalenian, Murchisonae Zone; SW Germany.

***Aphelocythere recta* Ohmert, 2004**
Fig. 11: 7

Material. 1 C in sample Ro19-4.
Occurrence. Upper Aalenian, Concavum Zone; SW Germany.

***Aphelocythere* aff. *recta* Ohmert, 2004**
Fig. 11: 8

Material. 1 RV in sample Ro19-4.
Occurrence. Upper Aalenian, Bradfordensis Zone (Gigantea Subzone) to Concavum Zone; SW Germany.
Remark. Ohmert (2004) mentioned this species as a probable ancestor of *Aphelocythere recta* from the top of the Concavabank.

? *Aphelocythere* sp. 1
Fig. 7: 7, Fig. 11: 9

Material. 2 C, 5 RV, 1 LV in samples G08Fr, G12 Fr, G13Fr, He19-6, He19-26–28.
Occurrence. Lower to Upper Aalenian, Opalinum to Concavum zones; SW Germany.
Description. Very small, subrectangular. Anterior margin rounded with extremity slightly below mid-height; posterior margin rounded, apex above mid-height. Cardinal angles rounded in both valves, slightly more pronounced in left valve. Dorsal margin straight, ventral margin slightly convex. The shell surface is smooth, with a number of pits, which are difficult to recognize due to bad preservation. Internal details not observed.

Family Cytherideidae Sars, 1925
Genus *Vernoniella* Oertli, 1957

***Vernoniella* ? *caytonensis* Bate, 1965**
Fig. 12: 10

Material. 1 C in sample Ro19-5.
Occurrence. Upper Aalenian, Concavum Zone; SW Germany.
Remark. *Vernoniella* ? *caytonensis* was described from the Blagdeni Subzone in England; our specimen comes from the Concavum Zone and therefore has been tentatively placed in this species.

Family Schulerideidae Mandelstam, 1959
Genus *Asciocythere* Swain, 1952

"*Asciocythere*" sp.
Fig. 11: 10

Material. 4 C, 3 LV in samples He19-25–26 and Ha19-4.
Occurrence. Upper Aalenian to Lower Bajocian; SW Germany.
Remark. We have set *Asciocythere* in quotation marks, because the generic assignment of this species is doubtful.

Genus *Eocytheridea* Bate, 1963

***Eocytheridea elongata* Bate, 1963**
Fig. 11: 11

Material. 2 C, 7 RV, 5 LV in samples He19-21, Mue19-1 and Ro19-1–5.
Distribution. Upper Aalenian; England, SW Germany.

***Eocytheridea lacunosa* Bate, 1963**
Fig. 11: 12

Material. 52 C, 183 RV, 209 LV in samples He19-23–29 and Ro19-1–5.
Distribution. Upper Aalenian to Lower Bajocian; England, SW Germany.

Genus *Praeschuleridea* Bate, 1963

***Praeschuleridea ornata* (Bate, 1963)**
Fig. 9: 9

Material. 57 C, 106 RV, 136 LV in samples He19-18–29, Ha19-1–5 and Ro19-1–5.
Distribution. Lower Aalenian to Lower Bajocian; England, Germany.

***Praeschuleridea punctulata* (Plumhoff, 1963)**
Fig. 8: 5

Material. 36 C, 49 RV, 47 LV in samples He19-13–29, Ha19-1–5 and Ro19-1–5.
Distribution. Upper Toarcian to Lower Bajocian; Germany, Spain, Switzerland.

***Praeschuleridea* cf. *subtrigona* (Jones & Sherborn, 1888)**
Fig. 11: 13, 14

Material. 4 C, 5 RV, 13 LV in samples Ro19-1–5.
Occurrence. Upper Aalenian, Concavum Zone; SW Germany.
Remark. The specimens from the Roschbach section closely resemble *Praeschuleridea subtrigona* from the Upper Bajocian to Upper Callovian. It is only tentatively placed in this species because of the remarkable difference in age.

***Praeschuleridea ventriosa* (Fischer in Plumhoff, 1963)**
Fig. 7: 10

Material. 118 C, 52 RV, 76 LV in samples He19-2–21, Mue19-1, Ha19-1–3 and Ro19-1–5.

Distribution. Upper Toarcian to Lower Bajocian; Germany, Spain, Switzerland.

***Praeschuleridea* sp. A (Ainsworth, 1986)**
Fig. 8: 6

Material. 1 C, 2 LV in samples He19-17–25.
Distribution. Toarcian to Aalenian; Germany, Ireland.

***Praeschuleridea* sp. 1**
Fig. 11: 15–17

Material. 4 C, 2 RV, 4 LV in samples He19-27 and Ha19-5.
Occurrence. Upper Aalenian, Concavum Zone to Early Bajocian; SW Germany.
Description. Medium-sized, subovate. Left valve larger than right valve, overlapping along complete outline. Anterior margin slightly asymmetrically rounded, extremity just below mid-height. Posterior margin triangular, upper margin straight, lower margin convex, the two joining at an angle below mid-height. Dorsal margin convex, ventral margin convex with slight concavity in front of mid-length in the right valve. Anterior cardinal angle rounded, posterior cardinal angle sloping straight to the posterior margin. Valve ventrolaterally swollen. Small-sized pits irregularly distributed over the anterior valve surface, significantly denser in the posterior third. A narrow channel with densely arranged pits parallels the anterior margin. Anteroventrally and posteroventrally there is a row of finest denticles.
The partly broken (? paleohemimerodont) hinge shows terminal serrated teeth and remains of teeth in the median hinge area of the right valve.

Family Protocytheridae Ljubimova, 1955
Genus *Southcavea* Bate, 1964

? *Southcavea* sp.
Fig. 9: 10, 11

Material. 3 C, 7 RV, 4 LV in samples He19-18–25 and Ro19-1–2.
Occurrence. Upper Aalenian, Bradfordensis Zone (Gigantea Subzone); SW Germany.

Genus *Pleurocythere* Triebel, 1951

***Pleurocythere kirtonensis* Bate, 1963**
Fig. 9: 12

Material. 1 RV, 1 LV in sample He19-18.
Distribution. Upper Aalenian, Bradfordensis Zone (Gigantea Subzone) to Lower Bajocian; England, southwest Germany.

***Pleurocythere ohmerti* Franz et al., 2018**
Fig. 11: 18

Material. 20 C, 29 RV, 27 LV in samples He19-24–29, Ha19-4–5 and Ro19-1–3.
Distribution. Upper Aalenian, Concavum Zone to Early Bajocian; SW Germany.

***Pleurocythere* sp. 1**
Fig. 8: 7

Material. 1 LV in sample He19-16.
Occurrence. Upper Aalenian, Murchisonae Zone; SW Germany.
Remark. This specimen resembles *Pleurocythere kirtonensis* in the arrangement of the ribs. In contrast to *P. kirtonensis* the ribs are broad and rounded. Possibly the median rib touches the ventral rib anteroventrally. More material is required for clarification.

? *Pleurocythere* sp.
Fig. 7: 8

Material. 1 RV, 1 LV in sample He19-1.
Occurrence. Lower Aalenian, Opalinum Zone; SW Germany.
Remark. The two specimens may represent an ancestor of the genus *Pleurocythere*.

Family Progonocytheridae Sylvester-Bradley, 1948
Genus *Acrocythere* Neale, 1960

***Acrocythere pumila* Plumhoff, 1963**
Fig. 7: 9

Material. 4 C, 2 RV, 4 LV in samples He19-1–12.
Distribution. Lower Aalenian, Opalinum Zone; Germany, Switzerland.

***Acrocythere* aff. *pumila* Plumhoff, 1963**
Fig. 9: 13

Material. 3 LV in samples He19-18 and He19-27.
Occurrence. Upper Aalenian, Bradfordensis Zone (Gigantea Subzone) to Concavum Zone; Germany.
Remark. In addition to the differentiation from *Acrocythere pumila* in Plumhoff, 1963, it should be noted that the reticulation between the median rib and the ventral rib in the posterior section is alternating here, whereas it is clearly linear in *A. pumila*.

Genus *Homocytheridea* Bate, 19 63

***Homocytheridea* sp. 1**
Fig. 8: 8

Material. 1 LV in sample He19-15.
Occurrence. Upper Aalenian, Murchisonae Zone; SW Germany.

***Homocytheridea* sp. 2**
Fig. 8: 9

Material. 22 C, 15 RV, 18 LV in samples He19-15–28, Mue19-1 and Ro19-4.
Occurrence. Upper Aalenian, Murchisonae to Concavum zones; SW Germany.

Genus *Camptocythere* Triebel, 1950

***Camptocythere pusilla* Plumhoff, 1963**
Fig. 12: 1

Material. 30 C, 43 RV, 36 LV in samples He19-24–28 and Ro 1–3.
Distribution. Upper Aalenian; Germany.

Genus *Aaleniella* Plumhoff, 1963

***Aaleniella* sp.**

Material. 1 C in sample He19-18.
Occurrence. Aalenian, Bradfordensis Zone; SW Germany.

Genus *Progonocythere* Sylvester-Bradley, 1948

***Progonocythere scutula* Franz et al., 2018**
Fig. 8: 10

Material. 1 C, 6 RV, 6 LV in sample He19-17.
Distribution. Upper Aalenian, Bradfordensis Zone; SW Germany.

***Progonocythere triangulata* Braun in Ohmert, 2004**
Fig. 12: 11

Material. 11 C, 34 RV, 34 LV in samples Ha19-4–5.
Distribution. Lower Bajocian; SW Germany. *Progonocythere triangulata* is the index species of the Triangulata ostracod Subzone (Ohmert 2004).

Genus *Kinkelinella* Martin, 1960

***Kinkelinella* (*Kinkelinella*) *adunca* Malz, 1966**
Fig. 12: 2

Material. 1 C, 4 RV, 16 LV in samples He19-23–29.
Distribution. Upper Aalenian to Lower Bajocian, Concavum to Discites zones; SW Germany.

***Kinkelinella* (*Kinkelinella*) *fischeri* Malz, 1966**
Fig. 8: 11

Material. 6 C, 18 RV, 22 LV in samples He19-14–18, Ha19-6, Lin 18-4, Mue19-1 and Ro19-1–5.
Distribution. Upper Toarcian to Upper Aalenian; France, Germany, Russia, Spain, Switzerland.

***Kinkelinella* (*Kinkelinella*) *levata* Ohmert, 2004**
Fig. 12: 3

Material. 4 C, 76 RV, 109 LV in samples He19-21–28 and Ro19-1–5.
Occurrence. Upper Aalenian to Lower Bajocian, Concavum to Discites zones; SW Germany.

***Kinkelinella* (*Kinkelinella*) *sermoisensis* (Apostolescu, 1959)**
Fig. 7: 11

Material. 2 C, 1 RV in sample He19-9.
Distribution. Lower Toarcian to Lower Bajocian; England, France, Germany, Ireland, Portugal, Russia, Spain, N Switzerland.

***Kinkelinella* (*Kinkelinella*) cf. *sermoisensis* (Apostolescu, 1959)**
Fig. 12: 4

Material. 9 C, 14 RV, 10 LV in samples Mue19-1 and Ro19-1–5.
Distribution. Upper Aalenian to Lower Bajocian; SW Germany.

***Kinkelinella* (*Ektyphocythere*) *triangula* (Brand, 1961)**
Fig. 12: 12

Material. 5 RV in samples Ha19-4–5.
Distribution. Early Bajocian; England, France, Germany, N Switzerland.

***Kinkelinella* sp. B Ohmert, 2004**
Fig. 12: 5

Material. 9 RV, 8 LV in samples He19-25–26, Mue19-1, Ha19-5 and Ro19-3–5.
Occurrence. Upper Aalenian to Early Bajocian, Concavum to Discites zones; SW Germany.

***Kinkelinella* sp. 2**
Fig. 8: 12

Material. 5 RV, 5 LV in samples He19-14–17 and Ro19-2.

Occurrence. Lower to Upper Aalenian, Opalinum Zone ("Comptum" Subzone) to Bradfordensis Zone; SW Germany.

Description. Anterior margin broadly rounded, accompanied by a flat marginal bulge. The dorsal margin slightly convex, with the greatest height in front of midlength of the valve. Posterior end flat, with narrowly rounded posterior margin. Ventral margin obscured by the the overhanging ventro-lateral curvature. The central part of the valve is ventrally strongly inflated, and clearly set off against the anterior and posterior ends. Remnants of two ventral ribs are visible parallel to the ventral margin. The remaining part of the valve shows only weak hints of a very fine, irregular reticulation.

***Ektyphocythere* aff. *anterocosta* Boomer, 1988**
Fig. 8: 13

Material. 1 RV in sample He19-14.

Occurrence. Toarcian to Lower Aalenian; England, SW Germany.

Family Neurocytheridae Gründel, 1975
Genus *Fuhrbergiella* Brand & Malz, 1962

***Fuhrbergiella* (*Praefuhrbergiella*) *horrida bicostata* Brand & Malz, 1962**
Fig. 12: 13

Material. 2 LV in samples Ha19-4–5.

Distribution. Lower Bajocian, Discites Zone; Germany.

Family Cytheridae Baird, 1850
Genus *Minyocythere* Lord et al., 2020

***Minyocythere tuberculata* (Luppold, 2012)**
Fig. 12: 6

Material. 5 C, 3 RV, 5 LV in samples Mue19-1 and Ro 3–5.

Distribution. Upper Aalenian to Lower Bajocian, Concavum to Humphriesianum zones; Germany.

Genus *Plumhofficythere* Luppold, 2003

***Plumhofficythere clavatoides* Luppold, 2003**
Fig. 12: 7

Material. 6 C, 30 RV, 24 LV in samples He19-23–28, Mue19-1 and Ro19-1–3.

Distribution. Upper Aalenian, Bradfordensis Zone (Gigantea Subzone) to ? Lower Bajocian; England, France, Germany, Luxembourg.

Ostracoda incertae sedis

aff. *Ostracode* A Ballent, 1991
Fig. 7: 12

Material. 2 RV in samples He19-2 and He19-12.

Distribution. Aalenian to Bajocian; Argentina, SW Germany.

Gen. et sp. 9 Tesakova, 2017
Fig. 8: 14

Material. 1 RV in sample He19-17.

Distribution. Lower to Upper Aalenian, Opalinum to Bradfordensis zones; SW Germany, N Switzerland.

Gen. et sp. indet. 3 Franz et al., 2018
Fig. 7: 13

Material. 2 RV in samples He19-2 and He19-5.

Occurrence. Lower Aalenian, Opalinum Zone; SW Germany.

Gen. et sp. indet. 5 Franz et al., 2018
Fig. 7: 14

Material. 4 RV, 1 LV in samples He19-3–27.

Distribution. Lower to Upper Aalenian, Opalinum to Concavum zones; SW Germany, N Switzerland.

Gen. et sp. indet. 7
Fig. 12: 8, 9

2019 Gen. et sp. indet. I. – Dietze et al., pl. 11, fig. 13.

Material. 4 RV, 1 LV in sample He19-22; one further RV from Thanheim.

Distribution. Upper Aalenian, Bradfordensis Zone (Gigantea Subzone) to Concavum Zone; SW Germany.

Gen. et sp. indet. 8
Fig. 7: 15

Material. 2 RV in samples He19-5–12.

Distribution. Lower Aalenian, Opalinum Zone; SW Germany.

Gen. et sp. indet. 9
Fig. 8: 15

Material. 1 RV, 1 LV in samples He19-17–18.

Occurrence. Upper Aalenian, Bradfordensis Zone; SW Germany.

Gen. et sp. indet. 10
Fig. 7: 16

Material. 1 RV, 2 LV in samples He19-12–15.

Occurrence. Lower to Upper Aalenian, Opalinum to Murchisonae zones; SW Germany.

Gen. et sp. indet. 11
Fig. 7: 17

Material. 1 LV in sample He19-8.

Occurrence. Lower Aalenian, Opalinum Zone; SW Germany.

Gen. et sp. indet. 12
Fig. 8: 16

Material. 1 LV in sample He19-16.

Occurrence. Upper Aalenian, Murchisonae Zone; SW Germany.

4. Description of the ammonite fauna

4.1 General remarks

The ammonite fauna of the Upper Aalenian of SW Germany is dominated by members of the subfamily Graphoceratinae Buckman, 1905, besides rare Hammatoceratinae Buckman, 1887. The Graphoceratinae originate in the subfamily Leioceratinae Spath, 1936. The family Graphoceratidae itself descends from the Upper Toarcian genus *Pleydellia* Buckman, 1899 (Grammoceratinae Buckman, 1905 within the family Hildoceratidae Hyatt, 1867) (Chandler 1997; Chandler et al. 2012, Howarth 2013).

The evolution within the Graphoceratidae occurred in a chronocline ranging from the lowermost Aalenian (Opalinum Zone, Opalinum Subzone) to the lowermost Bajocian (Discites Zone), with an immense morphological variability within each of the temporally succeeding faunas. In this plexus, individual morphologies sometimes have a long temporal range, whereas the variability of the succeeding faunas as a whole shifts – that is the reason why we can distinguish and define faunal biohorizons. Faunal biohorizons reflect the change of variation in the course of evolution of ammonites, here of Graphoceratidae (e.g., Chandler 1997, 2019; Chandler and Callomon 2009; Dietze et al. 2014, 2017). There is a gradual change from one genus to the next, so that we can – e.g., in the case of the ammonites under study here – find *Graphoceras* morphologies together with *Brasilia* morphologies coeval in a single bed, accompanied by specimens showing a mixture of characters of both morphogenera. For a slightly older (Bradfordensis Zone, Gigantea Subzone) overlap of the morphogenera *Brasilia* and *Graphoceras* (with a variability of the whole fauna closer to *Brasilia*) see Dietze et al. 2014 (ammonites therein were there described as chronospecies). An intersection of *Ludwiga* and *Brasilia* can be seen in the top of the Staufensisbank of the nearby Plettenberg/Hausen am Tann (Western Swabian Alb) sections (Dietze et al. 2017b; fauna described morphospecifically). Chandler (1997) demonstrated convincingly the evolution of the Graphoceratidae and the intersection of the nominal morphogenera in the Aalenian of Horn Park Quarry near Beaminster (Dorset, SW England).

In the literature, there are many attempts to classify the plexus of the Graphoceratidae into categories (families, subfamilies, morphogenera, morphospecies). The results of these attempts and the erection of new genera and species depended often by chance, depending on where the author had material from, often without any accurate stratigraphy. The great number of genera and species described in the literature (e.g. Buckman 1887–1907; Horn 1909; Hoffmann 1913; Althoff 1940; Rieber 1963; Géczy 1967; Contini 1969; Ureta Gil 1983; Henriques 1992; Chandler 1997; Howarth 2013) does by no means reflect the number of monophyletic genera and biological species, which was in fact much smaller (Chandler and Callomon 2009). These authors demonstrated the variation of a palaeobiospecies of the Leioceratinae, *Leioceras comptocostosum*, within one timeslice of the Scissum Zone (Lower Aalenian).

We here determined the ammonites conventionally as morphogenera and morphospecies, since we do not have enough material to describe these ammonites chrono- or (palaeo)biospecifically. However, it is most likely that all graphoceratid ammonites from the *cavatum* horizon described here represent a single palaeobiospecies.

4.2 Short comments on the ammonite fauna

4.2.1 Family Graphoceratidae Buckman, 1905, Subfamilies Leioceratinae Spath, 1936 and Graphoceratinae Buckman, 1905

Leioceras opalinum [m] and *L. opaliniforme* [M] occur about 10 m below the "Wasserfallschichten" in the Heiligenbach creek.

The ammonites from the "Comptum" Subzone are represented by *L.* "*comptum*", *L. crassicostatum*, *L. evolutum*, *L. paucicostatum* and *L. striatum*. They are significantly smaller than the *L.* "*comptum*" faunas from the Wochenberg and Gosheim (western Swabian Alb) which comprise more evolute morphs. These ammonites will be described later in detail.

A single *Brasilia bradfordensis* (Fig. 19: 1a, b) of the Bradfordensis Zone (Bradfordensis Subzone) was recovered from bed 2 of the Heiligenbach section.

The graphoceratid fauna of the Inopernabank (Bradfordensis Zone, Gigantea Subzone) and from the Kon-

glomeratbank to the Rostrote Kalkbank (Concavum Zone, Concavum Subzone) is characterized by the predominance of the morphogenus *Graphoceras*; less common are representatives of the morphogenus *Brasilia* and a substantial number of ammonites with various combinations of both morphogenera (cf. Rieber 1922: 47, 51). In the slightly older *decipiformis* horizon of the Gigantea Subzone (Bradfordensis Zone, see Fig. 26) ammonites of the genus *Brasilia* exhibit larger-sized and smooth shells, with generally broader whorl sections and a wider umbilicus compared to *Graphoceras* (Chandler 1997; Dietze et al. 2014). The ammonites determined as *B. decipiens* (Fig. 13: 1a, b, Fig. 18: 1), *B.* aff. *decipiens* (Fig. 20: 3a, b) and *B*. cf. *decipiformis* (Fig. 16: 2a, b, 5a, b) are very similar to examples of the genus *Brasilia* from the Bradfordensis Zone (Gigantea Subzone, *decipiformis* horizon) of Geisingen (SW Germany) and Dorset (SW England) (Dietze et al. 2014; Buckman 1887–1907; Chandler 1997). Some of the studied ammonites show mixed characters and are obviously intermediates between *Brasilia* and *Graphoceras*: *B.* aff. and *G.* cf. *decipiens* (Fig. 18: 4a, b; Fig. 19: 5a, b) show already the more compressed and involute morphology of *Graphoceras* (Howarth 2013), whereas in all other features it is still very close to *Brasilia*. *Graphoceras* aff. *magnum* (Fig. 20: 1a, b) and *G*. cf. *cavatum* (Fig. 20: 2a, b) show the broad whorls of *Brasilia*, but the ribbing style of primitive *Graphoceras*. The bulk of the ammonites belong to the genus *Graphoceras*. Besides *G*. cf. *concavum* (Fig. 16: 1, 4; Fig. 15: 1a, b) the poorly sculptured *G. cavatum* (Fig. 13: 2a, b, 9a, b; Fig. 18: 2; Fig. 21: 2a, b) and *G*. cf. *cavatum* (Fig. 21: 1a, b) are typical. *Graphoceras* with more sculptured flanks are assigned to *G. decorum* (Fig. 15: 2; Fig. 22: 1a, b), *G*. aff. *apertum* (Fig. 15: 3a, b), *G. pulchum* (Fig. 15: 5a, b; Fig. 22: 3a, b), *G*. cf. *pulchrum* (Fig. 15: 4a, b), *G*. cf. *v-scriptum* (Fig. 18: 3) and *G. formosum* (Fig. 22: 2a, b, 5a, b), respectively. The strongest sculptured *Graphoceras* belong to *G. fallax* (Fig. 18: 5; Fig. 22: 4), *G*. aff. *fallax* (Fig. 13: 3) and *G*. cf. *caduciferum* (Fig. 17: 1a, b).

We here follow Chandler (1997) in the determination of the microconchs and assign these to *Ludwigella*. They show often specifically distinguished morphologies (Buckman 1887–1907; Contini 1969; Chandler 1997) ranging from nearly smooth to strongly ribbed morphotypes: *Ludwigella tenuis* (Fig. 13: 4), *L. attenuata* (Fig. 13: 6), *L. arcitenens* (Fig. 16: 3a, b; Fig. 15: 6a, b; Fig. 17: 3), *L. cornu* (Fig. 19: 2) *L*. aff. *tenuis* (Fig. 13: 5), *L*. sp. (Fig. 17: 5), *L. micra* (Fig. 19: 4), and *L. attracta* (Fig. 13: 7, 8; Fig. 19: 3).

4.2.2 Family Hammatoceratidae Buckman, 1887, Subfamily Hammatoceratinae Buckman, 1887

A single record from the Inopernabank (Fig. 14: 1a–c) resembles in its nucleus *Bredyia diadematoides* (Mayer) as figured by Rieber (1963) from Kappishäusern near Metzingen (Rieber 1963); however, its body chamber recalls the slightly more evolute *Planammatoceras planiforme* Buckman (typical of the Lower and lower Upper Aalenian; Kovács 2009; Sandoval et al. 2020) or *Pl. lepsiusi* (Gemmellaro). Due to the combination of these characters we here determined this ammonite as *Planammatoceras* sp. Most of the few hammatoceratids from the *cavatum* biohorizon of the Concavum Subzone in the studied sections are rather large, with smooth, high-oval outer whorls, very complex suture lines and a narrow umbilicus on the inner whorls (Fig. 14: 2a, b; Fig. 17: 4). The best match in literature we could find is with *Euaptetoceras infernense* sensu Buckman. The original type series of *E. infernense* (Roman) consists of small nuclei, which are very similar to the innermost whorls of the ammonite figured on Fig. 14: 2a, b. A more evolute variant is *E*. cf. *kochi* (Prinz) (Fig. 24: 1a, b). There is a striking homoeomorphy of this specimen with *Brasilia decipiformis* or *Sonninia carinodiscus* (Quenstedt [LT: *Sonninia sowerbyi carinodiscus* Quenstedt, 1886, p. 502, pl. 63, Fig. 3]). A fragmentary *E*. cf. *euaptetum* (Fig. 23: 1a–c) recalls in its habitus already the slightly younger *E. amplectens*; however, the umbilicus of the latter is more involute. These smooth, large-sized hammatoceratids already resemble their presumed descendants, the Early Bajocian *Fissilobiceras ovale* (Quenstedt). A nearly complete compressed specimen from bed 49 of the Heiligenbach section (SMNS 70602) belongs to the genus *Euaptetoceras* as well; however, due to its bad preservation a specific determination is impossible.

5. Bio-/Chronostratigraphy

5.1 Ostracods (M. Franz)

5.1.1 Opalinum Zone

Pygmaea-pumila faunal assemblage (Franz et al. 2018; samples He19-1–12)

The ostracod assemblage consists of 360 individuals (average of 30 individuals per sample) representing 34 species. The assemblage is characterized by *Praeschuleridea ventriosa*, *Aphelocythere pygmaea*, *Metacytheropteron opalinum*, *Acrocythere pumila*, *Eucytherura transversiplicata*, *Euc. michelseni*, *Cardobairdia tesakovae*, *Eucytherura* sp. 1 Franz et al., *Euc*. sp. 3 Franz et al., and *Cytheropterina cribra*.

The zonal index species *Aphelocythere kuhni* (Ohmert 2004) is missing in our samples. Stratigraphically important are *Metacytheropteron opalinum*, *Cardobardia tesakovae*, *Eucytherura plumhoffi*, *Euc. foveolata* sp. nov. and *Procytherura euglyphea* in addition to the nominal species of this community. The very rare *Procytherura celtica* as well as Gen. et sp. indet. 3 and Gen. et sp. indet. 4 (Franz et al. 2018) have also only been found in the Opalinum Zone. A range chart is given in Appendix 1.

In samples He19-7–12, eight species have their last occurrences in this faunal assemblage: *Acrocythere pumila*, *Procytherura euglyphea*, *Eucytherura plumhoffi*, Ostracode A Ballent, *Eucytherura foveolata*, *Cardobairdia tesakovae*, *Metacytheropteron opalinum*, and *Eucytherura* sp. 1 Franz et al.

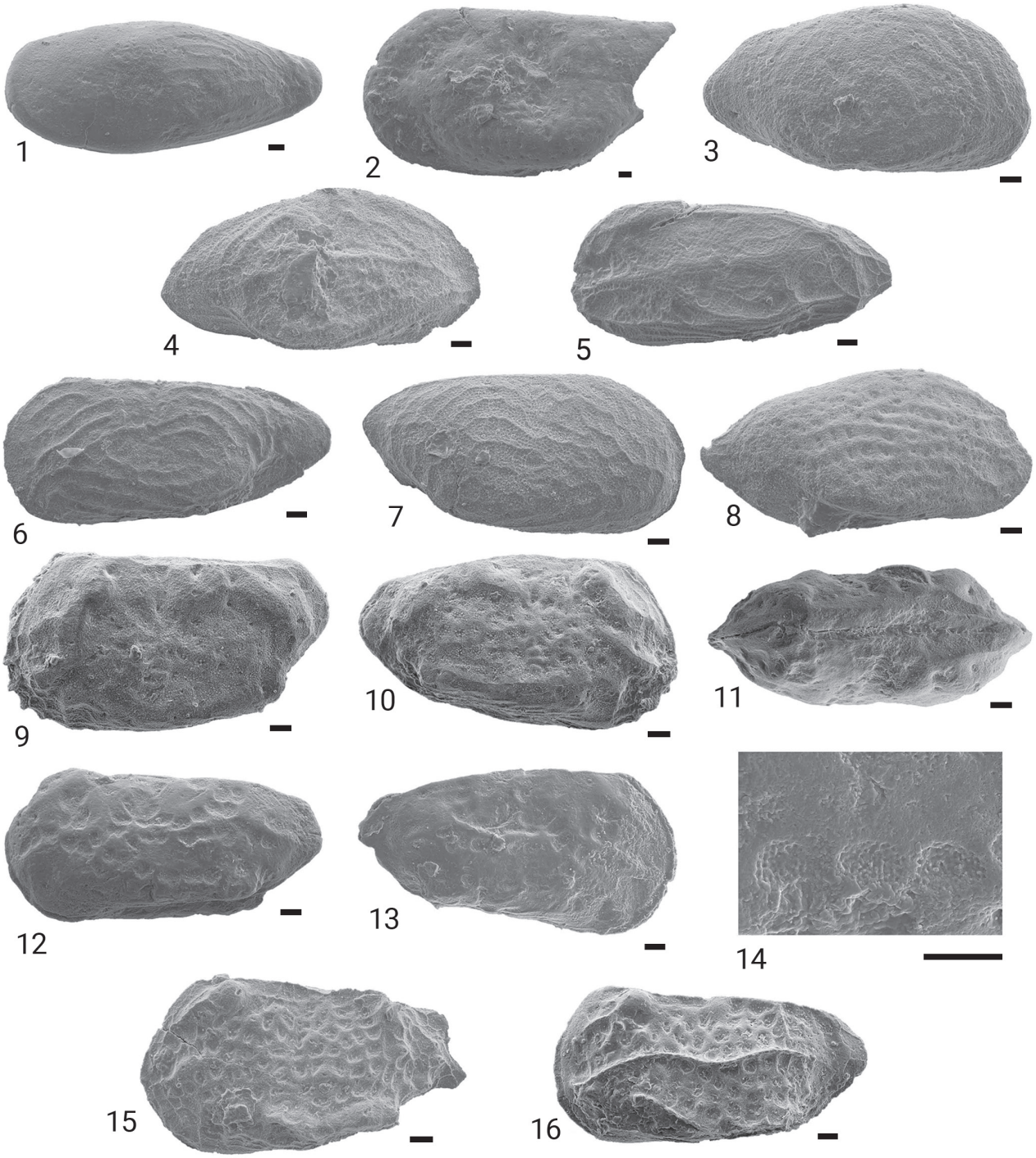

Figure 6. (1) *Cardobairdia tesakovae* Franz et al., SMNS 70521/1, LV, L: 0.426 mm; sample He19-6; **(2)** *Patellacythere* cf. *vulsa*, SMNS 70521/2, LV, L: 0.51 mm; sample He19-9; **(3)** *Procytherura celtica* Ainsworth, SMNS 70521/3, RV, L: 0.301 mm; sample He19-12. **(4, 5)** *Procytherura euglyphea* Ainsworth, **(4)** SMNS 70521/4, RV, L: 0.320 mm; sample He19-1; **(5)** SMNS 70521/5, LV, L: 0.327 mm; sample He19-12. **(6, 7)** *Procytherura multicostata* Ainsworth, **(6)** SMNS 70521/6, LV, L: 0.336 mm; sample He19-9; **(7)** SMNS 70521/7, RV, L: 0.319 mm; sample He19-16. **(8)** *Procytherura* sp. 2 Franz et al., SMNS 70521/8, RV, L: 0.325 mm; He19-8. **(9–11)** *Eucytherura eberti* sp. nov., **(9)** holotype, SMNS 70521/9, C, left view, L: 0.306 mm; sample He19-18; **(10)** Paratype, SMNS 70521/10, C, right view, L: 0.292 mm; sample He19-21; **(11)** paratype, SMNS 70521/11, C, dorsal view, L: 0.318 mm; sample He19-26. **(12–14)** *Eucytherura foveolata* sp. nov., **(12)** holotype, SMNS 70521/12, C, left view, L: 0.327 mm; sample G08Fr; **(13)** paratype, SMNS 70521/13, C, right view, L: 0.318 mm; sample G12Fr; **(14)** paratype, SMNS 70521/14, C, right view (detail), image width: 0.07 mm; sample G12Fr; **(15)** *Eucytherura liassica* Bate and Coleman, SMNS 70521/15, LV, L: 0.304 mm; sample He19-17. **(16)** *Eucytherura michelseni* (Finger), SMNS 70521/16, LV, L: 0.324 mm; sample He19-18. **(1–6, 8, 12–14)** Opalinuston Formation, Lower Aalenian, Opalinum Zone; **(7, 9–11, 15–16)** Achdorf Formation, Upper Aalenian, **(7)** Murchisonae Zone, **(15)** Bradfordensis Zone (Bradfordensis Subzone), **(9, 10, 16)** Bradfordensis Zone (Gigantea Subzone), **(11)** Concavum Zone. Scale bars (if not indicated otherwise): 20 µm.

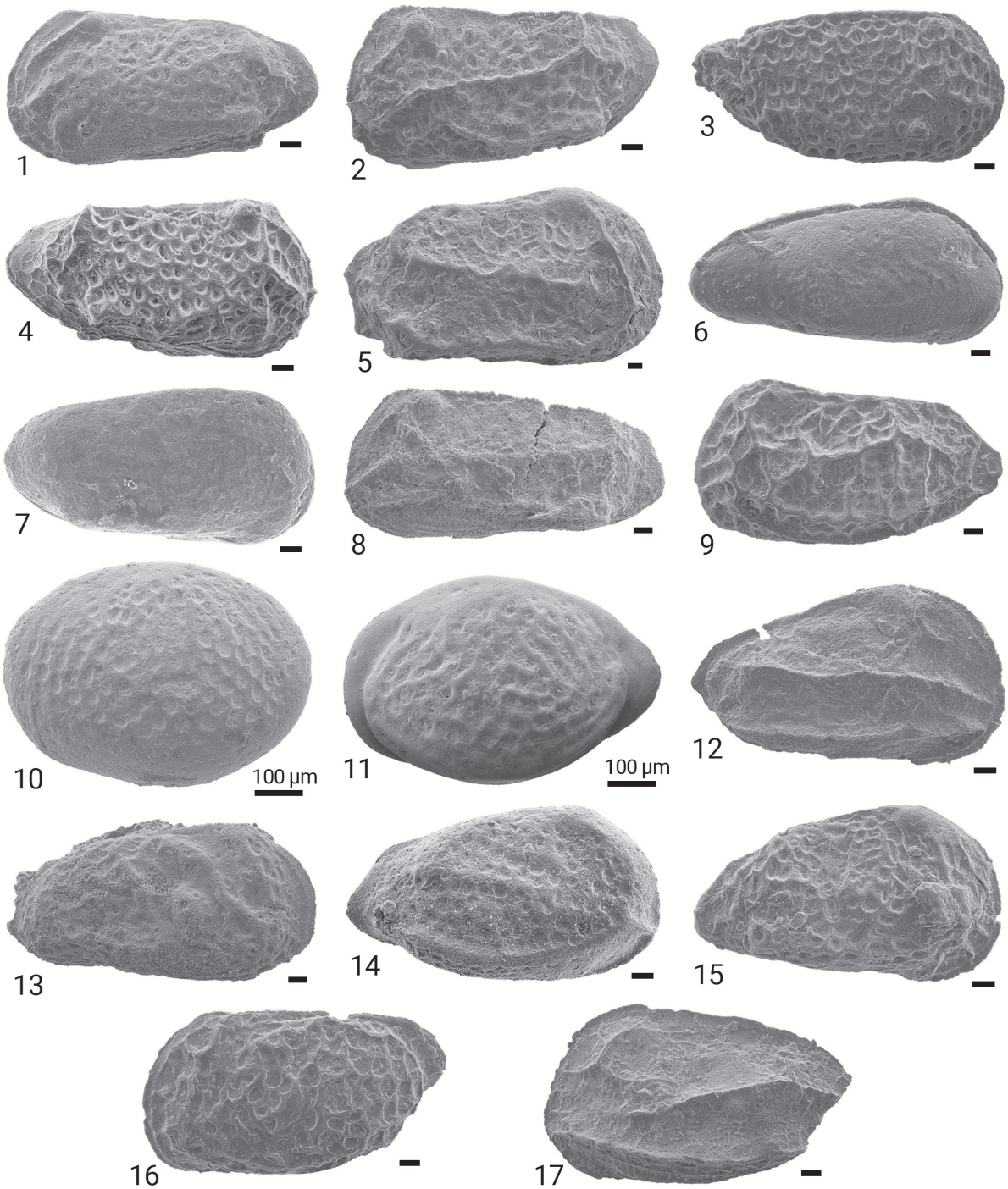

Figure 7. (1) *Eucytherura plumhoffi* Tesakova, SMNS 70521/17, C, left view, L: 0.309 mm; sample He19-7. **(2)** *Eucytherura transversiplicata* (Bate and Coleman), SMNS 70521/18, LV, L: 0.316 mm; sample He19-3. **(3)** *Eucytherura* sp. 1 Franz et al., SMNS 70521/19, RV, L: 0.320 mm; sample He19-12. **(4)** *Eucytherura* sp. 3 Franz, SMNS 70521/20, C, right view, L: 0.300 mm; sample He19-18; **(5)** *Aphelocythere dilgeri* Franz et al., SMNS 70521/21, RV, L: 0.460 mm; sample He19-18. **(6)** *Aphelocythere pygmaea* Plumhoff, SMNS 70521/22, C, right view, L: 0.343 mm; sample He19-12; **(7)** ? *Aphelocythere* sp. 1, SMNS 70423/119, C, right view, L: 0.308 mm; sample G08Fr; **(8)** ? *Pleurocythere* sp., SMNS 70521/23, LV, L: 0.354 mm; sample He19-1. **(9)** *Acrocythere pumila* Plumhoff, SMNS 70521/24, LV, L: 0.343 mm; He19-12. **(10)** *Praeschuleridea ventriosa* (Fischer in Plumhoff), SMNS 70521/25, LV, L: 0.650 mm; sample Mue19-1; **(11)** *Kinkelinella* (*Kink.*) *sermoisensis* (Apostolescu), SMNS 70521/26, LV, L: 0.656 mm; sample He19-9; **(12)** aff. Ostracode A Ballent, SMNS 70521/27, RV, L: 0.290 mm; sample He19-2. **(13)** Gen. et sp. indet. 3, Franz et al., SMNS 70521/28, RV, L: 0.342 mm; sample He19-5; **(14)** Gen. et sp. indet. 5 Franz et al., SMNS 70521/29, RV, L: 0.310 mm; He19-18; **(15)** Gen. et sp. indet. 8 Franz, SMNS 70521/30, RV, L: 0.280 mm; sample He19-12. **(16)** Gen. et sp. indet. 10, SMNS 70521/31, LV, L: 0.300 mm; sample He19-12. **(17)** Gen. et sp. indet. 11, SMNS 70521/32, LV, L: 0.324 mm; sample He19-8. **(1–3, 6–8, 10–12, 15–17)** Opalinuston Formation, Lower Aalenian, Opalinum Zone; **(4–5, 9, 14)** Achdorf Formation, Upper Aalenian, **(4–5, 14)** Bradfordensis Zone (Gigantea Subzone), **(9)** Concavum Zone. Scale bars (if not indicated otherwise): 20 µm.

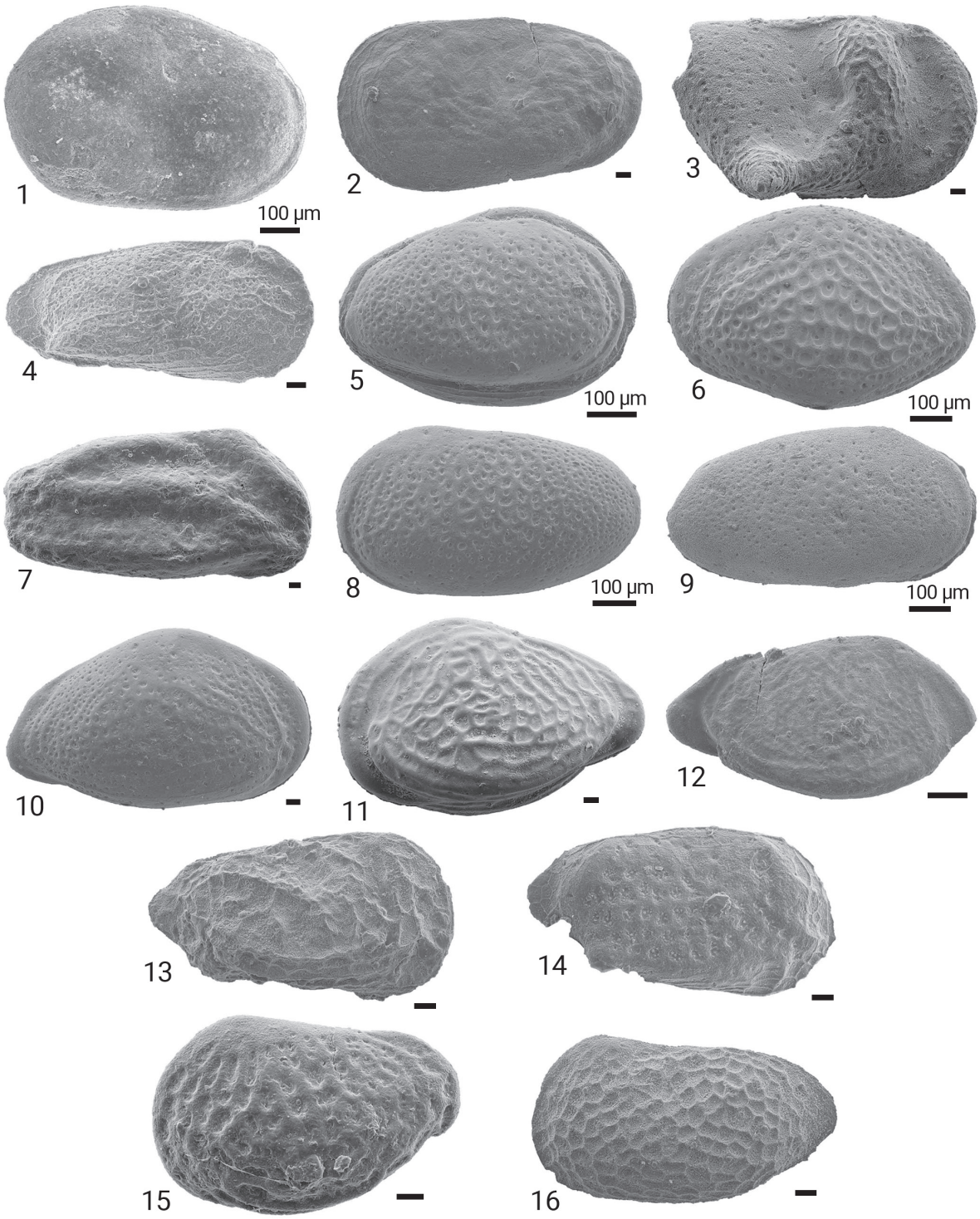

Figure 8. (1) *Cytherella apostolescui* Ainsworth, SMNS 70521/33, RV, L: 0.793 mm; sample He19-27. **(2)** *Cytherelloidea* cf. *catenulata* (Jones and Sherborn), SMNS 70521/34, LV, L: 0.438 mm; sample He19-17. **(3)** *Bythoceratina* (*Praebyth.*) sp. 1, SMNS 70521/35, RV, L: 0.416 mm; sample He19-18. **(4)** *Procytherura* cf. *serangodes* Ballent and Whatley, SMNS 70521/36, C, right view, L: 0.331 mm; sample He19-15; **(5)** *Praeschuleridea punctulata* (Plumhoff), SMNS 70521/37, C, right view, L: 0.606 mm; sample He19-15. **(6)** *Praeschuleridea* sp. A Ainsworth, SMNS 70521/38, LV, L: 0.733 mm; sample He19-17; **(7)** *Pleurocythere* sp. 1, SMNS 70521/39, RV, L: 0.585 mm; sample He19-16. **(8)** *Homocytheridea* sp. 1, SMNS 70521/40, LV, L: 0.707 mm; He19-15. **(9)** *Homocytheridea* sp. 2, SMNS 70521/41, RV, L: 750 mm; sample Mue19-1; **(10)** *Progonocythere scutula* Franz et al., SMNS 70521/42, RV, L: 0.464 mm; sample He19-17; **(11)** *Kinkelinella* (*Kink.*) *fischeri* Malz, SMNS 70521/43, C, left view, L: 0.412 mm; sample Lin18-4. **(12)** *Kinkelinella* sp. 2, SMNS 70521/44, RV, L: 0.444 mm; sample He19-17; **(13)** *Ektyphocythere* aff. *anterocosta* Boomer, SMNS 70521/45, RV, L: 0.281 mm; sample He19-14; **(14)** Gen. et sp. 9 Tesakova, SMNS 70521/46, RV, L: 0.296 mm; He19-17; **(15)** Gen. et sp. indet. 9, SMNS 70521/47, LV, L: 0.235 mm; sample He19-18. **(16)** Gen. et sp. indet. 12, SMNS 70521/48, LV, L: 0.306 mm; sample He19-16. Achdorf Formation **(13)** Opalinum Zone, ("Comptum" Subzone), **(4–5, 7–8, 16)** Murchisonae Zone, **(2, 6, 10, 12, 14)** Bradfordensis Zone (Bradfordensis Subzone), **(3, 15)** Bradfordensis Zone (Gigantea Subzone), **(1, 7)** Concavum Zone. Scale bars (if not indicated otherwise): 20 µm.

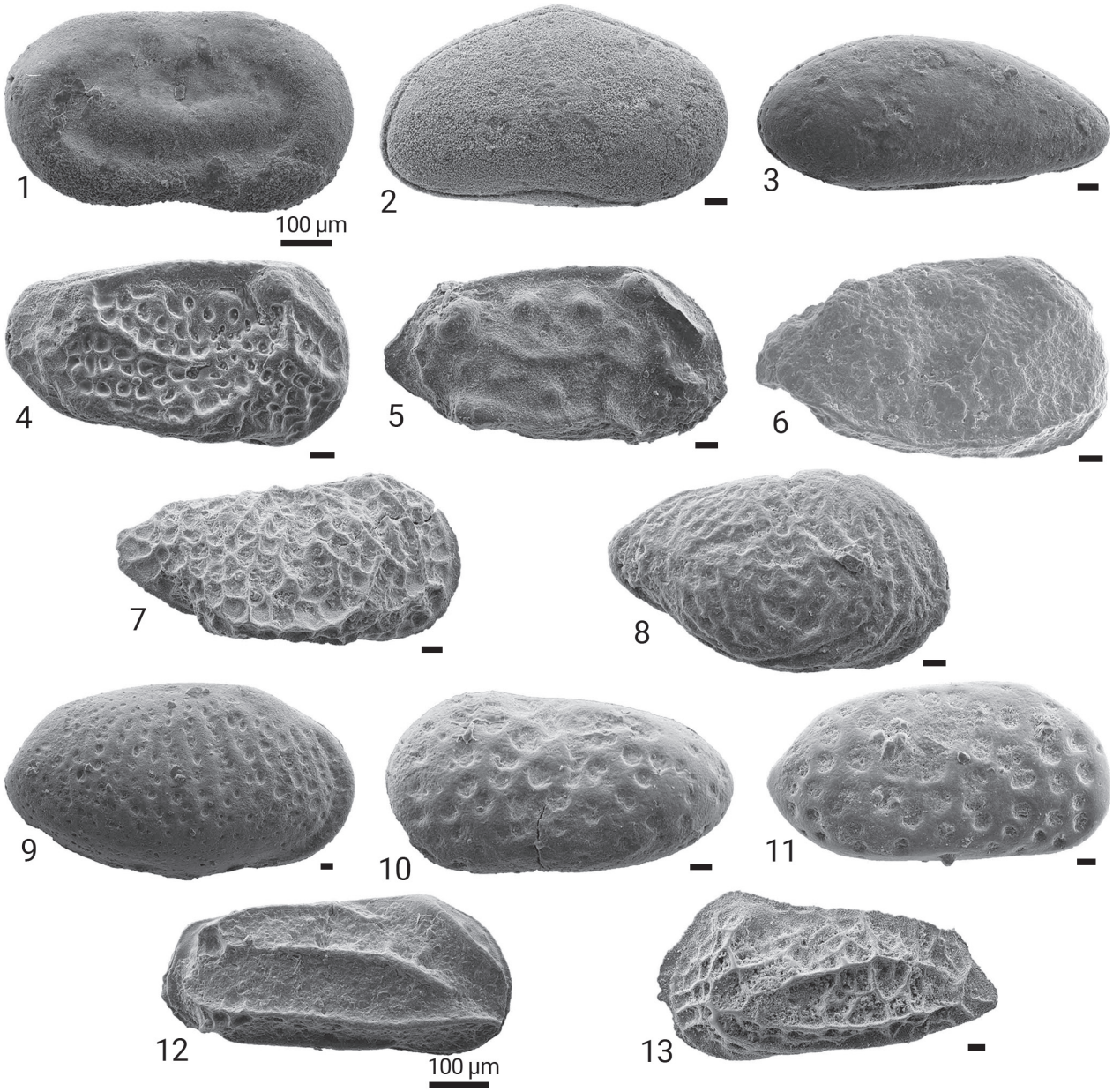

Figure 9. (1) *Cytherelloidea lordi* Ainsworth, SMNS 70521/49, C, right view, L: 0.688 mm; sample He19-19. **(2)** *Bairdiacypris triangularis* Ainsworth, SMNS 70521/50, C, right view, L: 0.309 mm; sample He19-19. **(3)** *Macrocypris aequabilis* Oertli, SMNS 70521/51, C, left view, L: 0.349 mm; sample He19-21. **(4)** *Eucytherura* cf. *parairregularis* Brand, SMNS 70521/52, C, right view, L: 0.281 mm; sample He19-19; **(5)** *Eucytherura* cf. *yunga* Ballent and Whatley, SMNS 70521/53, RV, L: 0.304 mm; sample He19-27. **(6)** *Eucytherura* sp. 5 Franz, SMNS 70521/54, RV, L: 0.295 mm; sample G11Fr; **(7)** *Eucytherura* sp. 11 Franz, SMNS 70521/55, RV, L: 0.327 mm; sample He19-25. **(8)** *Balowella catena* (Franz et al.), SMNS 70521/56, RV, L: 0.308 mm; sample He19-24. **(9)** *Praeschuleridea ornata* (Bate), SMNS 70521/57, RV, L: 0.578 mm; sample He19-21; **(10, 11)** ? *Southcavea* sp., **(10)** SMNS 70521/58, LV, L: 0.315 mm; **(11)** SMNS 70521/59, RV, L: 0.368 mm; sample He19-24; **(12)** *Pleurocythere kirtonensis* Bate, SMNS 70521/60, RV, L: 0.597 mm; sample He19-18. **(13)** *Acrocythere* aff. *pumila* Plumhoff, SMNS 70521/61, LV, L: 0.406 mm; sample He19-27; **(6)** Opalinuston Formation, Lower Aalenian, Opalinum Zone, **(1–5, 7–13)** Achdorf Formation, Upper Aalenian **(1–4, 9, 12)** Bradfordensis Zone (Gigantea Subzone), **(5, 7–8, 10–11, 13)** Concavum Zone. Scale bars (if not indicated otherwise): 20 µm.

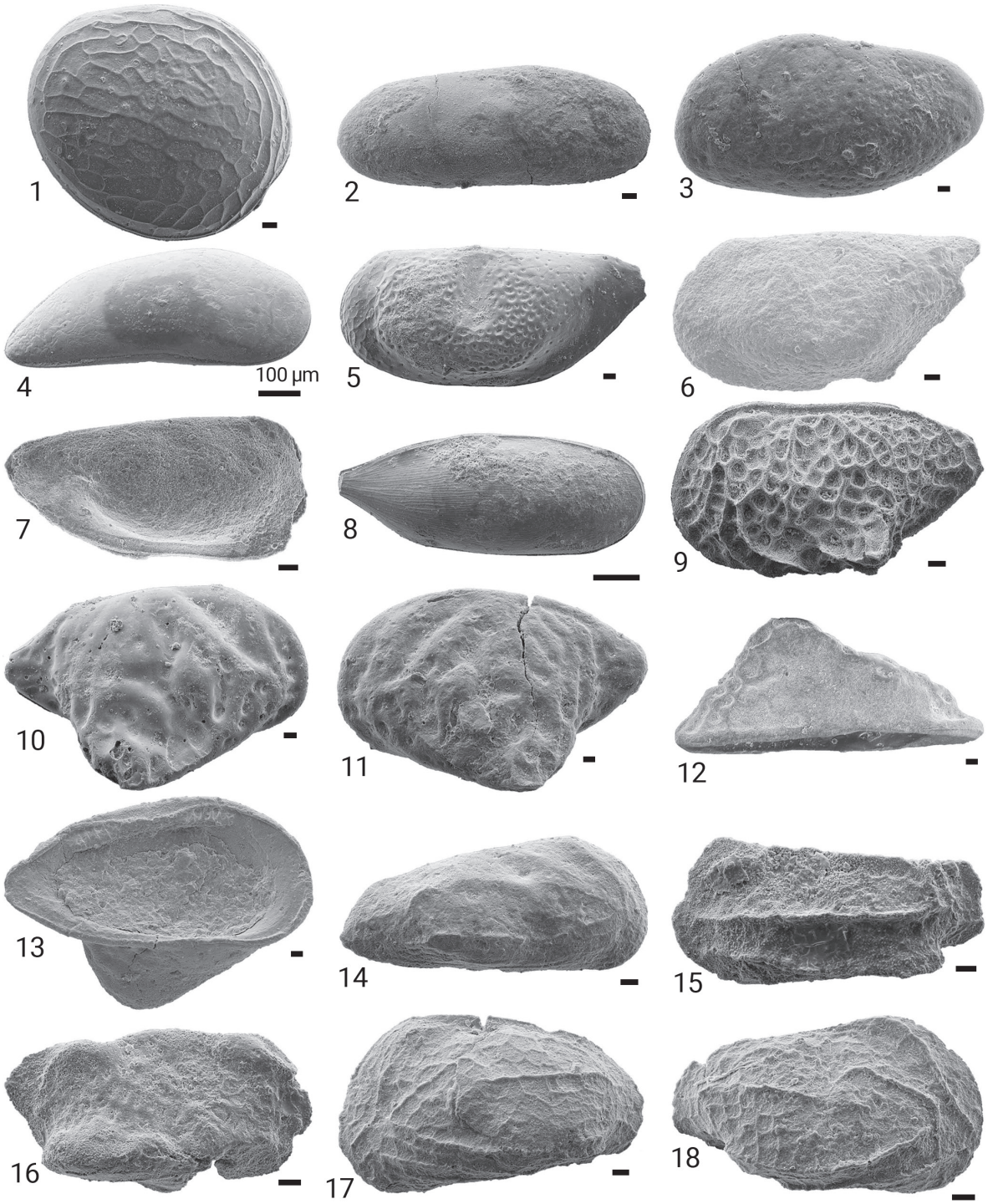

Figure 10. (1) *Polycope* cf. *riegrafi* Brand, SMNS 70521/62, C, right view, L: 0.345 mm; sample He19-27. **(2)** ? *Liasina cylindrica* Ainsworth, SMNS 70521/63, RV, L: 0.412 mm; sample Lin18-1. **(3)** *Cardobairdia toarcensis* Ainsworth, SMNS 70521/64, LV, L: 545 mm; sample He19-26. **(4)** *Macrocypris* ? *liassica* Bate and Coleman, SMNS 70521/65, C, right view, L: 0.750 mm; sample He19-27; **(5)** *Patellacythere paravulsa* cf. *tenuis* Brand, SMNS 70521/66, LV, L: 0.522 mm; sample He19-27. **(6)** *Patellacythere ungulina* (Triebel and Bartenstein), SMNS 70521/67, LV, L: 0.405; sample Mue19-1; **(7)** "*Monoceratina*" aff. *posterocarinata* Brand, SMNS 70521/68, C, right view, L: 0.324 mm; sample He19-21. **(8)** *Tanycythere posteroelongata* Cabral et al., SMNS 70521/69, C, right view, L: 0.676 mm; He19-27. **(9)** *Cytheropterina alacostata* Franz et al., SMNS 70521/70, LV, L: 0.368 mm; sample He19-27; **(10–13)** *Cytheropterina crassicostata* sp. nov., **(10)** holotype, SMNS 70521/71, RV, L: 0.516 mm; sample He19-27; **(11)** paratype, SMNS 70521/72, LV, L: 0.556 mm; sample He19-26, **(12)** paratype, SMNS 70521/73, RV, ventral view, L: 0.557 mm; sample He19-27; **(13)** paratype, SMNS 70521/74, LV, inner view, L: 0.555 mm; sample Ro19-4; **(14)** *Procytherura* sp. 5, SMNS 70521/75, RV, L: 0.363 mm; He19-24; **(15)** *Eucytherura* aff. *yunga* Ballent and Whatley, SMNS 70521/76, LV, L: 0.312 mm; sample He19-27. **(16)** *Eucytherura* sp. B Boomer and Ballent, SMNS 70521/77, RV, L: 0.277 mm; sample He19-25. **(17, 18)** *Eucytherura* sp. 10, **(17)** SMNS 70521/78, LV, L: 0.392; sample He19-25, **(18)** SMNS 70521/79, RV, L: 0.278 mm; sample He19-24. Achdorf Formation, Upper Aalenian, Concavum Zone. Scale bars (if not indicated otherwise): 20 µm.

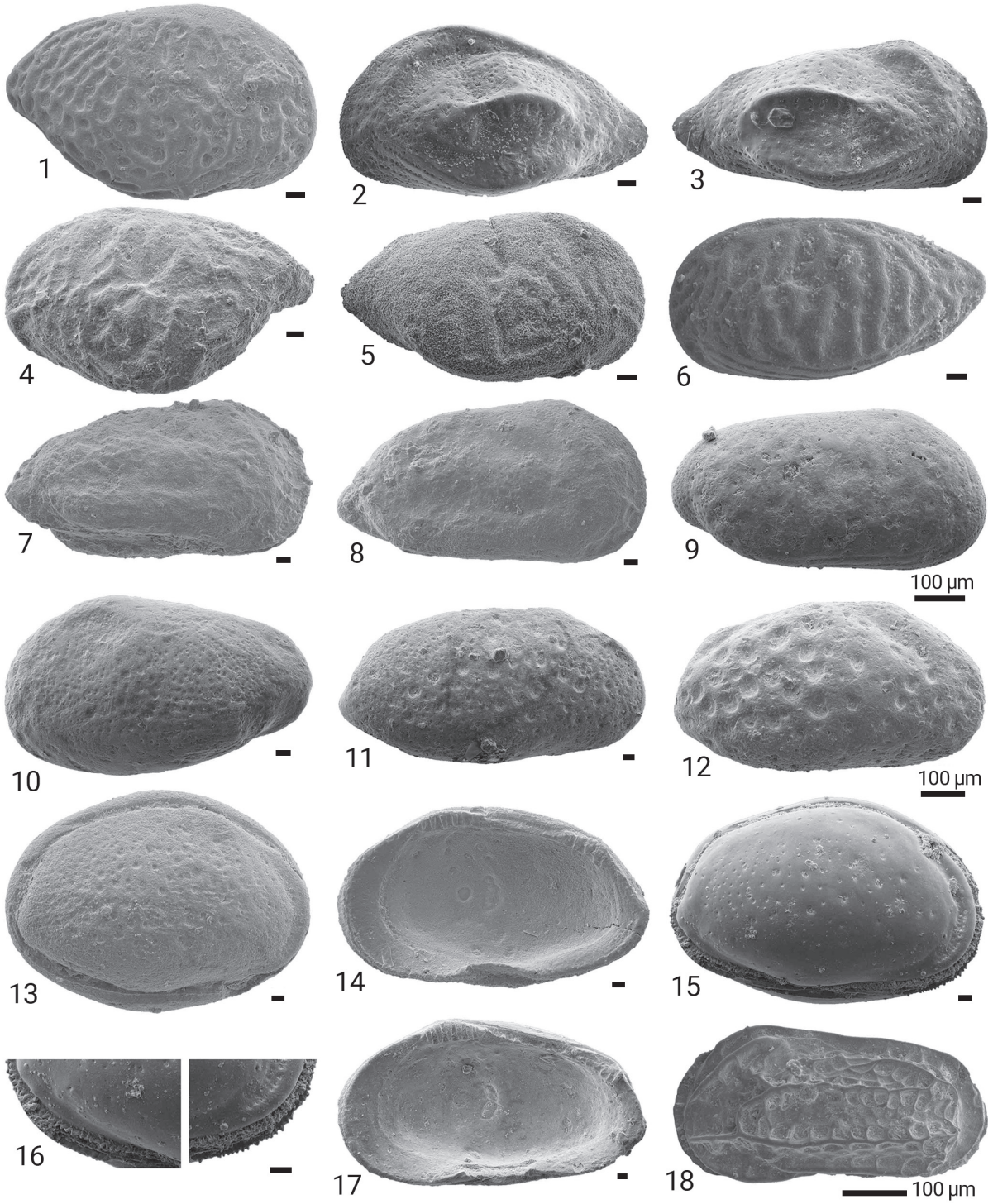

Figure 11. (1) *Balowella catena* (Franz et al.), SMNS 70521/80, C, right view, L: 0.329 mm; sample He19-18. **(2, 3);** ? *Cytheropteron* sp. 1, **(2)** SMNS 70521/81, LV, L: 0.322 mm; sample He19-27; **(3)** SMNS 70521/82, RV, L: 0.355 mm; sample He19-27. **(4, 5)** *Procytheropteron* aff. *gramanni* Brand, **(4)** SMNS 70521/83, LV, L: 0.373 mm; sample He19-26; **(5)** SMNS 70521/84, RV, L: 0.305 mm; sample He19-22. **(6)** *Procytheropteron* sp. 1 Franz et al., SMNS 70423/66, LV, L: 0.322 mm; sample G20b; **(7)** *Aphelocythere recta* Ohmert, SMNS 70521/85, C, right view, L: 0.460 mm; sample Ro19-4. **(8)** *Aphelocythere* aff. *recta*, SMNS 70521/86, C, right view, L: 0.466 mm; sample Ro19-4. **(9)** *Aphelocythere* sp. 1, SMNS 70521/87, RV, L: 0.630 mm; sample He19-27; **(10)** *"Asciocythere"* sp., SMNS 70521/88, RV, L: 436 mm; sample He19-26. **(11)** *Eocytheridea elongata* Bate, SMNS 70521/89, RV, L: 0.573 mm; sample He19-21. **(12)** *Eocytheridea lacunosa* Bate, SMNS 70521/90, RV, L: 0.705 mm; sample He19-25; **(13, 14)** *Praeschuleridea* cf. *subtrigona*, **(13)** SMNS 70521/91, C, right view, L: 0.512 mm; sample Ro19-5; **(14)** SMNS 70521/92, RV, inner view, L: 0.512 mm; sample Ro19-5; **(15–17)** *Praeschuleridea* sp. 1, **(15)** SMNS 70521/93, C, right view, L: 0.490 mm; sample He19-27, **(16)** SMNS 70521/93, C, right view, (detail); **(17)** SMNS 70521/94, RV, L: 0.620 mm; L: 0.620 mm; sample He19-27. **(18)** *Pleurocythere ohmerti* Franz et al., SMNS 70521/94, LV, L: 0.479 mm; sample Tst. 38-1988 (= He19-27). Achdorf Formation, Upper Aalenian, **(1, 6)** Bradfordensis Zone (Gigantea Subzone), **(2–5, 7–18)** Concavum Zone. Scale bars (if not indicated otherwise): 20 µm.

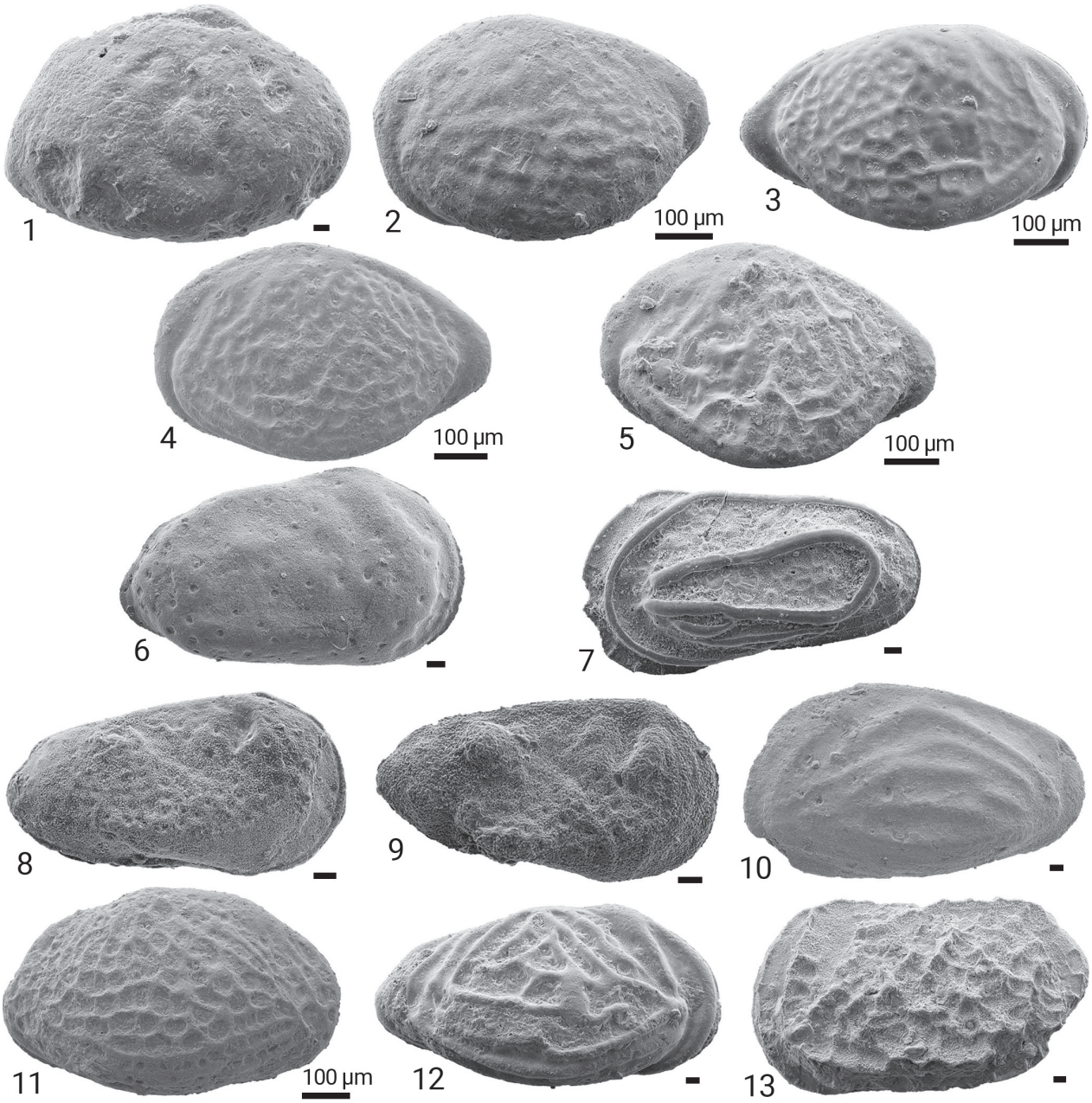

Figure 12. (1) *Camptocythere pusilla* Plumhoff, SMNS 70521/95, RV, L: 0.446 mm; sample He19-24; **(2)** *Kinkelinella* (*K.*) *adunca* Malz, SMNS 70521/96, LV, L: 0.598 mm; sample He19-24. **(3)** *Kinkelinella* (*Kink.*) *levata* Ohmert, SMNS 70521/97, RV, L: 0.636 mm; sample He19-27; **(4)** *Kinkelinella* (*Kink.*) cf. *sermoisensis*, SMNS 70521/98, LV, L: 0.640 mm; sample Mue19-1. **(5)** *Kinkelinella* sp. B Ohmert, SMNS 70521/99, LV, L: 0.623 mm; sample Ha19-5; **(6)** *Minyocythere tuberculata* (Luppold), SMNS 70521/100, RV, L: 0.400 mm; sample Mue19-1. **(7)** *Plumhofficythere clavatoides* Luppold, SMNS 70521/101, LV, L: 0.408 mm; sample He19-27; **(8, 9)** Gen. et sp. 7, **(8)** SMNS 70521/102, RV, L: 0.306 mm; sample He19-22; **(9)** SMNS 70521/103, RV, L: 0.291 mm, sample He19-22. **(10)** *Vernoniella* ? *caytonensis* Bate, SMNS 70521/104, C, left view, L: 0.535 mm; sample Ro19-5. **(11)** *Progonocythere triangulata* Braun in Ohmert, SMNS 70521/105, RV, L: 0.712 mm; sample Ha19-4; **(12)** *Kinkelinella* (*Ekt.*) *triangula* Brand, SMNS 70521/106, RV, L: 0.523 mm; sample Ha19-4. **(13)** *Fuhrbergiella horrida bicostata* Brand and Malz, SMNS 70521/107, LV, L: 0.560 mm; sample Ha19-5. Achdorf Formation, Upper Aalenian, **(5)** Bradfordensis Zone (Gigantea Subzone), **(1–4, 6–11)** Concavum Zone. Scale bars (if not indicated otherwise): 20 µm.

Figure 13. (1a, b) *Brasilia decipiens* (Buckman) [M], SMNS 70519/7. **(2a, b, 9a, b)** *Graphoceras cavatum* (Buckman) [M], (2) SMNS 70519/8, **(9)** SMNS 70519/9. **(3)** *G.* aff. *fallax* (Buckman) [M], SMNS 70519/10. **(4)** *Ludwigella tenuis* (Buckman) [m], SMNS 70519/11. **(5)** *L.* aff. *tenuis* (Buckman) [m], SMNS 70519/12. **(6)** *Ludwigella attenuata* (Buckman) [m], SMNS 70519/13. **(7, 8)** *L. attracta* (Buckman) [m], **(7)** SMNS 70519/14, **(8)** SMNS 70519/15**. (1a–8)** Jungingen (Starzel); Achdorf Formation, Bed 4, Upper Aalenian, Bradfordensis Zone (Gigantea Subzone). Asterisk marks beginning of the bodychamber. Scale bar: 5 cm.

Figure 14. (1a–c) *Planammatoceras* sp. [M], SMNS 70519/16. Jungingen (Starzel); Achdorf Formation, Bed 4, Upper Aalenian, Bradfordensis Zone (Gigantea Subzone). **(2a, b)** *Euaptetoceras infernense* sensu Buckman [M] (**2b**: innermost whorls from reverse flank), SMNS 70519/17. Hechingen-Beuren (Hanneswiesle); Achdorf Formation, Bed 4 [Calceolabank], Upper Aalenian, Concavum Zone (Concavum Subzone), *cavatum* biohorizon. Asterisk marks beginning of the bodychamber. Scale bar: 5 cm.

Figure 15. (1a, b) *G.* cf. *concavum* (Sowerby) [M], with *Propeamussium pumilum* (Lamarck), SMNS 70519/18. **(2)** *G. decorum* Buckman [M], SMNS 70519/19. **(3a, b)** *G.* aff. *apertum* (Buckman) [M], SMNS 70519/20. **(4a, b)** *G.* cf. *pulchrum* (Buckman) [M], SMNS 70519/21. **(5a, b)** *G. pulchrum* (Buckman) [M], SMNS 70519/22. **(6a, b)** *Ludwigella arcitenens* (Buckman) [m], SMNS 70519/23. **(1a–6b)** Hechingen-Beuren (Hanneswiesle); Achdorf Formation, Bed 4 [Calceolabank], Upper Aalenian, Concavum Zone (Concavum Subzone), *cavatum* biohorizon. Asterisk marks beginning of the bodychamber. Scale bar: 5 cm.

Figure 16. (1, 4) *Graphoceras* cf. *concavum* (Sowerby) [M], (1) SMNS 70519/24, (4) SMNS 70519/25. **(2a, b, 5a, b)** *Brasilia* cf. *decipiformis* Dietze et al. [M], (2) SMNS 70519/26, (5) SMNS 70519/27. **(3a, b)** *Ludwigella arcitenens* (Buckman) [m], SMNS 70519/28. **(1–5b)** Balingen-Zillhausen (Roschbach), Upper Aalenian, Achdorf Formation; Concavum Zone (Concavum Subzone); **(3a, b)** Bed 26; **(1–2b, 4–5b)** Bed 28 [Calceolabank], Upper Aalenian, Concavum Zone (Concavum Subzone), *cavatum* biohorizon. Asterisk marks beginning of the bodychamber. Scale bar: 5 cm.

Figure 17. (1a, b) *Graphoceras* cf. *caduciferum* (Buckman) [M], Bed 40 [Inopernabank], Bradfordensis Zone, (Gigantea Subzone), SMNS 70519/29. **(2)** *Graphoceras* sp., Bed 45 [Konglomeratbank], Bradfordensis Zone, (Gigantea Subzone), SMNS 70519/30. **(3)** *Ludwigella arcitenens* (Buckman) [m], Bed 45 [Calceolabank], SMNS 70519/31. **(4)** *Euaptetoceras infernense* sensu Buckman [M], Bed 45 [Calceolabank], SMNS 70519/32. **(5)** *L.* sp. [m], Bed 45 [Calceolabank], SMNS 70519/33. **(3–5)** Upper Aalenian, Concavum Zone (Concavum Subzone), *cavatum* biohorizon. **(1a–5)** Hechingen-Beuren (Heiligenbach), Achdorf Formation. Asterisk marks beginning of the body-chamber. Scale bar: 5 cm (shorter bar for Fig. 17.4).

Figure 18. (1) *Brasilia decipiens* (Buckman) [M], SMNS 70519/34. **(2)** *Graphoceras cavatum* (Buckman) [M], SMNS 70519/35. **(3)** *G.* cf. *v-scriptum* Buckman [M], SMNS 70519/36. **(4a, b)** *B.* aff. *decipiens* (Buckman) [M], SMNS 70519/37. **(5)** *G. fallax* (Buckman) [M], SMNS (70519/38. **(1–5)** Hechingen-Beuren (Heiligenbach), Achdorf Formation, Upper Aalenian, Concavum Zone (Concavum Subzone), *cavatum* biohorizon. Asterisk marks beginning of the bodychamber. Scale bar: 5 cm.

Figure 19. (1a, b) *Brasilia bradfordensis* (Buckman) [M], Bed 2, Bradfordensis Zone, (Bradfordensis Subzone), SMNS 70519/39. **(2)** *Ludwigella cornu* (Buckman) [m], SMNS 70519/40. **(3)** *L. attracta* (Buckman) [m], SMNS 70519/41. **(4)** *L. micra* (Buckman) [m], SMNS 70519/42. **(5a, b)** *B.* cf. *decipiens* (Buckman) [M], SMNS 70519/43. **(1a–5b)** Jungingen (Mühlbächle), Achdorf Formation, Bed 14 [Calceolabank], Upper Aalenian. **(2–5b)** Concavum Zone (Concavum Subzone), *cavatum* biohorizon. Asterisk marks beginning of the bodychamber. Scale bar: 5 cm.

Figure 20. (1a, b) *Graphoceras* aff. *magnum* (Buckman) [M], SMNS 70519/44. **(2a, b)** *G.* cf. *cavatum* (Buckman) [M], SMNS 70519/45. **(3a, b)** *B.* aff. *decipiens* (Buckman) [M], SMNS 70519/46. **(1a–3b)** Jungingen (Mühlbächle), Achdorf Formation, Bed 14 [Calceolabank], Upper Aalenian, Concavum Zone (Concavum Subzone), *cavatum* biohorizon. Asterisk marks beginning of the bodychamber. Scale bar: 5 cm.

Figure 21. (1a, b) *Graphoceras* cf. *cavatum* (Buckman) [M], SMNS 70519/47. **(2a, b)** *G. cavatum* (Buckman) [M], SMNS 70519/48. **(1a–2b)** Jungingen (Mühlbächle), Achdorf Formation, Bed 14 [Calceolabank], Upper Aalenian, Concavum Zone (Concavum Subzone), *cavatum* biohorizon. Asterisk marks beginning of the bodychamber. Scale bar: 5 cm.

Figure 22. (1a, b) *Graphoceras decorum* Buckman [M], SMNS 70519/49. **(2a, b, 5a, b)** *G. formosum* (Buckman) [M], (2) SMNS 70519/56, (5) SMNS 70519/50. **(3a, b)** *Graphoceras pulcrum* (Buckman) [M], SMNS 70519/51. **(4)** *G. fallax* (Buckman) [M], SMNS 70519/52. **(1a–5b)** Jungingen (Mühlbächle), Achdorf Formation, Bed 14 [Calceolabank], Upper Aalenian, Concavum Zone (Concavum Subzone), *cavatum* biohorizon. Asterisk marks beginning of the bodychamber. Scale bar: 5 cm.

Figure 23. (1a–c) *Euaptetoceras* cf. *euaptetum* Buckman [M], SMNS 70519/53. Jungingen (Mühlbächle), Achdorf Formation, Bed 14 [Calceolabank], Upper Aalenian, Concavum Zone (Concavum Subzone), *cavatum* biohorizon. Asterisk marks beginning of the body-chamber. Scale bar: 5 cm.

Figure 24. (1a, b) *Euaptetoceras* cf. *kochi* (Prinz) [M], collection S. Pfister. Jungingen (excavation pit in the street "Im Binder", about 0.5 km NW of the Mühlbächle stream), Achdorf Formation, Bed 14 [Calceolabank], Upper Aalenian, Concavum Zone (Concavum Subzone), *cavatum* biohorizon. Asterisk marks beginning of the bodychamber. Scale bar: 10 cm.

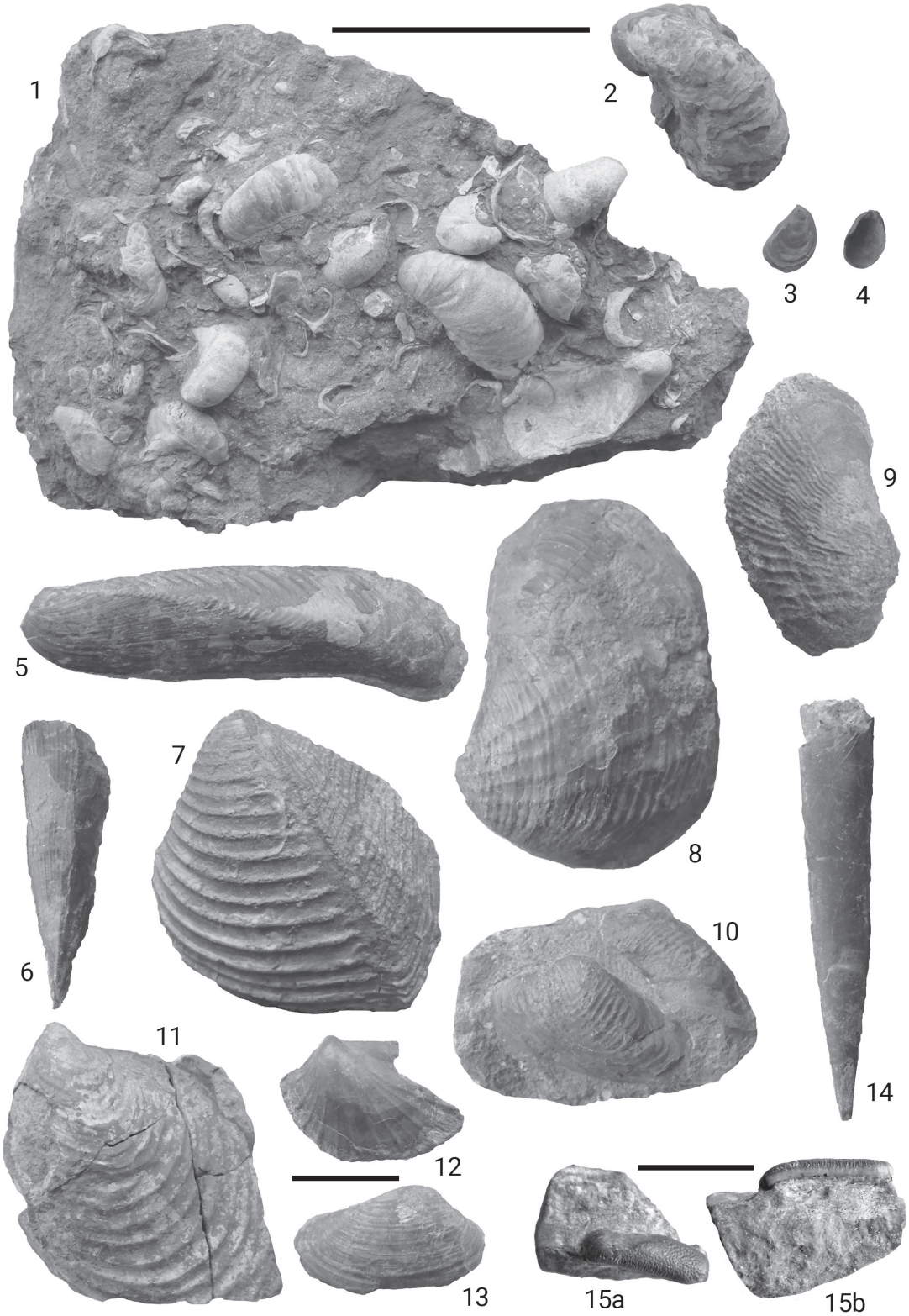

Figure 25. (1, 2) *Gryphaea calceola* Quenstedt, Jungingen, Mühlbächle, Calceolabank, SMNS 70528/1–2. **(3, 4)** juveniles of *Gryphaea calceola* Quenstedt, Jungingen, Mühlbächle, marlstone above Calceolabank, SMNS 70528/3–4. **(5)** *Inoperna sowerbyana* (d'Orbigny), Jungingen, Starzel river, Inopernabank, SMNS 70528/5. **(6)** *Pinna* sp., Jungingen, Starzel river, Inopernabank, SMNS 70528/6. **(7)** *Trigonia alemanica* Rollier, Balingen-Zillhausen, Roschbach, Calceolabank, SMNS 70528/7. **(8)** *Pholadomya lirata* (Sowerby), Jungingen, Starzel river, Inopernabank, SMNS 70528/8. **(9)** *Pholadomya fidicula* (Sowerby), Hechingen-Beuren, Heiligenbach, Inopernabank, SMNS 70528/9. **(10)** *Goniomya literata* (Sowerby), Hechingen-Beuren, Heiligenbach, Inopernabank, SMNS 70528/10. **(11)** *Mytiloceramus polyplocus* (Roemer), Jungingen, Mühlbächle, Rostrote Kalkbank, SMNS 70528/11. **(12)** *Oxytoma inaequivalvis* (Sowerby), Jungingen, Starzel river, Inopernabank, SMNS 70528/12. **(13)** *Pleuromya* cf. *uniformis* (Sowerby), Jungingen, Starzel river, Inopernabank, SMNS 70528/13. **(14)** Belemnite rostrum, Hechingen-Beuren, Heiligenbach, Calceolabank SMNS 70529. **(15)** *Asteracanthus personati* (Quenstedt), Zillhausen Member, Starzel river in Schlatt, SMNS 97005. Scale for 1, 2: 50 mm; for 3-14: 20 mm, for 15a, b: 20 mm.

5.1.2 "Comptum" Subzone (samples He19-13–14)

The stratigraphical significance of the ostracod assemblage from the "Comptum" Subzone is rather limited (8 species, represented by only 65 specimens). The assemblage is characterized by the extinction of the previously typical species *Aphelocythere pygmaea*, *Acrocythere pumila*, *Procytherura euglyphea*, *Proc. celtica*, *Eucytherura plumhoffi*, *Euc. foveolata*, *Euc.* sp. 1 Franz et al., *Metacytheropteron opalinum*, and *Cardobairdia tesakovae*. *Aphelocythere pygmaea* has its last appearance (very rare) in the claystones directly above the Comptumbank. Only *Cytherella apostolescui* appears for the first time, like in the Geisingen clay pit (Franz et al. 2018); the newly appearing species *Praeschuleridea punctulata*, *Kinkelinella* (*K.*) *fischeri*, *Kinkelinella* sp. 2 and *Ektyphocythere* aff. *anterocosta* are already known from older strata in Geisingen and some other sections.

Dominant species include *Praeschuleridea ventriosa*, *Pr. punctulata* and *Kinkelinella* (*K.*) *fischeri*.

5.1.3 Murchisonae Zone (samples He19-15–16)

The samples from the clays above the "Doppelbank" 20 + 21 yielded 126 specimens of 17 species, 12 of which were found in single specimens. Dominant species are *Praeschuleridea ventriosa*, *Pr. punctulata* and *Homocytheridea* sp. 1. Nine species are new; most important are *Homocytheridea* sp. 1, *Bythoceratina* (*Praebythoceratina*) sp. 1, *Eucytherura* sp. 3 Franz et al. and, to a minor degree, the very rare *Pleurocythere* sp. 1. The still undescribed Gen. et sp. indet. 10 Franz has its last appearance. *Homocytheridea* sp. 2, *Procytherura* aff. *serangodes*, *Aphelocythere* cf. *pygmaea*, *Pleurocythere* sp. 1 and Gen. et sp. indet. 12 were found only in single specimens in this assemblage.

Homocytheridea sp. 1 differs from *Homocytheridea* cf. *punctulata* from the Concavum Zone in the Geisingen clay pit. The stratigraphic distribution of *Homocytheridea* in the Upper Aalenian can be clarified only after investigation of further material.

5.1.4 Bradfordensis Zone, Bradfordensis Subzone (sample He19-17)

In this sample, we found 12 species (only 25 specimens), the majority of which are again represented by single specimens. Among the newly appearing species the solely abundant *Progonocythere scutula* (13 specimens) is particularly noteworthy. It was first described by Franz et al. (2018) from the Geisingen-Oolith (Gigantea Subzone). *Progonocythere scutula* and Gen. et sp. 9 Tesakova were observed in this sample only. A stratigraphical interpretation is not possible so far.

5.1.5 Bradfordensis Zone, Gigantea Subzone (samples He19-18–21)

The stratigraphical significance of this assemblage (35 species, represented by 169 specimens) is restricted. Eighteen species occur for the first time respectively reoccur in this part of the section: *Praeschuleridea ornata*, *Pr. ventriosa*, *Balowella catena*, *Cytherelloidea lordi*, *Pleurocythere kirtonensis* and rare *Kinkelinella levata* and *Eocytheridea elongata* in the uppermost sample. Dominant species are *Praeschuleridea ornata* and *Pr. ventriosa*, which alone account for > 22% of the total assemblage, *Cytheropterina bicuneata*, *Praeschuleridea punctulata* and *Balowella catena*. *Eucytherura michelseni*, *Eucyth*. sp. 3 Franz et al., *Cytherelloidea* cf. *catenulata* and Gen. et sp. indet. 9 have their last appearances in this section. *Cytherelloidea lordi*, *Pleurocythere kirtonensis*, *Aaleniella compressa* and *Eucytherura* sp. 5 Franz were found in this assemblage only.

As already observed in Geisingen (Franz et al. 2018) and Thanheim (Dietze et al. 2018), *Kinkelinella levata* – contrary to Ohmert (2004) – already occurs in the Bradfordensis Zone. The lower boundary of the Levata ostracod zone must therefore be significantly shifted downwards.

5.1.6 Concavum Zone (samples He19-21–28, Mue19-1, Ha19-1–3, Ro19-3–5)

The Concavum-Zone comprises the claystones immediately below and above the Inopernabank up to the Sowerbyi-Oolith. Since the claystones above the Rostrote Kalkbank are not exposed along the Heiligenbach creek, their basal part was sampled at the Mühlbächle creek in Jungingen and, for comparison purposes, at the Roschbach in Balingen-Zillhausen. The 14 samples obtained there show ostracod (and foraminifers) assemblages relatively rich in species and individuals. The upper half of these claystones and the basal Wedelsandstein Formation were sampled in the Hausterberg section. The claystones in this level are fine sandy and very poor in microfossils. In some samples only one foraminiferal and one ostracod species were found in small (foram.) to very small (ostr.) numbers.

This assemblage (including the samples from the Roschbach valley) comprises 2,365 specimens from 58 species, 34 of which appear for the first time in this section. Dominant species are *Cytherella apostolescui*, *Praeschuleridea ornata* and the newly appearing *Eocytheridea lacunosa* and *Camptocythere pusilla*. The still persisting *Praeschuleridea ventriosa*, *Pr. punctulata*, *Balowella catena*, *Cytheropterina bicuneata*, *Eucytherura eberti* and *Bythoceratina* (*Praebyth.*) sp. 1 are common as well. Of 34 species appearing here for the first time, the following ones are somewhat more common and useful for stratigraphic purposes (in the order of their first occurrence in this section): *Eocytheridea lacunosa*, *Plumhofficythere clavatoides*, *Kinkelinella* (*Kink.*) *adunca*, *Camptocythere pusilla*, *Pleurocythere ohmerti*, *Kinkelinella* (*Kink.*) sp. B Ohmert, *Cytheropterina crassicostata*, *Cyth. alacostata*, *Kinkelinella* (*Kink.*) cf. *sermoisensis*, *Praeschuleridea* cf. *subtrigona*, and *Minyocythere tuberculata*.

The two species of *Cytheropterina* are very conspicuous, but *Cytheropterina alacostata* is often represented by very small specimens.

Camptocythere pusilla, the index species of the Pusilla Ostracod Zone (Ohmert 2004), has been found here in

Zones	Subzones	Biohorizons	Localities
Concavum	Formosum	yet to be worked out	?Geisingen, Ringsheim, Wutach
	Concavum	*cavatum*	Zollernalb; ?Kappishäusern, ?Metzingen [Rieber 1963]
Bradfordensis	Gigantea	?	Zollernalb
		decipiformis	Geisingen
		?	Geisingen
		geisingensis	Geisingen, Öfingen
		gigantea sensu Contini	Geisingen, Wutach (condensed)
	Bradfordensis	yet to be worked out	Aalen, Kuchen, Geislingen, Wutach (condensed)
		staufensis	Swabian Alb, Wutach [Rieber 1963], Geisingen, Ringsheim
Murchisonae	Murchisonae	*discoidea*	Wochenberg [Rieber 1963]
		sehndensis	Wochenberg, Plettenberg, Gosheim [Rieber 1963]
	Haugi	*opalinoides*	Geisingen, Wutach, ?Aalen, Wochenberg [Rieber 1963]
Opalinum	"Comptum"	yet to be worked out	Aichelberg [Dietl 2013], Geisingen [Dietze et al. 2014]
		"comptum"	Swabian Alb, Wutach [Rieber 1963]
	Opalinum	*lineatum-"costosum"*	Middle Swabian Alb [Ohmert 1993], Zollernalb
		hansrieberi	Middle Swabian Alb [Dietze & Schweigert 2018], Zollernalb
		opaliniforme	Middle Swabian Alb [Ohmert 1993]
		misera	Wittnau [Ohmert 1993; non Schulbert 2001], Swabian Alb

Figure 26. Biohorizons in the Aalenian of SW Germany. The biohorizons recorded in the Zollernalb area are shaded in grey.

large numbers. The very noticeable *Plumhofficythere clavatoides*, which also occurs in Northern Germany (Plumhoff 1963; Luppold 2003) and England (Bate 1963b), is obviously limited to the Bradfordensis Zone (Gigantea subzone) and Concavum Zone and would therefore also have stratigraphic significance.

Eucytherura eberti sp. nov., which has been found in rare specimens from the uppermost Opalinum Zone upwards, has its acme at this level. A number of further, mostly small species appear here for the first time. Although they are partly very conspicuous (e.g., ? *Cytheropteron* sp. 1, *Eucytherura* sp. 10), they are rather unsuitable for stratigraphic purposes due to their scarcity. Additionally, some of these rare species occur earlier elsewhere. A range chart for the Achdorf Formation is given in Appendix 2.

Bajocian

5.1.7 Discites Zone (samples Ha19-4–6)

The appearance of *Kinkelinella* (*Ekt.*) *triangula* and *Progonocythere triangulata*, together with *Cytherelloidea* cf. *cadomensis* and rare *Fuhrbergiella horrida bicostata* in this assemblage (374 specimens) clearly indicates the base of the Triangula Ostracod Zone, Triangulata Ostracod Subzone (= Discites Zone; Ohmert 2004). All other of the 15 species persist from the Aalenian. *Praeschuleridea ornata*, *Progonocythere triangulata*, *Cytherella apostolescui* and *Cytherelloidea* cf. *cadomensis* are dominant. Nine of the 15 species, including the dominant and the zonal index species, were also found at this level in the Thanheim section (Dietze et al. 2019). In contrast to Ohmert (2004), *Kinkelinella* (*Ekt.*) *triangula* appears in the Hausterberg section directly at the base of the Lower Bajocian.

5.2 Ammonites

Aalenian

5.2.1 Opalinum Zone

Opalinum and **"Comptum" subzones:** The strata of the Opalinum Zone were not in the focus of this investigation. However, the Opalinum Subzone reaches at least up to the "Wasserfallschichten" in the area. About 8 m above the "Zopfplatten" of the Heiligenbach section the "Comptum" Subzone is verified by numerous small-sized ammonites of the *L.* "*comptum*" – *L. evolutum* group.

5.5.2 Murchisonae Zone

At present, we cannot confirm strata of this age with ammonites.

5.2.3 Bradfordensis Zone

Bradfordensis Subzone: Beds 20–22 in the Roschbach section and bed 2 of the Mühlbächle section belong to the Bradfordensis Subzone. Ammonites are *Brasilia bradfordensis* and *Staufenia staufensis*.

Gigantea Subzone: For the moment, we place the ammonite fauna of the Inopernabank bed into the uppermost Gigantea Subzone. The graphoceratid fauna of this bed itself is not diagnostic enough to decide definitely, if this bed should be placed in the youngest Gigantea Subzone (younger than *decipiformis* biohorizon) or in the oldest Concavum Subzone (older than *cavatum* biohorizon). However, the single *Planammatoceras* sp. is very close to some of the hammatoceratids from the *decipiformis* biohorizon (Gigantea Subzone) of Geisingen, but very different from the hammatoceratids of the *cavatum* biohorizon (Concavum Subzone). Hence, we tentatively assign these beds in the Gigantea Subzone. Ammonites: *Brasilia decipiens*, *Graphoceras cavatum*, *G.* cf. *caduciferum*, *G.* aff. *fallax*, *Ludwigella tenuis*, *L.* aff. *tenuis*, *L. attenuata*, *L. attracta*, *Planammatoceras* sp.

5.2.4 Concavum Zone

Concavum Subzone (*cavatum* horizon): The Calceolabank (Roschbach: Bed 28, Mühlbächle: Bed 14, Heiligenbach: Bed 45, Hanneswiesle: Bed 4) belongs to the *cavatum* biohorizon of the Concavum Subzone. The fauna is a mixture of *Brasilia* spp., the dominant *Graphoceras* spp. and transitional morphologies besides *Euaptetoceras infernense* sensu Buckman. Ammonites: *Brasilia decipiens*, *B.* cf. *decipiens*, *B.* aff. *decipiens*, *B.* cf. *decipiformis*, *Graphoceras cavatum*, *G.* cf. *cavatum*, *G.* cf. *concavum*, *G. fallax*, *G.* aff. *magnum*, *G. decorum*, *G. pulchrum*, *G. formosum*, *Ludwigella arcitenens*, *L. attracta*, *L. micra*, *L. cornu*, *Euaptetoceras* cf. *euaptetum*, *E. infernense* sensu Buckman, *E.* cf. *kochi*.

Formosum Subzone: There is no evidence for this subzone in the Zollernalb.

Bajocian

5.2.5 Discites Zone

The Sowerbyi-Oolith bed belongs to the Discites Zone (see Dietze et al. 2019).

Table 4. Number of species, genera and families in relation to zones and subzones. Indeterminable individuals were not considered. The maxima of the species within the zones are in bold. Indiv. = individuals.

Zone /Subzone	Heiligenbach							
	no. of indiv.	indiv. / sample	species /	new	genera /	new	families /	new
Discites-Ovale	374	125	15	4	9	1	7	1
Concavum	2572	**161**	**58**	**34**	**29**	**10**	**13**	**3**
Gigantea	169	42	35	18	20	6	9	1
Bradfordensis	25	25	12	5	7	1	5	
Murchisonae	126	63	17	9	11	2	7	
Comptum	65	33	8	1	6	2	4	1
Opalinum	360	28	**34**		15		**9**	
Total	**3691**		**109**		**38**		**15**	

6. Correlation

6.1 Ostracods (M. Franz)

As Plumhoff (1963: 59) already stated, species of the genera *Cytherella* and *Cytherelloidea* dominate in the Upper Aalenian of the Swabian Alb, while they are absent in NW Germany in sediments of the same age. Nevertheless, the correlation succeeds by means of the genera and species occurring at different frequencies in both parts of the basin as listed in Plumhoff (1963: 59). Additionally, *Plumhofficythere clavatoides* Luppold (= *Cytheridae*, n. gen. sp. nov. 1 in Plumhoff 1963) is now also known from several sections in SW Germany.

In the present study and in the Geisingen section, a total of 33 genera and species were identified which are also known from the English, Scottish and Irish Aalenian and Lower Bajocian. *Cytherella apostolescui*, *Cytherelloidea catenulata*, *Cyth. lordi*, *Cytheropterina cribra*, *Eocytheridea elongata*, *Eoc. lacunosa*, *Eucytherura liassica*, *Euc. michelseni*, *Euc. transversiplicata*, *Kinkelinella* (*Ekt.*) *triangula*, *Macrocypris aequabilis*, *M. liassica*, *Procytherura celtica*, *Proc. euglyphea*, *Proc. multicostata*, and many others indicate a marine connection between these two sedimentary basins across the Paris Basin.

6.1.1 Opalinum Zone

Of the 34 species detected in the Heiligenbach section in the upper part of the Opalinuston Formation, 21 species are restricted to the Opalinum Zone or occur here for the last time. In accordance with the Geisingen clay pit (Franz et al. 2018), these are, in the order of their first occurrence: *Aphelocythere pygmaea*, *Acrocythere pumila*, *Eucytherura plumhoffi*, *Eucytherura* sp. 1 Franz et al., Gen. et sp. indet. 3 Franz et al., *Eucytherura foveolata* sp. nov., *Cardobairdia tesakovae*, *Metacytheropteron opalinum*, Gen. et sp. indet. 4 Franz et al., *Procytherura* sp. 2 Franz et al., and *Procytherura celtica*.

The ostracod assemblage of the upper Opalinuston Formation, Zillhausen Subformation (Franz and Nitsch 2009) can be well correlated with neighbouring regions. Although the zonal index *Aphelocythere kuhni* is missing here, *Aphelocythere pygmaea*, *Acrocythere pumila* and *Metacytheropteron opalinum* are also indicative for the upper Opalinum Zone in the Western and Middle Swabian Alb (Dilger 1963; Franz et al. 2018), Northern Germany and Northern Switzerland – there additionally *Eucytherura plumhoffi* and *Cardobairdia tesakovae*.

6.1.2 Opalinum Zone ("Comptum" Subzone) to Murchisonae Zone

The stratigraphically insignificant ostracod faunal assemblage of the "Comptum" Subzone and Murchisonae Zone has little in common with previously studied sections of the Swabian Alb. According to Dilger (1963), only *Cytherella apostolescui* and *Cytheropterina bicuneata* are common in this section. Besides these two species Franz et al.

(2018) mentioned also *Praeschuleridea punctulata* and *Kinkelinella fischeri*. The composition of the ostracod assemblage in northern Germany is very different. According to Ainsworth (1986), *Cytherella apostolescui* is already present in the Toarcian of the Fastnet Basin (off Ireland).

6.1.3 Bradfordensis Zone

The ostracod assemblage of this part of the section shows good accordance with that of the Geisingen section with 15 common species. In contrast, the similarities with Dilger (1963) are limited to *Aphelocythere dilgeri* and *Cytherelloidea lordi*.

Progonocythere scutula, first described from the Geisingen Oolite (Gigantea Subzone; Franz et al. 2018: 78), occurs in the Heiligenbach section only in sample 17 (below the Staufensisbank), which presumably corresponds to the Bradfordensis Subzone. Due to the rarity of this species, a further stratigraphic interpretation is not possible.

The samples following higher up yielded *Balowella catena*, an index species of the Ohmerti-catena assemblage (Franz et al. 2018: 82). The second index species, *Pleurocythere ohmerti*, occurs here only above the Konglomeratbank, in the Concavum Zone.

6.1.4 Concavum Zone

Ohmert (2004) placed an ostracod assemblage with *Kinkelinella* (*Kink.*) *levata*, *Aphelocythere recta* and *Pleurocythere* cf. *kirtonensis* (= *Pleurocythere ohmerti*) from beds of the lower Discites Zone in the Pusilla ostracod zone (Concavum to Discites zones). The index species and additionally *Plumhofficythere clavatoides*, *Cytheropterina alacostata* and *C. crassicostata*, occur in the Zollernalb already in the Concavum Zone; *Kinkelinella* (*Kink.*) *levata* sporadically even in the uppermost Gigantea Subzone of the Bradfordensis Zone. Dilger (1963), who had summarized the interval from the Staufensisbank to the Sowerbyi-Oolith, also mentioned *Camptocythere pusilla* from the Balingen section (Zollernalb).

Apart from the zonal index species *Camptocythere pusilla*, *Plumhofficythere clavatoides* (Cytheridae, n. gen. sp. nov. 1 Plumhoff) is restricted to the Concavum Zone in northern Germany (Plumhoff 1963: 55). The latter occurs very rarely already in the Gigantea Subzone in Geisingen (Franz et al. 2018).

Reisdorf et al. (2016) and Tesakova (2017) did not mention any of the characteristic species of the Concavum Zone, which is a very thin interval in Northern Switzerland.

6.2 Ammonites

Herein we focus on the ammonites from the Inopernabank up to the Rostrote Kalkbank.

SW Germany: From the few data available it is most likely that the ammonites from the Inopernabank and the Rostrote Kalkbank are slightly younger compared to the ammonites from the *decipiformis* biohorizon of Geisingen (westernmost Swabian Alb). The few *Graphoceras* specimens from the Inopernabank are slightly more depressed and more involute compared to the "*Graphoceras*-morphology" of *B. decipiformis* (in a chronospecific sense as described in Dietze et al. 2014). Furthermore, *Euaptetoceras infernense* sensu Buckman – typical of the Concavum Subzone (Chandler and Sole 1996) – is unknown from the *decipiformis* biohorizon at Geisingen, where the highly variable *Bredyia diadematoides* and *Planammatoceras* spp. are the most common hammatoceratids; the latter was also recorded in the Inopernabank. Very close in depositional age to the Inopernabank and to the Calceolabank is the "Concava-Bank" around Metzingen and Kappishäusern (Middle Swabian Alb) (Rieber 1963). However, these outcrops and their ammonite content is still under investigation. Possibly the sections around Metzingen and Kappishäusern are slightly condensed.

The *cavatum* biohorizon (index species: *Graphoceras cavatum*; Calceolabank and Rostrote Kalkbank) is younger compared to the *decipiformis* biohorizon of Geisingen (Dietze et al. 2014) and younger than the ammonite faunas from the underlying Inopernabank and Konglomeratbank. The *decipiformis* biohorizon is characterised by smooth, large-sized *Brasilia decipiformis*, which occur only rarely in the *cavatum* biohorizon. The *Brasilia* fauna of the *cavatum* biohorizon consists of specimens with a smaller size, sometimes already showing the ribbing style of *Graphoceras*. The morphogenus *Graphoceras* is much more common in the *cavatum* biohorizon than in the *decipiformis* biohorizon, where most of the specimens belonging to the morphogenus *Graphoceras* are also less depressed. Variants of *Bredyia diadematoides* are abundant in the *decipiformis* biohorizon and not recorded in the *cavatum* biohorizon, where *Euaptetoceras infernense* sensu Buckman is common.

Ammonites of the Formosum Subzone occur in the "Bunte Mergel" and "Tonhorizont E1" of Ringsheim (Upper Rhine Valley) and in the Konglomeratbank/basal part of the Sowerbyi-Oolith near Achdorf (Wutach area). However, these beds are not yet subdivided into biohorizons.

SW England: The *decipiens* biohorizon (Bradfordensis Zone, Gigantea Subzone) is slightly older than the *cavatum* biohorizon of SW Germany, because therein occur *Graphoceras* and large-sized *Brasilia* (up to 0.4 m in diameter) in roughly equal numbers (Chandler 1997). The herein described *cavatum* biohorizon can be correlated with the *cavatum* biohorizon (Concavum Zone) of Dorset (Chandler 1997).

7. Additional macrofauna of the Upper Aalenian in the Zollernalb

Besides the ammonites described and discussed above, the macrofauna of the Achdorf Formation is mainly composed of bivalves. Only two species, *Gryphaea calceola* (Quenstedt, 1843) and *Inoperna sowerbyana* (d'Orbigny, 1850) are more abundant, especially the former, which oc-

curs in masses, but only in a few beds. *Gryphaea calceola* (Fig. 25: 1–4) was first described from the vicinity of Jungingen, which is hence considered the type locality. This small oyster is especially abundant in the name-bearing Calceolabank. The shells are embedded not in live position, but as isolated valves in a chaotic arrangement (Fig. 25: 1). In a few other beds only small-sized specimens occur (Fig. 25: 3, 4). Probably these small specimens did not reach the maximum size due to less favourable life conditions and thus represent ecophenotypes, very similar to Early and Middle Jurassic species of *Gryphaea* (e.g., Bayer et al. 1985). Despite their smaller size they undoubtedly belong to the same taxon and should not be confused – as Quenstedt (1843) did – with a superficially similar small oyster, *Ostrea calceola* Zieten, 1833, described from Upper Aalenian beds in eastern Swabia (Aalen-Wasseralfingen). The identity of the latter was checked by topotypic material in the SMNS collection. *Inoperna sowerbyana* (d'Orbigny, 1850) (Fig. 25: 5) was already mentioned by Quenstedt (1857, as *Modiola plicata*) from the vicinity of Jungingen. In the studied sections, it is restricted to the Inopernabank, which is why we here name the bed after this bivalve. *Inoperna* was probably a shallow endobenthic sediment stacker (Fürsich and Werner 1988), very similar in its life-style to *Pinna*, which is rarely recorded as well (Fig. 25: 6). Isolated calcitic valves of *Trigonia alemanica* Rollier, 1912 (Fig. 25: 7) occur in the Calceolabank and were probably washed out of the sediment during storm events. This observation corresponds to the chaotic embedding of the above mentioned *Gryphaea*. Epibenthic bivalves do not occur earlier than in the Lower Bajocian Sowerbyibank. They are represented by fragments of thick-shelled oysters (*Actinostreon* sp.) and limids (*Ctenostreon* sp.). Deeper endobenthic taxa such as *Pholadomya lirata* (Sowerby, 1818) (Fig. 25: 8), *Pholadomya fidicula* (J. de C. Sowerby, 1826) (Fig. 25: 9), *Goniomya literata* (Sowerby, 1819) (Fig. 25: 10), and *Pleuromya* cf. *uniformis* (Sowerby, 1813) (Fig. 25: 13), always preserved as steinkerns, are rare in the Upper Aalenian claystones.

Byssate bivalves are represented by isolated valves of *Mytiloceramus polyplocus* (Roemer, 1857), *Oxytoma inaequivalvis* (Sowerby, 1819) and the pectinids *Propeamussium pumilum* (Lamarck, 1819), *Chlamys textoria* (Schlotheim, 1820) and *Entolium corneolum* (Young & Bird, 1828). *Mytiloceramus polyplocus* (Fig. 25: 11) is a geographically wide-spread taxon, which was originally reported from the Aalenian of northern Germany. In the studied Aalenian sections of the Zollernalb, all records come from a single bed, the Rostrote Kalkbank (Mühlbächle, Starzel river near Killer), which is otherwise very poor in fossils. Possibly these bivalves lived attached to driftwood or empty ammonite shells and thus had a pseudoplanctic life-style. *Propeamussium pumilum* (Fig. 15: 1) is rare in the area, probably because of unfavourable environmental conditions. In contrast, it is extremely common in various sandstones of the coeval Eisensandstein Formation of eastern Swabia. *Chlamys textoria* and *Entolium corneolum* are stratigraphically long-ranging and geographically widespread taxa (Johnson 1984). In the studied sections, however, they have been only recorded by a few specimens. Other determinable molluscs comprise a single belemnite rostrum (Fig. 25: 14) and a poorly preserved nautiloid (*Cenoceras* sp.), both from the Heiligenbach section.

Crinoid remains were noticed in the field in some beds of the Zillhausen Member and in polished sections of the Onkoidbank bed. Among arthropods, in the Upper Aalenian claystones of the Zollernalb occasionally tanaidacean remains occur. Specimens preserved in claystones had been originally misidentified and described as tiny salamanders by F. v. Huene (see Schweigert and Etter 2008). A well-preserved new record comes from a microfossil sample below the Konglomeratbank in the Heiligenbach section and will be described in another context elsewhere.

Finally, a single tooth of *Asteracanthus personati* (Quenstedt, 1857) Fig. 25: 15) is the only vertebrate remain from our studied sections and outcrops. It was found in a bed of the Zillhausen Member of the Starzel river.

8. Conclusions

The consideration of small species results in a much higher diversity of the ostracod fauna of the Upper Aalenian in SW Germany than previously known. The Heiligenbach section and the Geisingen clay pit (Franz et al. 2018) yielded a total of 115 species from the Upper Aalenian (including the species 'incertae sedis'), 31 of which were recorded in both sections.

The uppermost Lower Aalenian is well characterized by the presence of *Aphelocythere pygmaea*, *Acrocythere pumila* and *Metacytheropteron opalinum*. *Eucytherura foveolata* and *Cardobairdia tesakovae* have also only been found in this part of the section so far. *Cytherella apostolescui* appears for the first time at the base of the Achdorf Formation. Higher up in the Achdorf Formation, especially from the Gigantea subzone on, several stratigraphically important species appear like *Balowella catena*, *Cytherelloidea lordi*, *Cytheropterina alacostata*, *Eucytherura eberti*, *Kinkelinella levata*, *Pleurocythere ohmerti*, *Procytherura multicostata*, and *Progonocythere scutula*.

Among the ostracod assemblages, cytherurids show the most striking development with the first appearance of five species in the Gigantea Subzone and 14 species in the Concavum Zone. During the same period the total number of genera increases from 7 (from 5 families) in the Bradfordensis Zone to 20 (9 families) in the Gigantea Subzone and 29 (13 families) in the Concavum Zone.

The variation within ammonites of the family Graphoceratidae in southwestern Germany reflects the evolution of Graphoceratidae from the *geisingensis* biohorizon via the *decipiformis* biohorizon (uppermost Bradfordensis Zone; see Dietze et al. 2014) to the here newly introduced *cavatum* biohorizon (basal Concavum Zone). The faunas gradually change in the successive biohorizons from the morphogenus *Brasilia* to the morphogenus *Graphoceras*, with numerous transitional forms and a gradual shift towards smaller, more involute and slender shells. In each biohorizon, the ammonites of the family Graphoceratidae

probably represent a single palaeobiospecies, the variation of which changes through time, whereas each morphospecies may range across several biohorizons. The integrative study of ammonite and ostracod faunas allows an excellent combination of both stratigraphic lines of evidence. This allows significantly improved correlations between sections and areas, where either ammonites or ostracods are absent or very rare.

Acknowledgements

We thank C. Tetzel (Freiburg i. Br.) for her assistance in describing and sampling the sections studied. N. Ainsworth (St. Albans), A. Lord (London/Frankfurt a. M.) and E. Tesakova (Moscow) gave numerous valuable hints, which is gratefully acknowledged. Special thanks go to S. Herbstritt, A. Schill, S. Wendt (all Freiburg i. Br.) for their help in processing the samples. C. Gasco-Martín (Stuttgart) is thanked for taking the SEM photographs, G. Fischer (Freiburg i. Br.) for preparing the illustrations and ostracod plates in customary high quality. S. Pfister (Ringingen) provided a stratigraphically important ammonite. M. Pfister (Ringingen) and H. Unmuth (Ringingen) are thanked for valuable information. R. B. Chandler (London) supported us in the determination of some of the ammonites. G. Stappenbeck (Sulz am Neckar) assisted in the field work. A. Hofbauer (Wendlingen) prepared the figured *Trigonia*. Special thanks go to A. Lord (London/Frankfurt a. M.) and B. Hostettler (Glovelier) for their valuable reviews.

References

Ainsworth NR (1986) Toarcian and Aalenian Ostracoda from the Fastnet Basin, offshore south-west Ireland. Bulletin of the Geological Survey of Ireland 3: 277–336.

Ainsworth NR (1990) Uppermost Rhaetian to Lower Bajocian Ostracoda from the Porcupine, Slyne, Erris and Donegal basins, offshore west Ireland. Bulletin of the Geological Survey of Ireland 4: 168–200.

Ainsworth NR (1991) Stratigraphy of the Triassic, Lower Jurassic and Middle Jurassic (Aalenian) from the Fastnet Basin, offshore south-west Ireland. Marine and Petroleum Geology 8: 417–429. https://doi.org/10.1016/0264-8172(91)90064-8

Ainsworth NR, O'Neill M, Rutherford MM (1989) Jurassic and Upper Triassic biostratigraphy of the North Celtic Sea and Fastnet Basins. In: Batten DJ, Keen MC (Eds) Northwest European Micropalaeontology and Palynology. Ellis Horwood, Chichester, 44 pp.

Alexander CI (1929) Ostracoda of the Cretaceous of North Texas. University of Texas Bulletin 2907: 1–137.

Althoff W (1940) Die Ammonitenzonen der oberen Ludwigienschichten von Bielefeld. Palaeontographica A 92: 1–44.

Apostolescu V (1959) Ostracodes du Lias du Bassin de Paris. Revue de l'Institut Francais du Pétrole et Annales des Combustibles liquides 14(6): 795–826.

Arias C, Garcia-Frank A, Canales ML, Ureta S (2009) Ostracods from the global stratotype section for the base of the Aalenian stage, Jurassic, at Fuentelsaz section (Cordillera Ibérica, Spain). Rivista Italiana di Paleontologia e Stratigrafia 115: 209–232.

Baird W (1850) The natural history of the British Entomostraca. The Ray Society, London, 364 pp. https://doi.org/10.5962/bhl.title.1807

Ballent SC (1991) Ostrácodos del Jurásico medio (límite Aaleniano-Bayociano) en la Provincia del Neuquén, centro-oeste de Argentina. Revista Española de Micropaleontología 23(3): 21–56.

Ballent SC, Whatley R (2000) The distribution of the Mesozoic ostracod genus *Procytherura* Whatley: palaeogeographical implications with special reference to Argentina. Alcheringa 24(3): 229–242. https://doi.org/10.1080/03115510008619209

Ballent SC, Whatley RC (2009) Taxonomy and zoogeography of the Mesozoic cytherurid Ostracoda from West-Central Argentina. Palaeontology 52(1): 193–218. https://doi.org/10.1111/j.1475-4983.2008.00827.x

Bate RH (1963a) Middle Jurassic Ostracoda from North Lincolnshire. – Bulletin of the British Museum (Natural History) 8(4): 175–219.

Bate RH (1963b) Middle Jurassic Ostracoda from South Yorkshire. Bulletin of the British Museum (Natural History) 9(2): 21–46.

Bate RH (1964) Middle Jurassic ostracoda from the Millepore Series, Yorkshire. Bulletin of the British Museum (Natural History) 10(1): 1–33.

Bate RH (1965) Middle Jurassic ostracoda from the Grey Limestone Series, Yorkshire. Bulletin of the British Museum (Natural History) 11(3): 73–133.

Bate RH (1968) *Praeschuleridea ventriosa ventriosa* (Plumhoff) and *Paraschuleridea ornata* Bate [Ostracoda] from the Bajocian of N.E. England. Journal of Natural History 1968(2): 205–214. https://doi.org/10.1080/00222936800770841

Bate RH (1978) The Jurassic Part 2 (Aalenian to Bathonian). In: Bate RH, Robinson E (Eds) A stratigraphical index of British Ostracoda. Geological Journal, Special issues 8: 213–258.

Bate RH (2009) Middle Jurassic (Aalenian–Bathonian). In: Whittaker JE, Hart MB (Eds) Ostracods in British Stratigraphy. The Micropalaeontological Society, Special Publications. The Micropalaeontological Society, London, 199–233. https://doi.org/10.1144/TMS003.9

Bate RH, Coleman B (1975) Upper Lias ostracoda from Rutland and Huntingdonshire. Bulletin of the Geological Survey of Great Britain 55: 1–42.

Bayer U (1969) *Euaptetoceras* und *Eudmetoceras* (Ammonoidea, Hammatoceratidae) aus der concava-Zone (Ober-Aalenium) Süddeutschlands. Neues Jahrbuch für Geologie und Paläontologie, Abhandlungen 133: 211–222.

Bayer U, Johnson ALA, Brannan J (1985) Ecological patterns in Middle Jurassic *Gryphaea*: The relationship between form and environment. Lecture Notes in Earth Sciences 1: 436–463. https://doi.org/10.1007/BFb0009855

Beisswenger H (1920) Beiträge zur Kenntnis der Schichten des Braunen Jura α–γ zwischen Kirchheim und Balingen. Dissertation Universität Tübingen [unpublished].

Bizon JJ (1960) Sur quelques ostracodes du Lias du Bassin Parisien. Revue de Micropaléontologie 2(4): 203–211.

Bodergat AM (1997) Les ostracodes marins du Jurassique Européen – Utilisation stratigraphique. In: Groupe française d'étude du Jurassique (Ed.) Biostratigraphie du Jurassique Ouest-Européen et Méditerranéen. Bulletin du Centre des Recherches Elf Exploration-Production, Mémoires 17: 197–223.

Bold WA van den (1960) Eocene and Oligocene ostracoda of Trinidad. Micropaleontology 6(2): 145–196. https://doi.org/10.2307/1484466

Boomer ID (1988) On *Ektyphocythere anterocosta* Boomer sp. nov. A Stereo-Atlas of Ostracod Shells 15: 93–96.

Boomer I, Ballent S (1996) Early–Middle Jurassic ostracod migration between the northern and southern hemispheres: further evidence for a proto Atlantic-Central American connection. Palaeogeography, Palaeoclimatology, Palaeoecology 121: 3–64. https://doi.org/10.1016/0031-0182(95)00049-6

Boomgaard WH (1948) Der Braunjura im Starzeltal. Neues Jahrbuch für Mineralogie, Geologie und Paläontologie Monatshefte Abt. B 1945–1948, 319–333.

Bradfield HH (1935) Pennsylvanian ostracoda of the Admore Basin, Oklahoma. Bulletins of American Paleontology 22(73): 1–173.

Brady GS (1868) A synopsis of the recent British Ostracoda. The Intellectual Observer 12: 110–130. https://doi.org/10.5962/bhl.title.84654

Brand E (1961) *Procytheridea triangula* n. sp. Brand. In: Brand E, Malz H (Eds) Ostracoden-Studien im Dogger, 3: Drei neue Procytheridea-Arten und *Ljubimovella* n. g. aus dem NW-deutschen Bajocien. Senckenbergiana Lethaea 42(1/2): 157–173.

Brand E (1990) Biostratigraphische Untergliederung des Ober-Bathonium im Raum Hildesheim, Nordwestdeutschland mittels Ostracoden und Korrelation ihrer Vertikalreichweiten mit Ammonitenzonen. Geologisches Jahrbuch A 121: 119–274.

Brand E, Malz H (1962) Ostracoden-Studien im Dogger, 4: *Fuhrbergiella* n. g. Senckenbergiana Lethaea 43(1): 1–39.

Brand E, Mönnig E (2009) Litho- und Biostratigraphie des Mittel-Jura (Dogger) in Bohrungen Norddeutschlands. Schriftenreihe der Deutschen Gesellschaft für Geowissenschaften 54: 5–73.

Buckman SS (1887–1907) A Monograph of the ammonites of the Inferior Oolite Series. Palaeontographical Society Monographs. The Palaeontographical Society, London, [ccixii +] 456 pp.

Cabral MC, Lord A, Boomer I, Loureiro I, Malz H (2014) *Tanycythere* new genus and its significance for Jurassic ostracod diversity. Journal of Paleontology 88(3): 519–530. https://doi.org/10.1666/13-127

Chandler RB (1997) The graphoceratid ammonite succession in the Aalenian and lowest Bajocian (Middle Jurassic) at Horn Park, Dorset, UK. Proceedings of the Dorset Natural History and Archaeological Society 118: 85–106.

Chandler RB (2019) A new ammonite faunal horizon in the Ovale Zone (Middle Jurassic, Lower Bajocian) and observations on the ammonite genus *Sonninia* at Coombe Quarry, Mapperton, near Beaminster, Dorset. Proceedings of the Geologists' Association 130: 772–791. https://doi.org/10.1016/j.pgeola.2019.10.004

Chandler RB, Callomon JH (2009) The Inferior Oolite at Coombe Quarry, near Mapperton, Dorset, and a new Middle Jurassic ammonite faunal horizon, Aa-3b, *Leioceras comptocostosum* n. biosp., in the Scissum Zone of the Lower Aalenian. Proceedings of the Dorset Natural History and Archaeological Society 130: 99–132.

Chandler RB, Dietze V, Auer W (2012) Die Graphoceratidae: *Leioceras* und seine Verwandten. Fossilien 2012/2: 110–119.

Chandler RB, Sole D (1996) The Inferior Oolite at East Hill Quarry, Bradford Abbas, Dorset. Proceedings of the Dorset Natural History and Archaeological Society 117: 101–108.

Contini D (1969) Les Graphoceratidae du Jura franc-comtois. Annales scientifiques de l'Université de Besançon, série 3, Géologie 7: 1–95.

Dépêche F (1985) Lias supérieur, Dogger, Malm. In: Oertli HJ (Ed.) Atlas des Ostracodes de France. Bulletin des Centres des Recherches Exploration-Production Elf-Aquitaine, Mémoires 9: 119–145.

Dietl G (2013) Der Braunjura am Fuß der Schwäbischen Alb. Fossilien, Sonderhefte 2013, 62 pp.

Dietze V, Rieber H, Auer W, Franz M, Schweigert G, Chandler RB, Rieter M, Chiarini R (2014) Aalenian (Middle Jurassic) ammonites and stratigraphy of the Geisingen clay pit (SW Germany). Palaeodiversity 7: 61–127.

Dietze V, Franz M, Kutz M, Waltschew A (2017a) Stratigraphy of the Middle Jurassic Sengenthal Formation of Polsingen-Ursheim (Nördlinger Ries, Bavaria, Southern Germany). Palaeodiversity 10: 49–95. https://doi.org/10.18476/pale.v10.a5

Dietze V, Rieber H, Wannenmacher N (2017b) Der *staufensis*-Horizont (Bradfordensis-Zone, Ober-Aalenium, Mittlerer Jura) am Plettenberg (westliche Schwäbische Alb, SW-Deutschland). Zitteliana 89: 235–252.

Dietze V, Schweigert G (2018) The *hansrieberi* biohorizon (Aalenian; Opalinum Zone) in the Opalinuston Formation of Donzdorf-Grünbach (Eastern Swabian Alb, Germany). Palaeodiversity 11: 29–57. https://doi.org/10.18476/pale.11.a4

Dietze V, Wannenmacher N, Franz M, Weis R (2019) Neue Erkenntnisse über die Wedelsandstein-Formation der Zollernalb (Schwäbische Alb, SW-Deutschland). Zitteliana 93: 47–81.

Dilger H (1963) Mikrofauna und Stratigraphie des Dogger beta Schwabens. Thesis, Universität Tübingen, 98 pp. [unpubl.]

Donze P (1975) *Tethysia*, nouveau genre d'ostracode bathyal du Jurassique supérieur – Crétacé inférieur mésogéen. Géobios 8(3): 185–190. https://doi.org/10.1016/S0016-6995(75)80037-4

d'Orbigny A (1850) Prodrome de paléontologie stratigraphique universelle des animaux mollusques et rayonnés. Masson, Paris, [IX + 394 +] 428 pp. https://doi.org/10.5962/bhl.title.62810

Erb H (1938) Die Geologie der Braun-Jura-Landschaft um Beuren bei Hechingen. Hohenzollerische Jahreshefte 5: 328–357.

Ernst M (1989) Bio- und Lithostratigraphie des Unter-Aalenium (Opalinumton) in der Tongrube von Feldberg bei Müllheim/Südbaden. Berichte der Naturforschenden Gesellschaft Freiburg i. Br. 77/78: 5–22.

Finger KL (1983) *Acrocythere michelseni*, a new name for *Acrocythere tricostata* Michelsen, 1975 (Ostracoda). Micropaleontology 28(1): 110–110. https://doi.org/10.2307/1485654

Fischer W (1961) Neue Arten der Ostracoden-Gattung *Polycope* Sars 1865 aus dem oberen Lias (Württemberg). Neues Jahrbuch für Geologie und Paläontologie, Monatshefte 1961(10): 497–501.

Fischer W (1962) Ostracoden der Gattungen *Monoceratina* Roth 1928, *Cytheropteron* G. O. Sars 1865 und andere im Lias zeta Schwabens. Neues Jahrbuch für Geologie und Paläontologie, Abhandlungen 114(3): 333–345.

Franz M (1986) Vergleichende Ökologie und Fazies der Oolithhorizonte im Bajocium Südwestdeutschlands. PhD Thesis, Heidelberg University, 313 pp.

Franz M, Beher E, Dietl G (2014) The Bathonian and Early Callovian Ostracoda of Baden-Wuerttemberg, southern Germany. Neues Jahrbuch für Geologie und Paläontologie, Abhandlungen 274(2/3): 149–185. https://doi.org/10.1127/0077-7749/2014/0431

Franz M, Ebert M, Stulpinaite R (2018) Aalenian – Early Bajocian (Middle Jurassic) ostracods from the Heiligenbach section near Hechingen, Swabian Alb (SW Germany). Palaeodiversity 11: 59–105. https://doi.org/10.18476/pale.11.a5

Franz M, Nitsch E (2009) Zur lithostratigraphischen Gliederung des Aalenium in Baden-Württemberg. LGRB Informationen 22: 123–146.

Franz M, Tesakova E, Beher E (2009) Documentation and revision of the index ostracods from the Lower and Middle Jurassic in SW Germany according to Buck (1954). Palaeodiversity 2: 119–167.

Fürsich FT, Werner W (1988) The Upper Jurassic Bivalvia of Portugal. Part I. Palaeotaxodonta and Pteriomorphia (Arcoida and Mytiloida). Comunicações dos Serviços Geológicos de Portugal 73: 103–144.

Géczy B (1967) Ammonoides jurassiques de Csernye, Montagne Bakony, Hongrie – Part II (excl. Hammatoceratidae). Geologica Hungarica, Series Palaeontologica 35: 1–413.

Gramann F (1963) *Liasina* n. gen. (Ostracoda) aus dem deutschen Lias. Geologisches Jahrbuch 82: 65–73.

Gründel J (1975) Zur Entwicklung der Trachyleberididae (Ostracoda) im Jura. Zeitschrift für Geologische Wissenschaften 3(3): 363–374.

Gründel J, Kozur H (1971) Zur Taxonomie der Bythocytheridae und Tricorninidae (Podocopida, Ostracoda). Monatsberichte der Deutschen Akademie der Wissenschaften zu Berlin 13(10/12): 907–937.

Hahn W (1975) Erläuterungen zu Blatt 7620 Jungingen. 1. Auflage, Geol. Kt. 1:25.000 Baden-Württemberg. Stuttgart (Landesvermessungsamt), 89 pp.

Harlton BH (1933) Micropaleontology of the Pennsylvanian Johns Valley shale of the Ouachita Mountains, Oklahoma, and its relationship to the Mississippian Caney Shaler. Journal of Paleontology 7(1): 3–29.

Henriques MH (1992) Biostratigrafia e Paleontologia (Ammonoidea) do Aaleniana em Portugal (Sector Setentrinal da Bacia Lusitaniana). Ph. D. Thesis. Centro de Geociencias da Universidade de Coimbra, Portugal, 301 + 7 pp.

Hiller D, Kunze T (1979) Der Braune Jura β (Ober-Aalenium) zwischen Nürtingen und Owen (Württemberg). Arbeiten aus dem Institut für Geologie und Paläontologie der Universität Stuttgart NF 74: 141–163.

Hoffmann G (1913) Stratigraphie und Ammoniten-Fauna des Unteren Doggers in Sehnde bei Hannover. Stuttgart, Schweizerbart, 202 pp.

Horn E (1909) Die Harpoceraten der Murchisonae-Schichten des Donau-Rhein-Zuges. Mitteilungen der Grossherzoglichen Badischen Geologischen Landesanstalt 6: 251–323.

Hornibrook N de B (1952) Tertiary and recent marine ostracoda of New Zealand. Their origin, affinities, and distribution. Palaeontological Bulletins, New Zealand Geological Survey 18: 1–82.

Howarth MK (2013) Treatise Online 57. Part L, Revised, Vol. 3B, Chapter 4: Psiloceratoidea, Eodoceratoidea, Hildoceratoidea, 1–139. https://doi.org/10.17161/to.v0i0.4441

Howe HvW, Laurencich L (1958) Introduction to the study of Cretaceous ostracoda. Louisiana State University Press, Baton Rouge, 536 pp.

Hyatt A (1867) The fossil cephalopods of the Museum of Comparative Zoology. Bulletin of the Museum of Comparative Zoology 1: 71–102.

Johnson ALA (1984) The palaeobiology of the bivalve families Pectinidae and Propeamussiidae in the Jurassic of Europe. Zitteliana 11: 3–235.

Jones TR (1849) A monograph of the Entomostraca of the Cretaceous Formation of England. Annual Volumes (Monographs) of the Palaeontographical Society 3(1): [I–IV,] 1–40. https://doi.org/10.1080/02693445.1850.12088362

Jones TR, Sherborn CD (1888) On some ostracoda from the Fullers-Earth oolite and Bradford clay. Proceedings of the Bath Natural History and Antiquarian Field Club 6(3): 249–278.

Kobler HU (1972) Geochemische, sedimentologische und ökologische Untersuchungen im Braunen Jura alpha (Opalinuston) der Schwäbischen Alb. Arbeiten aus dem Geologisch-Paläontologischen Institut der Universität Stuttgart NF 66: 134 pp.

Kochhann KGD, Bergue CT, Falahatgar M, Javidan M, Parent H (2015) Benthic foraminifera and Ostracoda from the Dalichai Formation (Aalenian–Bajocian) at Delma-Dareh, Alborz Mountains, northern Iran. Revista Brasileira de Paleontologia 18(1): 3–20. https://doi.org/10.4072/rbp.2015.1.01

Kovács Z (2009) Toarcian – Aalenian Hammatoceratinae (Ammonitina) from the Gerecse Mts (NE Transdanubian Range, Hungary). Fragmenta Palaeontologica Hungarica 27: 1–72.

Lamarck JPBA de (1819) Histoire naturelle des animaux sans vertèbres. Tome sixième, 1re partie. Déterville et Verdière, Paris, 232 pp.

Ljubimova PS (1955) Ostrakody Mezozoyskikh otlozheniy srednego Povolzhya i obshchego Syrta. Trudy Vsesoyuznogo Neftyanogo Nauchno-Issledovatelskogo Geologo-Razvedochnogo Instituta (VNIGRI), novaya seriya 84: 3–189.

Lörcher E (1939) Die Stratigraphie von Braun-Jura (Dogger) β und Ober-α im südwestlichen Württemberg. Jahreshefte des Vereins für vaterländische Naturkunde in Württemberg 95: 145–230.

Lord AR, Cabral MC, Danielopol DL (2020) Sieve-type normal pore canals in Jurassic ostracods: A review with description of a new genus. Acta Palaeontologica Polonica 65(X): 1–37. https://doi.org/10.4202/app.00632.2019

Luppold FW (2003) Neue und seltene Index-Foraminiferen und -Ostrakoden aus dem Jura NW-Deutschlands. Senckenbergiana lethaea 83(1/2): 15–37. https://doi.org/10.1007/BF03043303

Luppold FW (2012) Ostracod assemblages from the Middle Jurassic of NW Germany with special reference to the Sowerbyi ammonite Zone (Early Bajocian, Jurassic). Neues Jahrbuch für Geologie und Paläontologie, Abhandlungen 266(3): 217–238. https://doi.org/10.1127/0077-7749/2012/0280

Malz H (1966) Zur Kenntnis einiger Ostracoden-Arten der Gattungen *Kinkelinella* und *Praeschuleridea*. Senckenbergiana Lethaea 47(4): 385–404.

Mandelstam MI (1956) Ostracoda. In: Kiparisova, Markovski, Radchenko (Eds) Materialy po Paleontologii. Novie semeystva I rody. Trudy Vsesoyuznogo Neftyanogo Nauchno-Issledovatelskogo Geologicheskogo Instituta (VSEGEI), novaya seriya 12: 87–144.

Mandelstam MI (1959) Ostrakody iz otlozheniy Paleogena sredney Azii. Trudy Vsesoyuznogo Neftyanogo Nauchno-Issledovatelskogo Geologo-Razvedochnogo Instituta (VNIGRI), novaya seriya 136: 442–543.

Martin GPR (1960) 3. Die Mikrofauna. In: Hoffmann K, Martin GPR (Eds) Die Zone des *Dactylioceras tenuicostatum* (Toarcien, Lias) in NW- und SW-Deutschland. Paläontologische Zeitschrift 34: 119–132. https://doi.org/10.1007/BF02987046

Morris PH (1983) Palaeoecology and stratigraphic distribution of Middle Jurassic ostracods from the Lower Inferior Oolite of the Cotswolds, England. Palaeogeography, Palaeoclimatology, Palaeoecology 41: 289–324. https://doi.org/10.1016/0031-0182(83)90092-5

Müller GW (1894) Ostracoden des Golfes von Neapel und der angrenzenden Meeres-Abschnitte. Fauna und Flora des Golfes von Neapel und der angrenzenden Meeres-Abschnitte 21: [I–VIII,] 1–404.

Müller GW (1912) Crustacea: Ostracoda. Das Tierreich 31: [I–XXXIII,] 1–434.

Neale JW (1960) Marine lower Cretaceous ostracoda from Yorkshire, England. Micropaleontology 6(2): 203–224. https://doi.org/10.2307/1484468

Oertli HJ (1957) Ostracodes du Jurassique supérieur du Bassin de Paris (sondage Vernon 1). Revue de l'institut francais du pétrole et annales des combustibles liquides 12(6): 647–695.

Oertli HJ (1959) Malm-Ostrakoden aus dem Schweizerischen Juragebirge. Denkschriften der Schweizerischen Naturforschenden Gesellschaft 83(Abh. 1): [I–IV,] 1–44.

Ohmert W (1981) Fossilfunde aus der Freiburger Umgebung. Der Aufschluss 32: 379–390.

Ohmert W (1993) Zur Entwicklung der Grammoceratinae – Leioceratinae an der Toarcium-Aalenium-Grenze Südwestdeutschlands. Geologische Blätter für Nordost-Bayern und angrenzende Gebiete 43: 143–166.

Ohmert W (1996) 3.5.6.3 Ostracoden. In: Geologisches Landesamt Baden-Württemberg (Ed.) Die Grenzziehung Unter-/Mitteljura (Toarcium/Aalenium) bei Wittnau und Fuentelsaz – Beispiele interdisziplinärer Zusammenarbeit. Informationen 8: 39–40.

Ohmert W (2004) Ammoniten-Faunen im tiefen Unter-Bajocium des Reutlinger Gebiets (mittlere Schwäbische Alb) [mit einem Beitrag zur Ostracoden-Stratigraphie]. Jahreshefte des Landesamts für Geologie, Rohstoffe und Bergbau in Baden-Württemberg 40: 9–141.

Plumhoff F (1963) Die Ostracoden des Oberaalenium und tiefen Unterbajocium (Jura) des Gifhorner Troges, Nordwestdeutschland. Abhandlungen der Senckenbergischen Naturforschenden Gesellschaft 503: 1–100.

Quenstedt FA (1843) Das Flözgebirge Würtembergs. Tübingen (Laupp), [iv +] 558 pp.

Quenstedt FA (1856–1857) Der Jura. Stuttgart (Schweizerbart), [vi +] 842 pp.

Quenstedt FA (1886) Die Ammoniten des Schwäbischen Jura. 2. Der Braune Jura. Stuttgart (Schweizerbart), 441–672.

Reisdorf A, Hostettler B, Jaeggi D, Deplazes G, Bläsi H, Morard A, Feist-Burkhardt S, Waltschew A, Dietze V, Menkveld-Gfeller U (2016) Litho- and biostratigraphy of the 250 m-deep Mont Terri BDB-1 borehole through the Opalinus Clay and bounding formations, St-Ursanne, Switzerland. Mont Terri Project, Technical Report 2016-02, 59 pp.

Rieber A (1922) Die neuen Braun-Jura-Aufschlüsse bei Zillhausen im Vergleich mit den Nachbargebieten. Dissertation Universität Tübingen, 120 pp. [unpubl.]

Rieber A (1961) Drei neue Braunjura β-Profile in der Mittleren Alb. In: Einsele H, Seibold H (Eds) Die geologische Kartierung der Rohrgräben beim Bau der Bodensee-Fernwasserversorgung. Jahreshefte des geologischen Landesamtes Baden-Württemberg 4: 251–254.

Rieber H (1963) Ammoniten und Stratigraphie des Braunjura β der Schwäbischen Alb. Palaeontographica A 122: 1–89.

Roemer F (1857) Die jurassische Weserkette. Zeitschrift der Deutschen Geologischen Gesellschaft 9: 581–728.

Rollier L (1912) Fossiles nouveaux ou peu connus des terrains secondaires (mésozoiques) du Jura et de contrées environnantes. Mémoires de la Société Paléontologique Suisse: 2. partie: 38: 33–148.

Roth R (1928) Monoceratina: A new genus of ostracoda from the Pennsylvanian of Oklahoma. Journal of Paleontology 2(1): 15–19.

Sandoval J, Martinéz G, Ureta S (2020) Hammatoceratidae (Ammonitina) from the Upper Toarcian–Lowermost Bajocian (Jurassic) of the Betic Cordillera (Southern Spain). Palaeontographica A315, 4–6: 1–65. https://doi.org/10.1127/pala/2020/0092

Sanns M, Schweizer V (1987) Zur Fazies und Genese des Ober-Aalenium (Braunjura ß) der südwestlichen Schwäbischen Alb. Jahreshefte des Geologischen Landesamtes in Baden-Württemberg 29: 125–143.

Sars GO (1866) Oversigt af Norges marine ostracoder. Forhandlinger i videnskabs-selskabet i Christiania 1865: 1–130.

Sars GO (1888) Nye bidrag til Kundskaben om Middelhavets invertebratfauna: 4. Ostracoda mediterranea (sydeuropaeiske ostracoder). Archiv for Mathematik og Naturvidenskab 12: 173–324. https://doi.org/10.5962/bhl.title.10252

Sars GO (1923) An account of the crustacean of Norway with short descriptions and figures of all the species, vol. 9 (Ostracoda), parts 3–4: 33–72.

Sars GO (1925) An account of the crustacean of Norway with short descriptions and figures of all the species, vol. 9 (Ostracoda), parts 5–12: 73–208.

Sars GO (1926) An account of the crustacean of Norway with short descriptions and figures of all the species, vol. 9 (Ostracoda), parts 13–14: 209–240.

Schlotheim EF von (1820) Die Petrefactenkunde auf ihrem jetzigen Standpunkte durch die Beschreibung seiner Sammlung versteinerter und fossiler Überreste des Thier- und Pflanzenreichs der Vorwelt erläutert. Gotha (Becker'sche Buchhandlung), [LXI +] 437 pp.

Schmierer T (1925) Blatt Hechingen (Bodelshausen) Nr. 3640. Erläuterungen zur Geologischen Karte von Preußen und benachbarten deutschen Ländern. Preußische Geologische Landesanstalt, Berlin, 68 pp.

Schmierer T (1926) Blatt Thanheim (Balingen). Nr. 3648. Erläuterungen zur Geologischen Karte von Preußen und benachbarten deutschen Ländern. Preußische Geologische Landesanstalt, Berlin, 64 pp.

Schmidt M (1933) Blatt Mössingen (Nr. 109). Erläuterungen zur geologischen Spezialkarte von Württemberg. Württembergisches Statistisches Landesamt, Stuttgart, 184 pp.

Schulbert C (2001) Die Ammonitenfauna und Stratigraphie der Tongrube Mistelgau bei Bayreuth (Oberfranken). Beihefte zu den Berichten der Naturwissenschaftlichen Gesellschaft Bayreuth e. V. 4: 1–20.

Schweigert G, Etter W (2008) On the true nature of the supposed urodelan amphibian *Boomgaardia* v. Huene, 1948 from the Middle Jurassic of SW Germany – a tanaidacean! – Neues Jahrbuch für Geologie und Paläontologie, Abhandlungen 248: 123–127. https://doi.org/10.1127/0077-7749/2008/0248-0123

Sheppard LM (1981) Middle Jurassic Ostracoda from Southern England and Northern France. PhD Thesis, University of London, [XVIII +] 214 pp. [unpublished]

Sowerby J (1812–1822) The Mineral Conchology of Great Britain. Meredith, London 1(1): 9–32 (1812); 1(2): 33–96 (1813); 1(3): 97–178 (1814); 179–236 (1815); 2(1): 1–28 (1815); 2(2): 29–116 (1816); 2(3): 117–194 (1817); 2(4): 195–239 (1818); 3(1): 1–40 (1818); 3(2): 41–98 (1819); 3(3): 99–126 (1820); 3(4): 127–186; 4(1): 1–16 (1821); 4(2): 17–104 (1822).

Sowerby J de C (1822–1845) The Mineral Conchology of Great Britain. Meredith, London, 4(3): 105–114 (1822); 4(4): 115–151 (1823); 5(1) 1–64 (1823); 5(2): 65–138 (1824); 5(3): 139–171 (1825);

6(1): 1–86 (1826); 6(2): 87–156 (1827); 6(3): 157–200 (1828); Preface to general indices: 239–250 (1835); Alphabetical index to vol.1–6: 1–11 (1840); 7(1): 1–8 (?1840); 7(2): 9–16 (1841): 7(3): 17–24 (1843); 7(4): 25–56 (1844); 7(5): 57–80 (1846).

Spath LF (1936) On Bajocian ammonites and belemnites from eastern Persia (Iran). Palaeontologica Indica. Memoirs of the Geological Survey of India. New series 22, Memoir 3: 1–21.

Stahlecker R (1926) Brauner Jura und Tektonik im Kirchheim-Urach-er Vulkangebiet. Neues Jahrbuch für Mineralogie, Geologie und Paläontologie. Beilage-Band 54: 157–258.

Stahlecker G (1934) Stratigraphie und Tektonik des Braunen Jura im Gebiet des Stuifen und Rechberg. Jahreshefte des Vereins für vaterländische Naturkunde in Württemberg 90: 59–121.

Swain FM (1952) Ostracoda from wells in North Carolina, part 2: Mesozoic ostracoda. United States Geological Survey professional paper 234 B: [I–III,] 59–93. https://doi.org/10.3133/pp234B

Sylvester-Bradley PC (1948) Bathonian ostracods from the Boueti bed of Langton Herring, Dorset. Geological Magazine 85(4): 185–204. https://doi.org/10.1017/S001675680007309X

Tesakova EM (2017) Biostratigraphie du Jurassique moyen des sondages Benken et Schlattingen-1 (Nord de la Suisse) établie sur la base de la répartition des ostracodes. NAGRA NAB 17–41, 79 pp.

Triebel E (1950) *Camptocythere*, eine neue Ostracoden-Gattung aus dem Dogger Norddeutschlands. Senckenbergiana 31(3/4): 197–208.

Triebel E (1951) Einige stratigraphisch wertvolle Ostracoden aus dem höheren Dogger Deutschlands. Abhandlungen der Senckenbergischen Naturforschenden Gesellschaft 485: 87–101.

Triebel E, Bartenstein H (1938) Die Ostracoden des Deutschen Juras – 1: Monoceratina-Arten aus dem Lias und Dogger. Senckenbergiana 20(6): 502–518.

Triebel E, Klingler W (1959) Neue Ostracoden-Gattungen aus dem deutschen Lias. Geologisches Jahrbuch 76: 335–371.

Tröster J (1987) Biostratigraphie des Obertoarcium und der Toarcium/Aalenium-Grenze der Bohrungen Weiach, Beznau, Riniken und Schafisheim (Nordschweiz). Eclogae geologicae Helvetiae 80(2): 431–447.

Ureta Gil S (1983) Bioestratigrafia y Paleontologia (Ammonitina) del Aaleniense en el sector noroccidental de la Cordillara Iberica. Unpublished Ph. D. Thesis, Universidad Complutense de Madrid, [VIII +] 452 pp.

Whatley RC (1970) Scottish Callovian and Oxfordian Ostracoda. Bulletin of the British Museum (Natural History), Geology 19(6): 299–358.

Whittaker JE, Hart MB (2009) Ostracods in British Stratigraphy. The Micropalaeontological Society, Special Publications, London [The Geological Society], 485 pp.

Wienholz E (1967) Neue Ostracoden aus dem norddeutschen Callov. Freiberger Forschungshefte, Reihe C (Paläontologie) 213: 23–51.

Young G, Bird J (1828) A geological survey of the Yorkshire coast: describing the strata and fossils occurring between the Humber and the Tees, from the German Ocean to the plain of York. Whitby [published by the authors].

Zieten CH von (1830–1833) Die Versteinerungen Württembergs. Stuttgart (Schweizerbart), 102 pp.

Appendices

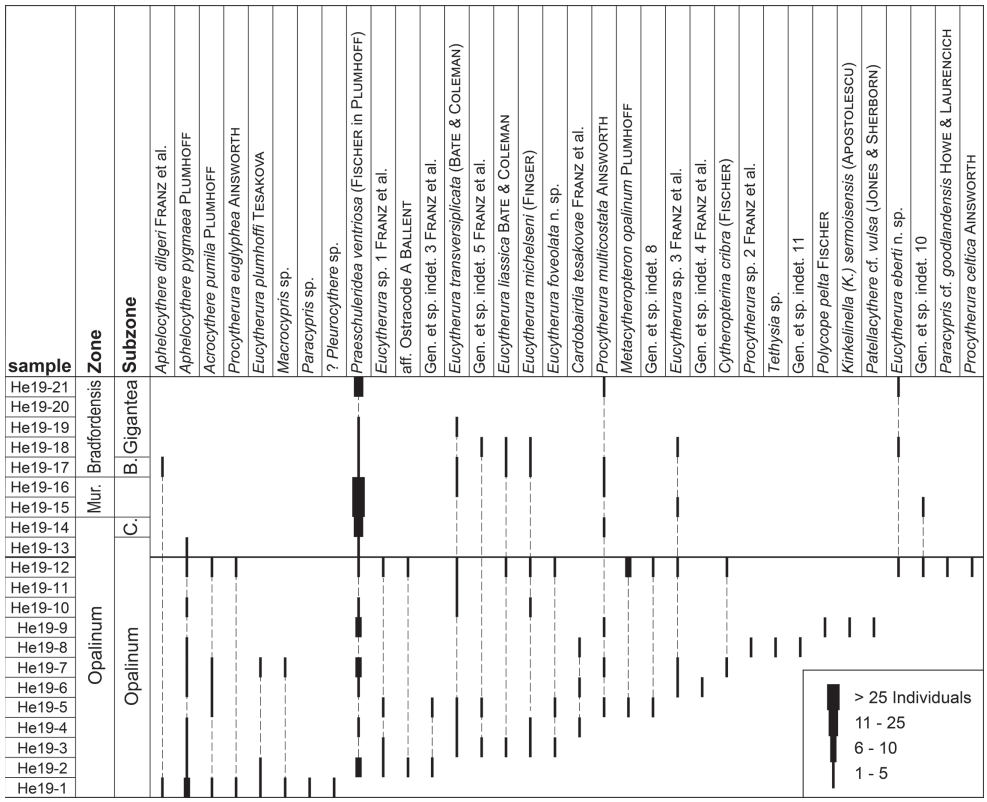

Appendix 1. Range chart of all taxa in the Opalinuston Formation determined to the specific level. Single representatives of a genus are also listed, even when the species in unkown.

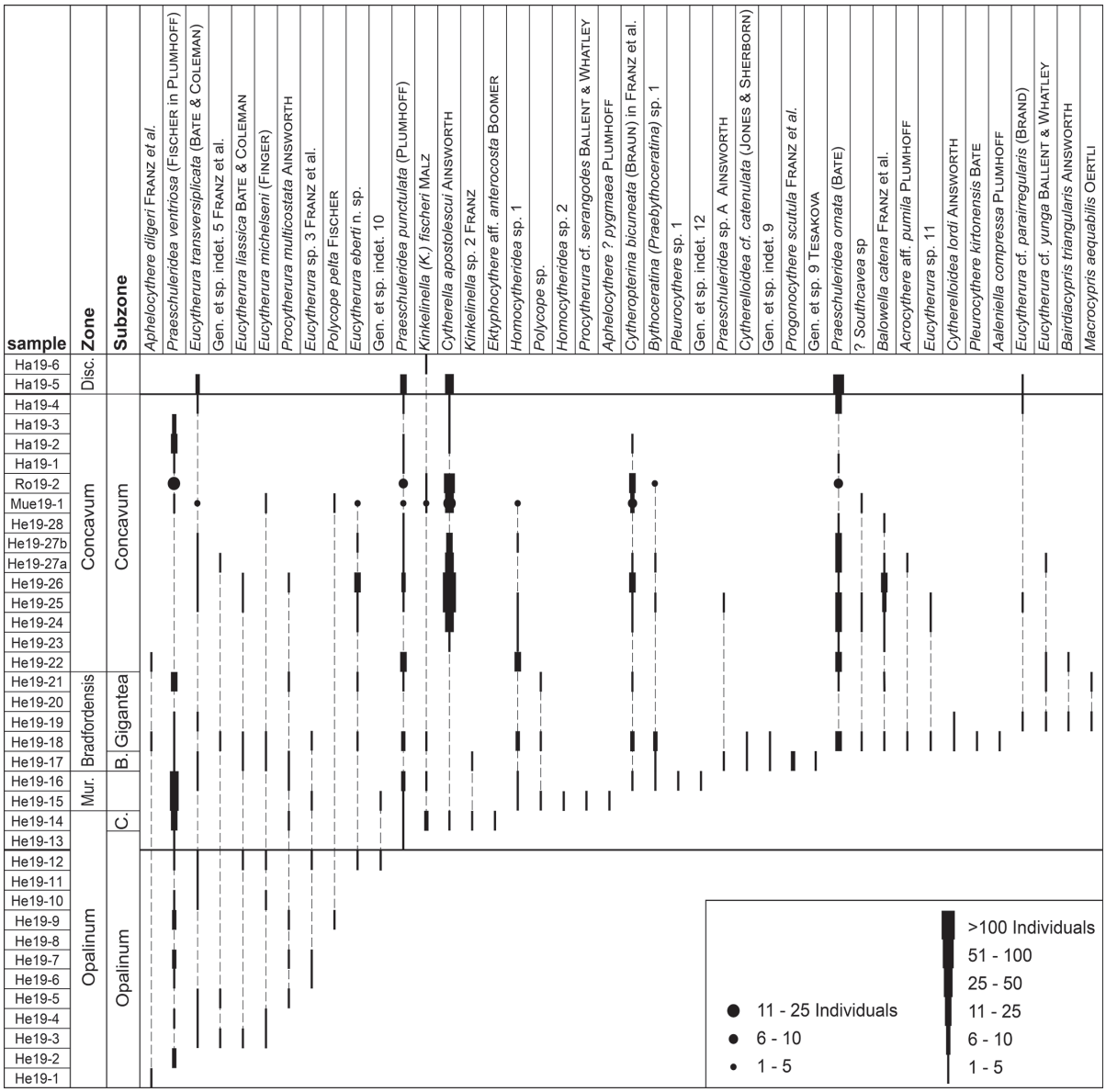

Appendix 2. Range chart of all taxa in the Achdorf Formation determined to the specific level. Species persisting from the Opalinuston Formation are also shown.

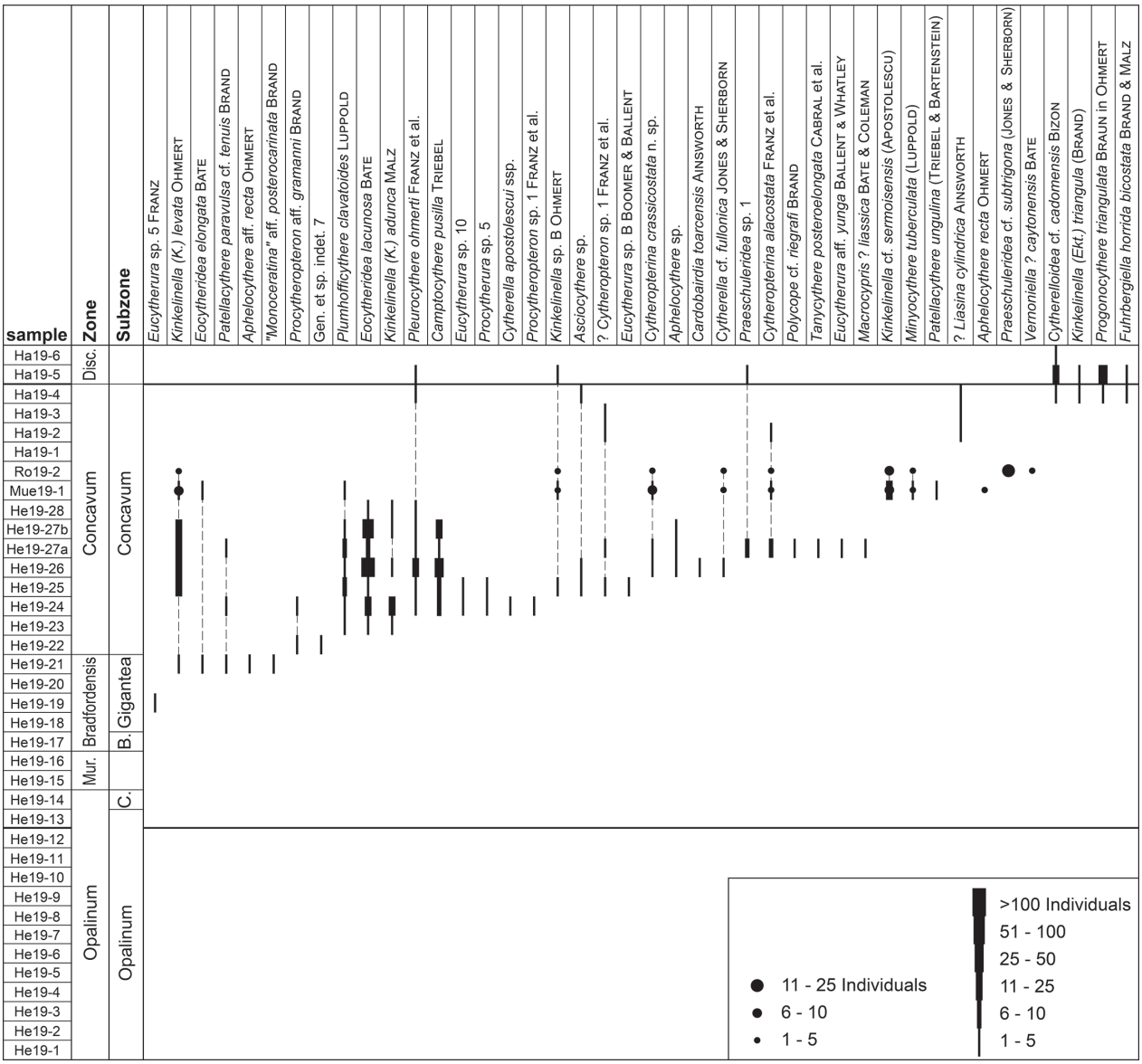

Appendix 2. Continued.

Addendum

After submission of the original draft of this manuscript, the "Comptum" Subzone of the Opalinum Zone has been renamed Bifidatum Subzone, and the number of distinguished biohorizons in the Opalinum Zone (Opalinum and Bifidatum subzones) (Fig. 26) has remarkably increased (see Dietze V, Gräbenstein S, Franz M, Schweigert G, Wetzel A (2021) The Middle Jurassic Opalinuston Formation (Aalenian, Opalinum Zone) at its type locality near Bad Boll and adjacent outcrops (Swabian Alb, SW Germany). Palaeodiversity 15: 14–113, published online 05 March 2021). These changes could not be included in the present paper and have to be considered.

Zitteliana 95, 2021, 57–94 | DOI 10.3897/zitteliana.95.56222

SNSB Bayerische Staatssammlung für Paläontologie und Geologie

ZITTELIANA
An International Journal of Paleontology and Geobiology

Biostratigraphy and sequence stratigraphy of the Toarcian Ludwigskanal section (Franconian Alb, Southern Germany)

Gernot Arp[1], Sebastian Gropengießer[1], Christian Schulbert[2], Dietmar Jung[3], Andreas Reimer[1]

1 *Georg-August-Universität Göttingen, Geowissenschaftliches Zentrum, Abteilung Geobiologie, Goldschmidtstraße 3, 37077 Göttingen, Germany*
2 *Friedrich-Alexander-Universität Erlangen-Nürnberg, GeoZentrum Nordbayern, PaläoUmwelt, Loewenichstraße 28, 91054 Erlangen, Germany*
3 *Bayerisches Landesamt für Umwelt, Geologischer Dienst, Hans-Högn-Str. 12, 95030 Hof/Saale, Germany*

http://zoobank.org/257141A1-1F3E-47AE-8D6F-8F08FDF4CBA0

Corresponding author: Gernot Arp (garp@gwdg.de)

Academic editor: A. Nützel ♦ **Received** 6 July 2020 ♦ **Accepted** 2 February 2021 ♦ **Published** 17 June 2021

Abstract

Extensive construction work at the canal cutting of the Ludwigskanal near Dörlbach, Franconian Alb, provided the opportunity to re-investigate a scientific-historical and biostratigraphically important reference section of the South-German Toarcian. The 16 m thick section, described bed by bed with respect to lithology and macrofossils, starts within the Upper Pliensbachian Amaltheenton Formation, covers the Toarcian Posidonienschiefer and Jurensismergel Formation, and ends in basal parts of the Opalinuston Formation. Carbonate contents are high in the Posidonienschiefer and successively decline within the Jurensismergel to basal parts of the Opalinuston. The high carbonate contents in the Posidonienschiefer are associated with comparatively low organic carbon contents. However, organic carbon contents normalized to the silicate fraction are similarily high if compared to other regions in Germany. Only the persistence of high organic carbon levels into middle parts of the Upper Toarcian differs from those of most regions in central Europe.

Ammonite biostratigraphy indicates a thickness of >9 m for the Upper Pliensbachian, 1.15–1.20 m for the Lower Toarcian, 5.04 m for the Upper Toarcian, and >0.5 m for the Lower Aalenian. Despite the low sediment thickness, all Toarcian ammonite zones and almost all subzones are present, except for major parts of the Tenuicostatum Zone and the Fallaciosum Subzone.

On the basis of discontinuities, condensed beds, and correlations with neighbouring sections in Southern Germany, a sequence stratigraphic interpretation is proposed for the Toarcian of this region: (i) The Posidonienschiefer Formation corresponds to one 3rd order T-R sequence, from the top of the Hawskerense Subzone to a fucoid bed at the top of the Variabilis Subzone, with a maximum flooding surface at the top of the Falciferum Zone. (ii) The Jurensismergel Formation exhibits two 3rd order T-R sequences: The first ranges from the basis of the Illustris Subzone (i.e., the Intra-Variabilis-Discontinuity) to the top of the Thouarsense Zone, with a maximum flooding surface within the Thouarsense Zone. The "belemnite battlefield" reflects a transgressive "ravinement surface" within the first Jurensismergel Sequence, not a maximum regression surface at its basis. The second sequence extents from the erosive basis of the Dispansum Zone to the top of the Aalensis Subzone, with a maximum flooding surface at the Pseudoradiosa-Aalensis Zone boundary. Finally, the Opalinuston starts with a new sequence at the basis of the Torulosum Subzone. Transgressive system tracts of these 3rd order T-R sequences are commonly phosphoritic, while some regressive system tracts show pyrite preservation of ammonites. The maximum regression surfaces at the basis of the Toarcian and within the Variabilis Zone reflect a significant submarine erosion and relief formation by seawater currents, while this effect is less pronounced at the basis of the Dispansum Zone and basis of the Torulosum Subzone (i.e., the boundary Jurensismergel-Opalinuston Formation).

Kurzfassung

Umfangreiche Bauarbeiten am Kanaleinschnitt des Ludwigskanals bei Dörlbach auf der Fränkischen Alb boten die Gelegenheit ein wissenschaftlich-historisch und biostratigraphisch wichtiges Referenzprofil des süddeutschen Toarciums neu zu untersuchen. Das 16 m mächtige Profil, dessen Lithologie und Makrofossilien Schicht für Schicht beschrieben werden, beginnt innerhalb der Amaltheenton-Formation des Oberpliensbachiums, umfasst die Posidonienschiefer- und Jurensismergel-Formationen des Toarciums und endet mit basalen Teilen der Opalinuston-Formation. Die Karbonatgehalte sind im Posidonienschiefer hoch und nehmen innerhalb des Juren-

Copyright *Gernot Arp et al.* This is an open access article distributed under the terms of the Creative Commons Attribution License (CC BY 4.0), which permits unrestricted use, distribution, and reproduction in any medium, provided the original author and source are credited.

PENSOFT®

sismergels sukzessive bis in basale Teile der Opalinuston-Formation ab. Die hohen Karbonatgehalte im Posidonienschiefer sind mit vergleichsweise niedrigen organischen Kohlenstoffgehalten verbunden. Die auf die Silikatfraktion normierten organischen Kohlenstoffgehalte sind jedoch im Vergleich zu anderen Regionen in Deutschland ähnlich hoch. Lediglich die anhaltend hohen organischen Kohlenstoffgehalte bis in den mittleren Teil des Obertoarciums unterscheiden sich von denen der meisten Regionen Mitteleuropas.

Biostratigraphisch verwertbare Ammoniten-Funde belegen eine Mächtigkeit von >9 m für das Obere Pliensbachium, 1.15–1.20 m für das Untere Toarcium, 5.04 m für das Obere Toarcium, und >0.5 m für das Untere Aalenium. Trotz der geringen Sedimentmächtigkeiten sind alle Ammoniten-Zonen und nahezu alle Subzonen nachweisbar, mit Ausnahme großer Teile der Tenuicostatum-Zone und der Fallaciosum-Subzone.

Auf Grundlage von Diskontinuitäten, kondensierten Horizonten und Korrelationen mit Nachbarprofilen in Süddeutschland wird eine sequenzstratigraphische Interpretation für das Toarcium dieser Region entwickelt: (i) Die Posidonienschiefer-Formation entspricht einer Sequenz dritter Ordnung, vom Top der Hawskerense-Subzone bis zu einem Fucoidenhorizont am Top der Variabilis-Subzone, mit einer maximalen Überflutung am Top der Falciferum-Zone. (ii) Die Jurensismergel-Formation weißt zwei Sequenzen dritter Ordnung auf: Die erste reicht von der Basis der Illustris-Subzone (d.h. der Intra-Variabilis-Diskontinuität) bis zum Top der Thouarsense-Zone. Das „Belemnitenschlachtfeld“ spiegelt einen transgressiven „Auswaschungshorizont“ innerhalb der ersten Jurensismergel-Sequenz wider, keinen Meeresspiegeltiefststand an ihrer Basis. Die zweite Sequenz reicht von der erosiven Basis der Dispansum-Zone bis zum Top der Aalensis-Subzone, mit einer maximalen Überflutung an der Grenze Pseudoradiosa-Aalensis Zone. Die Opalinuston-Formation beginnt schließlich mit einer neuen Sequenz an der Basis der Torulosum-Subzone. Transgressive Phasen dieser Sequenzen dritter Ordnung sind häufig phosphoritisch ausgebildet, während regressive Phasen eine Pyriterhaltung von Ammoniten aufzeigen. Die Meeresspiegeltiefststände nahe der Basis des Toarciums und innerhalb der Variabilis-Zone sind mit einer deutlichen submarinen Erosion und Reliefbildung durch grundberührende Meeresströmungen verbunden. Dieser Effekt ist an der Basis der Dispansum-Zone und Torulosum-Subzone (d.h. der Formationsgrenze Jurensismergel-Opalinuston) weniger stark ausgeprägt.

Keywords

Ammonoidea, Jurensismergel, Lower Jurassic, Posidonienschiefer, sealevel changes, Southern Germany, stratigraphy

Schlüsselwörter

Ammonoidea, Jurensismergel, Unterer Jura, Posidonienschiefer, Meeresspiegel-Schwankungen, Süddeutschland, Stratigraphie

Introduction

The Franconian Alb is a classical region of Jurassic geosciences in Europe, and specifically the area of Altdorf SE of Nürnberg has been of great importance in the early times of palaeontology (von Freyberg 1958a, b, c, 1972; Schmidt-Kaler 1974; Mayr 1995; Kursawe 1995, 1996; Mäuser 2001). Indeed, the construction of the Ludwigskanal cutting at Dörlbach south of Altdorf (Fig. 1) lead 1840–1841 to the first large-scale temporary exposure of the Schwarzjura-Group in Southern Germany and corresponding fossil discoveries such as one of the worldwide first finding of a large, 1.6 m long, *Temnodontosaurus* skull (von Freyberg 1972). Furthermore, the Ludwigskanal outcrop delivered many invertebrate type fossils, among them a number of ammonoids, described in the monographs of Quenstedt (1845–1849, 1851–1852, 1856–1858, 1865–1866, 1872–1875, 1876, 1881–1884, 1882–1885a, b).

However, the only contemporary description of the exposed strata was given by Beyschlag (1841), and it took over eight decades until more details on the section were provided by Reuter (1927), Kolb (1964) and Urlichs (1971), all of them focussing on the Posidonienschiefer Formation. Despite these previous descriptions, and despite that the sediment succession of the Schwarzjura Group in this region is generally well known (Reuter 1927; Meyer and Schmidt-Kaler 1996; Bloos et al. 2005), a number of crucial stratigraphic details are subject to controversial views and remained unclear to date. Above all, this applies to the extent and position of discontinuities and condensed beds. Consequently, no sequence stratigraphic interpretation of the Toarcian has been suggested for this region, except for the Posidonienschiefer (Röhl and Schmid-Röhl 2005).

Slope failure at the Ludwigskanal cutting near Dörlbach and following extensive construction activities re-exposed the section in 2010–2012, allowing a re-investigation of the complete succession from the middle part of the Amaltheenton, through the Posidonienschiefer and Jurensismergel, to the basis of the Opalinuston Formation (Fig. 2A, B). An overview and preliminary description of the new exposure was already given in Arp et al. (2014). Gastropods of the Amaltheenton were described by Gründel and Nützel (2015).

The aim of the present study is to provide a detailed description of the lithologic succession and its macrofossils.

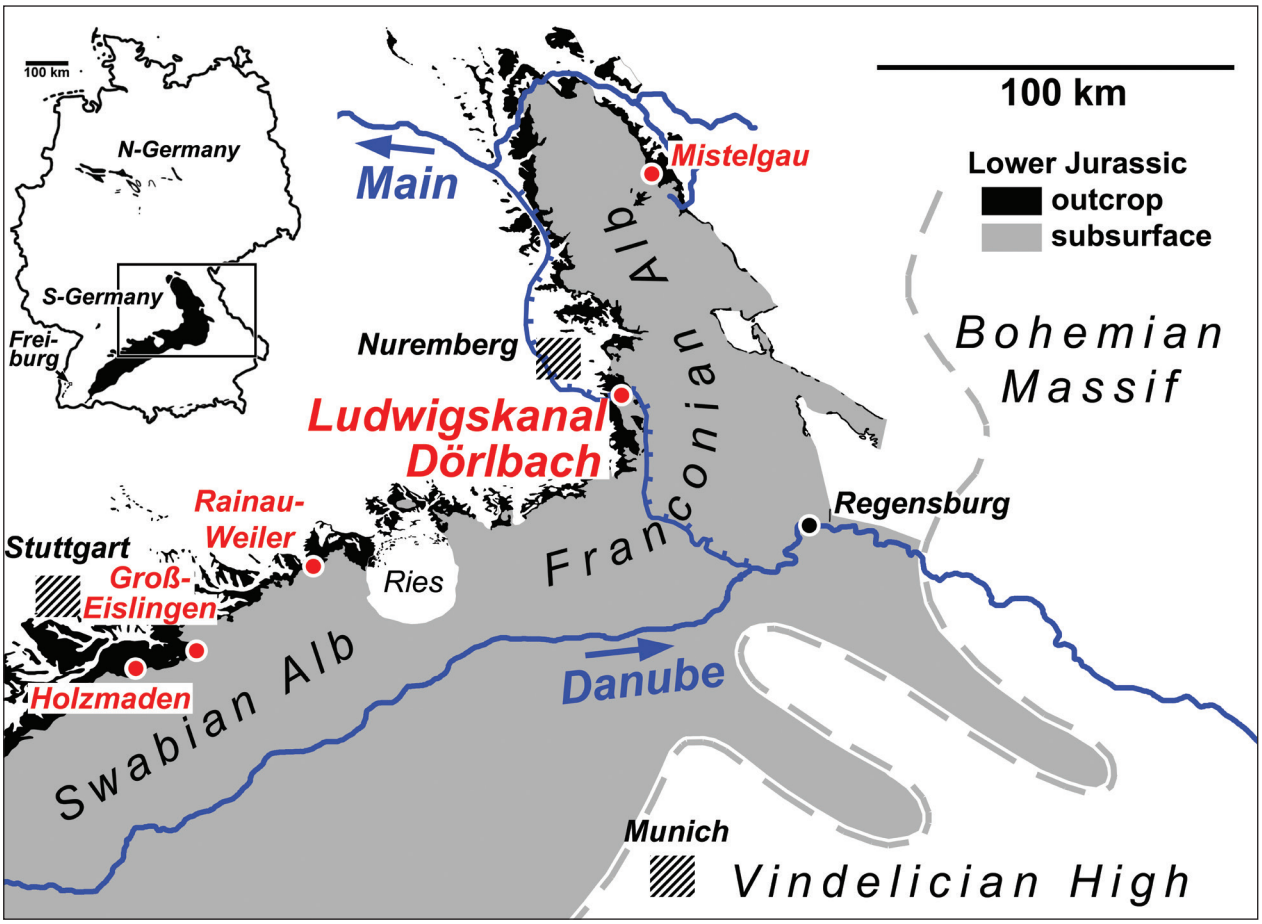

Figure 1. Geographic and geological overview with the location of the Ludwigskanal section (49°21.238938N, 11°21.534298E) at the western margin of the Franconian Alb (S-Germany, Bavaria). Outcrop and subsurface deposits of Lower Jurassic after Freudenberger and Schwerd (1996).

The high-resolution biostratigraphy and sequence stratigraphy may form a basis for further investigations on seawater temperatures ($\delta^{18}O$ of low-Mg calcite skeletons), seawater currents, sealevel changes, and causes for the persistence of the Toarcian Oceanic Anoxic Event (T-OAE; Jenkyns 1988) in the eastern part of the NW European Epicontinental Seaway. The present study focusses on the description and stratigraphic interpretation of this section.

Location and geological overview

The Ludwigskanal cutting is located in Southern Germany, Bavaria, approximately 20 km ESE of Nürnberg (Fig. 1) in the western foreland of the middle Franconian Alb. The village Dörlbach lies 1 km W of the cutting, while Altdorf/Mfr. is located 3 km N of it. The coordinates of the section, located on the topographic map 1:25000, sheet 6634 Altdorf b. Nürnberg, are 49°21.238938N, 11°21.534298E. The region is part of the South German Scarplands (Peterek and Schröder 2010 and references therein), and the escarpment of the Franconian Alb, i.e., the edge of the Upper Jurassic limestone plateau, is located approximately 5 km E of the investigated section (Schmidt-Kaler 1974).

Geologically, the deep subsurface of the region is formed by high-grade metamorphics and plutonites of the Variscan basement (Moldanubian gneiss and granite). These basement rocks are overlain by a Mesozoic cover sequence starting with Triassic fluvial coarse siliciclastics of the Buntsandstein (63 m), Muschelkalk (45 m) and Keuper Group (270 m) (drilling Eschertshofen: Salger and Schmid 1982). After a stratigraphic gap comprising the Rhaetian, the Lower Jurassic Schwarzjura Group (47–69 m) starts with fluvial arkoses of the Bayreuth Formation, followed by marine near-shore sandstones of the Gryphaeensandstein Formation, condensed dolomitic limestones of the Numismalismergel Formation, monotonous claystones of the Amaltheenton Formation, condensed bituminous limestones and shales of the Posidonienschiefer Formation, and finally fossiliferous marls of the Jurensismergel Formation (Schmidt-Kaler 1974; Salger and Schmid 1982; Fig. 3). The Middle Jurassic Braunjura Group (125 m) is composed of marine, monotonous claystones (Opalinuston Formation), iron-ore-bearing sandstones (Eisensandstein Formation) and a condensed, highly fossiliferous succession of iron-oolites and glauconitic siltstones (Sengenthal Formation). Up to 70 m of the Upper Jurassic Weißjura Group are preserved

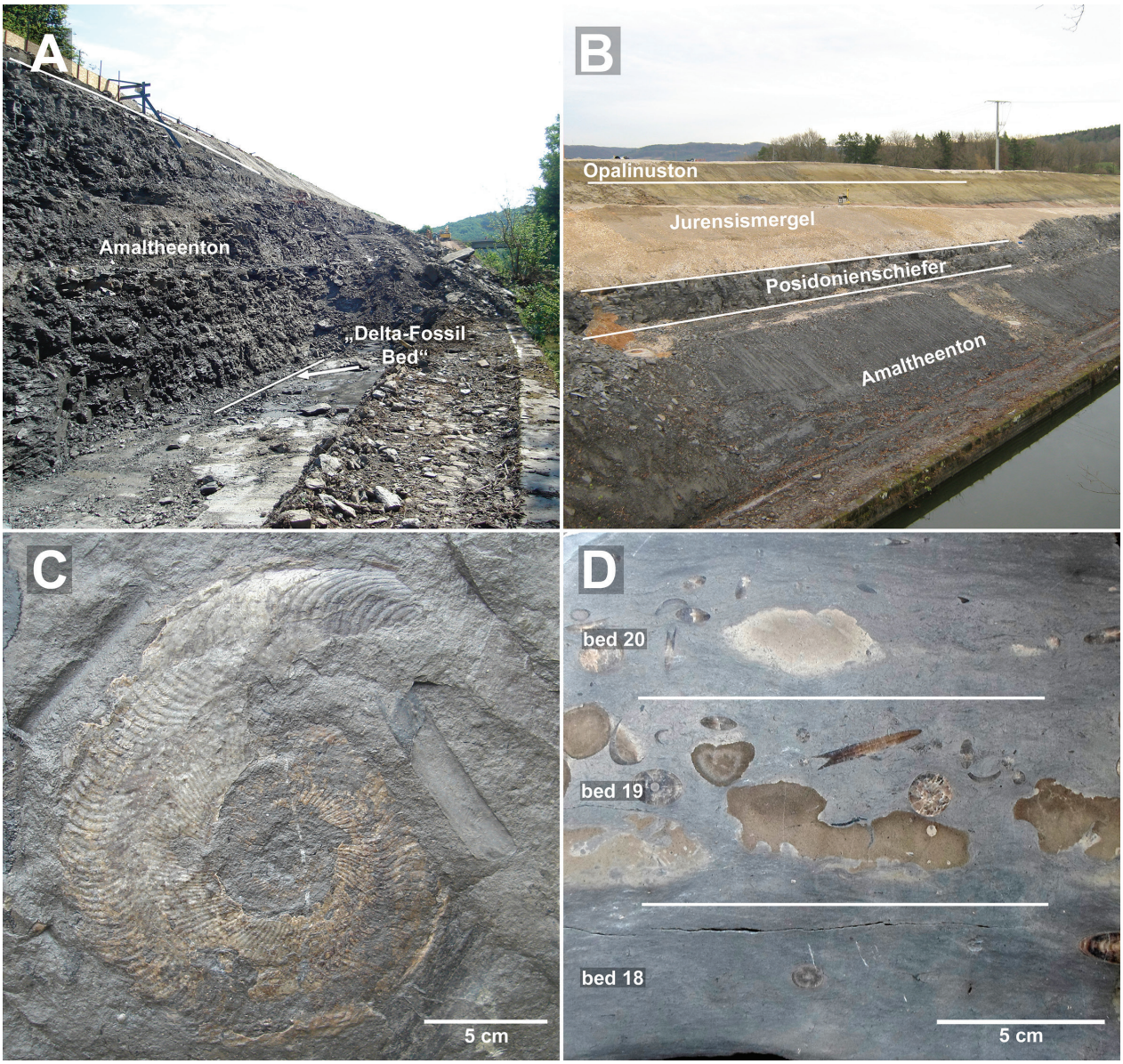

Figure 2. Field images of the Ludwigskanal section and ammonites. **A.** Western section of the canal cutting, showing basal parts of the exposure, from the "Delta-Fossil Bed" to the basis of the Posidonienschiefer Formation. **B.** Eastern section of the canal cutting, showing the Amaltheenton, Posidonienschiefer, Jurensismergel, and basal parts of the Opalinuston Formation. **C.** *Harpoceras falciferum* (Sowerby), "Falciferum Shale", bed 10, field image (specimen not recovered). **D.** Polished section of rock sample, from "Fucoid Bed" (bed 17), basal marl of Jurensismergel (bed 18) and "Belemnite Battlefield" (bed 19) to the "Main Phosphorite Bed" (bed 20).

in the Altdorf region, with bedded marine limestones and sponge-microbialite mounds, some of them dolomitized (Schmidt-Kaler 1974). Subaerial exposure, erosion and karstification during Cretaceous and Tertiary times led to the present-day landscape (Wagner 1960; Hofbauer 2001; Peterek and Schröder 2010).

Material and methods

Fieldwork and sampling was carried out on 16 days between September 2010 and August 2014. Lithological descriptions are based on field observation and binocular observations on hand specimens, supplemented by 21 thin sections between 5 × 7.5 cm and 7.5 × 10 cm in size, and about 80 µm thick.

Total carbon (C_{tot}), nitrogen (N_{tot}), and sulfur (S_{tot}) of bulk rock samples were analysed with a Euro EA 3000 Elemental Analyser (HEKAtech, Wegberg, Germany) applying 2,5-bis(5-tertbenzoxazol-2-yl)thiophene (BBOT) and atropine sulfate monohydrate (IVA Analysetechnik, Meerbusch, Germany) as reference material. Organic and carbonate carbon (C_{org}, C_{carb}) contents were determined by a LECO RC612 (Leco, St. Joseph, MI, USA) multi-phase carbon and water analyser. For calibration, Leco synthetic carbon (1 and 4.98 carbon %) and Leco calcium carbonate (12 carbon %) standards were used. All analyses were performed as duplicates. Analytical accuracy of all analyses was bet-

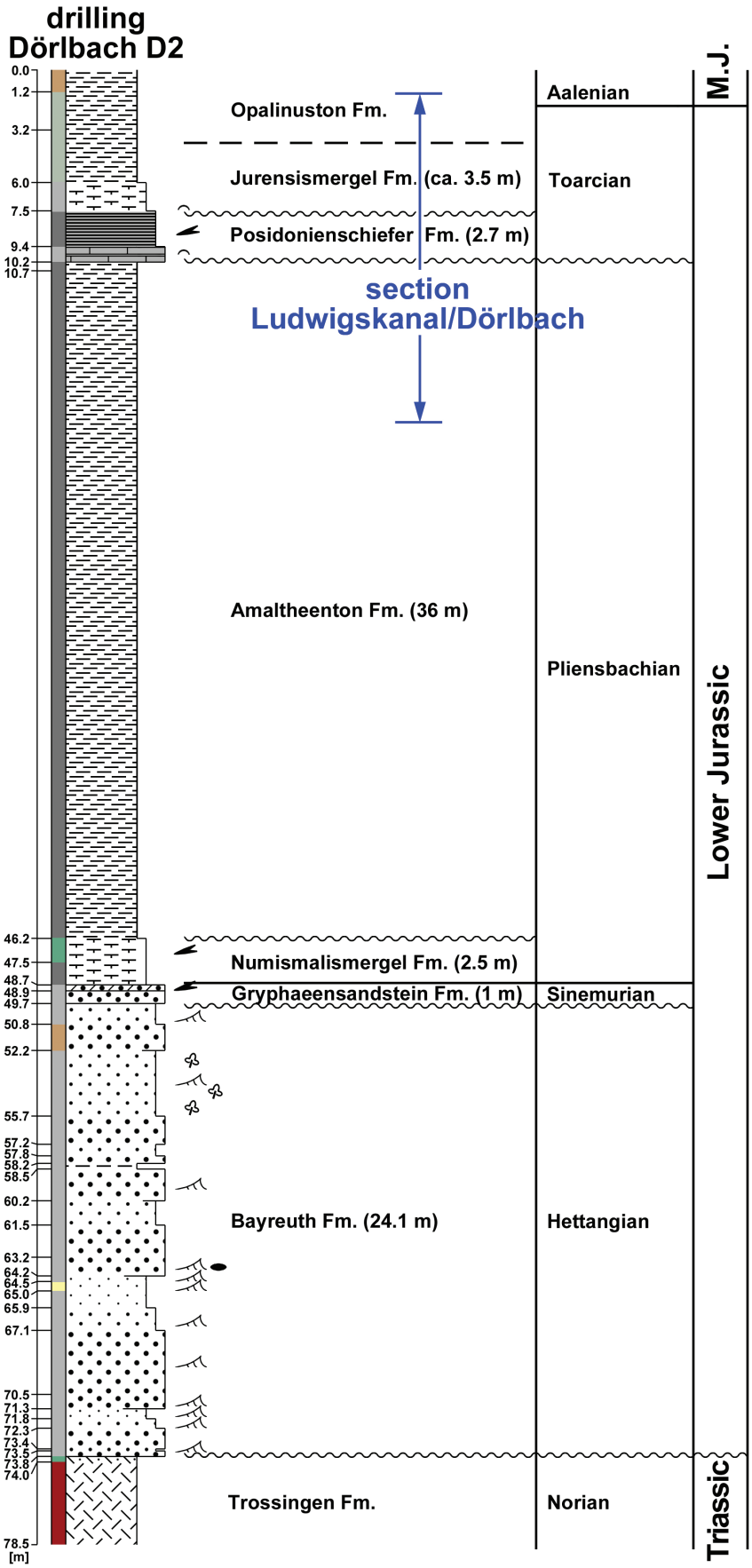

Figure 3. Overview of the Lower Jurassic Schwarzjura Group, Drilling Dörlbach D2 (top ground surface 436 m a.s.l., 49°21.679543N, 11°21.797843E; topographic map sheet 6634 Altdorf b. Nürnberg; unpublished drilling report), ca. 750 m N of the Ludwigskanal/Dörlbach section. For legend see Fig. 7.

ter than 3%. The carbonate-free fraction was calculated from the total weight minus the $CaCO_3$ and C_{org} content.

Biostratigraphy is based on approximetaly 425 determinable ammonites that were recovered *in situ*. Few additional ammonites recovered by private fossil collectors were taken into account. Ammonite determinations follow the systematic descriptions in Howarth (1958, 1978, 1992), Gabilly (1976a, b), Schulbert (2001a), Rulleau (2007), Hoffmann (2010, 2015), Arp (2010), and Di Cencio and Weis (2020).

Repository: The material is stored in the Museum and Collection of the Geoscience Centre, University of Göttingen, under the numbers GZG.INV.45641–GZG.INV.45644 and GZG.INV.70496–GZG.INV.70650.

Data Availability Statement: All data used in this publication are stored on the Göttingen Research Online Data repository (https://doi.org/10.25625/8PLFNS).

Figure captions: unless otherwise noted, all specimen are coated by ammonium chloride prior to photography. Abbreviations: diameter (d), diameter of penultimate half whorl (di), umbilical width (u), whorl height (wh), whorl breadth (wb), primary ribs per half whorl (rb/2).

Results

Description of the section

Informal bed names are given in quotation marks. From bottom to top:

Amaltheenton Formation:

Bed 1: >100 cm — bluish-grey, well bedded claystone;

Bed 2: 0–15 cm — "Septaria Bed": grey marlstone concretions with mm-thick, calcite-cemented shrinkage cracks;

Bed 3: 25 cm — bluish-grey, well bedded claystone with scattered cm-sized septarian concretions; ammonoids: at the top one juvenile *Pleuroceras solare* (Phillips);

Bed 4: 10 cm — "Delta-Fossil Bed": bluish-grey, fissile, calcareous claystone to argillaceous marl with abundant ammonoids, belemnites, echinoderm remains and bivalves; lower part of the bed with reworked bluish-grey marlstone concretions with borings and serpulid tubes; ammonoids: *Pleuroceras spinatum* (Bruguière); *Amaltheus* sp. (juvenile), *Pleuroceras solare* (Phillips) (within reworked concretions; Fig. 10: 1), *Pleuroceras solare* var. *solitarium* (Simpson) (within reworked concretions; Fig. 10: 2), *Amauroceras ferrugineum* (Simpson) (within reworked concretions; Fig. 10: 2); other fossils: *Passaloteuthis* sp., *Pseudopecten equivalvis* (Sowerby), *Eopecten velatus* (Goldfuss), *Pseudomytiloides* sp., *Nicaniella pumila* (Sowerby), *Harpax spinosus* (Sowerby), *Mactromya* sp., *Ryderia doris* (d'Orbigny), *Pseudolimea* sp., *Palaeoneilo elliptica* (Goldfuss), *Oxytoma inaequivalvis* (Sowerby), *Terquemia arietis* (Quenstedt), *Palmoxytoma cygnipes* (Young & Bird), *Pleurotomaria amalthei* Quenstedt, *Laeviconulus subimbricatus* (Koch & Dunker), *Levipleura blainvillei* (von Münster), rhynchonellid brachiopods, *Amaltheocrinus* sp., echinid spines, drift wood;

Bed 5: 800 cm — bluish-grey, slightly miceous, fissile claystone with scattered small bivalves; 15 and 75 cm below top layers of flat-lenticular, grey siderite nodules; ammonoids: *Pleuroceras spinatum* (Bruguière) (0.8 m, 1.5 m, 2.0 m, 3.0 m, 5.5 m, 7.25 m and 7.5 m below top: Fig. 10: 3, 4); other fossils: *Palaeoneilo* sp.;

Bed 6: 0–1 cm — reworked flat concretions composed of bluish-grey pyrite-rich argillaceous limestone, with corroded surfaces;

Posidonienschiefer Formation:

Bed 7: 5–15 cm — "Laibstein I": dark grey, laminated calcareous marl with coarse shell debris and one 15-cm-sized limestone concretion composed of laminated bituminous pellet packstone, with intercalated layers of coarse shell debris and fish scales; basis with reworked flat concretions from the Amaltheenton; ammonoids: *Tiltoniceras antiquum* (Wright) (1–2 cm above basis; and one juvenile specimen in middle part; Fig. 10: 5, 6); middle and upper part with *Cleviceras exaratum* (Young & Bird) (Fig. 10: 10), *Hildaites murleyi* (Moxon) (Fig. 10: 8, 9), and *Lytoceras ceratophagum* (Quenstedt) (Fig. 10: 7); other fossils: *Pseudomytiloides dubius* (Sowerby), *Nicaniella* sp., scattered *Coelodiscus minutus* (Schübler in Zieten);

Bed 8: 15 cm — "Laibstein II": dark grey, laminated bituminous limestone concretions (pellet packstone) up to 50 cm width, with abundant mm-sized holoplanktonic gastropods; ammonoids: *Cleviceras elegans* (Sowerby) (Fig. 11: 6), rare *Cleviceras* cf. *exaratum* (Young & Bird), *Phylloceras heterophyllum* (Sowerby) (Fig. 11: 5), *Harpoceras serpentinum*

(Schlotheim) (Fig. 11: 1), *"Peronoceras" desplacei* (d'Orbigny) (Fig. 11: 4), *Nodicoeloceras crassoides* (Simpson), *Dactylioceras semiannulatum* Howarth (Fig. 11: 7), *Dactylioceras anguinum* (Reinecke) (Fig. 11: 3); other fossils: *Meleagrinella* cf. *substriata* (von Münster), *Pseudomytiloides dubius* (Sowerby), *Goniomya rhombifera* (Goldfuss), *Camptonectes subulatus* (von Münster in Goldfuss), *Pleuromya* sp., abundant *Coelodiscus minutus* (Schübler in Zieten);

Bed 9: 5–6 cm "Fish Scale Bed": dark grey, bituminous argillaceous fissile limestone composed of mollusc shell fragments and fish scales, with abundant belemnites; ammonoids: *Dactylioceras* sp. (upper bedding plane), *Cleviceras* cf. *elegans*. (lower bedding plane); other fossils: *Meleagrinella* cf. *substriata* (von Münster), *Pseudomytiloides dubius* (Sowerby), belemnites, ichthyosaur vertebra;

Bed 10: 10 cm "Falciferum Shale": dark grey, laminated, bituminous marl; lower part with one dark grey, 8 × 12-cm-sized, poorly laminated bituminous limestone concretion (pellet packstone) with mollusk shell debris, few phosphatic vertebrate microfragments and abundant small *Dactylioceras* shells (spar filled); ammonids: *Harpoceras falciferum* (Sowerby) (middle part; Fig. 2C), *Phylloceras heterophyllum* (Sowerby); other fossils: *Pseudomytiloides dubius* (Sowerby) abundant on bedding planes, drift wood;

Bed 11: 3–4 cm grey, bituminous argillaceous fissile limestone with abundant fish scale and shell debris; fossils: few large (2-cm-sized) *Meleagrinella* cf. *substriata* (von Münster);

Bed 12: 25 cm "Dactylioceras Bed": grey, bituminous limestone consisting of densely packed *Meleagrinella* shells and shell fragments, faecal pellets, and scarce phosphatic vertebrate microfragments; abundant sparite and micrite filled casts of *Dactylioceras*; relictic cross-stratification in the lower part of the bed; ammonoids: *Dactylioceras athleticum* (Simpson) (abundant throughout the bed; Fig. 12: 3), *Dactylioceras* cf. *commune* (Sowerby) (lower bedding plane; Fig. 12: 1), *Hildoceras* cf. *lusitanicum* Meister (lower bedding plane; Fig. 12: 2)), *Pseudolioceras* sp. (juvenil); other fossils: *Meleagrinella substriata* (von Münster), belemnites;

Bed 13: 1–2 cm grey, bituminous argillaceous limestone consisting of densely packed *Meleagrinella* shells and scattered phosphatic vertebrate microfragments; fossils: *Meleagrinella substriata* (von Münster);

Bed 14: 10–12 cm "Monotis Bed": bituminous limestone (lumachelle) consisting of densely packed *Meleagrinella* shells, faecal pellets, and scarce phosphatic vertebrate microfragments; ammonoids: *Dactylioceras* cf. *athleticum* (Simpson); other fossils: *Meleagrinella substriata* (von Münster), *Pseudomytiloides dubius* (Sowerby);

Bed 15: 40 cm "Bifrons Shale": dark-grey, bituminous marl, laminated; with scattered shell debris in layers, scattered phosphatic scale and bone microfragments, abundant belemnites 26 cm and 38 cm below top; ammonoids: *Hildoceras semipolitum* Buckman (2 cm, 17 cm, 18 cm, and 22 cm below top; Fig. 12: 4, 5), *Pseudolioceras* cf. *lythense* (Young & Bird) (20 cm below top), *Phylloceras heterophyllum* (Sowerby) (28 cm below top); other fossils: *Pseudomytiloides dubius* (Sowerby), *Bositra buchi* var. *elongata* (Goldfuss), rare *Orbiculoidea papyracea* (von Münster), *Lenticulina* sp., rare echinoderm fragments, belemnites;

Bed 16: 70 cm "Variabilis Shale": dark-grey, laminated to well bedded, bituminous marl (lower 60 cm) to calcareous marl (top 10 cm) with scattered shell debris, rare phosphatic fish scale and bone microfragments; ammonoids compressed or as pyrite casts preserved, scattered pyrite nodules up to 3 cm in size; light-grey *Chondrites* horizons 5–6 cm and 18–19 cm below top; ammonoids: *Denckmannia* cf. *rude* (Simpson) (1 cm below top), *Haugia jugosa* (Sowerby) (3 cm below top; Fig. 12: 9), *Haugia* sp. (7 cm and 70 cm below top), *Haugia variabilis* (d'Orbigny) (13 cm below top; Fig. 12: 8), *Pseudolioceras compactile* (Simpson) (13 cm, 19 cm, 21 cm, 24 cm, 25 cm, 37 cm, and 65 cm below top; Fig. 12: 10, 11), *Pseudolioceras* sp. (23 cm and 25 cm below top), *Catacoeloceras raquinianum* (d'Orbigny) (3 cm, 7 cm, 13 cm, 15 cm, 19 cm, 22 cm, 37 cm, 38 cm, and 53 cm below top; Fig.

13: 2, 3), *Catacoeloceras* sp. (68 cm below top), *Mucrodactylites mucronatus* (d'Orbigny) (43 cm below top; Fig. 12: 7, 8), *Lytoceras* sp. (5 cm below top), *Lytoceras* cf. *cornucopia* (Young & Bird) (13 cm below top), *Lytoceras sublineatum* (Oppel) (26 cm and 38 cm below top; Fig. 13: 1), *Hildoceras* cf. *semipolitum* Buckman (70 cm below top); other fossils: *Salpingoteuthis* sp. (15 cm below top), further belemnites, *Bositra buchi* var. *elongata* (Goldfuss), *Pseudomytiloides dubius* (Sowerby), *Propeamussium pumilum* (Lamarck), *Grammatodon* sp., *Lenticulina* sp. (rare);

Bed 17: 2 cm "Fucoid Bed": grey to white-grey, bioturbated marl, slightly phosphoritic, with *Chondrites* burrows; with compressed and deformed phosphoritic casts of ammonoids; ammonoids: abundant *Catacoeloceras raquinianum* (d'Orbigny), *Haugia variabilis* (d'Orbigny), *Phylloceras heterophyllum* (Sowerby), *Lytoceras* cf. *cornucopia* (Young & Bird); other fossils: *Pseudomytiloides dubius* (Sowerby), *Camptonectes subulatus* (Münster);

Jurensismergel Formation:

Bed 18: 5 cm grey, well bedded calcareous marl; ammonoids: *Pseudogrammoceras subregale* (Pinna) (Fig. 13: 4), *Haugia* cf. *phillipsi* (Simpson) (Fig. 13: 5); abundant *Catacoleoceras raquinianum* (d'Orbigny); *Haugia* cf. *variabilis* (d'Orbigny) at basis of the bed; other fossils: *Bositra buchi* var. *elongata* (Goldfuss);

Bed 19: 6 cm "Belemnite Battlefield": grey, bituminous calcareous marl with abundant bivalve shell debris (*Propeamussium*), belemnite accumulation, and reworked phosphorite nodules; at the basis reworked plate-like, bored white-grey phosphorites nodules up to 2.5 × 5 × 10 cm in size; thin burrows; ammonoids: *Lytoceras* cf. *cornucopia* (Young & Bird), *Pseudogrammoceras* sp., lower bedding plane with *Catacoeloceras raquinianum* (d'Orbigny) (Fig. 13: 6); other fossils: *Dactyloteuthis irregularis* (Schlotheim);

Bed 20: 6–7 cm "Main Phosphorite Bed": grey, marl to calcareous marl, poorly bedded, with abundant bivalve shell debris (*Propeamussium*) with white-grey phosphorite nodules up to 1 × 3 × 6 cm and abundant belemnites; *Chondrites* burrows; ammonoids: *Lytoceras cornucopia* (Young & Bird) (Fig. 13: 8), *Pseudogrammoceras* sp., *Denckmannia rude* (Simpson) (Fig. 13: 9), *Osperleioceras bicarinatum* (Zieten) (Fig. 13: 7); other fossils: *Dactyloteuthis irregularis* (Schlotheim), *Chlamys textoria* (Schlotheim), *Camptonectes* cf. *subulatus* (Münster);

Bed 21: 14–15 cm "Toarcensis Shale": dark grey, well bedded, bituminous marl transected by numerous small branching burrows (*Chondrites*); abundant compressed ammonoids (solely *Grammoceras*) and bivalves (solely *Pseudomytiloides*); ammonoids: *Grammoceras thouarsense* (d'Orbigny) (Fig. 14: 1) throughout the bed; other fossils: *Pseudomytiloides dubius* (Sowerby), few belemnites;

Bed 22: 5 cm "Belemnite accumulation": grey, poorly stratified argillaceous marl full of belemnites (*Dactyloteuthis*); nubeculariid foraminifera on shell fragments and belemnites; one compressed *Lytoceras* shell fragment with stromatolithic crust at the top inside of the body chamber; one phosphorite nodule with microbialite-like corroded upper surface; locally small lenticular phosphorite nodules; basis with flat corroded phosphorites (11 × 7 × 1 cm in size) and double-sided-corroded belemnite rostra; ammonoids: *Alocolytoceras* cf. *rugiferum* (Pompeckj); other fossils: *Liostrea erina* (d'Orbigny) attached to belemnite rostra, *Chladocrinus* sp.;

Bed 23: 30 cm "Levesquei-Dispansum-Marl": grey, poorly bedded marl rich in nubeculariid foraminifera, shell debris, and with small phosphorite nodules; abundant mid-sized and large compressed ammonites (top 12 cm and at 20–25 cm below top); deformed phosphorite casts of smaller ammonoids, rare pyrite casts;
ammonoids: *Phlyseogrammoceras dispansum* (Lycett) (12–20 cm and 20–25 cm below top; Fig. 14: 5, 8), *Pseudolioceras* cf. *boulbiense* (Young & Bird) (12–20 cm below top; Fig. 14: 3), *Alocolytoceras rugiferum* (Pompeckj) (12–20 cm, 20–25 cm, and 29 cm below top; Fig. 14: 2, 4), *Hammatoceras insigne* (Schübler in Zieten) (15 cm below top; Fig. 15: 10,

12), *Hammatoceras* sp. (20–25 cm below top), *Dumortieria insignisimilis* (Brauns) (11 cm below top; Fig. 14: 6, 7), *Dumortieria levesquei* (d'Orbigny) (6 cm and 9 cm below top; Fig. 14: 11, 13), *Dumortieria radians* (Reinecke) (6 cm below top), *Dumortieria pseudoradiosa* (Branco) (4 cm below top; Fig. 14: 14), *Dumortieria radiosa* (Seebach) (4 cm below top), *Dumortieria striatulocostata* (Quenstedt) (4 cm below top), *Dumortieria* sp. (pyrite cast at 8 cm below top); other fossils: *Chlamys textoria* (Schlotheim), *Camptonectes subulatus* (Münster in Goldfuss), *Entolium* sp., *Eopecten velatus* (Goldfuss), *Plagiostoma giganteum* Sowerby, *Pseudolimea* sp., *Pseudomytiloides* sp., *Nicaniella voltzi* (Hoeninghaus in Roemer), *Liostrea erina* (d'Orbigny), belemnites;

Bed 24: 95 cm grey, well bedded argillaceous marl to marl with abundant shell microdebris; lower 60 cm rich in nubeculariid foraminifera; lower 45 cm with small marcasite nodules; 40–45 cm below top accumulation of phosphorite nodules and ammonites, 70 cm below top accumulation of compressed ammonites; ammonoids: *Paradumortieria* cf. *tectiforme* Elmi & Caloo-Fortier (20 cm, 25 cm, 40–45 cm, and 50 cm below top; Fig. 15: 5), *Dumortieria* cf. *kochi* Benecke (40 cm below top; Fig. 15: 11), *Dumortieria moorei* (Lycett) (7 cm, 40 cm, and 54 cm below top; Fig. 15: 10), *Dumortieria* cf. *moorei* (Lycett) (5 cm and 40 cm below top), *Dumortieria pseudoradiosa* (Branco) (40–45 cm and 70 cm below top), *Dumortieria* cf. *pseudoradiosa* (Branco) (65 cm and 94 cm below top), *Dumortieria radiosa* (Seebach) (40–45 cm, 73 cm, and 75 cm below top; Fig. 14: 9), *Dumortieria* cf. *radiosa* (Seebach) (40–45 cm, 70 cm, and 75 cm below top); other fossils: *Chlamys textoria* (Schlotheim), *Pseudomytiloides* sp., belemnites;

Bed 25: 2 cm grey, poorly bedded, argillaceous marl with shell microdebris and abundant ammonites (pyrite casts and marcasite-veneered imprints), abundant belemnites, and small phosphorite nodules; ammonoids: *Cotteswoldia mactra* (Dumortier) (Fig. 15: 3), *Dumortieria* cf. *moorei* (Lycett), *Dumortieria costula* (Reinecke), *Paradumortieria* cf. *tectiforme* Elmi & Caloo-Fortier, *Dumortieria* cf. *externicostata* (Branco), *Pleydellia* cf. *subcompta* (Branco) (transitional form to *C. mactra*), *Pleurolytoceras wrighti* (Buckman); other fossils: rhynchonellid brachiopode, belemnites;

Bed 26: 50 cm grey, well bedded, argillaceous marl rich in shell microdebris of *Bositra suessi*, with scattered small branching burrows (*Chondrites*), scarce nubeculariid foraminifera, small pyrite nodules and pyrite ammonite casts; *Bositra suessi* pavement 32 cm below top; *Pleydellia subcompta* (Branco) (35 cm below top; Fig. 15: 12), *Cotteswoldia aalensis* (Zieten) (5 cm, 22 cm, 25 cm, 30 cm, and 35 cm below top), *Cotteswoldia distans* (Buckman) (35 cm below top), *Cotteswoldia mactra* (Dumortier) (40 cm below top), *Dumortieria* cf. *moorei* (Lycett) (40 cm below top), *Dumortieria costula* (Reinecke) (30 cm below top; Fig. 15: 8), *Dumortieria externicostata* (Branco) (30 cm below top; Fig. 15: 7), *Pleurolytoceras wrighti* (Buckman) (25 cm below top), *Pleurolytoceras hircinum* (Schlotheim) (35 cm below top), other fossils: *Bositra suessi* (Oppel), belemnites;

Bed 27: 5–10 cm grey (unweathered) to yellowish-brown (weathered), well bedded, calcareous claystone with scattered small branching burrows (*Chondrites*), minor shell microdebris, very few nubeculariid foraminifera, and very few echinoderm bioclasts; abundant small pyrite casts of ammonites, especially near the basis of the bed; ammonoids: *Pleydellia subcompta* (Branco), *Pleydellia distans* (Buckman) (Fig. 15: 9), *Cotteswoldia aalensis* (Zieten) (Fig. 15: 6), *Pseudolioceras beyrichi* (Schloenbach), *Pleurolytoceras hircinum* (Schlotheim) (Fig. 15: 2), *Pleurolytoceras wrighti* (Buckman) (Fig. 15: 1), other fossils: belemnites;

Bed 28: 80–85 cm grey, well bedded, calcareous claystone rich in shell microdebris of *Bositra suessi* and nubeculariid foraminifera; with scattered small pyrite nodules and pyrite ammonite casts; at the top accumulation of small pyritic ammonites (embedded in various orientation); *Bositra suessi* pavement 50 cm below top; ammonoids: *Pleydellia subcompta* (Branco) (1 cm below top), *Pleydellia costulata* (Zieten) (1 cm below top; Fig. 15: 13), *Cotteswoldia aalensis* (Zieten) (1 cm below top), *Pseudolioceras bey-*

richi (Schloenbach) (1 cm below top; Fig. 15: 4), *Pleurolytoceras hircinum* (Schlotheim) (1 cm below top), *Pleurolytoceras wrighti* (Buckman) (1 cm and 25 cm below top); other fossils: *Toarctocera* sp., *Bositra suessi* (Oppel), *Palaeonucula* sp., *Chladocrinus* sp., belemnites;

Bed 29: 10–12 cm grey, poorly bedded, calcareous marlstone with abundant nubeculariid foraminifera;

Bed 30: 30 cm grey, well bedded, marl to calcareous claystone rich in shell microdebris of *Bositra suessi* (Oppel) and nubeculariid foraminifera;

Opalinuston Formation:

Bed 31: 2 cm grey (unweathered) to brownish-grey (weathered), poorly bedded calcareous claystone with abundant, partially aligned belemnites of the *Hastites* group;

Bed 32: 80 cm grey, well bedded, calcareous claystone rich in shell microdebris of *Bositra suessi* (Oppel); at 50 cm below top rich in nubeculariid foraminifera;

Bed 33: 2–3 cm grey (unweathered) to brownish-grey (weathered), poorly bedded calcareous claystone with few small phosphorite nodules, abundant belemnites and compressed ammonoids; one shell fragment of *Lytoceras* with a stromatolitic crust at the top inside of the body chamber; ammonoids: *Cotteswoldia lotharingica* (Branco) (Fig. 15: 15), *Pleydellia buckmani* Maubeuge (Fig. 15: 16), *Pleydellia* cf. *falcifer* Maubeuge (Fig. 15: 17), *Pleurolytoceras torulosum* (Schübler in Zieten) (Fig. 15: 14); other fossils: *Acrocoelites* sp., *Hastites subclavatus* (Voltz), *Thecocyathus mactrus* (Goldfuss), *Palaeonucula hammeri* (Defrance), *Nicaniella voltzii* (Hoeninghaus in Roemer), *Chlamys textoria* (Schlotheim), *Pseudomytiloides* sp., *Sphenodus* sp. (tooth 4 mm);

Bed 34: >50 cm grey (unweathered) to brownish-grey (weathered), well bedded clay;

Carbonate and organic carbon contents

The Amaltheenton Formation is characterized by low $CaCO_3$ contents (2.5–3.3 wt%) as well as low C_{org} contents (0.8–1.0 wt%) (Table 1, Fig. 4).

The Posidonienschiefer Formation, however, shows a sudden and strong increase in $CaCO_3$ to 94 wt% at its basis, followed by consistently high values (73–98 wt%) in the lower part of the formation (i.e. limestone and argillaceous limestone), with only the Falciferum Shale showing a lower value (45 wt%). Higher parts of Posidonienschiefer exhibit marl equivalent values around 50–65 wt% $CaCO_3$, with only two intercalations of reduced $CaCO_3$ content (35 wt%) in the upper third (Table 1, Fig. 4). C_{org} contents of the Posidonienschiefer vary between 0.3 and 2.0 wt% in limestone beds, and higher values up to 5.3 wt% in less $CaCO_3$-rich lithologies. The highest value (7.5 wt%) was measured in the Falciferum Shale. However, C_{org} contents calculated for the carbonate-free rock fraction demonstrate a different trend: Very high contents characterize Laibstein I and II near basis of formation (i.e., bed 7 and 8, with up to 17.6 wt%), while fish scale debris bed 9 shows a slightly lower value (7.4 wt%). It follows a further maximum in the interval Falciferum Shale to Monotis Bed (up to 14.1 wt%). Higher parts of the formation finally show fluctuating C_{org} contents (4.4–14.0 wt%), with two minima in top parts (1.5 and 1.8 wt%) (Table 1, Fig. 4).

$CaCO_3$ contents at the basis of the Jurensismergel Formation correspond to calcareous marl (65–71 wt%) and marl (44–53 wt%), then decrease to marls (37–62 wt%) and argillaceous marls (17–34 wt %). Near the top of the formation, one last bed of calcareous marl (66 wt%) is found. Increased C_{org} values (3.0 and 4.3 wt%) were found near basis (bed 18, "Belemnite Battlefield", "Toarcensis Shale"), followed by low values of 1–2 wt% in middle and upper parts of the formation. Only two horizons, basis of bed 24 and bed 25, show slightly increased C_{org} contents (2.5 and 2.8 wt%). Finally, the Opalinuston Formation revealed $CaCO_3$ contents only slightly lower than top parts of the Jurensismergel, and C_{org} as low as in the Amaltheenton (Table 1, Fig. 4).

Discussion

Lithostratigraphy

The assignment of beds to specific formations of the Schwarzjura Group follows the definitions given in Bloos et al. (2005), Mönnig et al. (2015), and Nitsch et al. (2015), with only minor modifications.

1. The lower part of section, i.e. beds 1–6, represent the top 9 m of the Amaltheenton Formation (Figs 2A, 5), which shows a total thickness of 36 m at this location (Fig. 3). The formation is characterized by monotonous bluish-grey claystones with disseminated pyrite, low $CaCO_3$ and low C_{org} contents.
2. The Posidonienschiefer Formation (Figs 2B, 4), with a total thickness of 1.85–1.90 m, is characterized by bituminous marls and limestones rich in fossils. The basis is drawn with the first bituminous and calcareous bed, i.e. "Laibstein I". The erosive discontinuity

Table 1. Carbon (C_{tot}, C_{org}, C_{carb}), total sulphur (S_{tot}), and total nitrogen (N_{tot}) contents of sedimentary rocks of the Ludwigskanal section.

Sample number	**Formation**	**Bed number**	**Section** from–to [cm]	**Lithology**	**Remarks**	**C_{tot}** mean [wt %]	**C_{org}** mean [wt %]	**C_{carb}** mean [wt %]	**$CaCO_3$** calculated [wt %]	**C_{org} carbonate-free** [wt %]	**N_{tot}** mean [wt %]	**S_{tot}** mean [wt %]	**S_{tot} carbonate-free** [wt %]
Lud 72	Opalinuston	34	639	calcareous clay-stone		3.23	0.33	2.90	24.2	0.44	0.035	0.013	0.02
Lud 1	Opalinuston	34	629	clay		0.37	0.35	0.02	0.2	0.35	0.057	0.016	0.02
Lud 2	Opalinuston	33	618	argillaceous limestone	stromatolitic crust	9.66	0.30	9.36	78.0	1.36	0.019	0.040	0.18
Lud 3	Opalinuston	33	617–619	calcareous clay-stone	matrix of belemnite accumulation	2.60	0.60	2.00	16.7	0.72	0.047	0.009	0.01
Lud 4	Opalinuston	32	607	calcareous clay-stone		2.70	0.42	2.28	19.0	0.52	0.039	0.011	0.01
Lud 73	Opalinuston	32	602	calcareous clay-stone		3.25	0.78	2.47	20.6	0.98	0.047	0.011	0.01
Lud 74	Opalinuston	32	567	calcareous clay-stone		3.33	0.55	2.78	23.2	0.72	0.041	0.014	0.02
Lud 75	Opalinuston	32	557	calcareous clay-stone	rich in nubeculariid foraminifera	2.93	0.66	2.27	18.9	0.81	0.046	0.010	0.01
Lud 76	Jurensismergel	30	533	calcareous clay-stone	rich in nubeculariid foraminifera	3.61	0.74	2.87	23.9	0.97	0.048	0.020	0.03
Lud 5	Jurensismergel	30	515	calcareous clay-stone	rich in nubeculariid foraminifera	3.16	0.68	2.48	20.7	0.86	0.046	0.014	0.02
Lud 6	Jurensismergel	29	495 to 505	calcareous marl		8.24	0.28	7.96	66.3	0.83	0.024	0.012	0.04
Lud 7	Jurensismergel	28	475 to 480	calcareous clay-stone	rich in nubeculariid foraminifera	3.39	1.07	2.32	19.3	1.33	0.061	0.015	0.02
Lud 8	Jurensismergel	28	465 to 470	calcareous clay-stone		3.20	0.43	2.77	23.1	0.6	0.05	0.03	0.04
Lud 9	Jurensismergel	28	455 to 460	calcareous clay-stone		3.49	0.52	2.97	24.7	0.7	0.04	0.02	0.02
Lud 10	Jurensismergel	28	445 to 450	calcareous clay-stone	rich in nubeculariid foraminifera	3.60	1.18	2.42	20.2	1.5	0.07	0.04	0.06
Lud 11	Jurensismergel	28	435 to 440	calcareous clay-stone	rich in nubeculariid foraminifera	4.01	1.35	2.66	22.2	1.7	0.07	0.06	0.07
Lud 12	Jurensismergel	28	425 to 430	calcareous clay-stone	rich in nubeculariid foraminifera	3.11	1.12	1.99	16.6	1.3	0.06	0.04	0.05
Lud 13	Jurensismergel	28	415 to 420	calcareous clay-stone		2.88	1.18	1.70	14.2	1.4	0.07	0.03	0.04
Lud 14	Jurensismergel	27	405 to 410	calcareous clay-stone	"Yellow Bed"	3.62	1.07	2.55	21.2	1.4	0.07	0.05	0.07
Lud 15	Jurensismergel	26	395 to 400	calcareous clay-stone		3.31	0.85	2.46	20.5	1.1	0.05	0.05	0.06
Lud 16	Jurensismergel	26	385 to 390	calcareous clay-stone		4.14	1.17	2.97	24.7	1.6	0.06	0.05	0.06
Lud 17	Jurensismergel	26	375 to 380	argillaceous marl		4.57	1.29	3.28	27.3	1.8	0.07	0.12	0.17
Lud 18	Jurensismergel	26	365 to 370	argillaceous marl		4.34	0.92	3.42	28.5	1.3	0.05	0.05	0.07
Lud 19	Jurensismergel	25	355 to 360	bituminous marl	matrix of "Mactra Bed"	10.26	2.83	7.43	61.9	7.4	0.09	0.61	1.60
Lud 20	Jurensismergel	24	345 to 350	argillaceous marl		4.82	1.01	3.81	31.7	1.5	0.06	0.16	0.23
Lud 21	Jurensismergel	24	335 to 340	argillaceous marl		5.02	1.36	3.66	30.5	2.0	0.07	0.80	1.15
Lud 22	Jurensismergel	24	325 to 330	argillaceous marl		5.09	1.09	4.00	33.3	1.6	0.07	0.94	1.41
Lud 23	Jurensismergel	24	315 to 320	calcareous clay-stone	rich in nubeculariid foraminifera	3.60	1.03	2.57	21.4	1.3	0.07	0.52	0.67
Lud 24	Jurensismergel	24	305 to 310	calcareous clay-stone	rich in nubeculariid foraminifera	3.53	1.04	2.49	20.7	1.3	0.07	0.60	0.75
Lud 25	Jurensismergel	24	295 to 300	argillaceous marl	rich in nubeculariid foraminifera	4.75	0.94	3.81	31.7	1.4	0.06	0.51	0.75
Lud 26	Jurensismergel	24	285 to 290	marl	rich in nubeculariid foraminifera	6.22	0.90	5.32	44.3	1.6	0.05	0.66	1.18
Lud 27	Jurensismergel	24	275 to 280	argillaceous marl	rich in nubeculariid foraminifera	5.89	1.78	4.11	34.2	2.7	0.08	1.45	2.20
Lud 28	Jurensismergel	24	265 to 270	poorly bituminous, argillaceous marl	rich in nubeculariid foraminifera	5.83	2.54	3.29	27.4	3.5	0.08	1.53	2.11
Lud 29	Jurensismergel	23	255 to 260	marl	rich in nubeculariid foraminifera	5.41	1.09	4.32	36.0	1.7	0.05	0.18	0.28
Lud 30	Jurensismergel	23	245 to 250	marl		5.65	1.06	4.59	38.2	1.7	0.04	0.25	0.40

Sample number	Formation	Bed number	Section from–to [cm]	Lithology	Remarks	C_{tot} mean [wt %]	C_{org} mean [wt %]	C_{carb} mean [wt %]	$CaCO_3$ calculated [wt %]	C_{org} carbonate-free [wt %]	N_{tot} mean [wt %]	S_{tot} mean [wt %]	S_{tot} carbonate-free [wt %]
Lud 31	Jurensismergel	23	235 to 240	marl	rich in nubeculariid foraminifera	5.30	0.88	4.42	36.8	1.4	0.04	0.25	0.39
Lud 32	Jurensismergel	23	225 to 230	argillaceous marl	rich in nubeculariid foraminifera	4.59	1.04	3.55	29.6	1.5	0.07	0.10	0.15
Lud 33	Jurensismergel	22	220 to 225	argillaceous marl	matrix of belemnite accumulation	4.24	1.03	3.18	26.5	1.4	0.06	0.16	0.21
Lud 34	Jurensismergel	21	205 to 220	bituminous marl	"Toarcensis Shale"	8.49	3.00	5.49	45.7	5.5	0.10	1.23	2.26
Lud 35	Jurensismergel	20	198 to 205	marl	matrix of "Main Phosphorite Bed"	5.96	0.73	5.23	43.6	1.3	0.04	0.69	1.21
Lud 36	Jurensismergel	19	195 to 198	poorly bituminous, calcareous marl	"Belemnite Battlefield"	9.87	1.30	8.57	71.4	4.5	0.04	0.69	2.41
Lud 37	Jurensismergel	19	192 to 195	bituminous marl	"Belemnite Battlefield"	10.62	4.30	6.32	52.7	9.1	0.12	0.99	2.10
Lud 38	Jurensismergel	18	187 to 192	poorly bituminous, calcareous marl		9.58	1.75	7.83	65.2	5.0	0.06	0.99	2.84
Lud 39	Posidonien-schiefer	17	185 to 187	poorly bituminous marl	"Fucoid Bed"	8.69	1.88	6.81	56.7	4.3	0.06	1.09	2.52
Lud 40	Posidonien-schiefer	16	180	bituminous, calcar-eous marl	"Variabilis Shale"	11.69	3.57	8.12	67.7	11.0	0.11	0.66	2.05
Lud 41	Posidonien-schiefer	16	179	bituminous, calcar-eous marl	"Variabilis Shale"	11.44	3.40	8.04	67.0	10.3	0.10	0.83	2.50
Lud 42	Posidonien-schiefer	16	175	bituminous, calcar-eous marl	"Variabilis Shale"	12.68	4.79	7.89	65.7	14.0	0.15	0.75	2.18
Lud 43	Posidonien-schiefer	16	165	poorly bituminous, argillaceous marl	"Variabilis Shale"	4.93	1.04	3.89	32.4	1.5	0.05	0.10	0.15
Lud 44	Posidonien-schiefer	16	155	bituminous marl	"Variabilis Shale"	11.63	4.70	6.93	57.7	11.1	0.14	0.72	1.69
Lud 45	Posidonien-schiefer	16	145	poorly bituminous marl	"Variabilis Shale"	5.70	1.08	4.62	38.5	1.8	0.05	1.03	1.68
Lud 46	Posidonien-schiefer	16	135	bituminous marl	"Variabilis Shale"	11.63	5.34	6.29	52.4	11.2	0.16	1.27	2.66
Lud 47	Posidonien-schiefer	16	125	bituminous marl	"Variabilis Shale"	10.23	3.81	6.42	53.5	8.2	0.11	0.64	1.38
Lud 48	Posidonien-schiefer	15	115	bituminous marl	"Bifrons Shale"	11.29	5.01	6.28	52.3	10.5	0.14	1.41	2.95
Lud 49	Posidonien-schiefer	15	105	bituminous marl	"Bifrons Shale"	10.26	3.80	6.46	53.8	8.2	0.11	1.05	2.28
Lud 50	Posidonien-schiefer	15	95	bituminous marl	"Bifrons Shale"	10.82	4.02	6.80	56.7	9.3	0.13	1.39	3.20
Lud 51	Posidonien-schiefer	15	85	bituminous marl	"Bifrons Shale"	9.67	2.88	6.79	56.6	6.6	0.10	1.25	2.89
Lud 52	Posidonien-schiefer	15	76	bituminous marl	"Bifrons Shale"	11.58	4.58	7.00	58.3	11.0	0.14	1.14	2.74
Lud 53	Posidonien-schiefer	14	66 to 75	poorly bituminous limestone	"Monotis Bed"	12.02	0.31	11.71	97.6	12.8	0.02	0.05	2.11
Lud 54	Posidonien-schiefer	13	65 to 66	poorly bituminous, argillaceous limestone		12.04	2.44	9.60	80.0	12.2	0.09	0.60	3.00
Lud 55	Posidonien-schiefer	12	40 to 65	poorly bituminous limestone	"Dactylioceras Bed"	12.12	0.80	11.32	94.3	14.1	0.03	0.24	4.22
Lud 56	Posidonien-schiefer	11	37 to 40	poorly bituminous, argillaceous limestone		12.31	2.17	10.14	84.5	14.0	0.07	0.18	1.13
Lud 57	Posidonien-schiefer	10	27 to 37	bituminous marl	"Falciferum Shale"	12.84	7.47	5.37	44.7	13.5	0.21	2.18	3.94
Lud 58	Posidonien-schiefer	9	22 to 27	poorly bituminous, argillaceous limestone	"Fish Scale Bed"	11.89	1.29	10.60	88.3	11.1	0.05	0.28	2.38
Lud 59	Posidonien-schiefer	8	17 to 22	poorly bituminous, argillaceous limestone	"Laibstein II" (top)	11.63	1.97	9.66	80.5	10.1	0.06	0.77	3.92
Lud 60	Posidonien-schiefer	8	12 to 17	poorly bituminous limestone	"Laibstein II" (centre)	12.01	0.56	11.45	95.4	12.2	0.02	0.09	1.92
Lud 61	Posidonien-schiefer	8	7 to 12	poorly bituminous, argillaceous limestone	"Laibstein II" (bottom)	11.64	1.75	9.89	82.4	10.0	0.06	0.59	3.35
Lud 62	Posidonien-schiefer	7	0 to 7	poorly bituminous, calcareous marl	lateral to "Laib-stein I"	10.75	1.99	8.76	73.0	7.4	0.07	1.32	4.88
Lud 63	Posidonien-schiefer	7	5 to 7	poorly bituminous, argillaceous limestone	"Laibstein I" (top)	11.57	1.02	10.55	87.9	8.4	0.04	0.68	5.59
Lud 64	Posidonien-schiefer	7	2 to 5	poorly bituminous limestone	"Laibstein I" (centre)	12.33	1.03	11.30	94.2	17.7	0.03	0.33	5.67
Lud 65	Posidonien-schiefer	7	0 to 2	poorly bituminous, argillaceous limestone	"Laibstein I" (bottom)	12.02	1.07	10.95	91.2	12.2	0.05	0.38	4.35

Sample number	Formation	Bed number	Section from–to [cm]	Lithology	Remarks	C_{tot} mean [wt %]	C_{org} mean [wt %]	C_{carb} mean [wt %]	$CaCO_3$ calculated [wt %]	C_{org} carbonate-free [wt %]	N_{tot} mean [wt %]	S_{tot} mean [wt %]	S_{tot} carbonate-free [wt %]
Lud 66	Amaltheenton	5	-15	claystone		1.23	0.88	0.35	2.9	0.9	0.06	2.00	2.06
Lud 67	Amaltheenton	5	-40	claystone		1.11	0.82	0.29	2.4	0.8	0.05	2.05	2.10
Lud 68	Amaltheenton	5	-230	claystone		1.33	0.94	0.39	3.2	1.0	0.06	0.73	0.76
Lud 69	Amaltheenton	5	-300	claystone		1.31	0.98	0.33	2.7	1.0	0.06	0.64	0.66
Lud 70	Amaltheenton	4	-800 to -810	calcareous clay-stone	matrix of "Del-ta-Fossil Bed"	2.16	0.78	1.38	11.5	0.9	0.05	0.56	0.63
Lud 71	Amaltheenton	1	-930	claystone		1.24	0.84	0.40	3.3	0.9	0.06	2.48	2.57

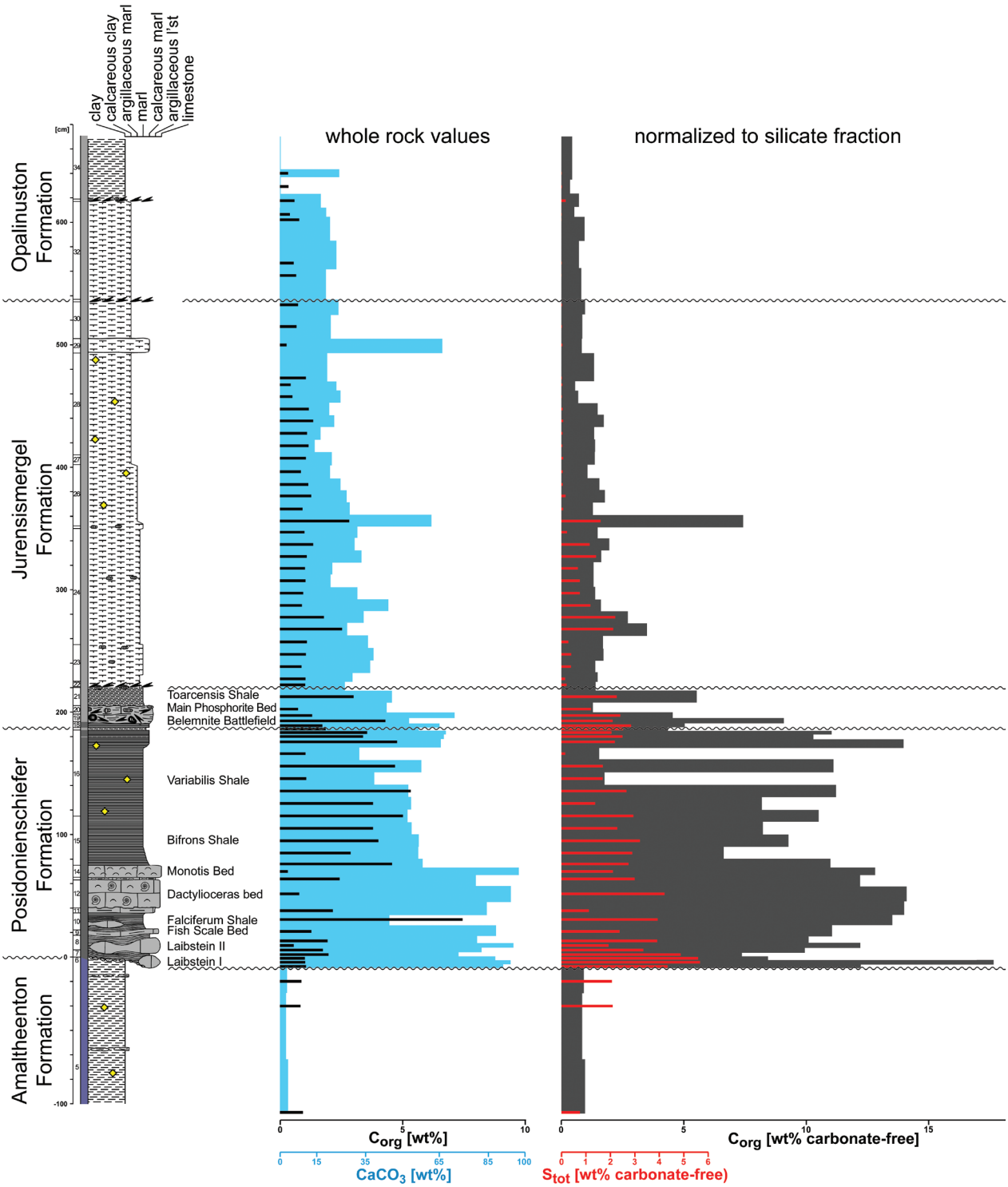

Figure 4. Lithology and lithostratigraphy of the Ludwigskanal section (top Amaltheenton to basis Opalinuston Formation) with $CaCO_3$ and organic carbon contents. For legend see Fig. 7.

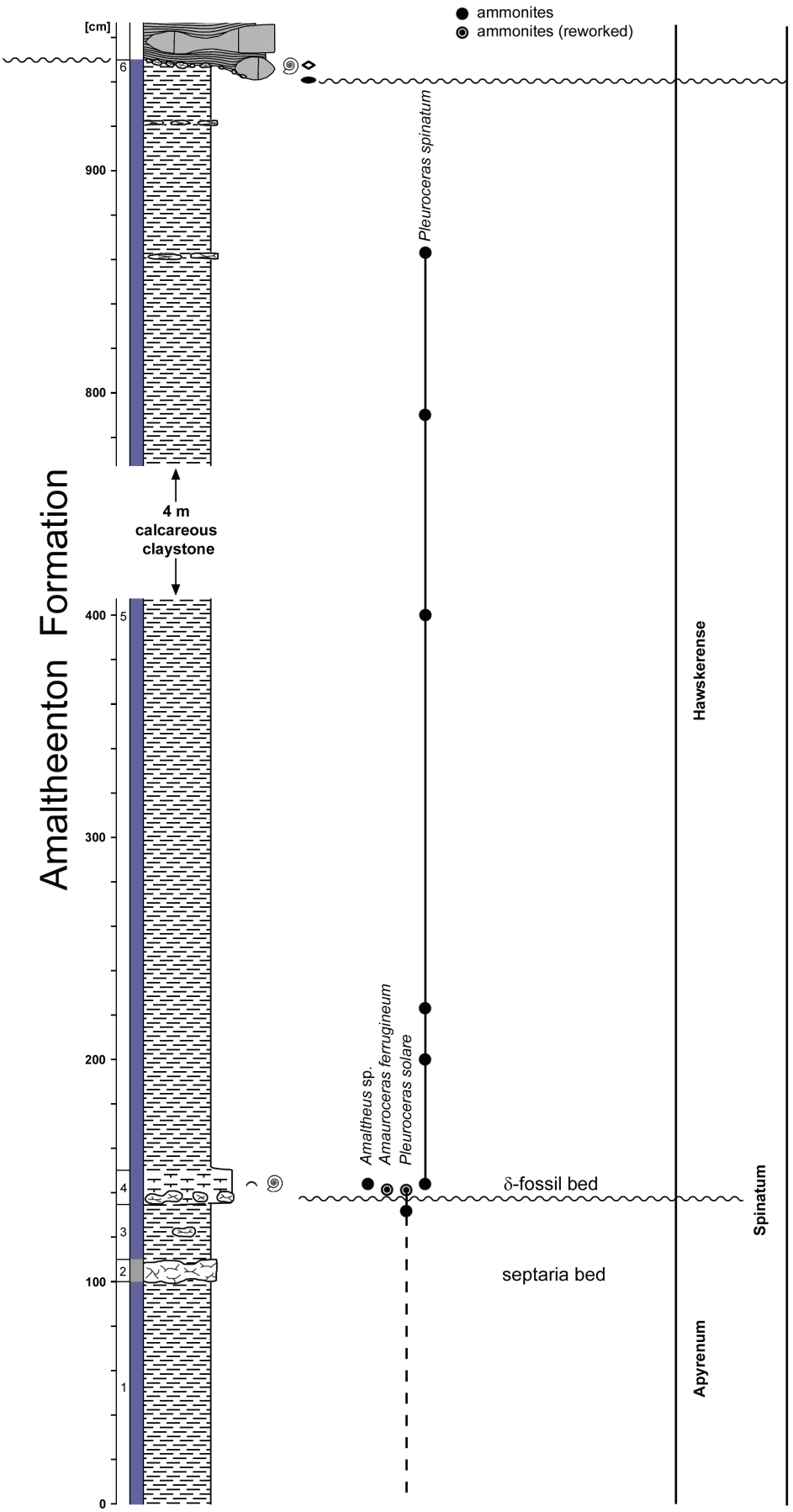

Figure 5. Litho- and biostratigraphy of the upper Amaltheenton Formation, Upper Pliensbachian, exposed at the Ludwigskanal. For legend see Fig. 7.

at its basis is indicated by reworked concretions of the Amaltheenton. Accordingly, the basal alternation of marls, bituminous marls and *Chondrites*-rich beds, as seen in the Swabian Posidonienschiefer (Urlichs 1977a; Riegraf et al. 1984; Riegraf 1985a; Bloos et al. 2005), is absent in this region. While the total rock C_{org} contents are clearly lower than in the Swabian sections (mean C_{org} = 2.45 wt% at Ludwigskanal versus 6.77 wt% at Dotternhausen, for top Semicelatum to Bifrons Zone), C_{org} contents of the carbonate-free fraction are almost identical (mean C_{org} carbonate-free = 11.18 wt% at Ludwigskanal versus 12.22 wt% at Dotternhausen; Frimmel 2003; Frimmel et al. 2004). Therefore, the comparatively low C_{org} values at Ludwigskanal section reflect a "dilution effect" by increased carbonate contents.

3. The Jurensismergel Formation (Figs 2B, 4), with a total thickness of 3.50 m, is formed by highly fossiliferous marls with phosphorite (lower part) or pyrite nodules (higher part). Major parts of the formation show abundant nubeculariid foraminifera as a significant component of the sediment. Increased C_{org} contents were only detected near the basis ("Belemnite Battlefield", "Toarcensis Shale") and in bed 25, a condensed bed in the middle of the formation. Carbonate contents are generally lower (predominantly argillaceous marls; Table 1), if compared to sections of the Swabian alb (e.g. Göppingen-Ursenwang and Aselfingen: marls and argillaceous limestone beds: Bruder 1968, his tab 4.).

The lower boundary of the Jurensismergel has previously been drawn at the top of the "Belemnite Battlefield": Urlichs (1971: p. 70f) argued that earlier publications (von Gümbel 1891: p. 359; Reuter 1927: p. 56) assigned this belemnite accumulation to the Posidonienschiefer, and that its components are reworked from the Posidonienschiefer below. However, the phosphorite nodules with borings (Fig. 2D) are not derived from bituminous shales below, and correlations with sections in the Swabian Alb (Figs 7, 9) indicate an erosive discontinuity at the basis of the marl bed 18 below the "Belemnite Battlefield" (see discussion of sequence stratigraphy below). Therefore, the "Fucoid Bed" (bed 17) forms, in our view, the top of the Posidonienschiefer Formation, and the poorly bituminous marls of bed 18 form the basis of a new stratigraphic sequence, i.e., the basis of the Jurensismergel Formation.

4. The basis of the comparatively thick Opalinuston Formation (Figs 2B, 4) should be drawn with the lithological change from marl (Jurensismergel) to claystone (Opalinuston). While this change appears gradual in the northern Franconian Alb (e.g., Mistelgau; Schulbert 2001a, b), the Ludwigskanal section still shows a clear calcareous marl bed 308–318 cm above the basis of the Jurensismergel. A calcareous marl bed has also been found in a similar position in the neighbouring section Pölling and likewise assigned to the Jurensismergel (Arp 2010). Therefore, the change from marl to claystone occurs above this bed, and the belemnite accumulation of bed 31, marking a 3rd order sequence boundary (see sequence stratigraphic discussion below) could be taken as the lithostratigraphic lower boundary of the Opalinuston Formation. This suggested boundary definition coincides with change from pyritic to phosphoritic or compressed preservation of ammonoids in this region.

Biostratigraphy

The biostratigraphic subdivision of the investigated section follows the standard scheme by Dean et al. (1961), with revisions for the Lower Toarcian by Howarth (1973) and Riegraf et al. (1984: p. 19), and for the Upper Toarcian by Knitter and Ohmert (1983), Ohmert et al. (1996), Elmi et al. (1997), Cresta et al.(2001), and Schulbert (2001a) (Fig. 8). As a principal, the lower boundaries of subzones are drawn in the present paper by the first appearance datum (FAD) of the corresponding index species, with the exception of the Hawskerense Subzone (last appearance datum LAD of *Pleuroceras solare*: Dean et al. 1961). The distribution of each of the ammonite genera and species along the investigated section is given in Figs 5 and 6.

(i) Upper Pliensbachian (>9 m)

The first *Pleuroceras solare* of the investigated section has been found 5 cm below the "Delta-Fossil Bed" (bed 4), indicating the Apyrenum Subzone of the Spinatum Zone. Abundant specimens of this species were found enclosed within reworked concretions of the "Delta-Fossil Bed" (bed 4), together with rare *Amauroceras ferrugineum* (Fig. 10: 1, 2). Few of the *Pleuroceras solare* specimens already show minor tubercles, corresponding to var. *solitarium* (Fig. 10: 2).

The marl matrix of the "Delta-Fossil Bed" (bed 4) enclosing the reworked concretions already yielded compressed *Pleuroceras spinatum* with clear tubercles, while *P. solare* is absent. This suggests that the conglomeratic bed represents the base of the Hawskerense Subzone (sensu Dean et al. 1961: "lower boundary [...] drawn immediately above the highest *Pleuroceras solare*"; equivalent to "Upper Spinatum Zone" sensu Hoffmann et al. 2007). Besides, a juvenile *Amaltheus* sp. (possibly a *Pseudoamaltheus*) was recovered.

The following top 8 m claystones of the Amaltheenton (bed 5) contain siderite concretions with typical morphotypes of *Pleuroceras spinatum* (strong ribs with clear tubercles, whorl section square; Fig. 10: 3, 4). However, neither *Pleuroceras hawskerense* nor *Pleuroceras buckmani*, characteristic for the top parts of the Hawskerense Subzone (see e.g. Jordan 1960), were found at the Ludwigskanal/Dörlbach, although they are known from the very top of the Amaltheenton in this region (Zeiss and Schirmer 1965; Arp 1989).

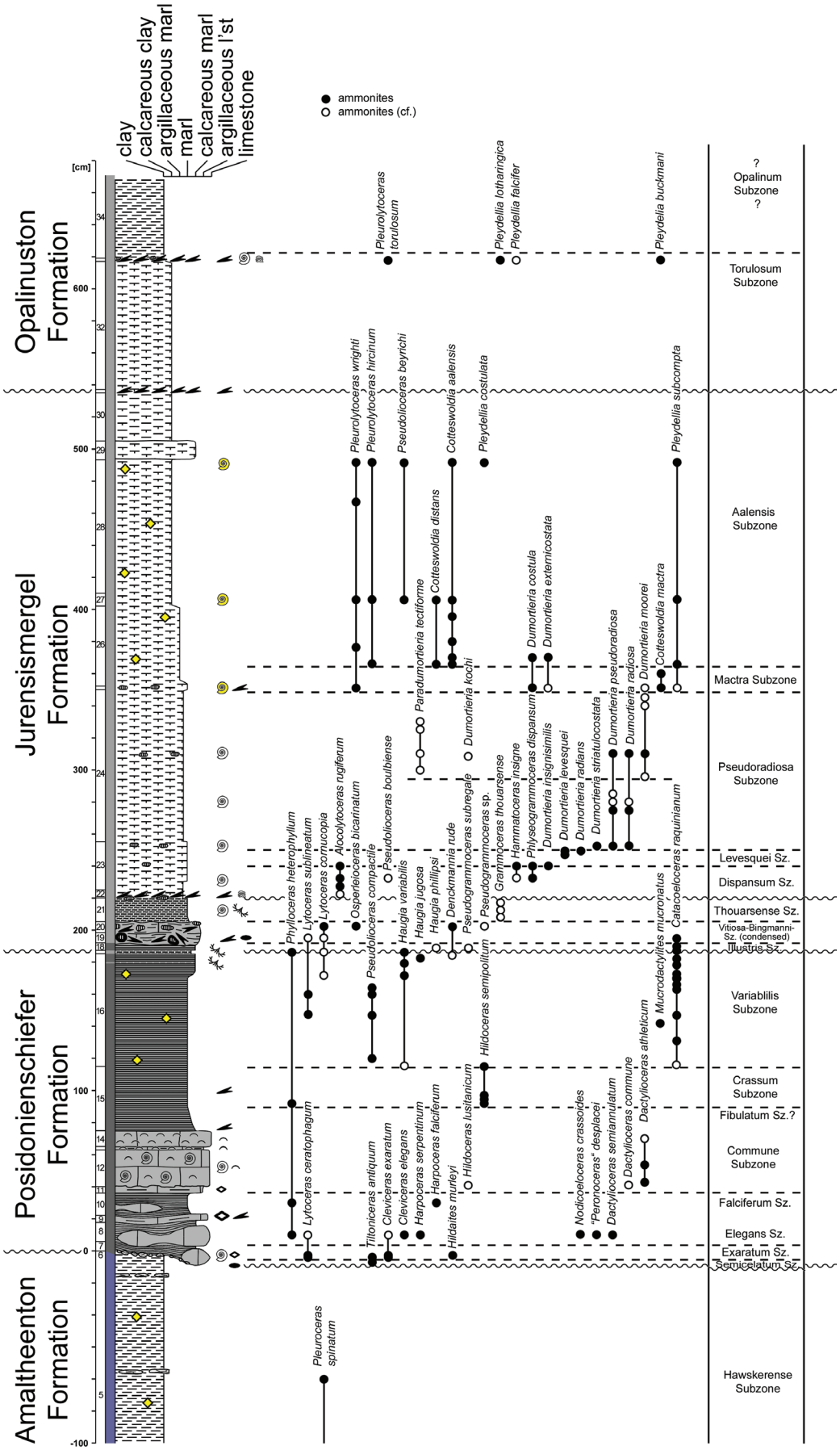

Figure 6. Litho- and biostratigraphy of the Posidonienschiefer, Jurensismergel, and basal Opalinuston Formation, Toarcian, exposed at the Ludwigskanal near Dörlbach. For legend see Fig. 7.

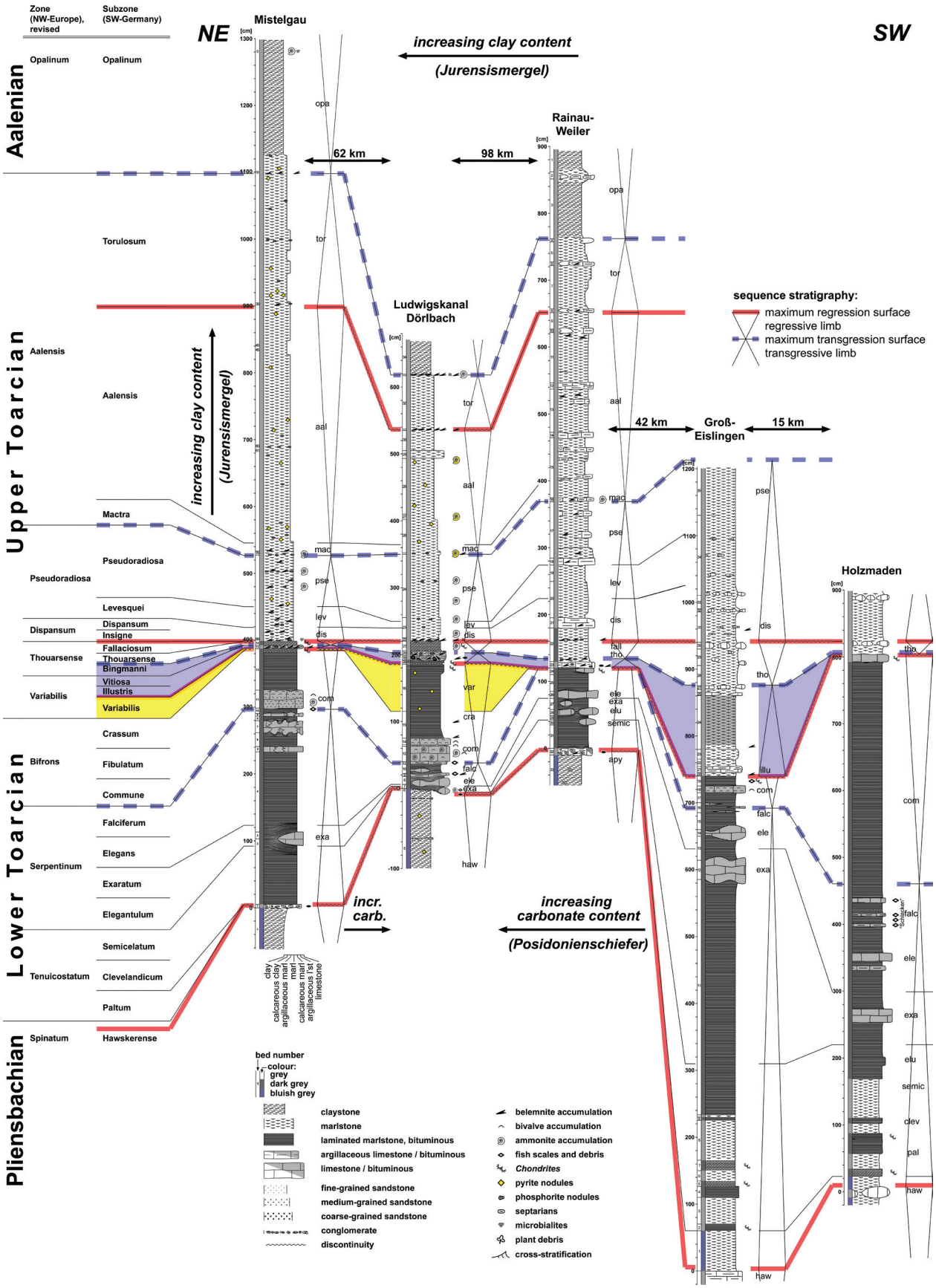

Figure 7. Correlation of the investigated section Ludwigskanal/Dörlbach with sections from the northern Franconian Alb (Mistelgau: Krumbeck 1932c; Schulbert 2001a, b; Arp and Gropengießer 2015; Basis Mactra Subzone drawn with the "Dumortieria bed I"; Basis Aalensis Subzone defined by FAD of *P. subcompta*) and Swabian Alb (Rainau-Weiler: Etzold et al. 1989; Gross-Eislingen: Wiedemann 1966; Holzmaden: Hauff 1921; Riegraf 1985a; Urlichs 1977a), with suggested T-R cycles.

(ii) Lower Toarcian (1.15–1.20 m)

Posidonienschiefer Formation starts with a clear discontinuity and Amaltheenton-derived intraclasts within the shell-debris-rich "Laibstein I" (bed 7). These laminated limestone concretions revealed a layer with several *Tiltoniceras antiquum* 2–3 cm above their basis (Fig. 10: 5, 6), representing the latest interval of the Semicelatum Subzone (Antiquum Horizon; Page 2003, 2004). This finding confirms previous rare reports on *Tiltoniceras antiquum* (syn.: *T. schroederi*: Krumbeck 1932a; Kolb 1964; *T. antiquum*: Kraus 1983: his fig. on p. 415), which – together with "*Lytoceras siemensi*" (most of them belong to *L. ceratophagum*: see Riegraf 1985b) – have initially lead to the assumption that the Laibstein concretions are representing the Tenuicostatum Zone (e.g., Urlichs 1971). However, no dactylioceratid ammonoids of the *tenuicostatum* group have been reported from the working area. Likewise, in middle and upper parts of the "Laibstein I"-bed abundant *Cleviceras exaratum* (Fig. 10: 10), *Lytoceras ceratophagum* (Fig. 10: 7), and *Hildaites murleyi* (Fig. 10: 8, 9) clearly indicate the Exaratum Subzone of the Falciferum Zone. Rare reports of *Eleganticeras* (Weißmüller 2017: his fig. 187) suggest that the Elegantulum Zone might be present, too, condensed within the "Laibstein I" (bed 7). Nonetheless, the Laibstein I bed largely represents the Exaratum Subzone, as previously shown by Riegraf (1985b) and Arp (1989).

The following "Laibstein II" (bed 8), with the abundant holoplanktic gastropod *Coelodiscus minutus*, comprises an ammonoid assemblage typical of the Elegans Subzone: *Cleviceras exaratum* (Fig. 11: 6), *Harpoceras serpentinum* (Fig. 11: 1), and a number of dactylioceratids (*Dactylioceras anguinum*, *D. semiannulatum*, *Nodicoeloceras crassoides*, *"Peronoceras" desplacei*; Fig. 11: 2–4, 7). *Phylloceras heterophyllum* (Fig. 11: 5), which is absent in "Laibstein I", has also been found in this limestone concretion bed (Kolb 1964; Arp 1989; Weissmüller 2017).

Higher parts of the Falciferum Zone are less well documented at the Ludwigskanal section as well as in the whole region. One compressed specimen of *Harpoceras falciferum* (Fig. 2C) has been found within the "Falciferum Shale" (bed 10), indicating that these bituminous marlstones above the "Fish Scale Bed" (bed 9) belong to the Falciferum Subzone.

The lower bedding plane of "Dactylioceras Bed" (bed 12) and the fish-scale-rich argillaceous limestone layer at its base (bed 11) exhibit poorly preserved specimen of *Dactylioceras commune* (Fig. 12: 1), marking the basis of the Bifrons Zone. The lowermost part of "Dactylioceras Bed" (bed 12) also revealed a poorly preserved *Hildoceras* cf. *lusitanicum* (Fig. 12: 2), consistent with basis of the Bifrons Zone. In addition, *Frechiella subcarinata* has been reported for this bed 5.5 km ESE of the Ludwigskanal section (Krumbeck 1932a; Weiß and Freitag 1991). No indication of the Ovatum Horizon (Howarth 1992; Page 2003) was found. Within the "Dactylioceras" to "Monotis Bed", however, *Dactylioceras athleticum* (Fig. 12: 3) is most abundant. Therefore, the complete event bed (Arp and Gropengießer 2016) as well as the fish-scale-rich layer below, belongs to the Commune Subzone.

Between 18 and 38 cm above the basis of the "Bifrons Shale" (bed 15), the occurrence of compressed *Hildoceras semipolitum* (Fig. 12: 4, 5) defines the Semipolitum Horizon at the top of the Bifrons Zone, as known from France and the Mediterranean (Guex 1975; Gabilly 1976a; Elmi et al. 1994, 1997). *Hildoceras semipolitum* has also been recovered from the condensed Variabilis Zone immediately below the "Belemnite Battlefield" of Mistelgau, together with *Haugia jugosa* and *Denckmannia tumefacta* (Simonsen 2013). Associated ammonoids are *Pseudolioceras* cf. *lythensis* and *Phylloceras heterophyllum*. Neither *Hildoceras bifrons*, *Catacoeloceras crassum* nor representatives of the genus *Peronoceras* were found in this bed at Dörlbach. However, a poorly preserved *H.* cf. *bifrons* 5 cm above the Monotis Bed in the neighbouring section Altdorf-Hirschbühler Bach and findings noted in Kolb (1964: p. 131) and Urlichs (1971: p. 70) suggest that the Fibulatum Subzone (see Dean et al. 1961: p. 482) is present.

(iii) Upper Toarcian (5.04 m)

The first appearance of *Haugia* sp. at the basis of bed 16 ("Variabilis Shale"), i.e. one compressed fragment at 40 cm above the "Monotis Bed", indicated the lower boundary of the Variabilis Subzone, Upper Toarcian. Only a minor overlap of this genus with *Hildoceras* was observed at the Ludwigskanal/Dörlbach. Pyritized and compressed *Catacoeloceras raquinianum* (Fig. 13: 2, 3), *Pseudolioceras compactile* (Fig. 12: 10, 11), and *Lytoceras sublineatum* (Fig. 13: 1) are abundant in this zone, while compressed *Haugia variabilis* (Fig. 12: 8) concentrate in the top 15 cm. *Phylloceras heterophyllum*, *Mucrodactylites mucronatus* (Fig. 12: 6, 7), and *Lytoceras* cf. *cornucopia* are present, too.

One compressed *Haugia jugosa* 3 cm below top (Fig. 12: 9) and one compressed *Denckmannia rude* 1 cm below top of bed 16 are consistent with the Jugosa Horizon (Elmi et al. 1997) at the top of the Variabilis Subzone. A finding of *Haugia ogerieni* from Berg by Krumbeck (1943), which is a coarse ribbed variety of *Haugia jugosa* according to Lacroix (2011), may further support this interpretation. The following "Fucoid Bed" (bed 17), containing *Haugia variabilis*, *Catacoeloceras raquinianum*, *Phylloceras heterophyllum*, and *Lytoceras* cf. *cornucopia* may also belong to this horizon.

A change in the ammonoid assemblage, however, is evident for bed 18, i.e., the 5 cm calcareous marl below the "Belemnite Battlefield": *Pseudogrammoceras subregale* (Pinna) (Fig. 13: 4) and *Haugia* cf. *phillipsi* (Simpson) (Fig. 13: 5) point to the Illustris Subzone (Gabilly 1976a: p. 126), with *Catacoeloceras raquinianum* still abundant. Likewise, Krumbeck (1943: p. 298) reported a *Haugia* cf. *illustris* from shales just below the Belemnite Battlefield of the Teufelsgraben.

The "Belemnite Battlefield" (bed 19) is rather poor in ammonoids. *Catacoeloceras raquinianum* (d'Orbigny) has been recovered at the lower bedding plane (Fig. 13: 6), and deformed phosphoritic casts of *Lytoceras* cf. *cornucopia* occur within the bed. One fragmentary *Pseudogrammoceras* sp. is poorly preserved. This rather unspecific assemblage is, nonetheless, consistent with the view of Urlichs (1971) that the Belemnite Battlefield still belongs to the (upper) Variabilis Zone, with no elements of the Thouarsense Zone. However, no direct evidence of the Vitiosa Subzone was found at Dörlbach.

The following "Main Phosphorite Bed" (bed 20) has been assigned by Krumbeck (1943: p. 305) to the Thouarsense Zone because of findings of *Grammoceras thouarsense* in the neighbouring section Hausheim. At the Ludwigskanal/Dörlbach, this bed yielded a number of *Lytoceras cornucopia* (Fig. 13: 8) specimens, one coarsely ribbed *Pseudogrammoceras* sp., one *Osperleioceras bicarinatum* (Fig. 13: 7), and one phosphoritic cast of *Denckmannia rude* (Fig. 13: 9). While *D. rude* is restricted to the Variabilis Zone (Becaud et al. 2005; Lacroix 2011: p. 235), *O. bicarinatum* ranges from the Semipolitum Horizon to the Bingmanni Horizon (Lacroix 2011: p. 113). The "Main Phosphorite Bed" (bed 20), therefore, represents a condensation horizon comprising the top of Variabilis and the basis of Thouarsense Zone.

Numerous, compressed *Grammoceras* cf. *thouarsense* (Fig. 14: 1) occur as a monospecific assemblage in the overlying "Toarcensis Shale" (bed 21), which consequently represents the Thouarsense Subzone. Neither lytoceratids nor any other ammonite genus was found in this bed. Indication of the Fallaciosum Subzone is absent at the Ludwigskanal/Dörlbach, but phosphoritic casts of *Pseudogrammoceras* gr. *fallaciosum* were mentioned by Krumbeck (1943: p. 305) from a belemnite-rich marl at the neighbouring section Hausheim (4.4 km SE of Dörlbach).

The "belemnite accumulation" of bed 22 yielded, except for *Alocolytoceras* cf. *rugiferum*, no determinable ammonoids. The range of *A. rugiferum* is not well constrained, but shows a maximum abundance in the Dispansum Zone in northern and southwestern Germany (Wunstorf 1904; Ernst 1923; Knitter and Riegraf 1984). Therefore, this bed is considered as erosive basis of the Dispansum Zone, and may contain reworked components of the Fallaciosum Subzone, as the ones described by Krumbeck (1943).

First *Phlyseogrammoceras dispansum* (Fig. 14: 5, 8), however, have been found 5 cm above the "belemnite accumulation bed 22", in bed 23. This ammonoid extents up to 18 cm above basis of bed 23 and is associated with abundant *Alocolytoceras rugiferum* (Fig. 14: 2, 4) and rare *Pseudolioceras* cf. *boulbiense* (Fig. 14: 3). 10 and 15 cm above basis of bed 23, *Hammatoceras insigne* (Fig. 14: 10, 12) has been detected, clearly overlapping with the range of *Phlyseogrammoceras dispansum* in this section, so that the Dispansum Zone cannot be subdivided at the Ludwigskanal/Dörlbach.

At 11 cm below top of bed 23, first *Dumortieria* occur, specifically *Dumortieria insignisimilis* (Fig. 14: 6, 7), corresponding to the basis of the Levesquei Subzone ("Dumortieri Horizon": Elmi et al. 1997; "Insignisimilis Zonule": Page 2003). The index fossil *Dumortieria levesquei* (Fig. 14: 11, 13) was detected slightly above (i.e., 6 and 9 cm below top of bed 23), together with *Dumortieria radians*.

The top 4 cm of bed 23 finally show an ammonite accumulation with *Dumortieria pseudoradiosa* (Fig. 14: 14), *D. radiosa*, and *D. striatulocostata*, marking the onset of the Pseudoradiosa Subzone. The first appearance of *Dumortieria moorei* (Fig. 15: 10), which decends from *D. radiosa*, is delayed relative to *D. pseudoradiosa*, and falls into the upper part of the Pseudoradiosa Subzone. The (chrono)species also shows an overlap with its successor *Cotteswoldia mactra*, in accordance with data from sections from France (Rulleau 2007: p. 32). Consequently, the Moorei Subzone sensu Dean et al. (1961) in England is, in our view, not equivalent to the Pseudoradiosa Subzone sensu Gabilly 1976a and Elmi et al. 1997 (Fig. 8). However, the Moorei Subzone sensu Knitter and Ohmert (1983) in SW Germany (defined by the FAD of *Dumortieria pseudoradiosa*) is identical to the Pseudoradiosa Subzone used in the present paper. Moreover, top parts of the Pseudoradiosa Subzone at the Ludwigskanal/Dörlbach yielded *Paradumortieria* cf. *tectiforme* (Fig. 15: 5), forming the transition to the subsequent *Cotteswoldia aalensis* group.

Bed 25 clearly forms a minor condensation with the enrichment of phosphorite nodules, ammonites and belemnites. *Cotteswoldia mactra* (Fig. 15: 3) obtained from this bed indicates the basis of the Mactra Subzone, Aalensis Zone, still occuring together with the latest *D.* cf. *moorei*. This lowermost part of the Aalenis Zone, which is a comparatively short interval of only 20 cm thickness, is characterized by the persistent occurrence of coarse-ribbed *Dumortieria*, specifically *D. costula* und *D. externicostata*, which appear to be absent (or rare) in the upper part of the section. Also, first *Pleurolytoceras wrighti* were found in this bed.

With a minor overlap with *Cotteswoldia mactra*, *Cotteswoldia aalensis* (Fig. 15: 6), *C. distans* (Fig. 15: 9), *Pleydellia subcompta* (Fig. 15: 12) and *Pleurolytoceras hircinum* (Fig. 15: 2) occur from 15 cm above the basis of bed 26 to the top of bed 28, i.e. an ammonoid accumulation just below the calcareous marlstone bed 29. This ammonoid assemblage is characteristic for the Aalensis Subzone. From the following 120 cm of the section (beds 29 to 32), no ammonoids were recovered (lack of collection). However, according to the section Pölling 6.3 km SSE of Dörlbach (Arp 2010), the marlstone bed (equivalent to bed 29) and 30 cm marls above (equivalent to bed 30) still belong to the Aalensis Subzone, and the basis of the Torulosum Subzone is drawn at a belemnite accumulation of bed 31. Bed 33, a condensed horizon with phosphorite nodules, enrichment of belemnites, ammonites, and bivalves provided compressed specimens of *Pleydellia buckmani* (Fig. 15: 16), *P.* cf. *falcifer* (Fig. 15: 17), *P. lotharingica* (Fig. 15: 15), and *Pleurolytoceras torulosum* (Fig. 15: 14). The bed clearly belongs to the youngest ammonite subzone of the Lower Jurassic, i.e., the Torulosum Subzone.

Stage	Zone (NW-Europe)[1]	Subzone (Great Britain)[1]	Horizon (Yorkshire, Scotland)[2]	Subzone (SW-Germany)[3]	Subzone (France)[4]	Horizon (France)[4]	Zone (NW-Europe), revised[4]
Aal.	Opalinum			Opalinum			Opalinum
Upper Toarcian				Torulosum	Pseudo-lotharingicum	Buckmani	Aalensis
						Pseudolotharingicum	
	Levesquei	Aalensis		Aalensis	Mactra	Celtica	
		Moorei		Mactra		Mactra	
						Tectiforme	
				Moorei	Pseudoradiosa	Pseudoradiosa	Pseudoradiosa
		Levesquei		Levesquei	Levesquei	Munieri	
						Dumortieri	
		Dispansum	< not defined >	Dispansum	Gruneri	Gruneri	Dispansum
				Insigne	Insigne	Pachu	
						Cappucinum	
	Thouarsense	Struckmanni		Fallaciosum	Fallaciosum	Fallaciosum	Thouarsense
					Fascigerum	Fascigerum	
		Striatulum		Thouarsense	Thouarsense	Thouarsense	
						Doerntense	
	Variabilis	<not defined>		Bingmanni	Bingmanni	Bingmanni	
				Vitiosa	Vitiosa	Vitiosa	Variabilis
				Illustris	Illustris	Phillipsi	
						Illustris	
				Variabilis	Variabilis	Jugosa	
						Navis	
Lower Toarcian	Bifrons	Braunianus/ Crassum	Crassum-Semipolitum	Crassum	Bifrons	Semipolitum	Bifrons
			Crassum-Bifrons			Bifrons	
		Fibulatum	Vortex	Fibulatum			
			Braunianus			Apertum	
			Turriculatum				
		Commune	Athleticum	Commune		Lusitanicum	
			Commune		Sublevisoni	Tethysi	
			Ovatum			Sublevisoni	
	Falcifer	Falcifer	Falciferum	Falciferum	Falciferum	Douvillei	Serpentinum
			Pseudoserpentinum			Pseudoserpentinum	
		Exaratum	Elegans	Elegans	Elegantulum	Strangewaysi	
			Exaratum	Exaratum			
			Elegantulum	Elegantulum		Elegantulum	
	Tenuicostatum	Semicelatum	Antiquum	Semicelatum	Semicelatum	Semicelatum	Tenuicostatum
			Semicelatum				
		Tenuicostatum	Tenuicostatum			Tenuicostatum	
		Clevelandicum	Clevelandicum	Clevelandicum		Crosbeyi	
			Crosbeyi				
		Paltum	Paltum	Paltum	Paltus	Paltum	
Pliensb.	Spinatum	Hawskerense	Hawskerense	Hawskerense	Hawskerense	Hawskerense	Spinatum
			Elaboratum			Lotta	
		Apyrenum	Solare	Apyrenum	Apyrenum	Solare	
			Transiens			Transiens	
			Salebrosum			Salebrosum	

Figure 8. Ammonite zones, subzones, and horizons for the NW-European Toarcian according to different authors. 1) Dean et al. 1961; Howarth 1978. 2) Page 2003, 2004. 3) Knitter and Ohmert 1983; Riegraf et al. 1984; Riegraf 1985a; Ohmert et al. 1996; Cresta et al. 2001. 4) Gabilly 1976a; Elmi et al. 1997). Note that *Pleydellia* (*Walkericeras*) *lugdunensis* Elmi & Rulleau, 1997 is considered by Di Cencio and Weis (2020) as junior synonym of *P.* (*W.*) *pseudolotharingicum* Maubeuge, 1950, so that the subzone and horizon is termed accordingly.

(iv) Lower Aalenian (>0.5 m)

No *Leioceras opalinum* has been found in the Ludwigskanal/Dörlbach section. However, compressed *Leioceras opalinum* found in a drill core (highway viaduct Pilsach, unpublished observations) immediately above the equivalent of bed 33 suggests that the Toarcian-Aalenian boundary is located at the basis of bed 34.

Sequence stratigraphy

Sequence stratigraphic interpretations require correlation and comparison of sections across the shelf with respect to discontinuities, facies trends, geometry and stacking patterns (e.g., Catuneanu et al. 2011). In the present paper, the definition of sequences as "transgressive-regressive cycles" (T-R cycles) follows Embry and Johannessen (1992), with "sequence boundaries" at maximum regression surfaces (mrs; for further discussion see Catuneanu et al. 2011 and Simmons 2012). However, it remains difficult to distinguish stratigraphic gaps at maximum regression surfaces (with reworked fauna in the following transgressive "ravinement surface"; Nummedal and Swift 1987) from condensation or non-deposition of maximum flooding surfaces (mfs) in sections distant from siliciclastic sediment influx.

This also applies to the South German Toarcian succession, because of low sedimentation rates and high distance to deltaic siliciclastic influx, no evident subaerial exposure surfaces, and (with respect to the Upper Toarcian) a limited number of sections with both, detailed sedimentological plus biostratigraphic observations. The following sequence stratigraphic interpretations, therefore, remain preliminary (Figs 7, 9).

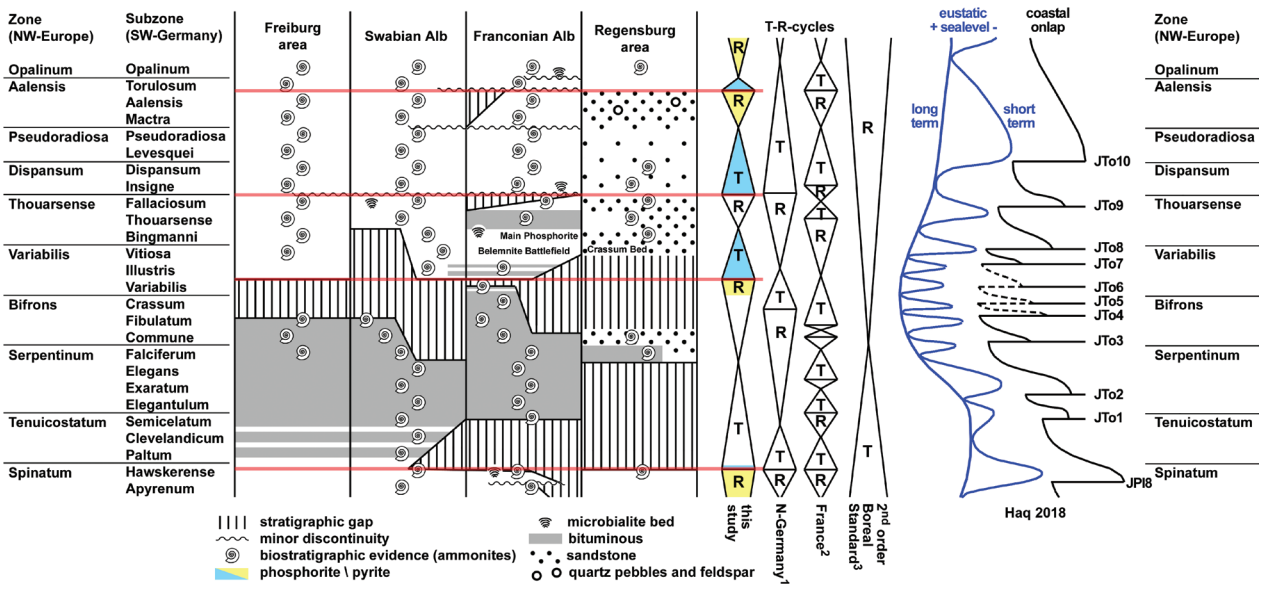

Figure 9. Sequence stratigraphic interpretation of the Toarcian succession in the Franconian Alb (including Ludwigskanal/Dörlbach section) and adjacent areas. Sedimentary succession and ammonite biostratigraphic evidence according to Pompeckj (1901), Krumbeck (1932b, 1943), Putzer (1939), Bauberger et al. (1969), Meyer and Bauberger (1998) (Regensburg area), Brockert (1959), Fischer (1964), Wiedemann (1966), Urlichs (1977a), Riegraf et al. (1984), Riegraf (1985a), Etzold et al. (1989) (Swabian Alb), Ohmert (1976), Knitter and Ohmert (1983), Ohmert et al. (1996) (Freiburg area), T-R cycles: 1 = third order sequences N-Germany (Zimmermann et al. 2015), 2 = third order sequences France (de Graciansky et al. 1998); 3 = second order sequences Boreal standard (de Graciansky et al. 1998; Jacquin et al. 1998). Eustatic sea level and coastal onlap according to Haq (2018). Note that the definition of sequence boundaries in Haq (2018) differs from the concept of T-R-sequences, with the latter bounded by maximum regression surfaces (Embry and Johannessen 1992; see also Simmons 2012).

A sequence stratigraphic framework, however, has been developed for the Toarcian of Northern Germany, based on a comprehensive analysis of drillings (sedimentology and gamma ray logs) covering the transition from marine to fluviodeltaic deposits of the NE-German Basin to fully marine deposits of the NW-German Basin (Zimmermann et al. 2015). Nonetheless, the biostratigraphic calibration of the drillings relies on a combination of microfossil records and comparatively rare ammonite records, with limited resolution at the subzone level. Furthermore, a sequence stratigraphic interpretation was given by Röhl and Schmid-Röhl (2005) for the Lower Toarcian in Southern Germany, specifically based on the biostratigraphically and sedimentologically well investigated sections Dotternhausen (Swabian Alb) and Schesslitz (Franconian Alb).

For the Upper Toarcian of Southern Germany, no such detailed analysis exists, but important information can be derived from proximal sections near Regensburg, where minor coarse siliciclastic influx during regressive phases intercalate between fine-grained open-marine sediments with ammonoids (Fig. 9). Furthermore, sequence stratigraphic interpretations based on well dated drillings and outcrops exist for the Toarcian of France (de Graciansky et al. 1998), including Quercy (Cubaynes et al. 1984; Lezin et al. 1997) and the type region of the Toarcian (Galbrun et al. 1994). Indeed, the most recent interpretation of the Toarcian eustatic sealevel curve by Haq (2018) is largely based on European sections from France, United Kingdom, Poland, and Switzerland, with additional data from sections in Argentina, Tibet, and the Arabian Platform (partially with tentative correlations).

The total duration of the Toarcian is about 8.5 Ma (Gradstein et al. 2012: from 182.7 to 174.1 Ma, i.e. 8.6 Ma; Boulila et al. 2014: 8.3 Ma), while the duration of each of the ammonite zones is to date under discussion (Gradstein et al. 2012; Boulila et al. 2014; Rübsam and Al-Husseini 2020). In the following, vertical thickness and facies trends as well as discontinuities of the Ludwigskanal/Dörlbach section are discussed in comparison with neighbouring sections (Fig. 7) and areas to reveal T-R cycles for the top Pliensbachian to basis Aalenian succession in Southern Germany (Fig. 9).

(i) Amaltheenton Formation

Only two stratigraphic gaps in the otherwise monotonous claystones of the Amaltheenton are evident: The first gap is located within higher parts of the formation. Here, the "Delta-Fossil Bed" (Fig. 5) forms a distinct intraformational discontinuity at the basis of the Hawskerense Subzone. This discontinuity is also evident in neighbouring sections farther north (Buttenheim: Hoffmann et al. 2007) and south, where the section Sulzkirchen exhibits a clear erosional relief with compensation of the gap by sediment of the Hawskerense Subzone (Keupp and Arp 1990).

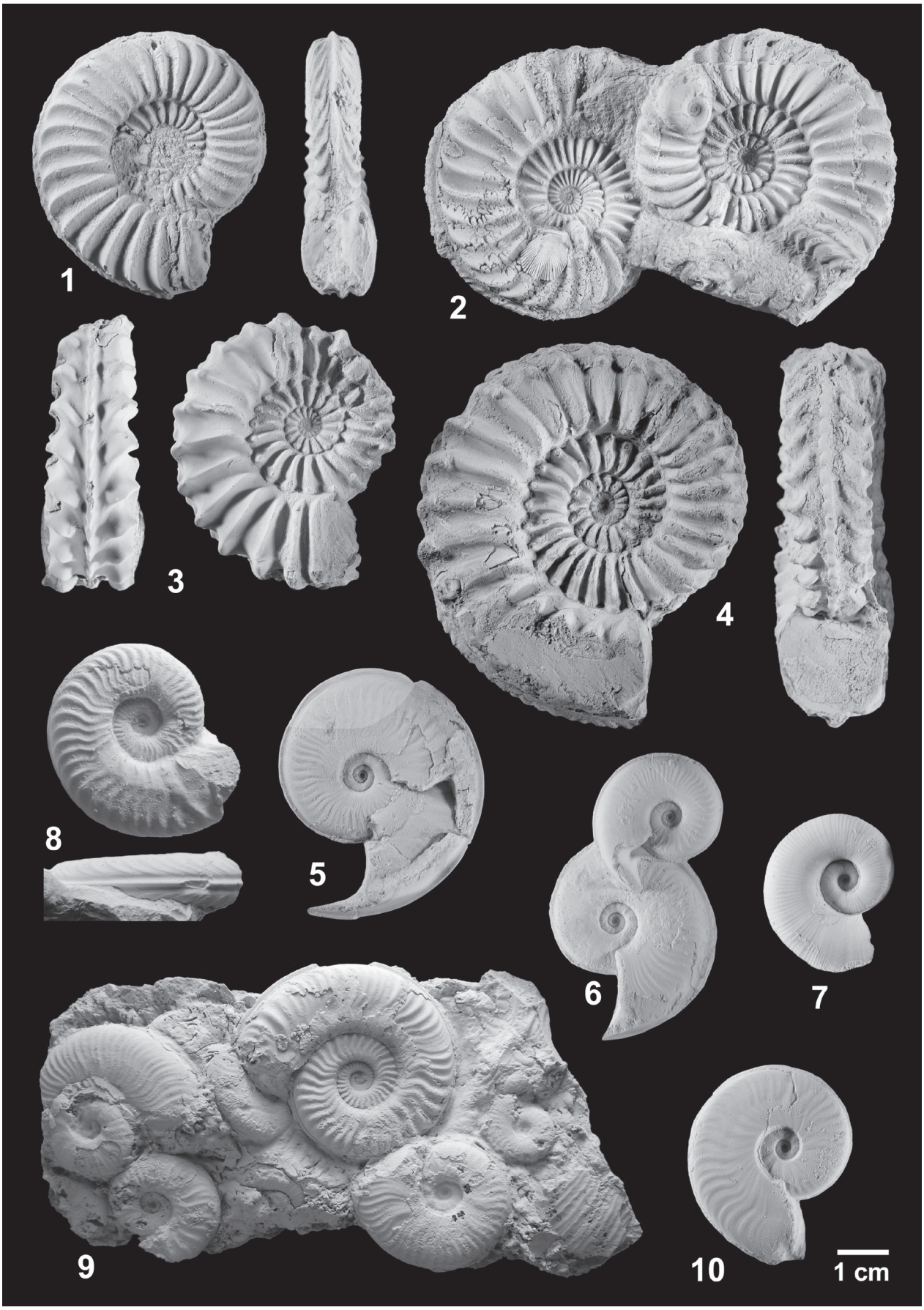
1
2
3
4
5
6
7
8
9
10
1 cm

Figure 10. 1. *Pleuroceras solare* (Phillips), reworked concretion in bed 4, basis of Hawskerense Subzone, Amaltheenton Formation. GZG.INV.70496: d = 53 mm, di = 39 mm, u = 22 mm, wh = 17 mm, wb = 15 mm, rb/2 = 15. **2.** Two specimens of *Pleuroceras solare* var. *solitarium* (Simpson), together with a juvenile *Amauroceras ferrugineum* (Simpson), reworked concretion in bed 4, basis of Hawskerense Subzone, Amaltheenton Formation. GZG.INV.70497a: d = 54 mm, di = 39 mm, u = 21 mm, wh = 17 mm, wb = 15 mm, rb/2 = 15; GZG.INV.70497b: d = 56 mm, di = 40 mm, u = 24 mm, wh = 18 mm, wb = 14 mm, rb/2 = 15; GZG.INV.70497c: d = 11 mm, di = 7 mm, u = 3 mm, wh = 5 mm, wb = 3 mm, rb/2 = 28. **3.** *Pleuroceras spinatum* (Bruguière), 2 m below top of bed 5, Hawskerense Subzone, Amaltheenton Formation. GZG.INV.70498: d = 54 mm, di = 37 mm, u = 23 mm, wh = 19 mm, wb = 18 mm, rb/2 = 11. **4.** *Pleuroceras spinatum* (Bruguière), 50 cm above basis of bed 5, Hawskerense Subzone, Amaltheenton Formation. GZG.INV.70499: d = 76 mm, di = 58 mm, u = 36 mm, wh = 24 mm, wb = 24 mm, rb/2 = 14. **5.** *Tiltoniceras antiquum* (Wright), 1–2 cm above basis of bed 7, Semicelatum Subzone, Posidonienschiefer Formation. Minor part (bright area) of the body chamber restored. GZG.INV.45641a: d = 48 mm, di = 33 mm, u = 12 mm, wh = 20 mm, wb = 12 mm, rb/2 = 22. **6.** *Tiltoniceras antiquum* (Wright), 1–2 cm above basis of bed 7, Semicelatum Subzone, Posidonienschiefer Formation. GZG.INV.45641b: d = 38 mm, di = 26 mm, u = 9 mm, wh = 17 mm, wb = 9 mm, rb/2 = (33); GZG.INV.45641c: d = 27 mm, di = 18 mm, u = 6.5 mm, wh = 11 mm, wb = 7 mm, rb/2 = (30). **7.** *Lytoceras ceratophagum* (Quenstedt), middle part of bed 7, Exaratum Subzone, Posidonienschiefer Formation. GZG.INV.70500: d = 29 mm, di = 18 mm, u = 9 mm, wh = 12 mm, wb = 11 mm, rb/2 = 46. **8.** *Hildaites murleyi* (Moxon), bed 7, Exaratum Subzone, Posidonienschiefer Formation. GZG.INV.70501: d = 41 mm, di = 27 mm, u = 14 mm, wh = 16 mm, wb = 12 mm, rb/2 = 21; (leg. Arno Garbe). **9.** *Hildaites murleyi* (Moxon), together with juvenile *Cleviceras exaratum* (Young and Bird), bed 7, Exaratum Subzone, Posidonienschiefer Formation. GZG.INV.70502: d = 44 mm, di = 32 mm, u = 17 mm, wh = 15.5 mm, wb = 10 mm, rb/2 = 24; (leg. Arno Garbe). **10.** *Cleviceras exaratum* (Young and Bird), middle part of bed 7, Exaratum Subzone, Posidonienschiefer Formation.GZG.INV.70503: d = 39 mm, di = 27 mm, u = 10 mm, wh = 17 mm, wb = 8 mm, rb/2 = 24.

The second gap is developed at the top of the Amaltheenton, where reworked nodules indicate an erosion at the Ludwigskanal (Fig. 5). In neighbourig sections, these nodules are commonly accumulated to form the so-called "Bollernkalk" (Bandel and Knitter 1983; Böhm and Brachert 1993), which shows a non-bituminous bioclastic micrite matrix with minor phosphorite. This conglomeratic bed is probably still Upper Pliensbachian in age (Riegraf 1985a: his fig. 17) and coincides with the formation of an erosional relief including the "Altdorf High" and a coast-parallel strip devoid of Amaltheenton sediments, compensated by later sediments of the Posidonienschiefer (Knitter 1983: p. 240; Arp et al. 2014). Strikingly, the Spinatum Zone in the Franconian Alb shows a considerably higher thickness compared to sections of the Swabian Alb. In turn, the carbonate contents of the Spinatum Zone sediments increase towards the Swabian Alb ("Costatenkalke": alternation of marls and concretionary limestone beds; Quenstedt 1858: p. 164; Urlichs 1977a, b).

Based on these observations, sediments of the Spinatum Zone in the Franconian Alb are considered to reflect a regression with prograding siliciclastics from NE, and a corresponding maximum regression surface in top parts of the Hawskerense Subzone (Fig. 9). This is in accordance with delta progradation and regression seen in N-Germany (Zimmermann et al. 2015) and a sequence boundary near the top of the Spinatum Zone (JPl8 sensu Haq 2018). Hence, the reduced thickness and increasing carbonate content towards the SW (Swabian Alb) mirrors the greater distance to the source of siliciclastics from NE (see Paul et al. 2008: fig. 5). An additional, minor, intermittent regression (with changes in bottom currents) might be seen in the erosional discontinuity at basis of the Hawskerense Subzone, while the coast-parallel lack of the total Amaltheenton mirrors a coast-parallel current intensification during the Pliensbachian-Toarcian transition (Fig. 9). Röhl and Schmid-Röhl (2005), however, suggest that the sequence boundary at the Pliensbachian-Toarcian transition in Southern Germany is located within the Tenuicostatum Zone, which might correspond to the medium sequence boundary JTo1 sensu Haq (2018). No decision can be made on that from the present data of the condensed Ludwigskanal section. In any case, the Upper Pliensbachian is generally known as a period of low sealevel, reflecting a cold climate interval with polar ice caps (Price 1999), glendonites (Teichert and Luppold 2013), and cool-water faunal elements (Arp and Seppelt 2012). Nonetheless, no evidence of subaerial exposure was found to date at basin margin sections (Regensburg area). However, these oolitic and laminated iron ores are poorly investigated with respect to sedimentology and geochemistry.

(ii) Posidonienschiefer Formation

The Posidonienschiefer shows a very low thickness, combined with high carbonate contents. C_{org} contents normalized to the silicate sediment fraction show that the T-OAE clearly peaks in the Exaratum Subzone (Fig. 4). A second maximum is developed in the Falciferum-Commune Subzones. Strikingly, first Posidonienschiefer beds (Laibstein I and II) show endo- and epibenthic bivalves (*Nicaniella* sp., *Pleuromya* sp., *Goniomya rhombifera*, *Camptonectes subulatus*), which are absent farther up the section, suggesting a delayed overstepping of anoxic bottom waters on the Altdorf High. Ammonite zones and subzones are densely spaced, however, with only one clear stratigraphic gap at the basis of the formation (Fig. 6). Here, the

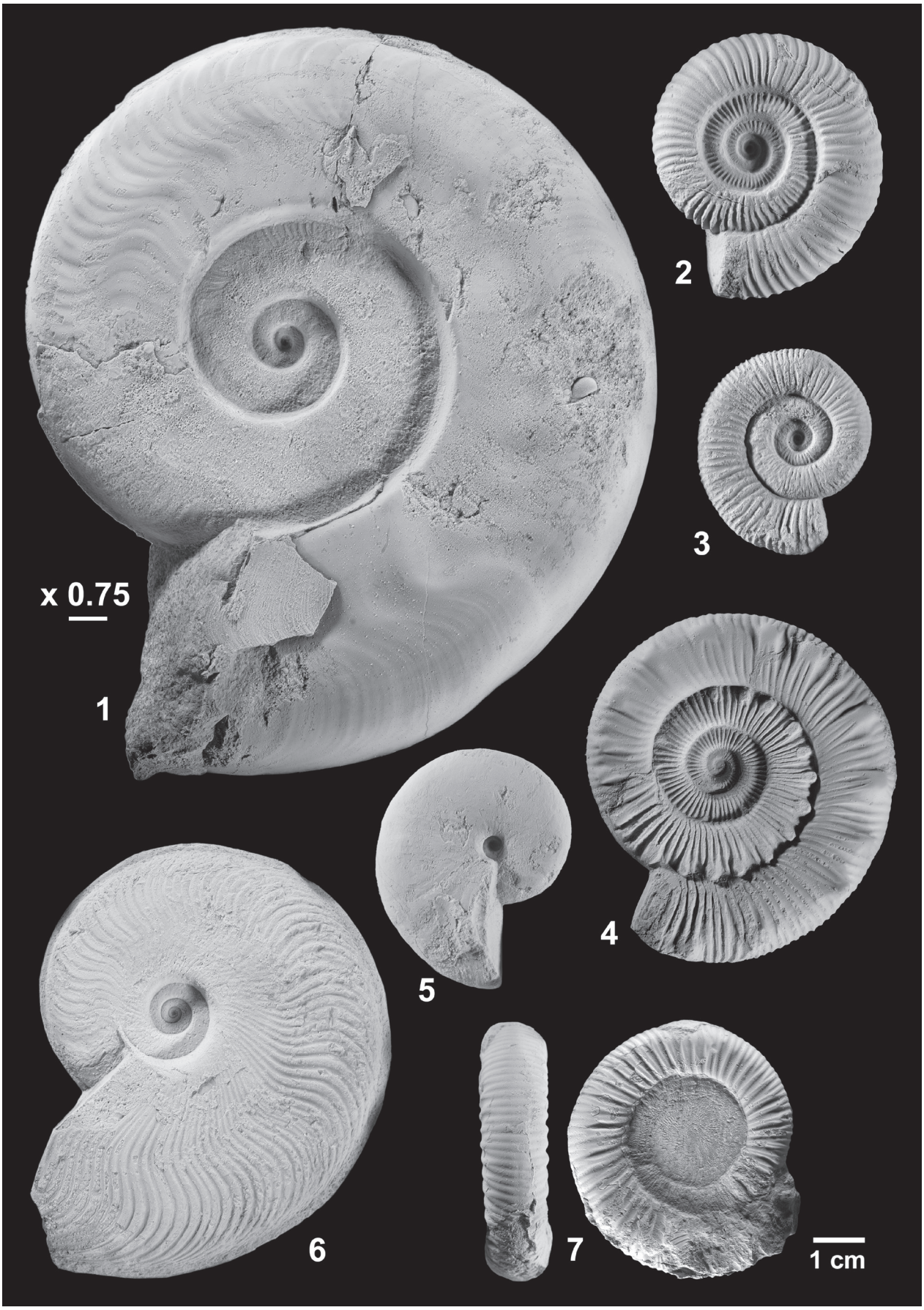
x 0.75
1
2
3
4
5
6
7
1 cm

Figure 11. 1. *Harpoceras serpentinum* (Schlotheim), bed 8, Elegans Subzone, Posidonienschiefer Formation. GZG.INV.70504: d = 197 mm, di = 144 mm, u = 80 mm, wh = 70 mm, wb = 40 mm, rb/2 = n.a.; (leg. Matthias Weißmüller). **2.** *Dactylioceras* sp. forma aegra *circumdata* (Martin 1858) Hölder 1956, bed 8, Elegans Subzone, Posidonienschiefer Formation. GZG.INV.70505a: d = 53 mm, di = 40.5 mm, u = 22 mm, wh = 13.5 mm, wb = 15 mm, rb/2 = 30. **3.** *Dactylioceras anguinum* (Reinecke), bed 8, Elegans Subzone, Posidonienschiefer Formation. GZG.INV.70505b: d = 40 mm, di = 30 mm, u = 14.5 mm, wh = 11 mm, wb = (11 mm), rb/2 = 31. **4.** "*Peronoceras" desplacei* (d'Orbigny), bed 8, Elegans Subzone, Posidonienschiefer Formation. GZG.INV.70506: d = 68 mm, di = 53 mm, u = 38 mm (56%), wh = 16 mm (24%), wb = 16 mm, rb/2 = 41. **5.** *Phylloceras heterophyllum* (Sowerby), bed 8, Elegans Subzone, Posidonienschiefer Formation. GZG.INV.70507: d = 44 mm, di = 29 mm, u = 4.5 mm, wh = 24 mm, wb = 12 mm, rb/2 = n.a. **6.** *Cleviceras elegans* (Sowerby), bed 8, Elegans Subzone, Posidonienschiefer Formation. GZG.INV.70508: d = 86 mm, di = 53 mm, u = 15 mm, wh = 43 mm, wb = 19 mm, rb/2 = 49. **7.** *Dactylioceras semiannulatum* Howarth, bed 8, Elegans Subzone, Posidonienschiefer Formation. GZG.INV.70509: d = 49 mm, di = 39 mm, u = 26 mm, wh = 12 mm, wb = 13 mm, rb/2 = 30.

Posidonienschiefer Formation unconformably overlies the Hawskerense Subzone, with a stratigraphic gap comprising the Paltum- to midth of Semicelatum Subzone (Riegraf 1985a, b).

All other ammonite subzones from top of the Semicelatum to the Crassum Subzone are present in the bituminous and laminated sediments of the Ludwigskanal/Dörlbach area (Fig. 6), although minor sedimentary gaps below the ammonite subzone resolution may be developed. The laminated bituminous marls continue into the lower Variabilis Zone with non-bituminous intercalations, fucoid beds, and scattered re-occurrence of benthic fauna (*Grammatodon* sp.). The fish scale-rich beds in the Falciferum Zone and at the basis of the Bifrons Zone, however, may reflect considerable sedimentological condensation, while the Dactylioceras-Monotis bed itself is an exceptional event bed with an erosional basis, possibly formed by a tsunami (Arp and Gropengießer 2015).

Towards the basin margin (Regensburg area), bituminous shales of the Falciferum Zone are overlain by prograding sandstones containing *Dactylioceras commune* and *D. athlecticum* (Pompeckj 1901; Putzer 1939; Krumbeck 1932b), followed by a discontinuity comprising the Fibulatum and Crassum Subzones (Fig. 9). Note that the "Crassum Bed" in this area does not contain *Catacoeloceras crassum*, but the younger species *Catacoeloceras raquinianum*, and is an equivalent of the "Belemnite Battlefield" (see below). In the Posidonienschiefer of Swabian Alb a number of fish scale-rich beds ("Schlacken") at top of Falciferum Zone (Riegraf et al. 1984; Riegraf 1985a) reflect a sedimentological condensation. Contrary to the Franconian Alb, bituminous sedimentation in the Swabian Posidonienschiefer ends with the Fibulatum Subzone.

Consequently, the sequence stratigraphic interpretation is as follows (Fig. 9): The transgression in the lower half of the Posidonienschiefer is documented by the successive onlap of subzones from SW to NE (Riegraf et al. 1984: p. 26, fig. 7; Riegraf 1985a: p. 55, fig. 27), delayed onset of sedimentation on the Altdorf High and basin margin (Regensburg area), and delayed benthos elimination on the Altdorf High. Minor sediment condensation (fish scale rich beds) at the Falciferum-Commune Subzone transition (bed 11; Fig. 6) may correspond to a maximum flooding surface, probably equivalent to fish-scale-rich intercalations ("Schlacken"; Hauff 1921; Riegraf et al. 1984: p. 16 ff) in a similar lithostratigraphic position in the Swabian Posidonienschiefer (Fig. 7). Hence, higher Bifrons and Variabilis Subzone reflect regression with increasing siliciclastic influx, associated with pyrite preservation of ammonites (only Variabilis Subzone), and temporary re-oxygenation of the seafloor.

This interpretation is similar to the 3rd order T-R cycle previously proposed for the Swabian and Franconian Posidonienschiefer by Röhl and Schmid-Röhl (2005) (Fig. 9). The only addition to be made is, that the regressive system tract of the cycle extents into the lower Variablilis Zone. In N-Germany, this T-R cycle appears slightly shifted, with a maximum flooding surface already in top parts of the Tenuicostatum Zone (mfs Toa 1), followed by regression and maximum regression surface in top parts of the Bifrons Zone (mrs Toa 1) (Zimmermann et al. 2015). A possible explanation for this minor shift is the higher subsidence as well as higher sediment supply in North-German Basin at that time.

Considerable differences exist with respect to the proposed 3rd order sequences in France. De Graciansky et al. (1998) suggest four 3rd order sequences for the Lower Toarcian, and a fifth sequence for the Fibulatum to Thouarsense Subzone. None of these T-R cycles appear recognizable in Germany, and may refer to minor superimposed changes (4th oder sequences) only seen in areas of high sedimentation rate. Strikingly, there is also a continuous sedimentation from the higher Bifrons throughout the complete Variabilis Zone, in contrast to the erosive Intra-Variabilis-Discontinuity in S-Germany (Fig. 9).

(iii) Jurensismergel

Similar to the previous formation, the thickness of the Jurensismergel Formation is low (5 m). Ammonite zones and subzones are densely spaced and condensed at the phosphoritic and (slightly) bituminous basis of the formation (Fig. 6). Similar to the section Mistelgau (Schulbert 2001a, b), an increasing subzone thickness, decreasing carbonate content, and change from phosphoritic to pyritic ammonite preservation is observed towards the top of the formation (Fig. 7). A trend of increasing clay content is also recognizable from SW to NE, when compared to the increasingly

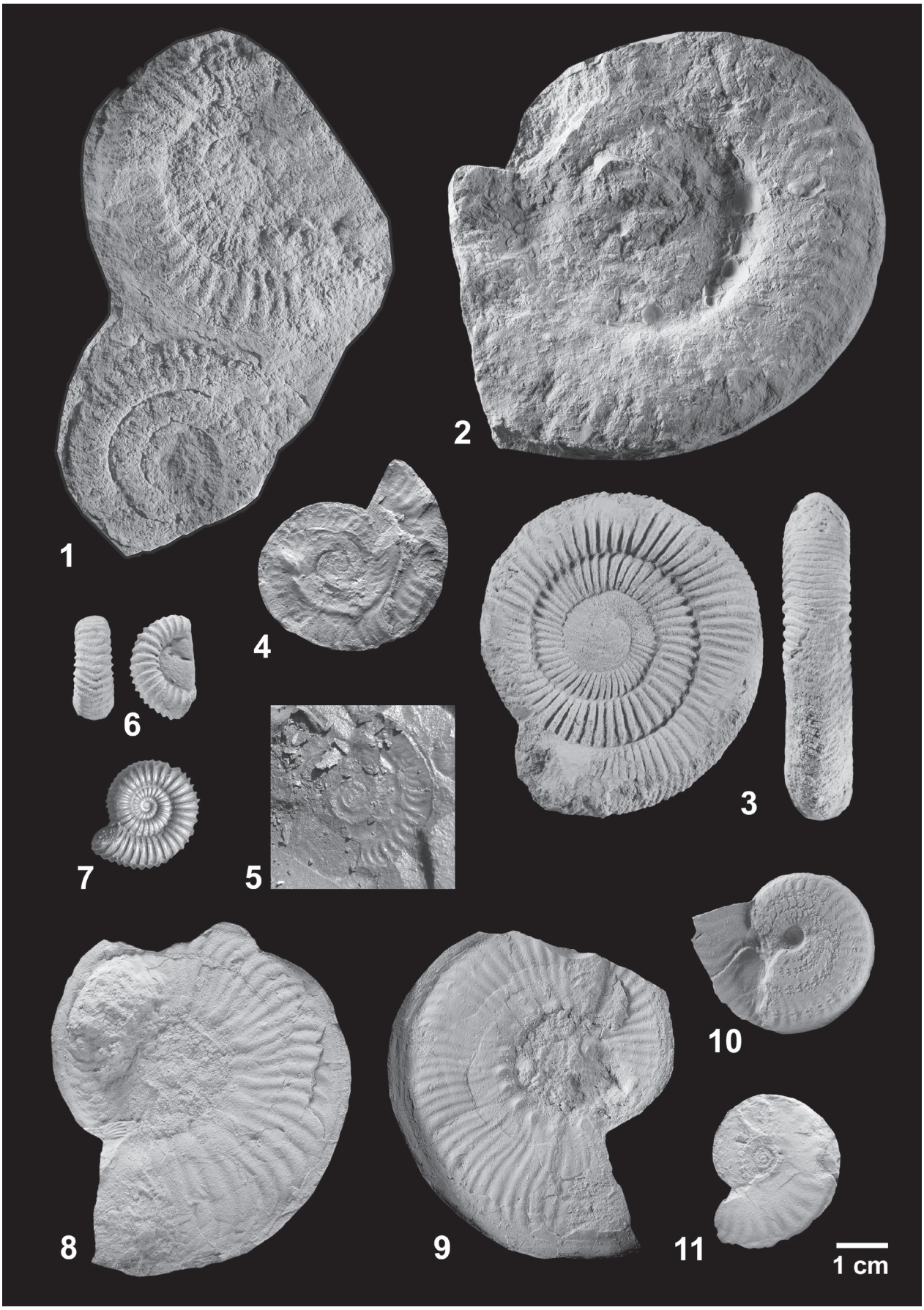
1
2
3
4
5
6
7
8
9
10
11
1 cm

Figure 12. 1. *Dactylioceras* cf. *commune* (Sowerby), lower bedding plane of bed 12, Commune Subzone, Posidonienschiefer Formation. GZG.INV.70510a: d = 61 mm, di = 49 mm, u = 34 mm, wh = 14 mm, wb = n.a., rb/2 = (24); GZG.INV.70510b: d = 45 mm, di = 35 mm, u = 27 mm, wh = 10 mm, wb = n.a., rb/2 = (25). **2.** *Hildoceras* cf. *lusitanicum* Meister, lower bedding plane of bed 12, Commune Subzone, Posidonienschiefer Formation. GZG.INV.70511: d = 92, di = (68 mm), u = 43 mm, wh = 26 mm, wb = (12 mm), rb/2 = (27). **3.** *Dactylioceras athleticum* (Simpson), middle part of bed 12, Commune Subzone, Posidonienschiefer Formation. GZG.INV.70512: d = 64 mm, di = 51 mm, u = 38 mm, wh = 13.5 mm, wb = 13.5 mm, rb/2 = 37. **4.** *Hildoceras semipolitum* Buckman, 18 cm below top of bed 15, Crassum Subzone, Posidonienschiefer Formation. GZG.INV.70513: d = 40 mm, di = 28 mm, u = 12 mm, wh = 16.5 mm, wb = n.a., rb/2 = (23). **5.** *Hildoceras semipolitum* Buckman, 18 cm below top of bed 15, Crassum Subzone, Posidonienschiefer Formation. Field image: d = (30 mm), di = (23 mm), u = 11 mm, wh = 10 mm, wb = n.a., rb/2 = (24). **6.** *Mucrodactylites mucronatus* (d'Orbigny), 43 cm below top of bed 16, Variabilis Subzone, Posidonienschiefer Formation. GZG.INV.70514: d = 20 mm, di = (15 mm), u = 9 mm, wh = 6.5 mm, wb = 8 mm, rb/2 = 17. **7.** *Mucrodactylites mucronatus* (d'Orbigny), bed 16 *ex situ*, Variabilis Subzone, Posidonienschiefer Formation. leg. Volker Münzner: d = 22 mm, di = 16.5, u = 10 mm, wh = 6 mm, wb = 6 mm, rb/2 = 18. **8.** *Haugia variabilis* (d'Orbigny), 13 cm below top of bed 16, Variabilis Subzone, Posidonienschiefer Formation. GZG.INV.45642: d = 67 mm, di = 44 mm, u = 20 mm, wh = 27 mm, wb = n.a., rb/2 = 27. **9.** *Haugia jugosa* (Sowerby), 3 cm below top of bed 16, Variabilis Subzone, Posidonienschiefer Formation. GZG.INV.70515: d = 71 mm, di = 46 mm, u = 19 mm, wh = 30 mm, wb = n.a., rb/2 = 34. **10.** *Pseudolioceras compactile* (Simpson), 37 cm below top of bed 16, Crassum Subzone, Posidonienschiefer Formation. GZG.INV.70516: d = 32 mm, di = 19 mm, u = 4.5 mm, wh = 17 mm, wb = 7 mm, rb/2 = 21. **11.** *Pseudolioceras compactile* (Simpson), 32 cm below top of bed 16, Crassum Subzone, Posidonienschiefer Formation. GZG.INV.70517: d = 30 mm, di = 20 mm, u = 5 mm, wh = 15 mm, wb = n.a., rb/2 = 15.

carbonate-rich sections in the Swabian Alb (Fig. 7). This points to a general progradation of deltas in N-Germany at that time, affecting the Franconian realm, with the Swabian area more proximal to the warm Tethyan Ocean.

The erosive basis of the Jurensismergel Formation, forming a sequence boundary, has early been recognized in the Swabian Alb, with an apparent transgression beginning with the Variabilis Zone (Stier 1922; Fischer 1964: p. 99; Bruder 1968: p. 150; Riegraf 1985a: his fig. 18; Etzold et al. 1989: p. 44 f). Indeed, a continuous sequence of ammonite subzones across the Posidonienschiefer-Jurensismergel boundary is only developed in the Wutach area SW of the Swabian Alb (Straub 1946: p. 56; Riegraf 1985a: p. 31). At the Ludwigskanal/Dörlbach, however, a continuous sedimentation across the Bifrons-Variabilis Zone boundary is evident, and a major stratigraphic gap appears developed at the "Belemnite Battlefield", i.e. the top of the Variabilis Zone (Figs 6, 7). These contracting observations require a detailed look on the actual biostratigraphic evidence, i.e. ammonite records:

At the Ludwigskanal/Dörlbach, the Semipolitum Subzone is overlain by a Variabilis Subzone, characterized by abundant *Catacoeloceras raquinianum*, *Pseudolioceras compactile*, and *Mucrodactylites mucronatus* (Fig. 6). The Illustris Subzone follows after a thin, but evident fucoid bed, and grades in the "Belemnite Battlerfield" containing reworked as well as autochthonous ammonite fossils of the higher Variabilis Zone (e.g., Urlichs 1971). On the other hand, the oldest ammonite assemblages of the channel-like occurrences of the Variabilis Zone in the Swabian Jurensismergel already comprise representatives of the Illustris (*Haugia illustris*, Holzheim-Ursenwang: Stolz 1911 in Straub 1946: p. 27; *Pseudogrammoceras doerntense*, Groß-Eislingen: Wiedemann 1966: p. 104) and Vitiosa Subzones (*Haugia vitiosa*, Jebenhausen: Urlichs 1977a; *Haugia* cf. *vitiosa*, Weilheim: Knitter and Riegraf 1984: p. 75, their fig. 4). These ammonites co-occur with *Haugia variabilis* and *Haugia navis*, but – contrary to Ludwigskanal/Dörlbach – *Catacoeloceras*, *Pseudolioceras* and *Collina* are absent. The same applies to sections of the Freiburg area, with the Illustris and Vitiosa Subzone erosive on top of a partially eroded Posidonienschiefer (Ohmert 1976; Knitter and Ohmert 1983).

Therefore, we suggest that the erosive basis of the Jurensismergel Formation and sequence boundary lies within the Variabilis Zone, specifically at the basis of the Illustris Subzone (Figs 7, 9). While no Intra-Variabilis-Zone mrs (maximum regression surface) is seen in N-German sections (Zimmermann et al. 2015), an equivalent mrs and sequence boundary at the basis of the Illustris Subzone was identified in the Toarcian type area in western France (Galbrun et al. 1994: their fig. 5).

Consequently, the "Belemnite Battlefield" with its fossil accumulation and phosphorite nodules rather represents a transgressive sediment, and indeed grades in basin margin sections into a cephalopod-rich sandstone bed ("Crassum Bed" with *Dactylotheutis irregularis*, *Catacoeloceras raquinianum*, *Haugia* sp., *Mucrodactylites mucronatus* and *Pseudolioceras compactile*: Meyer and Bauberger 1998: p. 40–41, fig. 10; "nodule bed a" with *Catacoeloceras raquinianum*, *Mucrodactylites mucronatus*, *Hildoceras* cf. *bifrons*: Krumbeck 1943: p. 332). At Dörlbach and other sections of the Franconian Alb (e.g. Mistelgau, Fig. 7), the "Belemnite Battlefield" is overlain by the "Main Phosphorite Bed" and the bituminous "Toarcensis Shale" (Krumbeck 1943), with a time-equivalent calcareous sandstone bed in basin margin sections ("Grammoceras limestone": Putzer 1939; "nodule bed b" with *Pseudogrammoceras* aff. *subquadratum*; "nodule bed c" with *G. thouarsense*, *P.* cf. *saemanni*, *P. fallaciosum*: Krumbeck 1943: p. 332). These cephalopod-rich beds indicate flooding and highstand conditions at the basin margin.

In the Swabian Alb, submarine "swells" (i.e., remaining topographic highs after erosion within Variabilis Zone;

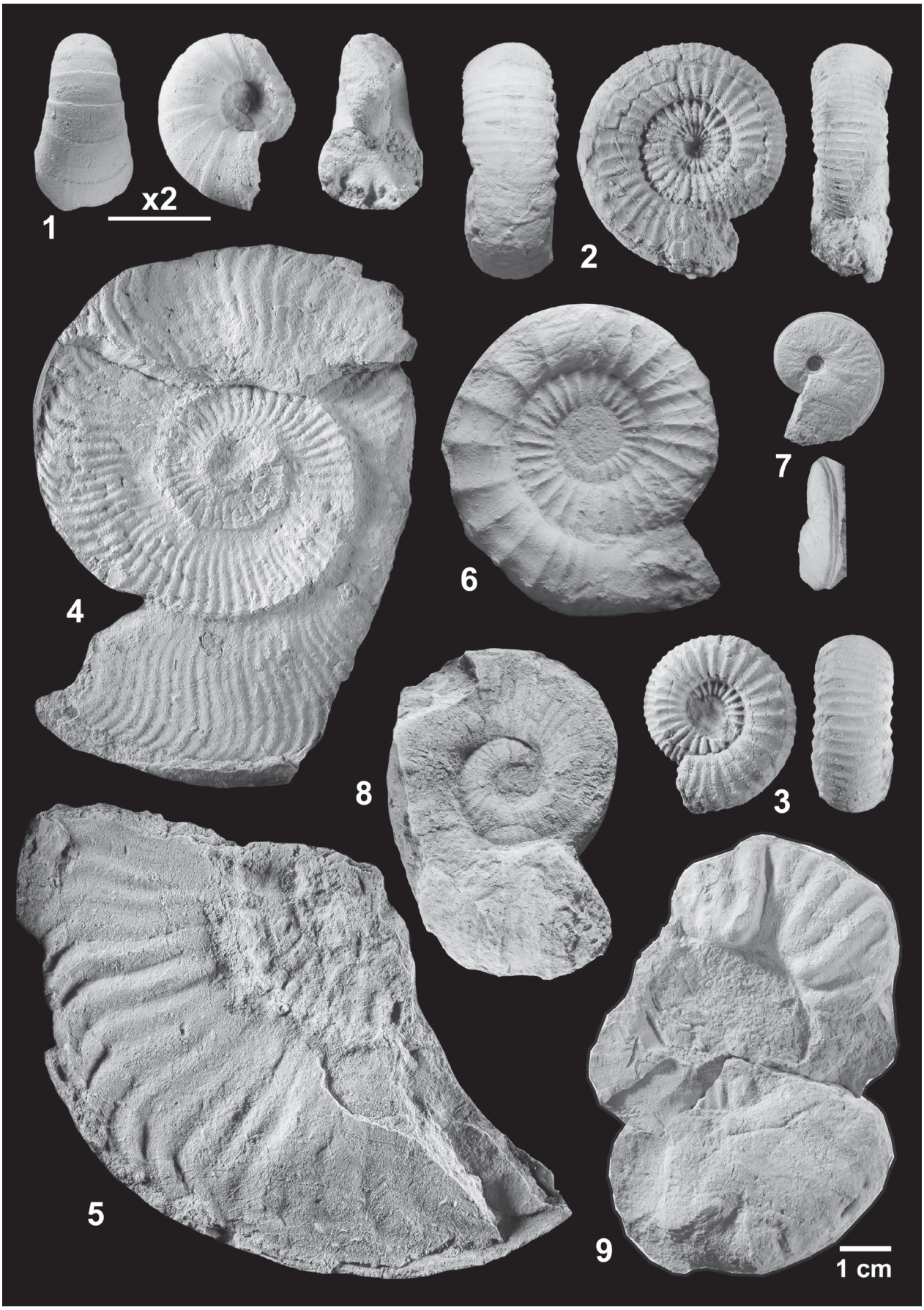
x2
1
2
4
6
7
8
3
5
9
1 cm

Figure 13. 1. *Lytoceras sublineatum* (Oppel), 38 cm below top of bed 16, Variabilis Subzone, Posidonienschiefer Formation. The telescope-like, shallow constrictions in this juvenile specimen are reminiscent of *Pleurolytoceras propehircinum* Krumbeck of the Aalensis Subzone, but the high wb/wh ratio points to *Lytoceras sublineatum* (Oppel). GZG.INV.70518: d = 17 mm, di = 10.5 mm, u = 5 mm, wh = 7.5 mm, wb = 10 mm, rb/2 = 10. **2.** *Catacoeloceras raquinianum* (d'Orbigny), 19 cm below top of bed 16, Variabilis Subzone, Posidonienschiefer Formation. GZG.INV.70519: d = 45 mm, di = 35 mm, u = 21 mm, wh = 12.5 mm, wb = 16 mm, rb/2 = 18. **3.** *Catacoeloceras raquinianum* (d'Orbigny), 13 cm below top of bed 16, Variabilis Subzone, Posidonienschiefer Formation. GZG.INV.70520: d = 35 mm, di = 26 mm, u = 14 mm, wh = 11.5 mm, wb = 15 mm, rb/2 = 13. **4.** *Pseudogrammoceras subregale* (Pinna), 4 cm below top of bed 18, Illustris Subzone, Jurensismergel Formation. GZG.INV.70521; d = 107 mm, di = 77 mm, u = 46 mm, wh = 34 mm, wb = n.a., rb/2 = (48). **5.** *Haugia* cf. *phillipsi* (Simpson), 3 cm below top of bed 18, Illustris Subzone, Jurensismergel Formation. GZG.INV.70522; d = (125 mm), di = n.a., u = n.a., wh = 46 mm, wb = n.a., rb/2 = (22). **6.** *Catacoeloceras raquinianum* (d'Orbigny), basis of bed 19, Variabilis Subzone, Posidonienschiefer Formation. GZG.INV.70523: d = 62 mm, di = 49 mm, u = 31 mm, wh = 15 mm, wb = (16 mm), rb/2 = 13. **7.** *Osperleioceras bicarinatum* (Zieten), phosphorite nodule in bed 20, condensed transition Variabilis-Thouarsense Zone, Jurensismergel Formation. GZG.INV.70524: d = 25 mm, di = 15 mm, u = 3.5 mm, wh = 14 mm, wb = 6 mm, rb/2 = (18). **8.** *Lytoceras cornucopia* (Young & Bird), marl matrix of bed 20, condensed transition Variabilis-Thouarsense Zone, Jurensismergel Formation. GZG.INV.70525: d = 66 mm, di = 46 mm, u = 23 mm, wh = 27 mm, wb = (28 mm), rb/2 = n.a. **9.** *Denckmannia rude* (Simpson), phosphorite nodule in bed 20, condensed transition Variabilis-Thouarsense Zone, Jurensismergel Formation. GZG.INV.70526: d = 86 mm, di = 58 mm, u = 32 mm, wh = 32 mm, wb = (26 mm), rb/2 = n.a.

Stier 1922; Etzold et al. 1989), show aphotic microbialites in the Toarcensis Zone (e.g., Aalen-Weidenfeld: Dietl and Etzold 1977; Keupp and Arp 1990; Ohmden: Arp and Heyng 2013), indicating highly reduced sedimentation (Keupp and Arp 1990). These condensed deposits may represent a maximum flooding, while the Fallaciosum Subzone shows a very discontinuous distribution of sediments, in the Swabian as well as in the Franconian Alb. High sealevel, however is still indicated by the sporadic occurrence of *P. fallaciosum* at the basin margin ("nodule bed c", see above).

A clear and significant discontinuity is developed at the basis of the Dispansum Zone in the Franconian Alb. This erosive sequence boundary, commonly associated with a belemnite accumulation and aphotic microbialites (Dörlbach, Mistelgau: Fig. 7) is also recognizable in the Swabian Alb (Bad Boll: Wiedemann 1966: p. 91, Taf. 9; Bruder 1968: p. 15f.; middle part of bed 22 Rainau-Weiler, and KB4 Reutehau: Etzold et al. 1989). In N-Germany, the basis of the Dispansum Zone is a significant erosive surface (Heidorn 1928; Hoffmann 1968a: p. 465: "Zeta-Konglomerat") and coincides with the mrs Toa 2 proposed by Zimmermann et al. (2015). Likewise, the Fallaciosum-Insigne Subzone boundary represents a mrs and sequence boundary in SW-France (Cubaynes et al. 1984: their fig. 18). The widespread erosion of the Fallaciosum Subzone in the Franconian Alb explains the scarcity of *Lytoceras jurense* findings in this area, as this species is most common in this subzone.

Subsequently, condensation and phosphorites characterize the transgressive sediments of the Dispansum Zone at the Ludwigskanal/Dörlbach and elsewhere in the Franconian Alb, while in the following Pseudoradiosa Subzone with several beds of compressed *Dumortieria* accumulations may reflect further deepening. A flooding at the basin margin area might be indicated by findings of Pompeckj (1901: p. 143), who noted the occurrence of *Phlyseogrammoceras* cf. *dispansum*, *Hammatoceras insigne* and *Dumortieria dumortieri* (syn.: *D. insignisimilis*) from the Regensburg area.

The condensed bed 25 (i.e., basis of Mactra Subzone; Fig. 7) at Dörlbach, with abundant ammonites, belemnites and phosphorite, may correspond to maximum flooding. The same horizon has also been described from Mistelgau (Dumortieria bed I: Schulbert 2001a) and Rainau-Weiler (Etzold et al. 1989: p. 49, their bed 16 with abundant phosphoritic *Dumortieria* and belemnites) (Fig. 6). By contrast, Galbrun et al. (1994: their fig. 5) infer a possible mrs and sequence boundary at the Pseudoradiosa/Aalensis Zone boundary from sections in western France.

Finally, the increasingly thick marls with pyritic ammonites of the Aalensis Subzone could reflect the regressive system tract of this 3rd order cycle, with increasing clay supply from N. Indeed, at the basin margin (Regensburg area) quartz-pebble and feldspar-containing calcareous sandstones document this regressive interval (Putzer 1939: p. 93, 107) (Fig. 9). Consistent with this interpretation, the sedimentary succession in Quercy/France appears regressive for the Mactra to Aalensis Subzone, followed by a discontinuity and sequence boundary (Lezin et al. 1997).

(iv) Opalinuston

While basal parts of this formation, i.e., the Torulosum Subzone, still show a low thickness, discontinuities, phosphorite, and some carbonate, major parts are composed of a thick monotonous series of claystones. Discontinuities within the formation and lateral facies trends are poorly documented. However, the sections Grossenbuch (middle Franconian Alb) and Wittelshofen (southern Franconian Alb) described by Krumbeck (1943) demonstrate that the Aalensis-Torulosum Subzone boundary is associated with erosion, locally removing the complete Aalensis Subzone.

Therefore, the belemnite accumulation (bed 31) at the Aalensis-Torulosum Subzone boundary of the Ludwigskanal/Dörlbach section (Fig. 6), although unspectacular at first glance, can be interpreted as a mrs and sequence

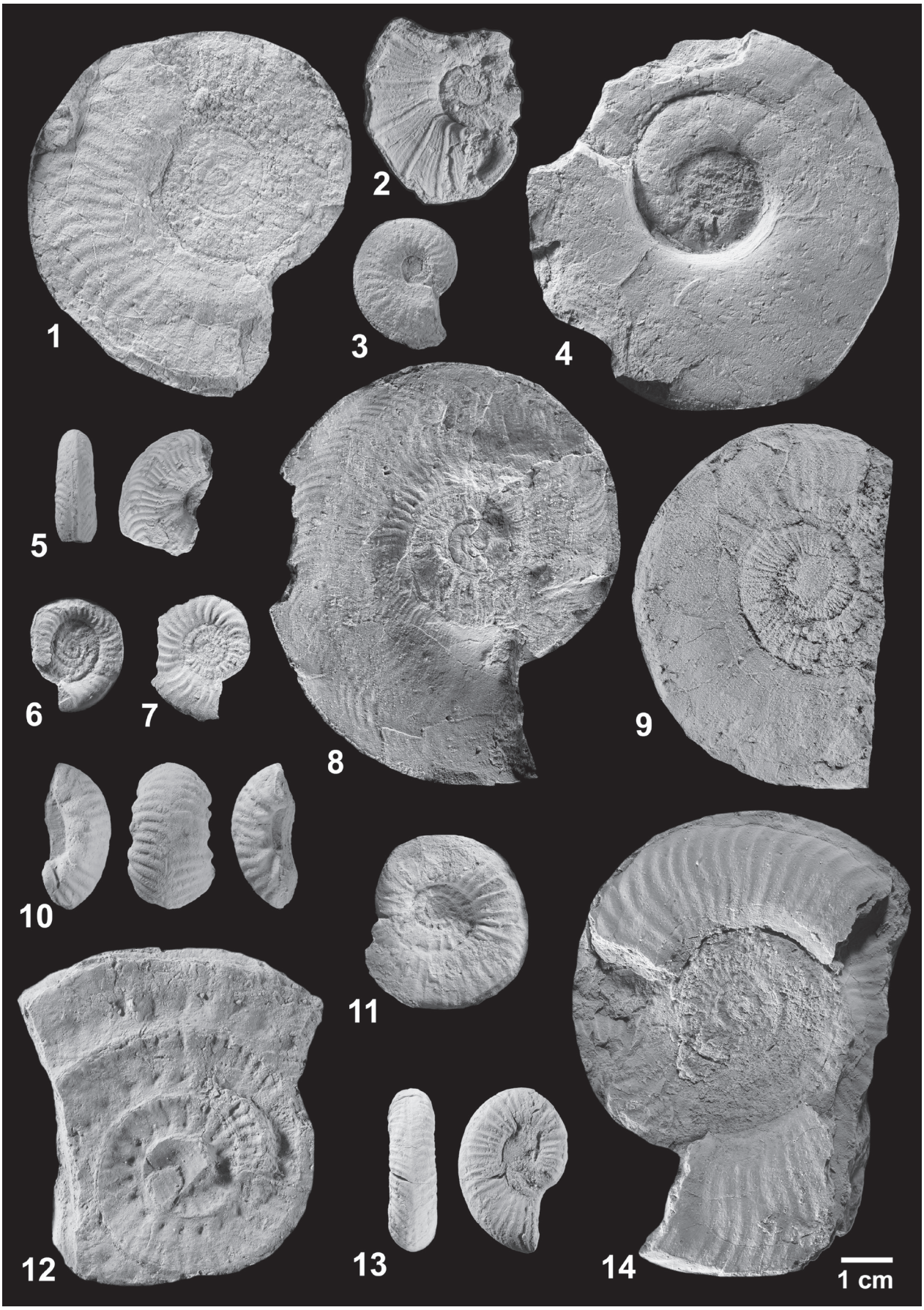
1
2
3
4
5
6
7
8
9
10
11
12
13
14
1 cm

Figure 14. 1. *Grammoceras thouarsense* (d'Orbigny), 10 cm below top of bed 21, Thouarsense Subzone, Jurensismergel Formation. GZG. INV.70527: d = 72 mm, di = 50 mm, u = 25 mm, wh = 27 mm, wb = n.a., rb/2 = (25). **2.** *Alocolytoceras rugiferum* (Pompeckj), 20–25 cm below top of bed 23, Dispansum Subzone, Jurensismergel Formation. GZG.INV.70528: d = (39 mm), di = (27 mm), u = 12 mm, wh = 16 mm, wb = n.a., rb/2 = (42). **3.** *Pseudolioceras* cf. *boulbiense* (Young and Bird), 12–20 cm below top of bed 23, Dispansum Subzone, Jurensismergel Formation. GZG.INV.70529: d = 26 mm, di = 17 mm, u = 5.5 mm, wh = 13 mm, wb = n.a., rb/2 = 13. **4.** *Alocolytoceras rugiferum* (Pompeckj), 20–25 cm below top of bed 23, Dispansum Subzone, Jurensismergel Formation. GZG.INV.70530: d = 76 mm, di = 56 mm, u = 21 mm, wh = 31 mm, wb = n.a., rb/2 = n.a. **5.** *Phlyseogrammoceras dispansum* (Lycett), 12–20 cm below top of bed 23, Dispansum Subzone, Jurensismergel Formation. GZG.INV.70531: d = (30 mm), di = n.a., u = (9 mm), wh = 12 mm, wb = 9 mm, rb/2 = n.a. **6.** *Dumortieria insignisimilis* (Brauns), 11 cm below top of bed 23, basis of Levesquei Subzone, Jurensismergel Formation. GZG.INV.70532: d = 22 mm, di = 17 mm, u = 12 mm, wh = 6 mm, wb = n.a., rb/2 = 20. **7.** *Dumortieria insignisimilis* (Brauns), 11 cm below top of bed 23, basis of Levesquei Subzone, Jurensismergel Formation. GZG.INV.70533: d = 25 mm, di = 17 mm, u = 10.5 mm, wh = 8.5 mm, wb = n.a., rb/2 = 18. **8.** *Phlyseogrammoceras dispansum* (Lycett), 20–25 cm below top of bed 23, Dispansum Subzone, Jurensismergel Formation. GZG. INV.70534: d = 83 mm, di = 61 mm, u = 27 mm, wh = 31 mm, wb = n.a., rb/2 = (45). **9.** *Dumortieria radiosa* (Seebach), 75 cm below top of bed 24, Pseudoradiosa Subzone, Jurensismergel Formation. GZG.INV.70535: d = 73 mm, di = (54 mm), u = 30 mm, wh = 23 mm, wb = n.a., rb/2 = n.a. **10.** *Hammatoceras insigne* (Schübler in Zieten), 15 cm below top of bed 23, Dispansum Subzone, Jurensismergel Formation. GZG.INV.70536: d = (56 mm), di = (42 mm), u = 26 mm, wh = (16 mm), wb = n.a., rb/2 = (28). **11.** *Dumortieria levesquei* (d'Orbigny), 6 cm below top of bed 23, Levesquei Subzone, Jurensismergel Formation. GZG.INV.70537a: d = 34 mm, di = 24 mm, u = 13 mm, wh = 12 mm, wb = n.a., rb/2 = 18. **12.** *Hammatoceras insigne* (Schübler in Zieten), 15 cm below top of bed 23, Dispansum Subzone, Jurensismergel Formation. GZG.INV.70538: d = 29 mm, di = (22 mm), u = (10 mm), wh = 10 mm, wb = 17 mm, rb/2 = (16). **13.** *Dumortieria levesquei* (d'Orbigny), 9 cm below top of bed 23, Levesquei Subzone, Jurensismergel Formation. GZG.INV.70539: d = 32 mm, di = (23 mm), u = (13 mm), wh = 11 mm, wb = 10 mm, rb/2 = 21. **14.** *Dumortieria pseudoradiosa* (Branco), 4 cm below top of bed 23, Levesquei Subzone, Jurensismergel Formation. GZG.INV.70537c: d = 92 mm, di = 70 mm, u = 41 mm, wh = 28 mm, wb = n.a., rb/2 = 32.

boundary (Fig. 7). Indeed, time-equivalent discontinuities have been described from N-Germany (e.g., Schlewecke, Dörnten: Ernst 1923; Heidorn 1928) and Quercy (Lezin et al. 1997). At the latter region, the discontinuity is associated with a lack of the Pseudolotharingicum (syn.: Lugdunensis) Horizon (Lezin et al. 1997), which also has not yet been detected in the Franconian Alb.

In the Ludwigskanal/Dörlbach section (Figs 6, 7), marls of bed 32 could reflect a subsequent sealevel rise, with condensed sediments, phosphorites, and the fossil accumulation in bed 33 representing a mfs, possibly equivalent to mfs Aal 1 in N-Germany (Zimmermann et al. 2015).

The monotonous and about 50 m thick claystone succession of the Opalinum Subzone, with only the lowermost 0.5 m exposed in the Ludwigskanal/Dörlbach section, reflects a progradation of siliciclastic influx from North, finally leading to shallow water conditions during deposition of the Upper Aalenian Eisensandstein Formation.

Conclusions

- The 16 m thick Ludwigskanal/Dörlbach section exposed upper parts of the Schwarzjura Group, from top parts of the Amaltheenton (>9 m), through the Posidonienschiefer (1.8–1.9 m) and Jurensismergel (3.5 m) to basal parts of the Opalinuston (>1.3 m). All formation boundaries are erosional discontinuities. Carbonate contents are low in the Amaltheenton, high in lower and middle parts of the Posidonienschiefer, followed by a successive decline to basal parts of the Opalinuston, with a last calcareous marl bed near the top of the Jurensismergel. The Posidonienschiefer shows increased organic carbon contents, which are, nonetheless, significantly lower than in other N- and SW-German sections due to the "dilution effect" by high carbonate contents. However, normalized to the sediment silicate fraction, organic carbon contents show a clear first maximum in the Exaratum Subzone and high values in the Falciferum and Bifrons Zone, similar to SW-German reference sections. Highly fluctuating values characterize the Variabilis and Thouarsense Zone, while low organic carbon contents were found in the Dispansum and younger zones, with one single spike at the basis of the Aalensis Zone (Mactra Subzone).
- Despite of the low thickness of the formations and a number of sedimentological gaps and condensation, all ammonite zones and subzones from the top of the Pliensbachian to the top of the Toarcian are present, with the following exceptions: Paltum and Clevelandicum (sedimentary gap), Vitiosa and Bingmanni (probably present, but no definite ammonite proof), and Fallaciosum Subzone (sedimentary gap). The erosive basis of the Torulosum Subzone may explain the lack of evidence for the Pseudolotharingicum (syn.: Lugdunensis) Horizon at the top of the Aalensis Subzone. The basis of the Aalenian is drawn in analogy to a neighbouring drill section that yielded *Leioceras opalinum*. Three subzones and horizons were detected for the first time in the investigated area: The Semipolitum Horizon, the Illustris Subzone, and the Dumortieri Horizon. The standard zone index ammonite *Harpoceras falciferum*, previously mentioned only by Urlichs (1971: p. 69), is figured for the first time for the Franconian Alb.

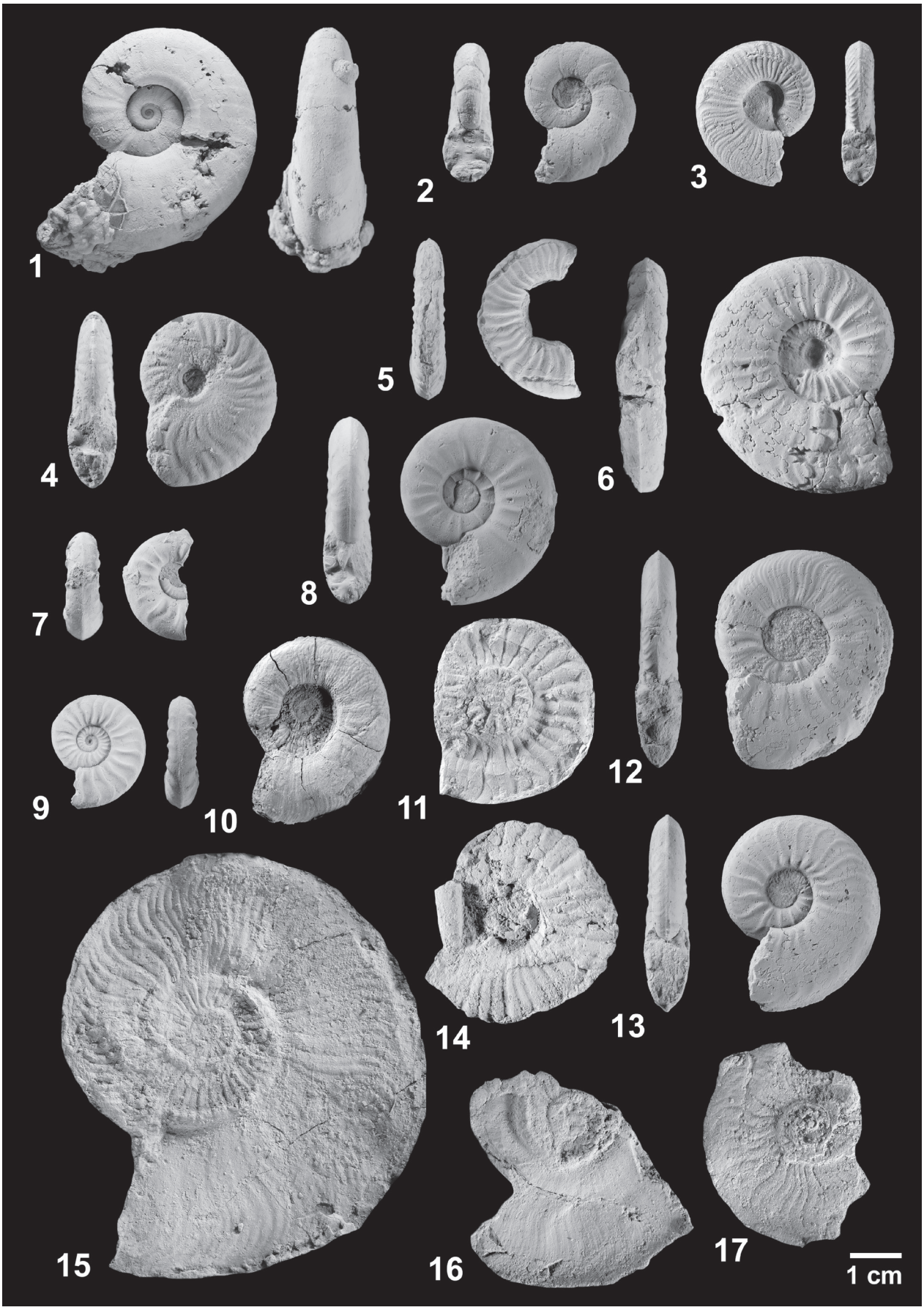
1
2
3
4
5
6
7
8
9
10
11
12
13
14
15
16
17
1 cm

Figure 15. 1. *Pleurolytoceras wrighti* (Buckman), bed 27, Aalensis Subzone, Jurensismergel Formation. This species has previously been assigned to *Pachylytoceras* Buckman 1905, which is a junior subjective synonym of *Pleurolytoceras* Hyatt 1900 (Hoffmann 2010, 2015). GZG.INV.70540: d = 44 mm, di = 27 mm, u = 14 mm, wh = 19 mm, wb = 15.5 mm, rb/2 = 19. **2.** *Pleurolytoceras hircinum* (Schlotheim), bed 27, Aalensis Subzone, Jurensismergel Formation. GZG.INV.70541: d = 27 mm, di = 18 mm, u = 10 mm, wh = 10.5 mm, wb = 10 mm, constr/2 = 6. **3.** *Cotteswoldia mactra* (Dumortier), bed 25, Mactra Subzone, Jurensismergel Formation. GZG.INV.70542; d = 29 mm, di = 20 mm, u = 10 mm, wh = 11 mm, wb = 7 mm, rb/2 = 35. **4.** *Pseudolioceras beyrichi* (Schloenbach), 1 cm below top of bed 28, Aalensis Subzone, Jurensismergel Formation. GZG.INV.45644: d = 34 mm, di = 21 mm, u = 6 mm, wh = 17.5 mm, wb = 10 mm, rb/2 = 15; (leg. Sebastian Demmel). **5.** *Paradumortieria* cf. *tectiforme* Elmi and Caloo-Fortier, 45 cm below top of bed 24, Pseudoradiosa Subzone, Jurensismergel Formation. GZG.INV.70543: d = 32 mm, di = 23 mm, u = 13 mm, wh = 11 mm, wb = 7.5 mm; rb/2 = 20. **6.** *Cotteswoldia aalensis* (Zieten), bed 27, Aalensis Subzone, Jurensismergel Formation. GZG.INV.70544: d = 46 mm, di = 31 mm, u = 16 mm, wh = 18 mm, wb = 9.5 mm, rb/2 = 19. **7.** *Dumortieria externicostata* (Branco), 30 cm below top of bed 26, Aalensis Subzone, Jurensismergel Formation. GZG.INV.70545: d = 21 mm, di = 14 mm, u = 7.5 mm, wh = 8 mm, wb = 8 mm, rb/2 = 10. **8.** *Dumortieria costula* (Reinecke), 30 cm below top of bed 26, Aalensis Subzone, Jurensismergel Formation. GZG.INV.70546: d = 36 mm, di = 26 mm, u = 12 mm, wh = 14 mm, wb = 9.5 mm, rb/2 = 11. **9.** *Pleydellia distans* (Buckman), bed 27, Aalensis Subzone, Jurensismergel Formation. GZG.INV.70547: d = 22 mm, di = 15 mm, u = 8 mm, wh = 8 mm, wb = 6.5 mm, rb/2 = 11. **10.** *Dumortieria moorei* (Lycett), 40 cm below top of bed 24, Pseudoradiosa Subzone, Jurensismergel Formation. GZG.INV.70548: d = 38 mm, di = 27 mm, u = 15 mm, wh = 13 mm, wb = (7 mm), rb/2 = 62. **11.** *Dumortieria* cf. *kochi* Benecke, 40 cm below top of bed 24, Pseudoradiosa Subzone, Jurensismergel Formation. GZG.INV.70549: d = 37 mm, di = (27 mm), u = 14 mm, wh = 13 mm, wb = n.a., rb/2 = 17. **12.** *Pleydellia subcompta* (Branco), 35 cm below top of bed 26, basis of Aalensis Subzone, Jurensismergel Formation. GZG.INV.70550: d = 44 mm, di = 29 mm, u = 16 mm, wh = 17 mm, wb = 9 mm, rb/2 = 30. **13.** *Pleydellia costulata* (Zieten), 1 cm below bed 28, Aalensis Subzone, Jurensismergel Formation. GZG.INV.70551: d = 39 mm, di = 26 mm, u = 11.5 mm, wh = 16.5 mm, wb = 9 mm, rb/2 = 12. **14.** *Pleurolytoceras torulosum* (Schübler in Zieten), bed 33, Torulosum Subzone, Opalinuston Formation. This species has previously been assigned to *Pachylytoceras* Buckman 1905, which is a junior subjective synonym of *Pleurolytoceras* Hyatt 1900 (Hoffmann 2010, 2015). GZG.INV.70552a: d = 40 mm, di = (29 mm), u = 12 mm, wh = 16 mm, wb = n.a., cstr/2 = 20. **15.** *Cotteswoldia lotharingica* (Branco), bed 33, Torulosum Subzone, Opalinuston For-mation. GZG.INV.70553: d = 84 mm; di = 60 mm, u = 32 mm, wh = 28 mm, wb = n.a., rb/2 = (48). **16.** *Pleydellia buckmani* Maubeuge, bed 33, Torulosum Subzone, Opalinuston Formation. GZG.INV.70554; d = (55 mm), di = n.a., u = 18 mm, wh = 26 mm, wb = n.a., rb/2 = n.a. **17.** *Pleydellia* cf. *falcifer* Maubeuge, bed 33, Torulosum Subzone, Opalinuston Formation. GZG.INV.70552b: d = 40 mm, di = (27 mm), u = 12 mm, wh = 17 mm, wb = n.a., rb/2 = 20.

- The sequence stratigraphic standard Boreal 2nd order cycle (de Graciansky et al. 1998), with a transgression during the Lower Toarcian, maximum flooding at the basis of the Bifrons Zone, and a regressive succession in the remaining Toarcian to Aalenian, is clearly developed in Southern Germany. Superimposed to that, three 3rd order T-R cycles are recognized at the Ludwigskanal/Dörlbach and adjacent sections, with a maximum regression near the basis of the Toarcian (i.e., within the lower Tenuicostatum Zon of Swabian Alb), within the Variabilis Zone (i.e., at the basis of the Illustris Subzone), at the basis of the Dispansum Zone, and less prominent at the basis of the Torulosum Zone. In turn, maximum flooding surfaces are developed at the basis of the Commune Subzone, basis of the Thouarsense Subzone, basis of Mactra Subzone, and basis of Opalinum Zone. While transgressive sediments of the Franconian Toarcian commonly show phosphorites (similar to other epicontinental marine deposits: Loutit et al. 1988; Glenn et al. 1994: p. 767; Glenn and Garrison 2003: p. 524), regressive sediments frequently show pyrite preservation of fossils, especially ammonites. The extraordinary "Belemnite Battlefield" near the basis of the Jurensismergel is considered as transgressive sediment, consistent with the previous formation model by Urlichs (1971) of winnowing by a coast-parallel seawater current.
- The litho-, bio-, and sequence stratigraphic framework of the Ludwigskanal section may serve as a basis for further isotope and biogeochemical studies on the Toarcian Oceanic Anoxic Event, and its recovery phase, in this seawater current-affected part of the NW-European Epicontinental Seaway.

Acknowledgements

We are grateful for the permission by the water management office Nürnberg, Rainer Ketterle, to investigate and sample at the construction site of the Ludwigskanal cutting. Thin sections were prepared by Axel Hackmann, geochemical analyses were performed with the help of Birgit Röhring and Wolfgang Dröse, and fieldwork was supported by Christian Strobl, Barbara Seuß, and Georg Maier. We thank Matthias Weissmüller, Arno Garbe, Martin Görlich, Sebastian Demmel, Volker Münzner, and Gernot Smolle for their generous donation of ammonites. Difficult ammonite preparations were preformed by Klaus Weiß and Stephan Seppelt. Photographs of the ammonites were taken by Max Hundertmark. Günter Schweigert and Ingmar Werneburg are gratefully acknowledged for access to original ammonite specimens hosted at the Stuttgart State Museum of Natural History and the Paleontological Collection of the University of Tübingen IGPT, respectively. We thank the engineering office Dr. Ing. Johann Spotka for the report on the landfill exploratory drilling Dörlbach

D2. The manuscript significantly benefited from discussions with René Hoffmann. Charlotte Kniest helped with the acquisition of rare papers. We thank Eckhard Mönnig and Matthias Franz (Göttingen) for their constructive and helpful reviews of the manuscript.

References

Arp G (1989) Neue Profile des Unteren Toarciums aus dem Altdorf-Neumarkter Raum. Geologische Blätter für Nordost-Bayern 39: 99–116.

Arp G (2010) Ammonitenfauna und Stratigraphie des Grenzbereichs Jurensismergel/Opalinuston-Formation bei Neumarkt i.d. Opf. (oberstes Toarcium, Fränkische Alb). Zitteliana A 50: 25–54.

Arp G, Heyng AM (2013) Jurassic Fossil Lagerstätten of Southern Germany. In: Reitner J, Reich M (Eds) Palaeobiology and Geobiology of Fossil Lagerstätten through Earth History. A Joint Conference of the "Paläontologische Gesellschaft" and the "Palaeontological Society of China", Göttingen. Field Guide to Excursions, Göttingen, 1–16.

Arp G, Gropengießer S (2016) The Monotis–Dactylioceras Bed in the Posidonienschiefer Formation (Toarcian, southern Germany): condensed section, tempestite, or tsunami-generated deposit? Paläontologische Zeitschrift 90: 271–286. https://doi.org/10.1007/s12542-015-0271-7

Arp G, Seppelt S (2012) The bipolar bivalve *Oxytoma* (*Palmoxytoma*) *cygnipes* (Young and Bird, 1822) in the Upper Pliensbachian of Germany. Paläontologische Zeitschrift 86: 43–57. https://doi.org/10.1007/s12542-011-0113-1

Arp G, Aiglstorfer M, Havlik P, Krause T, Schulbert C, Seppelt S (2014) New exposure of the Ludwigskanal section near Dörlbach – a key section for the Lower Jurassic in the Franconian Alb, Southern Germany. Zeitschrift der Deutschen Gesellschaft für Geowissenschaften 165: 163–177. https://doi.org/10.1127/1860-1804/2014/0054

Bandel K, Knitter H (1983) Litho- und biofazielle Untersuchung eines Posidonienschieferprofils in Oberfranken. Geologische Blätter für Nordost-Bayern 32: 95–129.

Bauberger W, Cramer P, Tillmann H (1969) Erläuterungen zur Geologischen Karte von Bayern 1:25000, Blatt Nr. 6938 Regensburg [mit Beiträgen von Bader, K., Berger, K., Buchner, A., Claus, G., Hauner, U., Stroh, A. and Wittmann, O.]. Bayerisches Geologisches Landesamt, München, 414 pp. [+ 1 map]

Becaud M, Rulleau L, Elmi S (2005) The ammonite fauna renewal at the boundary middle-late Toarcian: new data and consequences. Bulletin de la Société Géologique de France 176(1): 23–35. https://doi.org/10.2113/176.1.23

Beyschlag (1841) Über die geognostische Stellung der Gebirgsschichten, welche beim Bau des Ludwigskanales aufgedeckt oder durchschnitten wurden. Amtlicher Bericht über die 18. Versammlung der Naturforscher und Ärzte zu Erlangen im September 1840: 101–108.

Bloos G, Dietl G, Schweigert G (2005) Der Jura Süddeutschlands in der Stratigraphischen Tabelle von Deutschland 2002. Newsletters on Stratigraphy 41: 263–277. https://doi.org/10.1127/0078-0421/2005/0041-0263

Böhm F, Brachert TC (1993) Deepwater Stromatolites and *Frutexites* Maslov from the Early and Middle Jurassic of S-Germany and Austria. Facies 28: 145–168. https://doi.org/10.1007/BF02539734

Boulila S, Galbrun B, Huret E, Hinnov LA, Rouget I, Gardin S, Bartolini A (2014) Astronomical calibration of the Toarcian Stage: implications for sequence stratigraphy and duration of the early Toarcian OAE. Earth and Planetary Science Letters 386: 98–111. https://doi.org/10.1016/j.epsl.2013.10.047

Brachmann H (1991) Die Ammonitenfauna der "Dörntener Schichten" (Ober-Toarcium) von der Typlokalität bei Dörnten (N Harzvorland). Arbeitskreis Paläontologie Hannover 19(3/4): 88–115.

Brockert M (1959) Zur Ammonitenfauna und Stratigraphie des Lias zeta in Baden-Württemberg. Dissertation Eberhard Karls Universität, Tübingen, 155 pp.

Bruder HJ (1968) Ökologische, geochemische und sedimentologische Untersuchungen im Lias zeta (Oberes Toarcium) Schwabens, mit Berücksichtigung des obersten Lias epsilon. Arbeiten aus dem Geologisch-Paläontologischen Institut der Technischen Hochschule Stuttgart, Neue Folge 56: 1–65.

Buckman SS (1919–1921) Type Ammonites III. Wheldon and Wesley, London, 64 pp. [+ pls 131–266b]

Catuneanu O, Galloway WE, Kendall CGSC, Miall AD, Posamentier HW, Strasser A, Tucker ME (2011) Sequence stratigraphy: Methodology and Nomenclature. Newsletters on Stratigraphy 44: 173–245. https://doi.org/10.1127/0078-0421/2011/0011

Cresta S, Goy A, Ureta S, Arias C, Barrón E, Bernad J, Canales ML, García-Joral F, García-Romero E, Gialanella PR, Gómez JJ, González JA, Herrero C, Martínez G, Osete ML, Perilli N, Villalaín JJ (2001) The Global Boundary Stratotype Section and Point (GSSP) of the Toarcian-Aalenian Boundary (Lower-Middle Jurassic). Episodes 24: 166–175. https://doi.org/10.18814/epiiugs/2001/v24i3/003

Cubaynes R, Boutet C, Delfaud J, Faure P (1984) La megasequence d'ouverture du Lias quercynois (Bordure sud-ouest du Massif Central français). Bull. Centres Rech. Explor.-Prod Elf-Aquitaine 8(2): 333–370.

de Graciansky PC, Dardeau G, Dommergues JL, Durlet C, Marchand D, Dumont T, Hesselbo SP, Jacquin T, Goggin V, Meister C, Mouterde R, Rey J, Vail PR (1998) Ammonite biostratigraphic correlation and Early Jurassic sequence stratigraphy in France: comparisons with some U.K. sections. In: de Graciansky PC, Hardenbol J, Jacquin T, Vail PR (Eds) Mesozoic and Cenozoic Sequence Stratigraphy of European Basins, SEPM, Tulsa, 583–622. https://doi.org/10.2110/pec.98.02.0583

Dean WT, Donovan DT, Howarth MK (1961) The Liassic ammonite zones and subzones of the north-west European Province. Bulletin of the British Museum (Natural History) Geology Series 4: 435–505.

Di Cencio A, Weis R (2020) Revision of upper Toarcian ammonites (Lytoceratidae, Graphoceratidae and Hammatoceratidae) from the Minette ironstones, southern Luxembourg. Ferrantia 83: 5–103.

Dietl G, Etzold A (1977) The Aalenian at the type locality. Stuttgarter Beiträge zur Naturkunde B 30: 1–13.

Elmi S, Gabilly J, Mouterde R, Rulleau L, Rocha RB (1994) L'étage Toarcien de l'Europe et de la Téthys; divisions et corrélations. Geobios Mémoire Spécial 17: 149–159. https://doi.org/10.1016/S0016-6995(94)80135-5

Elmi S, Rulleau L, Gabilly J, Mouterde R (1997) Toarcien. In: Cariou E, Hantzpergue P (Coord.) Biostratigraphie du Jurassique ouest-européen et méditerranéen. Bulletin du Centre de Recherches Elf Exploration et Production, Mémoir 17: 25–36.

Embry AF, Johannessen EP (1992) T-R sequence stratigraphy, facies analysis and reservoir distribution in the uppermost Triassic-Lower Jurassic succession, western Sverdrup Basin, Arctic Canada. In: Vorren TO, Bergsager E, Dahl-Stamnes OA, Holter E, Johansen B, Lie E, Lund TB (Eds) Arctic Geology and Petroleum Potential, vol. 2 (Special Publication). Norwegian Petroleum Society (NPF), 121–146. https://doi.org/10.1016/B978-0-444-88943-0.50013-7

Ernst W (1923–1924) Zur Stratigraphie und Fauna des Lias Zeta im nordwestlichen Deutschland. Palaeontographica 65(1923): 1–96, plates 1–6; 66(1924): 97–222, plates 7–14.

Etzold A, Ohmert W, Balle T (1989) Toarcium und unterstes Aalenium im Gebiet der oberen Jagst nordöstlich Aalen. Jahreshefte des geologischen Landesamtes Baden-Württemberg 31: 23–68.

Fischer W (1964) Die *jurensis*-Schichten (Oberes Toarcien) im Vorland der Schwäbischen Alb. Neues Jahrbuch für Geologie und Paläontologie, Abhandlungen 120: 81–106.

Freudenberger W, Schwerd K [Eds] (1996) Erläuterungen zur Geologischen Karte von Bayern 1 : 500 000. 4th edn. Bayerisches Geologisches Landesamt, München, 329 pp. [+ 1 map]

Frimmel A (2003) Hochauflösende Untersuchungen von Biomarkern an epikontinentalen Schwarzschiefern des Unteren Toarciums (Posidonienschiefer, Lias ε) von SW-Deutschland. Dissertation Eberhard-Karls-Universität Tübingen, 108 pp.

Frimmel A, Oschmann W, Schwark L (2004) Chemostratigraphy of the Posidonia Black Shale, SW Germany. I. Influence of sea-level variation on organic facies evolution. Chemical Geology 206: 199–230. https://doi.org/10.1016/j.chemgeo.2003.12.007

Gabilly J (1976a) Le Toarcien à Thouars et dans le centra-ouest de la France. Les Stratotypes français 3: 217 pp. [+ 29 pls]

Gabilly J (1976b) Évolution et systématique des Phymatoceratinae et des Grammoceratinae (Hildocerataceae Ammonitina) de la région de Thouars, stratotype du Toarcien. Mémoires de la Société Géologique de France, Nouvelle Série 124: 1–196. [+ 36 pls]

Galácz A, Császár G, Géczy B, Kovács Z (2010) Ammonite stratigraphy of a Toarcian (Lower Jurassic) section on Nagy-Pisznice Hill (Gerecse Mts, Hungary). Central European Geology 53(4): 311–342. https://doi.org/10.1556/CEuGeol.53.2010.4.1

Galbrun B, Baudin F, Bassoullet JP, Depeche F, Emmanuel L, Lachkar G, Renard M, Riveline J, Gabilly J, Hantzpergue P, Manivit H, Ruget C (1994) Stratigraphie intégrée du Toarcien stratotypique (coupes de Thouars et Airvault, Deux-Sèvres, France). Geobios Mémoire Spécial 17: 575–595. https://doi.org/10.1016/S0016-6995(94)80222-X

Géczy B (1966) Upper Liassic Dactylioceratids of Úrkút. Acta Geologica Academiae Scientiarum Hungaricae 10: 427–443.

Glenn CR, Garrison RE (2003) Phosphorites. In: Middleton GV, Church MJ, Coniglio M, Hardie LA, Longstaffe FJ (Eds) Encyclopedia of Sediments and Sedimentary Rocks, Kluwer, Dordrecht, 519–526.

Glenn CR, Föllmi KB, Riggs SR, Baturin GN, Grimm KA, Trappe J, Abed AM, Galli-Olivier C, Garrison RE, Ilyin AV, Jehl C, Rohrlich V, Sadaqah RMY, Schidlowski M, Sheldon RE, Siegmund H (1994) Phosphorus and phosphorites: sedimentology and environments of formation. Eclogae geologicae Helvetiae 87: 747–788.

Gradstein FM, Ogg JG, Schmitz K, Ogg G (2012) The Geologic Time Scale 2012. Vol. 2. Elsevier, Amsterdam, 1144 pp.

Gründel J, Nützel A (2015) Gastropoden aus dem oberen Pliensbachium (Amaltheenton-Formation) NE Bayerns (Umgebung von Stauf/Dörlbach/Altdorf) (Franken, Süddeutschland). Zitteliana A 55: 45–76.

Guex J (1973) Aperçu biostratigraphique sur le Toarcien inférieur du Moyen-Atlas marocain et discussion sur la zonation de ce sous-étage dans les séries méditerranéennes. Eclogae Geologicae Helvetiae 66: 493–523.

Guex J (1975) Description biostratigraphique du Toarcien supérieur de la bordure sud des Causses (France). Eclogae geologicae Helvetiae 68: 97–129.

Haq BU (2018) Jurassic sea-level variations: a reappraisal. GSA Today 28(1): 4–10. https://doi.org/10.1130/GSATG359A.1

Hauff B (1921) Untersuchung der Fossilfundstätten von Holzmaden im Posidonienschiefer des Oberen Lias Württembergs. Palaeontographica 64: 1–42. [+ 21 pls]

Heidorn F (1928) Paläogeographisch-tektonische Untersuchungen im Lias Zeta von Nordwestdeutschland. Neues Jahrbuch für Mineralogie, Geologie und Paläontologie, Beilage-Bände 59(Abt. B): 117–244.

Hofbauer G (2001) Die Diskussion um die Entstehung der Süddeutschen Schichtstufenlandschaft: Eine historischmethodologische Skizze mit einem Modell zur fluviatil gesteuerten Schichtstufen-Morphogenese. Natur und Mensch, Jahresmitteilungen der Naturhistorischen Gesellschaft Nürnberg eV, Jubiläumsausgabe 200: 85–108.

Hoffmann K (1968a) Die Stratigraphie und Paläogeographie der bituminösen Fazies des nordwestdeutschen Oberlias (Toarcium). Geologisches Jahrbuch, Beihefte 58: 443–498.

Hoffmann K (1968b) Neue Ammonitenfunde aus dem tieferen Unter-Toarcium (Lias e) des nördlichen Harzvorlandes und ihre feinstratigraphische Bedeutung. Geologisches Jahrbuch 85: 1–32.

Hoffmann R (2010) New insights on the phylogeny of the Lytoceratoidea (Ammonitina) from the septal lobe and its functional interpretation. Revue de Paléobiologie 29: 1–156.

Hoffmann R (2015) Part L, Revised, Volume 3B, Chapter 3: Systematic Descriptions of the Lytoceratoidea. Treatise Online 70: 1–34. [Lawrence, Kansas]

Hoffmann R, Keupp H, Gradl H (2007) Zur Korrelation der Lias-Tongruben von Unterstürmig und Buttenheim (Frankenalb). Jahresberichte und Mitteilungen des oberrheinischen geologischen Vereins, Neue Folge 89: 37–48. https://doi.org/10.1127/jmogv/89/2007/37

Howarth MK (1958) A monograph of the ammonites of the Liassic family Amaltheidae in Britain. Monograph of the Palaeontographical Society, 111: i–xvi, 1–26, pls 1–4; 112: xv–xxxvii, 27–53, pls 5–10.

Howarth MK (1962) The Jet Rock Series and the Alum Shale Series of the Yorkshire coast. Proceedings of the Yorkshire Geological Society 33: 381–422. https://doi.org/10.1144/pygs.33.4.381

Howarth MK (1973) The stratigraphy and ammonite fauna of the Upper Liassic Grey Shales of the Yorkshire coast. Bulletin of the British Museum (Natural History), Geology Series 24: 235–277.

Howarth MK (1978) The stratigraphy and ammonite fauna of the Upper Lias of Northamptonshire. Bulletin of the British Museum (Natural History), Geology Series 29: 235–288.

Howarth MK (1992) The ammonite family Hildoceratidae in the Lower Jurassic of Britain. Monograph of the Paleontolographical Society 586: 1–106, pls 1–16; 590: 107–200, pls 17–38.

Howarth MK (2013) Chapter 4: Psiloceratoidea, Eodoceratoidea, Hildoceratoidea. In: Selden PA (Ed.) Treatise Online 57 (Part L (Revised) Mollusca 4, vol. 3B, Triassic and Jurassic Ammonoidea), Lawrence, Kansas (University of Kansas), 1–139. https://doi.org/10.17161/to.v0i0.4441

Jacquin T, Dardeau C, Durlet C, de Graciansky PC, Hantzpergue P (1998) An overview of 2nd-order transgressive/regressive facies cycles in Western Europe. In: de Graciansky PC, Hardenbol J, Jacquin T, Vail P (Eds) Mesozoic and Cenozoic Sequence Stratigraphy of European Basin. SEPM Special Publication 60: 445–467. https://doi.org/10.2110/pec.98.02.0445

Jattiot R, Fara E, Brayard A, Vennin E (2016) Revised stratigraphic range of the Toarcian ammonite genus *Porpoceras* Buckman, 1911. Geodiversitas 38: 505–513. https://doi.org/10.5252/g2016n4a3

Jenkyns HC (1988) The early Toarcian (Jurassic) anoxic event: Stratigraphic, sedimentary, and geochemical evidence. American Journal of Science 288: 101–151. https://doi.org/10.2475/ajs.288.2.101

Jordan R (1960) Paläontologische und stratigraphische Untersuchungen im Lias delta (Domerium) Nordwestdeutschlands. Dissertation Eberhard-Karls-Universität, Tübingen, 178 pp. [+ 9 pls]

Keupp H, Arp G (1990) Aphotische Stromatolithe aus dem süddeutschen Jura (Lias, Dogger). Berliner Geowissenschaftliche Abhandlungen A 124: 3–33.

Knitter H, Ohmert W (1983) Das Toarcium an der Schwärze bei Badenweiler (Oberrheingebiet S Freiburg). Jahreshefte des geologischen Landesamtes Baden-Württemberg 25: 233–281.

Knitter H, Riegraf W (1984) Biostratigraphie (Cephalopoden, Ostracoden) des Oberen Toarcium von Blumberg-Achdorf/Wutach und Weilheim/Teck (Baden-Württemberg). Jahreshefte des geologischen Landesamtes Baden-Württemberg 26: 57–97.

Knitter H (1983) Biostratigraphische Untersuchungen mit Ostracoden im Toarcien Süddeutschlands. Facies 8: 213–262. https://doi.org/10.1007/BF02536743

Kolb H (1964) Der Lias ε im Gebiet zwischen Altdorf und Neumarkt. Geologische Blätter für Nordost-Bayern 14: 129–144.

Kottek A (1963) Die Ammonitenabfolge des griechischen Toarcium. Annales Géologiques des Pays Helléniques, première série 17: 1–157. [+ 17 pls]

Kovács Z (2011) Lower Toarcian Ammonitida fauna and biostratigraphy of the Gerecse Mountains (Hungary). Fragmenta Palaeontologica Hungarica 29: 1–48.

Kraus W (1983) Paläontologische Notizen aus Mittelfranken. Mineralien Magazin 7(9): 414–416.

Krumbeck L (1932a) Über den Lias von Kalchreuth bei Erlangen, besonders γ und ε. Centralblatt für Mineralogie, Geologie und Paläontologie, Abteilung B (Geologie und Paläontologie) 1932: 43–64, 73–90.

Krumbeck L (1932b) Über den Fallaciosus-Horizont im Lias Mittel-ζ von Irlbach bei Regensburg. Centralblatt für Mineralogie, Geologie und Paläontologie, Abt. B Geologie und Paläontologie 1932: 499–518.

Krumbeck L (1932c) Über die Höckerfazies im Lias ε Nordbayerns. Fortschritte der Geologie und Paläontologie 35: 245–259.

Krumbeck L (1943–1944) Zur Stratigraphie und Faunenkunde des Lias ζ in Nordbayern. Zeitschrift der Deutschen Geologischen Gesellschaft 95(1943): 279–340; 96(1944): 1–74.

Kursawe U (1995) 300 Jahre Fossiliensammeln in Altdorf. Geologische Blätter für Nordost-Bayern 45: 271–288.

Kursawe U (1996) Bauder'scher Marmor – Vom Ausgangsgestein zum „kostbarn Ammonitenmarmor". Geologische Blätter für Nordost-Bayern 46: 53–70.

Lacroix P (2011) Les Hildoceratidae du Lias Moyen et Supérieur des domaines NW Européen et Téthysien. Une histoire de Famille. Dédale Editions, St-Just-la-Pendue, 354 pp. [+ 152 pls]

Lezin C, Cubaynes R, Fauré P, Pelissié T, Rey J (1997) Le Toarcien supérieur-Aalénien dans la région de Villefranche-du-Rouegue (sud-ouest de la France). Biostratigraphie et évolution sédimentaire. Géologie de la France 4: 3–14.

Loutit TS, Hardenbol J, Vail PR, Baum GR (1988) Condensed sections, the key to age determination and correlation of continental margin sequences. In: Wilgus CK, Hastings BS, Kendall CGSC, Posamentier HW, Ross CA, Van Wagoner JC (Eds) Sea-Level Changes—An Integrated Approach. SEPM Special Publication 42: 183–213. https://doi.org/10.2110/pec.88.01.0183

Mäuser M (2001) Altdorf bei Nürnberg. In: Weidert WK (Ed.) Klassische Fundstellen der Paläontologie 4: 97–110. [Korb (Goldschneck Verlag)]

Mayr H (1995) Über Medusenhäupter, marine Palmen und Liliensteine. Jahresbericht der Freunde der Bayerischen Staatssammlung für Paläontologie und historische Geologie 23(1994): 18–31.

Meyer RKF, Bauberger W (1998) Erläuterungen zur Geologische Karte von Bayern 1:25000, Blatt Nr. 6739 Bruck i. d. OPf. [mit Beiträgen von Apel, R., Bader, K., Gregor, H.J., Poschlod, K., Dobner, A., Eckbauer, M., Schmidt, F., Förster, H. and Schneider, G.]. Bayerisches Geologisches Landesamt, München, 164 pp. [+ 1 map]

Meyer RKF, Schmidt-Kaler H (1996) Jura. In: Freudenberger W, Schwerd K (Eds) Erläuterungen zur Geologischen Karte von Bayern 1 : 500 000. 4th edn., München (Bayerisches Geologisches Landesamt), 90–111.

Mönnig E, Nitsch E, Arp G (2015) Posidonienschiefer-Formation. In: LithoLex [Online-Datenbank]. Hannover: BGR. Last updated 19.10.2015 [cited 14.04.2020]. Record No. 4012098. https://litholex.bgr.de

Nitsch E, Arp G, Mönnig E (2015) Jurensismergel-Formation. In: LithoLex [Online-Datenbank]. Hannover: BGR. Last updated 19.10.2015 [cited 14.04.2020]. Record No. 4012084. https://litholex.bgr.de

Nummedal D, Swift DJP (1987) Transgressive stratigraphy at sequence-bounding unconformities: some principles derived from Holocene and Cretaceous examples. In: Nummedal D, Pilkey OH, Howard JD (Eds) Sealevel fluctuation and coastal evolution. SEPM Special Publication 41: 241–260. https://doi.org/10.2110/pec.87.41.0241

Ohmert W (1976) Das Toarcium-Profil von Ballrechten (Oberrheingebiet südlich Freiburg). Jahreshefte des geologischen Landesamtes Baden-Württemberg 18: 79–103.

Ohmert W, Wonik T, Rolf C, Martin M, Höhndorf A, Wetzel A, Allia V, Riegraf W, Baldanza A, Mattioli E, Bucefalo Palliani R, de Kaenel E, Bergen JA, Goy A, Ureta S, Arias C, Canales ML, Garcia Joral F, Herrero C, Martinez G, Perilli N (1996) Die Grenzziehung Unter-, Mitteljura (Toarcium, Aalenium) bei Wittnau und Fuentelsaz. Beispiele interdisziplinärer geowissenschaftlicher Zusammenarbeit. Informationen Geologisches Landesamt Baden-Württemberg 8: 52 pp.

Page KN (2003) The Lower Jurassic of Europe: its subdivision and correlation. Geological Survey of Denmark and Greenland Bulletin 1: 23–59. https://doi.org/10.34194/geusb.v1.4646

Page KN (2004) A sequence of biohorizons for the Subboreal Province Lower Toarcian in northern Britain and their correlation with a Submediterranean Standard. Rivista Italiana di Paleontologia e Stratigrafia 110(1): 109–114.

Paul J, Wemmer K, Ahrendt H (2008) Provenance of siliciclastic sediments (Permian to Jurassic) in the Central European Basin. Z. dt. Ges. Geowiss. 159: 641–650. https://doi.org/10.1127/1860-1804/2008/0159-0641

Peterek A, Schröder B (2010) Geomorphologic evolution of the cuesta landscapes around the Northern Franconian Alb – review and synthesis. Zeitschrift für Geomorphologie 54: 305–345. https://doi.org/10.1127/0372-8854/2010/0054-0037

Pinna G, Levi-Setti F (1971) I Dactylioceratidae della Provincia Mediterranea (Cephalopoda Ammonoidea). Memorie della Societa Italiana di Scienze Naturali Museo Civico di Storia Naturale die Milano 19: 49–136. [+ 12 pls]

Pompeckj JF (1901) Der Jura zwischen Regensburg und Regenstauf. Geognostische Jahreshefte 14: 139–220.

Price GD (1999) The evidence and implications of polar ice during the Mesozoic. Earth-Science Reviews 48: 183–210. https://doi.org/10.1016/S0012-8252(99)00048-3

Putzer H (1939) Der Jura am Keilberg bei Regensburg. Neues Jahrbuch für Mineralogie, Geologie und Paläontologie, Beilage-Bände 82(Abt. B): 90–154.

Quenstedt FA (1845–1849) Cephalopoden. Petrefactenkunde Deutschlands, 1.Abt. 1845: 1–104, Taf. 1–6; 1846: 105–184, Taf. 7–12; 1847: 185–264, Taf. 13–18; 1848: 265–472, Taf. 19–30; 1849: 473–580, Taf. 31–36; Tübingen (Fues).

Quenstedt FA (1851–1852, 1865–1866, 1882–1885a) Handbuch der Petrefaktenkunde. 1. Aufl.: 792 pp., 62 pls; 2nd edn.: 982 pp., 86 pls; 3rd edn.: 1239 pp., 100 pls; Tübingen (Laupp).

Quenstedt FA (1856–1858) Der Jura. 1856: 1–576, Taf. 1–72; 1857: 577–824, Taf. 73–100; 1858: 825–843; Tübingen (Laupp).

Quenstedt FA (1872–1875) Petrefactenkunde Deutschlands. III. Echinodermen (Echiniden). Text und Atlas, 720 pp., Taf. 62–89; Tübingen (Fues).

Quenstedt FA (1876) Petrefactenkunde Deutschlands. IV. Die Echinodermen (Asteriden und Encriniden nebst Cysti- und Blastoideen). Text und Atlas, 720 S., Taf. 90–114; Tübingen (Fues).

Quenstedt FA (1881–1884) Petrefaktenkunde Deutschlands. Erste Abteilung, 7: Gasteropoden. 1881: 1–192, Taf. 185–190; 1882: 193–320, Taf. 191–196; 1882: 321–464, Taf. 197–202; 1883: 465–592, Taf. 203–208; 1884: 593–736, Taf. 209–214; 1884: 737–867, Taf. 215–218; Leipzig (Fues).

Quenstedt FA (1882–1885b) Die Ammoniten des Schwäbischen Jura. 1. Band. Der Schwarze Jura (Lias). 1882: 1–48; 1883: 49–56; 1884: 97–240; 1885b: 241–440; Stuttgart (Schweizerbart).

Reuter L (1927) Geologische Darstellung des schwäbisch-fränkischen Juras, seines triasischen Vorlandes und des südlich angrenzenden Molasse-Gebietes. In: Schuster M (Ed.) Abriß der Geologie von Bayern r. d. Rh., Abt. IV: 1–132, München (Oldenburg and Piloty).

Riegraf W, Werner G, Lörcher F (1984) Der Posidonienschiefer – Biostratigraphie, Fauna und Fazies des südwestdeutschen Untertoarciums (Lias epsilon). Enke, Stuttgart, 195 pp.

Riegraf W (1985a) Mikrofauna, Biostratigraphie und Fazies im Unteren Toarcium Südwestdeutschlands und Vergleiche mit benachbarten Gebieten. Tübinger Mikropaläontologische Mitteilungen 3: 1–232.

Riegraf W (1985b) Biostratigraphie, Fauna und Mikropaläontologie des Untertoarcium-Profiles von Unterstürmig (Oberfranken, Süddeutschland). Geologische Blätter für Nordost-Bayern 34/35: 241–272.

Röhl HJ, Schmid-Röhl A (2005) Lower Toarcian (Upper Liassic) Black Shales of the Central European Epicontinental Basin: A Sequence Stratigraphic Case Study from the SW German Posidonia Shale. In: Harris NB (Ed.) The Deposition of Organic-Carbon-Rich Sediments. Models, Mechanisms, and Consequences. SEPM Special Publication 82: 165–189. https://doi.org/10.2110/pec.05.82.0165

Rübsam W, Al-Husseini M (2020) Calibrating the Early Toarcian (Early Jurassic) with stratigraphic black holes (SBH). Gondwana Research 82: 317–336. https://doi.org/10.1016/j.gr.2020.01.011

Rulleau L (2007) Biostratigraphie et paléontologique du Lias supérieur et du Dogger de la région Lyonnaise. Tome 1. Dédale Editions, Lafarge Ciments, 129 pp.

Salger M, Schmid H (1982) Die Forschungsbohrung Eschertshofen 1981 (Vorläufige Mitteilung). Geologica Bavarica 83: 145–161.

Schmidt-Kaler H (1974) Geologischen Karte von Bayern 1:25000, Erläuterungen zu Blatt Nr. 6634 Altdorf b. Nürnberg [mit Beiträgen von Apel, R., Bader, K., Berger, K., Diez, T., Gauckler, P.]. Bayerisches Geologisches Landesamt, München, 152 pp.

Schulbert C (2001a) Die Ammonitenfauna und Stratigraphie der Tongrube Mistelgau bei Bayreuth (Oberfranken). Beihefte zu den Berichten der Naturwissenschaftlichen Gesellschaft Bayreuth 4: 1–183.

Schulbert C (2001b) Geologische Kartierung der Umgebung von Mistelgau bei Bayreuth (Oberfranken). Diploma mapping, Friedrich–Alexander–Universität Erlangen–Nürnberg, 58 pp. [+ XXVIII pp., 1 map]

Simmons MD (2012) Sequence Stratigraphy and Sea-Level Change. In: Gradstein FM, Ogg JG, Schmitz M, Ogg GM (Eds) The geologic time scale 2012, vol 1. Elsevier, Amsterdam, 239–267. https://doi.org/10.1016/B978-0-444-59425-9.00013-5

Simonsen S (2013) Fossilien aus dem Posidonienschiefer der Tongrube Mistelgau. Der Steinkern 15: 28–46.

Stankievitch ES (1964) Amoniti yurskih peschano-glinitovih otlojenii severo-zapadnogo Kavkaza [Ammonites in the Jurassic sandy clay deposits of the northwestern Caucasus]. Nauka, Moscow-Leningrad, 99 pp. [in Russian]

Stier K (1922) Vorläufige Mitteilung über das Ergebnis der Untersuchung der württemb. Ölschiefer-und Eisenerzvorkommen. Jahresberichte und Mitteilungen des oberrheinischen geologischen Vereins, Neue Folge 11: 94–97. https://doi.org/10.1127/jmogv/11/1922/94

Straub W (1946) Stratigraphie und Bildungsgeschichte des Lias z in Mittelwürttemberg und Südbaden. Dissertation Technische Hochschule Stuttgart, 72 pp.

Teichert BMA, Luppold FW (2013) Glendonites from an Early Jurassic methane seep — Climate or methane indicators? Palaeogeography, Palaeoclimatology, Palaeoecology 390: 81–93. https://doi.org/10.1016/j.palaeo.2013.03.001

Urlichs M (1971) Alter und Genese des Belemnitenschlachtfeldes im Toarcium von Franken. Geologische Blätter für Nordost-Bayern 21: 65–83.

Urlichs M (1977a) The Lower Jurassic in Southwestern Germany. Stuttgarter Beiträge zur Naturkunde B 24: 1–41.

Urlichs M (1977b) Stratigraphy, ammonite fauna and some ostracods of the Upper Pliensbachian at the type locality (Lias, SW-Germany). Stuttgarter Beiträge zur Naturkunde B 28: 1–13.

Venturi F, Ferri R (2001) Ammoniti liassici dell' Appennino Centrale. Medesimi, Città di Castello, 268 pp.

von Freyberg B (1958a) 250 Jahre geologische Forschung in der Fränkischen Alb. Geologische Blätter für Nordost-Bayern 8: 34–43.

von Freyberg B (1958b) Johann Friedrich Bauder (1713–1791) und seine Bedeutung für die Versteinerungskunde in Franken. Geologische Blätter für Nordost-Bayern 8: 76–106.

von Freyberg B (1958c) Johann Jacob Baiers Oryctographia Norica nebst Supplementen. Erlanger Geologische Abhandlungen 29, 133 pp.

von Freyberg B (1972) Funde und Fortschritte zur Erdgeschichte beim Bau des Ludwig-Donau-Main-Kanals (1836–1845). Geologische Blätter für Nordost-Bayern 22: 100–125.

von Gümbel CW (1891) Geognostische Beschreibung des Koenigreichs Bayern. 4. Abtheilung, Geognostische Beschreibung der Fränkischen Alb (Frankenalb) mit dem anstossenden Fränkischen Keupergebiete. Fischer, Kassel, 763 pp.

Wagner G (1960) Einführung in die Erd-und Landschaftsgeschichte: mit besonderer Berücksichtigung Süddeutschlands. Ferdinand Rau, Öhringen, 694 pp.

Weiß KP, Freitag D (1991) *Frechiella subcarinata* (Young and Bird, 1822), ein bemerkenswerter Ammonit aus dem höheren Untertoarcium (*bifrons*-Zone) der Fränkischen Alb. Geologische Blätter für Nordost-Bayern 41: 125–132.

Weißmüller M (2017) Eine Reise in den unteren Jura der Region Altdorf. Self publisher, Berg, 200 pp.

Wiedemann HU (1966) Die Geologie der Blätter Göppingen (7223) und Lorch (7224) in Württemberg mit Nachträgen zu Blatt Weilheim (7323) 1:25000. Arbeiten aus dem Geologisch-Paläontologischen Institut der Technischen Hochschule Stuttgart, Neue Folge 53, 226 pp.

Wunstorf W (1904) Die Fauna der Schichten mit Harpoceras dispansum Lyc. vom Gallberg bei Salzgitter. Jahrbuch der Königlich Preussischen Geologischen Landesanstalt und Bergakademie zu Berlin 25: 488–525. [+ pls 17–20]

Zeiss A, Schirmer W (1965) Ober den obersten Lias delta bei Hetzles ostwärts Erlangen. Geologische Blätter für Nordost-Bayern 15: 189–193.

Zimmermann J, Franz M, Heunisch C, Luppold FW, Mönnig E, Wolfgramm M (2015) Sequence stratigraphic framework of the Lower and Middle Jurassic in the North German Basin: Epicontinental sequences controlled by Boreal cycles. Palaeogeography, Palaeoclimatology, Palaeoecology 440: 395–416. https://doi.org/10.1016/j.palaeo.2015.08.045

Zitteliana 95, 2021, 95–134 | DOI 10.3897/zitteliana.95.73026

SNSB Bayerische Staatssammlung für Paläontologie und Geologie

ZITTELIANA
An International Journal of Paleontology and Geobiology

Paleontological inventory of Paleozoic, Late Mesozoic, and Cenozoic plant, invertebrate, and vertebrate fossil species from Big Bend National Park, Texas, USA – over a century of paleontological discovery

Steven L. Wick[1]

1 *Texas Vertebrate Paleontology Collections, 10100 Burnet Road, Austin, TX 78758, USA*

http://zoobank.org/AE8073E6-878D-41F8-A1A4-8335713E7547

Corresponding author: Steven L. Wick (utpaleontology@gmail.com)

Academic editor: Oliver Rauhut ♦ **Received** 14 August 2021 ♦ **Accepted** 8 October 2021 ♦ **Published** 19 November 2021

Abstract

The extraordinary paleontological record from Big Bend National Park (BIBE), Texas chronicles nearly 120 million years of largely uninterrupted deposition through Late Cretaceous, Paleogene and Neogene time. Therefore, the park records one of the most complete and continuous fossil records of its kind in North America, if not the world. Paleontologists have collected and studied fossils from BIBE for over a century and nearly 1400 fossil species have been reported thus far. The BIBE paleontological record includes type specimens representing 44 scientifically valid species (five plants, nine invertebrates, and 30 vertebrates). Numerous other reported specimens are very likely new to science but have yet to be formally named. The present catalog presents the currently known assemblage of fossil plant, invertebrate, and vertebrate species from BIBE within a single, comprehensive record with significant references for each. This work is designed and written to be a research and resource management tool for scientists and non-scientists alike.

Keywords

Cretaceous, Neogene, paleobiodiversity, Paleogene, paleontology, taxonomy

Introduction

For more than 100 years, paleontological researchers have made some of North America's most important fossil discoveries in the Big Bend region of West Texas, USA – many of those in what is now Big Bend National Park (BIBE) (Fig. 1). Many other 'fossil' parks within the National Park Service (NPS) system contain strata which represent a relatively brief geologic interval providing a snapshot of the paleoenvironment represented in the rocks (e.g., Petrified Forest, Dinosaur, and Florissant national parks). On the other hand, BIBE's fossils come from a geologically long (ca. 120 Ma) and mostly uninterrupted series of strata which make it possible to study the succession of paleocommunities over geologic time. This is especially important in that the significance of fossil resources is directly related to degree of scientific information provided by the environmental contexts in which they are preserved. In fact, Big Bend National Park contains more than fossilized plants and animals; it contains a succession of "fossilized" aquatic and terrestrial ecosystems spanning ca. 120 Ma of Earth's history. Aside from the sheer number of fossil species discovered within the park, Big Bend is also known for several iconic fossil species including the largest flying creature known – the giant pterosaur *Quetzalcoatlus northropi* (Lawson), the colossal titanosaur *Alamosaurus* (Gilmore) and the hyper-giant alligatoroid *Deinosuchus riograndensis* (Colbert and Bird).

The updated taxonomic catalog herein is derived from a seminal paleontological inventory of Big Bend National Park produced by Wick and Corrick (2015). The present fossil inventory represents the most significant portion of that earlier work. It involves a comprehensive listing of

Copyright *Steven L. Wick.* This is an open access article distributed under the terms of the Creative Commons Attribution License (CC BY 4.0), which permits unrestricted use, distribution, and reproduction in any medium, provided the original author and source are credited.

PENSOFT®

all reported fossil species (currently around 1300) having been discovered in BIBE by professional paleontologists and academic researchers so that the astonishing number and variety of fossil taxa from BIBE are included in a single published reference. Along with the taxonomic tables are brief descriptions of the park's geologic history and formations so that the reader has a convenient point of reference. Each reported species is accompanied by at least one (or more) significant references so that researchers can use them as a springboard for further research.

The original 2015 (unpublished) catalog was developed as an internal NPS document so that NPS interpretive and law enforcement personnel, resource managers, and qualified permitted academics might better explain, protect, manage, and research the diversity and significance of the park's fossil resources. Hence, it was written using uncomplicated language so that it could be better understood by readers with variable levels of interest and expertise. That approach is maintained here. Whatever the case, it must be noted that this catalog (like all projects of its type) remains a work-in-progress. New discoveries will undoubtedly add to the park's paleobiodiversity and new explorers will emerge over the coming decades to expand upon what we have discovered thus far. It must also be noted that several fossil species relevant to the BIBE paleontological story have been discovered just outside of the park in the same geologic formations exposed within it. These were also included in the present catalog under the assumption that these species are very likely present in the park as well but have yet to be found there.

Relevant references involving the various individual species reported here is provided within each of the taxonomic lists and so specific references are not included within the preliminary text. Repositories and accession numbers for the specimens representing the species listed in the catalog can be found in their respective referenced works. Furthermore, understanding the changing landscape of Big Bend is critical to understanding its paleontological story. The reader is, therefore, strongly encouraged to review Blakey and Ranney (2018) as their work provides an excellent and coherent geotectonic synthesis involving the changing landscape of western North America during Late Cretaceous, Paleogene, and Neogene time. Finally, in order to better understand the geologic context of the park, as well as the stratigraphic and geospatial relationships of the formations outlined in this report, the reader is encouraged to visit https://pubs.usgs.gov/sim/3142/ for the online version of the latest geologic map of BIBE produced by the U.S Geological Survey (Turner et al. 2011).

Overview of Big Bend geologic history and paleoenvironments

Paleozoic era

Fossils from Big Bend National Park are widespread within Mesozoic and Cenozoic strata which are well-exposed throughout the park. Paleozoic strata are not well exposed within the park and are largely confined to its northern margins and so fossils from this time are not well known. These older rocks were laid down some 330–285 million years ago then subsequently deformed during the Ouachita orogeny. They appear in the configuration that we see today as the subsequent result of Laramide compression, faulting, and erosion during more recent times (e.g., Page et al. 2008). Those fossils that that have been found (e.g., conodonts, graptolites, and brachiopods) suggest deposition generally within deep-water, basinal marine habitats. Within the park, the Paleozoic and Mesozoic stratigraphic sequences are separated by a significant unconformity representing a depositional hiatus and/or erosion during Triassic, Jurassic, and early Cretaceous time.

Late Cretaceous system

Around 120 million years ago, a warm, shallow sea (the Western Interior Seaway) bisected North America dividing the continent in half from today's Gulf of Mexico to the Arctic Ocean (Blakey and Ranney 2018), providing the setting for deposition of limy, marine muds and calcareous oozes. Today, these limestones and shales preserve the remains of sea-dwelling invertebrates such as urchins, foraminifera, and mollusks. Within and around BIBE, these strata create the sheer walls of Santa Elena, Mariscal, and Boquillas Canyons, almost the entire range of the Dead Horse Mountains, as well as the magnificent cliffs of the Sierra Ponce and Sierra del Carmen in nearby Mexico. Strata from this interval comprise the Lower Cretaceous, Comanchean Series (marine carbonate) rocks of the Glen Rose, Telephone Canyon, Del Carmen, Sue Peaks, Santa Elena, Del Rio, and Buda formations (Maxwell et al. 1967; Busbey and Lehman 1989; Turner et al. 2011).

Approximately 90 million years ago, the shallow Cretaceous seaway began a gradual retreat to its present location – today's Gulf of Mexico. Calcareous marine muds, and silty clay containing more terrigenously-derived sediments were deposited on the nearby shallow, marine shelf along with the remains of giant bivalves, oysters, sharks, fish, ammonites, and mosasaurs. Gulfian Series limestones and shales of the flaggy Boquillas Formation and soft bentonitic clays of the Pen Formation were deposited during this time (Maxwell et al. 1967; Cooper et al. 2017).

Around 78 million years ago, Big Bend was situated upon the shore of the ancient seaway (Blakey and Ranney 2018). A complex of coastal rivers, meandering streams, estuaries, and marshlands developed in the tropical climate. Alternating periods of marine transgression and shoreline progradation are responsible for the cyclic deposition of the sandstones, mudstones, and shales contained within the Aguja Formation's complex ensemble of inter-tonguing facies (Lehman 1985). These deposits have yielded fossilized trees, oysters, turtles, crocodiles, dinosaurs, and mammals. This was a time of remarkable

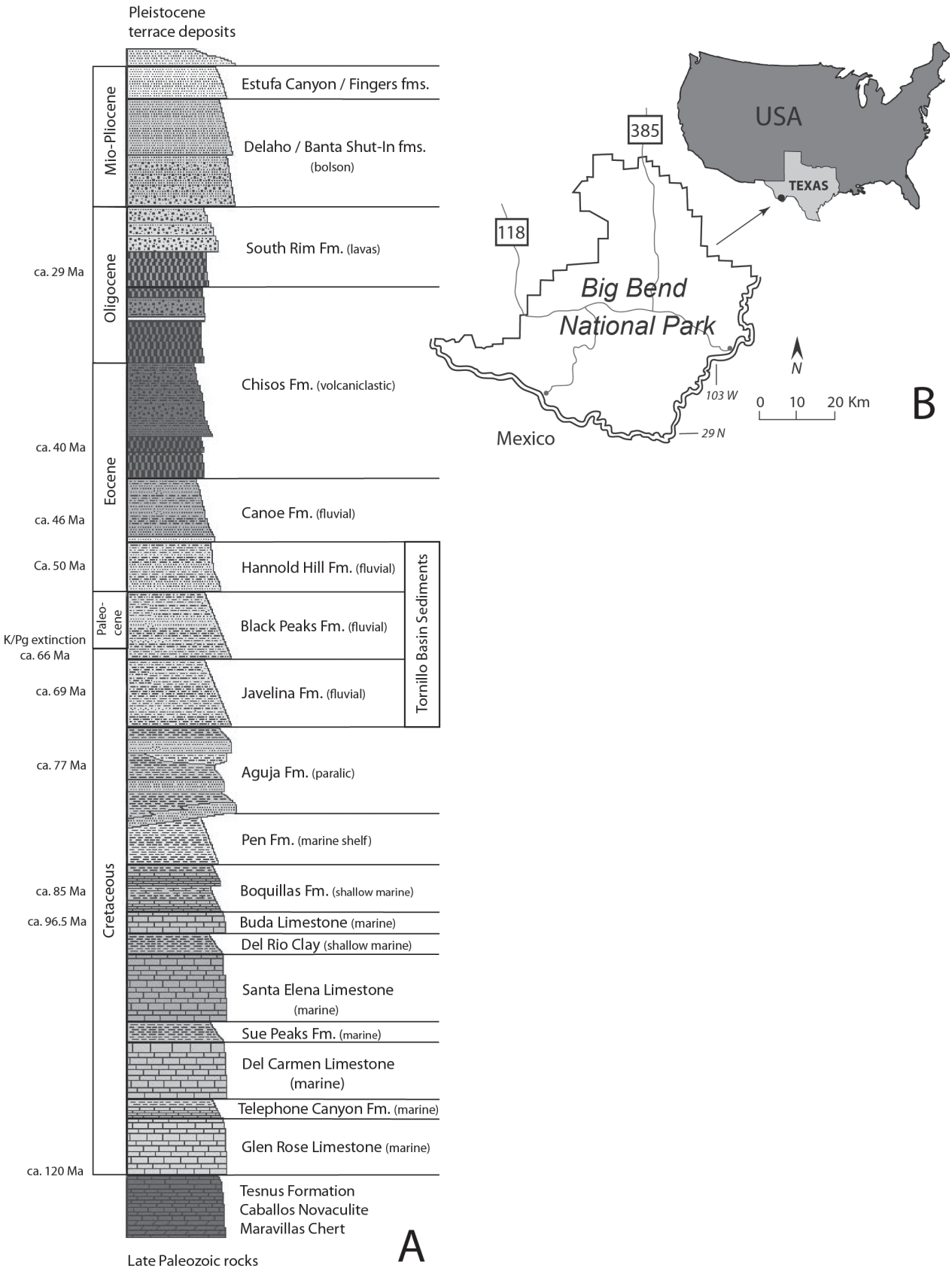

Figure 1. Generalized stratigraphic column (**A**) exposed within Big Bend National Park, Texas, USA (**B**). Approximate absolute stratigraphic ages are based upon biostratigraphic and radiometric information from multiple sources (Maxwell et al. 1967; Lehman et al. 2006; Befus et al. 2008; Tiedemann 2010; Cooper and Cooper 2018). Chart modified from USGS (public domain).

diversity within the ancient ecosystem of ancient BIBE as marine, brackish, and fresh-water subaquatic habitats were situated very near to each other as well as to better drained, terrestrial floodplain environs.

Some 70 to 65 million years ago, Laramide tectonism began uplifting the proto-Rocky Mountains to the west. As a result, the Late Cretaceous shoreline had retreated well to the east of today's park (Blakey and Ranney 2018). This new tectonic regime resulted in significant changes involving deposition and resultant lithology compared to deposits of the older Aguja Formation (Lehman et al. 2018). The most significant of these changes was the development of the Tornillo Basin across the Big Bend region (e.g., Lehman 1986) (Fig. 1). During this time, a river-floodplain environment dominated the deposition of fluvial sands and muds within the Tornillo Basin which are preserved within the Javelina and Black Peaks Formations within the Park. Today, fluvial channel sandstones, colorful overbank mudstones, and thin lacustrine facies can be found in many areas of BIBE which harbor the remains of many creatures including dinosaurs, pterosaurs, and many types of smaller reptiles, as well as conifer trees and flowering plants. The climate had changed since Aguja time and it was becoming cooler and more seasonal (e.g., Linnert et al. 2014). Dinosaurs reached their largest sizes during this time (e.g., Woodward 2005; Woodward and Lehman 2009).

The end of the Cretaceous Period was also a time of great change for life on Earth. Although there are several hypotheses for the extinction of the dinosaurs some 66 million years ago, their disappearance at the end of the Cretaceous gave rise to the 'Age' of mammals. Whether caused by climate change, disease, or the impact of a large meteor in the Yucatan of Mexico, this extinction event occurred during deposition of the Black Peaks formation in BIBE, one of the few public lands in North America which contain strata that span the Cretaceous-Paleogene (K-Pg) extinction boundary.

Paleogene system

Around 63 million years ago (Paleocene time) the dinosaurs were gone. However, ancient mammals survived the K-Pg extinction event (as did avian dinosaurs – the birds) and began to evolve on the ancient river floodplains in BIBE. Although this was the same river system which originated millions of years earlier during Javelina Formation time, the Rocky Mountains continued their unrelenting uplift (e.g., Lehman 1986; Blakey and Ranney 2018). Therefore, the fluvially-derived Black Peaks Formation continued to be deposited even further inland as the sea continued its slow retreat to the east. Bright maroon and somber grey/black 'candy-striped' paleosol (ancient soil) horizons characterize this portion of the Black Peaks section and signal a time when silty, fluvial muds were deposited on a stable, well-developed inland floodplain (Lehman et al. 2018). Huge trees that lined these sandy drainages and were often undercut by the currents, causing them to topple into the river where they became oriented to the paleocurrent direction (now informally called the "log jam sandstone" interval of the Black Peaks). The fossils of these trees show no growth rings, whereas those from the surrounding floodplain (conifers) do have them (Wheeler and Lehman 2005; 2009). This circumstance suggests that the climate afforded constant growth for only those trees along the river and that others went seasonally dormant as rainfall became scarce. Mammals thrived; however, they were small during this time with the largest being only the size of a medium- to small-sized dog.

55 million years ago during early Eocene time, the Tornillo Basin continued to aggrade with fluvial sediments of the Hannold Hill Formation in BIBE (Maxwell et al. 1967; Beatty 1992) (Fig. 1). These deposits consisted of coarser sands deposited in higher gradient river channels. The bright purple and peach-colored paleosol horizons we see now are today's expressions of the confined, muddy overbank deposits emplaced during deposition. Interestingly, some Hannold Hill exposures exhibit striking evidence for compressional deformation during deposition (Lehman and Busbey 2007) which records the final "push" of the Laramide Orogeny in Big Bend as well as the conclusion of basinal development within BIBE. As a result, the Hannold Hill Formation is limited to the northeast portion of the park as the Tornillo Basin, by this time, was almost completely infilled elsewhere by fluvial deposits. At long last, the ancient river system which had long coursed through the basin had reached its closing stages. Paleogene time saw an explosion of new species; mammals diversified in BIBE and became larger (e.g., Wilson 1967).

During mid-Eocene time (about 46 million years ago), the Laramide Orogeny had almost reached its culmination and the Big Bend region was now elevated several thousand feet. Erosion then became the dominant regime, stripping away much of the Hannold Hill, Black Peaks, Javelina, and Aguja formations throughout BIBE and surrounds. All of these strata (as well as the fossils preserved within) might have been lost. However, what remained of them was then covered by deposits laid down by a new river system that developed atop the ancient, infilled basin. As a result, sediments of the Canoe Formation were laid down unconformably on the previously eroded surface. These new rocks were made up of thick fluvial channel sands and gravels (the Big Yellow Sandstone in the park) as part of a braided river system (Maxwell et al. 1967; Rigsby 1986). Mammals had flourished and were now of many types and sizes. Turtles also inhabited the new river corridor which was lined with conifers and flowering plants.

Approximately 42 million to 32 million years ago (during middle Eocene to early Oligocene time) Big Bend experienced a strikingly different depositional regime as widespread volcanism commenced. Strata deposited during this time differ markedly across the region as the result of the changing loci and composition of various igneous intrusions, lavas, ash-falls, as well as the fluvial

volcaniclastics derived from them via weathering (Maxwell et al. 1967). Within BIBE, these deposits became the Chisos Formation, a colorfully diverse collection of tuffs, conglomerates, fluvially re-worked ash deposits, stream channel sandstones, and variegated mudstones situated between ensembles of extrusive lavas (e.g., the Alamo Creek Basalt). Portions of the Chisos Formation are locally fossiliferous whereas others are completely devoid of fossils. It is generally believed that the volcanism involved here was subduction-related and that a temporary shallowing of the angle of subduction of the Farallon plate (descending eastward, below the western edge of North America) resulted in the emplacement of various plutons and volcanoes far inland from the margin of subduction along western North America. Because of their complexity, these deposits are named differently in different areas (e.g., Canoe and Chisos formations within BIBE and Devil's Graveyard Formation outside of the park to the northwest) (e.g., Maxwell et al. 1967; Wilson and Runkel 1989). Whatever the case, similarities involving their geologic make-up and fossil evidence suggest that these formations are broadly coeval. Although the Devil's Graveyard Formation is very fossiliferous, these taxa were not included in the present catalog as that formation does not crop out within the park.

During early Oligocene time (around 32 to 26 million years ago), volcanism continued with a series of eruptions in what is today BIBE (Maxwell et al. 1967; Lehman and Busbey 2007). Higher in section, the un-fossiliferous South Rim Formation (along with the so-called "Burro Mesa" Formation of Turner et al. 2011) capped the Chisos Formation with a series of thick, brightly colored rhyolitic lavas which are particularly striking along the Ross Maxell Scenic Drive in the western part of the park. The Chisos Mountains within BIBE were fully formed by this time and, along their flanks, new and even larger mammals replaced older forms. Volcanic deposition in the region ended some 26 million years ago (Henry et al. 1989). As a result, erosion again resumed.

Neogene system

By the end of Oligocene time (around 20 million years ago), the Rocky Mountains stood in bold relief above the western plains. Compressional stresses involved in mountain-building finally eased across the North American continent resulting in a 'relaxation' of continental crust. As a result of this trans-continental stretching, rift zones developed which, over time, allowed large bodies of rock to slide downward along active faults, producing a horst-and-graben topography. This created the North American, Basin and Range Province which spans southern Canada to northern Mexico including Big Bend. The Big Bend region saw the development of several grabens and resultant bolsons including one within the central part of today's BIBE (from the Sierra del Carmen to the east to the Mesa de Anguila to the west). This graben formed a "sunken block" of strata, down-dropped several thousand feet by faulting (Maxwell et al. 1967; Lehman and Busbey 2007). As a result, two half-bolsons formed in BIBE (one on either flank of the eroding Chisos Mountains): the Delaho Bolson in the west and Estufa Bolson in the east (Stevens and Stevens 1985, 1989). During Miocene and Pliocene times, these bolsons slowly aggraded with alluvium and colluvium transported in streams and deposited as alluvial fans along the flanks of the nearby eroding Chisos Mountains. These coarsely-laminated sands and gravels formed today's Delaho and Banta Shut-In formations. On the Maxwell et. al, (1967) geologic map of the park, these bolson-fill deposits were mapped collectively as Quaternary/Tertiary "old gravels" (abbreviated thereon as QTog). Portions of these alluvial fans supported intermittent faunal communities comprised of mammals such as early camels, skunks, and carnivores, as well as turtles, lizards, and amphibians.

Eventually, similar bolsons throughout west Texas were infilled and subsequently linked by the Rio Grande (achieving through-flow to the Gulf of Mexico only within the last 2 million years or so). Once established, the downcutting Rio Grande and its tributaries (forerunners of today's Terlingua and Tornillo creeks within BIBE) largely gutted the infilled bolsons during Pleistocene time leaving only remnants of them today. The Rio Grande is the youngest major river system in the United States and continues to serve as the principal erosional conduit in the region.

Geologic formations within Big Bend National Park: a primer

The geologic formations within BIBE vary widely regarding composition, thickness, depositional environments, and fossil content. However, many are fossiliferous. Many formations exposed within the park also crop out on private lands just outside of its boundaries and so some fossils from just outside the park are also included here as well. In general, older, Late Cretaceous open marine carbonate strata are separated by unconformities representing relatively brief geologic intervals. Younger, Late Cretaceous (marine shelf) strata generally grade conformably into, and sometimes inter-tongue with, broadly coeval terrestrial rocks. These deposits then grade conformably into overlying Paleocene strata. Some localized unconformities are present in some strata (e.g., the Aguja/Javelina formations contact) as the result of penecontemporaneous erosion (i.e., stream downcutting which occurred simultaneously with overbank deposition in some areas), but these minor depositional gaps generally do not represent geologically significant intervals. Significant erosion of Cretaceous and Paleocene strata did occur as the result of Laramide uplifting in Eocene time however these eroded deposits were then covered by even younger fluvial deposits, volcaniclastics, and extrusive rocks. Basin and range development along with continued erosion of

the Chisos Mountains volcanic complex initiated yet another period of deposition which resulted in infilling of the surrounding bolson. Despite the presence of unconformities, many of the strata within the park and immediate surrounds preserve a relatively continuous, 135 million-year-long depositional sequence. The following formations are arranged in stratigraphic succession (low to high) (Fig. 1).

Paleozoic Era

Maravillas Chert (Baker and Bowman 1917)

Ordovician, marine, around 50 m thick. The Maravillas was deposited in a deep-water, basinal environment (Turner et al. 2011). The formation is exposed along the northern margins of the park northward (Persimmon Gap and Dog Canyon areas within BIBE) and is convolutedly deformed in some areas by pre- and post-Cretaceous thrusting. The formation contains dark brown/blackish cherts and thin conglomerate lenses, and a few limestone beds Fossils from BIBE include graptolites, brachiopods, bryozoans, and conodonts. Extensive deformation and poor exposures make sectional thickness measurements and definition of individual members within BIBE difficult.

Caballos Novaculite (Udden et al. 1916)

Silurian–Devonian, marine, only 20 m thick. The origin of both the novaculite and chert members leads to contrasting interpretations of water depth during deposition (e.g., Folk and McBride 1978). This formation contains chert and silicious shale with thin but conspicuous, white novaculite beds. The unit is modestly exposed near Persimmon Gap near the entrance of the park however no fossils have been reported from BIBE.

Tesnus Formation (Udden et al. 1916)

Mississippian – Pennsylvanian, marine, variably thick from 15–200 m. Deep-water sediments, thin to thickly bedded sandstone and dark gray, brown, and black shale. Several small outcrops are situated in the northernmost part of BIBE. No fossils have been collected from the park however nearby areas have produced conodonts, foraminifera, and a few Pennsylvanian Period plant fossils (King 1937).

Mesozoic Era – Lower Cretaceous (Comanchian Series)

Glen Rose Limestone (Hill 1891)

Marine, massive, about 100–150 m thick. Primarily a massive limestone but contains clay, minor sandstone, marl, and conglomerate deposited in near-shore tidal and sub-tidal marine environs (Maxwell 1967; Busbey 1989). This unit is exposed in several areas of BIBE including Persimmon Gap and Dog Canyon in the north, Marufo Vega trail in the southeast and Santa Elena Canyon in the southwest (Turner et al. 2011). These outcrops are generally exposed in areas which have been subjected to Cretaceous Laramide folding and/or the development of horst and graben structures emplaced during Miocene time. Invertebrate fossils include ammonites, oysters, gastropods, and echinoids. Rarely, dinosaur fossils have been found elsewhere in Texas from this formation (Upchurch et al. 2004). Although dinosaur trackways are somewhat common in the Glen Rose of Texas (e.g., Bird 1985) none have been reported in BIBE. However, several theropod dinosaur tracks are preserved along the Rio Grande in the Glen Rose Formation of Mexico just east of the park within the lower canyons (photos shown to the author by D. Corrick, BIBE Geologist).

Telephone Canyon Formation (Maxwell et al. 1967)

Marine, generally 20–45 m thick. Lagoonal sediments (Busbey 1989) containing thin nodular limestone with marl beds This formation can be seen in several areas of BIBE including Heath Creek, along the Marufo Vega Trail in the east, and Santa Elena Canyon in the southwest where folding and faulting have exposed it (Turner et al. 2011). Common invertebrate fossils in this formation include gastropods, oysters, and echinoids. Ammonites have also been reported.

Del Carmen Limestone (Maxwell et al. 1967)

Marine, massive, from 100–150 m thick. Open lagoon, tidal flat, and rudistid biostromal facies (Busbey 1989). Generally, a massive, dense limestone with abundant rudistids. This karstic formation also contains lenticular cherts and minor marl beds. Within the park, it is exposed in areas of tectonic folding and faulting such as Santa Elena Canyon in the southeast and Marufo Vega Trail, and Sierra del Caballo Muerto in the east (Turner et al. 2011). Typical invertebrate fossils include bivalves and gastropods although recovery of them from the hard matrix is difficult which makes their identification problematic.

Sue Peaks Formation (Maxwell et al. 1967)

Marine, around 25–30 m thick. Transgressional marine sediments containing shale, marl, thin nodular limestone ledges (Maxwell 1967; Busbey 1989). The formation is exposed in eastern and southwestern areas of the park including portions of the Sierra del Carmen, as well as Santa Elena Canyon where faults and folding have exposed it. Common invertebrate fossils include oysters, echinoids, gastropods, and numerous types of ammonites.

Santa Elena Limestone (Maxwell et al. 1967)

Marine, massive, up to 225 m thick. Open shelf carbonate environments (Busbey 1989). The Santa Elena is a massive, karstic limestone, hard, with some finely crystalline bedding along with nodular chert masses. Upper portions of this formation contain massive limestones with interbedded marls that weather to form a terrace-like topography. The formation can be found in eastern and southwestern parts of the park (and surrounds) such as the Sierra del Carmen, Santa Elena Canyon, and Sierra Ponce where faulting and folding have exposed it (Maxwell et al. 1967; Turner et al. 2011). Common invertebrate fossils include rudists with other pelycopods and gastropods being uncommon.

Del Rio Clay (Hill and Vaughn 1898)

Marine, fissile, around 1–35 m thick. A regressive marine environment facilitated development of this shaly, shallow-water facies (Busbey 1989). This formation consists mostly of claystone with interbeds of limestone and friable sandstone. It is exposed in the eastern and southwestern portions of the park including Mesa de Anguila, Dog Canyon, Alto Relex, and Sierra del Caballo Muerto (Turner et al. 2011). Invertebrate fossils include oysters, echinoids, and gastropods.

Buda Limestone (Vaughan 1900)

Marine, 20–30 m thick. Shallow, inner-shelf environment. This formation primarily crops out in eastern, southern. and southwestern areas of the park such as Dog Canyon, Dagger Mountain, Mariscal Mountain, and Mesa de Anguila (Turner et al. 2011). Invertebrate fossils are rare in fine-grained limestones and more common in marls including echinoids, gastropods, and bivalves. West of the park along route 170, the Buda/Boquillas limestone contact interval harbors the typical reddish tint of cinnabar.

Mesozoic Era – Upper Cretaceous (Gulfian Series)

Boquillas Formation (Udden 1907)

Marine, massive to shaley, from 220–245 m thick. Foraminiferal limestone and shale deposited in relatively shallow, open marine (platform) conditions (Lehman 1989b; Cooper et al. 2017). This formation contains two members including the lower Ernst Member and upper San Vicente Member (Maxwell et al. 1967). The Ernst Member contains silty limestone flags, siltstone, and calcarious clay while the San Vicente Member contains chalk, marly clay, and shale. It is exposed widely in the park in areas such as San Vicente, Hot Springs, Mariscal Mountain, McKinney Hills and Mesa de Anguila (Turner et al. 2011). The Boquillas Formation is very fossiliferous. Fossils include invertebrates such as cephalopods, bivalves, and echinoids as well as a few vertebrate fossils from mosasaurs, fish, and sharks. Even soft-bodied organisms (squids) have been discovered in the Boquillas.

Pen Formation (Maxwell et al. 1967)

Marine shelf, 70–200 m thick. Calcareous clay shale and chalky limestone with concretionary intervals. The Pen Formation was deposited upon a shallow marine shelf. This unit also includes a westerly-thinning wedge of dark gray marine shale within the overlying Aguja Formation (e.g., Lehman 1985). This formation is widely exposed in the park in areas such as San Vicente, Mariscal Mountain, Maverick Mountain and the McKinney Hills (Turner et al. 2011). Invertebrate fossils include echinoids, bivalves, gastropods, and ammonites. Vertebrate fossils are uncommon but include fragmentary sharks, fish, and mosasaurs. However, shed shark teeth and fish vertebrae are common throughout the formation. Rarely, reworked dinosaur bones (resulting from floods washing carcasses seaward) are also encountered (pers obs. by the author).

Aguja Formation (Adkins 1933)

Originally named “Rattlesnake Beds” by Udden (1907), these strata were later re-named the Aguja Formation as the previous name was already in use elsewhere. Nearshore marine, deltaic, and continental facies including paralic, estuarial, and coastal marsh and swamp deposits (Maxwell et al. 1967; Lehman 1985), 120–280 m thick. The coastal Aguja Formation records fluctuating periods of marine transgression and shoreline progradation. Transgressive and regressive marine Aguja facies include thicker, well-indurated marine sandstones, poorly developed coals, lignitic shales, and thin cross-bedded fluvial channel sandstones. The upper part of the formation contains coastal floodplain mudstones; some with incipient paleosol development. The Aguja Formation is widely exposed in BIBE in areas such as Dawson Creek, Rattlesnake Mountain, San Vicente, and McKinney Springs (Turner et al. 2011).

Some facies within these units are very fossiliferous while others are not. Plant fossils are locally abundant in the Aguja Formation. These usually include fossilized woods from conifers, palms (monocots), and flowering plants (dicots). Rarely, tree stumps are found upright, situated in their original growing positions. Fossil leaves have been found in a couple areas preserved as carbonate films within mudstone horizons or, in one area, as impressions within reworked volcanic ash. This ash bed and its fossils are currently under study by the author (S.W.). Aguja invertebrate fossils include bivalves, gastropods, cephalopods and rarely, crustaceans. Trace fossils from

some of these taxa are also relatively common (e.g., *Ophiomorpha* burrows).

Occasionally, vertebrate fossils (and microfossils) are also found at various stratigraphic intervals in strata representing numerous environs. Taxa include sharks, fish, turtles, crocodilians, as well as dinosaurs among other reptiles. Very rarely, small fossil mammals are encountered (mostly teeth) as are dinosaur eggshell fragments. The vertebrate fossil assemblage of the Aguja Formation is the most inclusive of its kind reported from southernmost North America.

Javelina Formation (Maxwell et al. 1967)

Continental, 100–190 m thick. The formation can be found along the flanks of the Chisos Mountains and is well exposed along the drainages of Tornillo, Terlingua, and Dawson creeks, as well as Rough Run (Turner et al. 2011). This formation contains facies from inland floodplain environs. Sedimentary strata include well-cemented fluvial sandstones, rhythmically-bedded lacustrine deposits, and floodplain mudstones – some containing fairly well-developed paleosol and paleocaliche horizons (Lehman et al. 2018). Generally, fossils are uncommon throughout this formation; however, several discreet areas (and representative habitats) are quite fossiliferous (e.g., Lehman and Langston 1996). Fossil wood is common in the Javelina Formation and includes fossils from fan palms as well as conifers and flowering plants. Abundant prone fossil logs can be found along a few stratigraphic horizons while others harbor stumps in their original growing positions. Invertebrate fossils are very rare but include fresh-water gastropods and crustacean burrows.

Isolated, broken vertebrate fossils are somewhat common within scree along deflated surfaces atop fluvial sandstone hogbacks but are also found in-situ at local intervals within overbank mudstones. Vertebrate fossils include those from fish, turtles, pterosaurs, dinosaurs, and small mammals (represented mostly by teeth). Vertebrate fossils usually occur as isolated, fragmentary bones. However, a few dinosaur skeletons have been found partially articulated or with bones in close association. Although typically well-preserved, Javelina Formation fossils are seemingly not as numerous as those of the underlying Aguja Formation. As such, I surmise that the paralic Aguja environment favored a greater variety (and populations) of vertebrate species and/or the paralic environment was more conducive the burial and preservation of remains. Lehman et al. (2006) obtained a radiometric date of around 69 Ma. for the middle of the formation

Black Peaks Formation (Maxwell et al. 1967) – Cretaceous interval

Continental, around 40 m thick (widely variable) (e.g., Lehman et al. 2018). The Black Peaks Formation contains inland flood plain deposits with interstitial fluvial sandstones. The formation is exposed widely in BIBE especially near Grapevine Hills, Dogie Mountain, and Tornillo Flat. Paleosols are sometimes well developed, appearing as somber red and black bands which are, in places, interrupted stratigraphically by fluvial sandstones. The bottom third of the formation is Cretaceous in age. Plant fossils present in the lower Black Peaks Formation including conifers and flowering plants. Invertebrate fossils are virtually unknown; however, freshwater ?crustacean burrow structures have been observed. Vertebrate fossils are uncommon in this portion of the formation but include those of fish, reptiles, as well as dinosaurs (especially those of the huge titanosaur *Alamosaurus*). Usually, vertebrate fossils are found isolated, weathering out of fluvial channel sandstones. Rarely, associated dinosaur bones have been located eroding from overbank mudstones.

The Cretaceous-Paleogene (K-Pg) boundary is situated in the lower third of the Black Peaks Formation although its exact stratigraphic position remains obscure. It has been defined within a two-meter section near the Grapevine Hills (Lehman and Coulson 2002). However, it has not been this well-defined elsewhere in BIBE (see discussion in Lehman et al. 2018, p. 2225). It is possible that there was a depositional hiatus during the K/Pg time interval and that the K/Pg boundary is only preserved in very localized lenses of deposition (if at all) within the park.

Cenozoic Era – Paleogene (Paleocene Series)

Black Peaks Formation (Maxwell et al. 1967) – Paleogene interval

Continental, up to 400 m thick (widely variable). The Black Peaks Formation straddles the K-Pg boundary. The Paleogene portion of the formation contains inland floodplain deposits with thick, fluvial sandstones. It is exposed near Dogie Mountain, Grapevine Hills, and Tornillo Flat (Turner et al. 2011). Paleosol horizons are often striking, appearing maroon, black or somber gray sometimes with interstitial, tan fluvial channel sandstones. Paleosols within the Cretaceous, Aguja and Javelina formations are often poorly developed. However, they become increasingly better developed higher in section with the Black Peaks having the most conspicuous forms. Typical vertebrate fossils include garfish, turtles, and mammals.

Plant fossils (mostly conifers) are rarely found in the lower part of the formation but are more common higher in section. Two, closely-space stratigraphic intervals of very large fossil dicot logs (*Paraphylanthoxylon*) in the middle portion (Torrejonian-Tiffinian) of the Black Peaks section (informally called the “log jam sandstone”) suggest the post K-Pg resurgence of trees during this time.

This fossil log horizon is conspicuous in many areas of the park and is a useful stratigraphic marker (Lehman et al. 2018).

Cenozoic Era – Paleogene (Eocene Series)

Hannold Hill Formation (Maxwell et al. 1967)

Continental, varies from around 30 to 70 m in thickness (e.g., Lehman et al. 2018). This relatively thin formation is very limited in area with all known outcrops in the Tornillo Flat region of BIBE and represents the final infilling of the Tornillo Basin (Turner et al. 2011). The inland floodplain formation contains variegated mudstone-dominated facies along with coarse fluvial sandstones and conglomerates. Vertebrate fossils include those from several mammalian taxa. The fossil bone exhibit in BIBE is situated atop fluvial channel sandstones of the Hannold Hill Formation (Exhibit Ridge Sandstone Member) where numerous specimens of *Coryphodon* were excavated and displayed as part of the park's original Fossil Bone Exhibit.

Canoe Formation (Maxwell et al. 1967)

Continental (upland), up to 350 m thick. This formation is exposed in the north-central portion of BIBE especially on Tornillo Flat (Turner et al. 2011). It contains rocks from a sandy, braided fluvial system with associated flood plain deposits (e.g., Rigsby 1986; Runkel 1988) which rest unconformably on the Hannold Hill Formation. Thick sandstones and conglomerates comprising the conspicuous Big Yellow Sandstone Member are present in the lowest part of the Canoe Formation with gray and variegated mudstones situated a bit higher in section. These paleosol horizons (along with interstitial sandstones and tuffaceous mudstones) make up a large portion of the Canoe Formation section above the Big Yellow Sandstone.

Vertebrate fossils are widespread within the formation in BIBE as well as areas northwest of the park in the Devil's Graveyard Formation which is temporally coeval with the Canoe Formation (e.g., Runkel 1988). The reader is cautioned that the Devil's Graveyard Fm. is not exposed within the park so its reported taxa are not included herein. Vertebrate fossils in the Canoe include those from mammals, turtles, and crocodilians. Fossilized wood is also common in the Big Yellow Sandstone including not only Eocene conifers and dicots but reworked and abraded, fossilized Cretaceous wood fragments exhumed during entrenchment of the younger, Eocene fluvial system. A striking example of its fossil ensemble includes a dense 'forest' of at least 92 fossil tree stumps in their original growing position observed by the author near the McKinney Hills. Whether these represent conifers or dicot trees is not yet known. However, these stumps (~10 to 15 cm in diameter) are the remains of smaller trees that apparently grew on islets within the confines of the braided fluvial corridor.

Cenozoic Era – Paleogene Period (Late Eocene and Oligocene Series)

Chisos Formation (Udden 1907)

Continental (upland), from 500–700 m thick. The Chisos Formation is exposed in many areas of BIBE along the flanks of the Chisos Mountains (Turner et al. 2011). This widely variable formation contains lavas, tuff, tuffaceous sandstone, clay, and conglomerates. Vertebrate fossils include turtles and large mammals while invertebrates include fresh-water gastropods and snails). Fossil wood is present but not common.

South Rim Formation and "Burro Mesa" Formation (Maxwell et al. 1967; Turner et al. 2011, respectively)

Please note that the Burro Mesa Formation is not considered valid by all researchers and so both are included together here. Continental (volcanic), from 300–500 m thick. These typically massive, volcanically-derived strata are exposed in the central and southwest portions of BIBE in the Chisos Mountains and near Burro Mesa. They contain lavas, flow breccias, conglomerates, tuff, and tuffaceous sediments from various localized eruptive events and are apparently non-fossiliferous.

Neogene (Miocene Series)

Delaho Formation (Stevens et al. 1969)

Continental (bolson deposits), up to 300 m thick. The formation is exposed on the west side of BIBE near Castolon (Lehman and Busbey 2007; Turner et al. 2011). Originally identified by Maxwell et al. (1967) as 'older gravels', the Delaho has two members including the lower member and Smokey Creek Member. These contain pink friable sandstone and gray conglomerate representing mid and distal alluvial fan deposits that accumulated in a fault bounded basin in the western half of BIBE (the Delaho Bolson). Vertebrate fossils include those from small and large mammals as well as from several reptiles including a unique Gila monster.

Banta Shut-In formation (informally proposed by Stevens and Stevens 1985)

Continental (bolson deposits), up to 150 m thick. This formation is exposed in the east-central portion of BIBE near Banta Shut-In. These include pink fine-grained sandstone, siltstone and red mudstone which represent distal alluvial fan facies in the eastern half of BIBE (Estufa Bolson). Vertebrate fossils include amphibians, reptiles, and mammals (including those from canids, camels, and primitive

horses). This formation is exposed in areas along Tornillo Creek that are not easy to reach and it is likely that its fossiliferous nature has yet to be fully realized.

Neogene (Pliocene – Pleistocene series)

Fingers and Estufa Canyon formations (informally named by Stevens and Stevens 1989)

Continental (bolson deposits), variably thick up to 300 m. These formations are exposed in the western portion of BIBE near Sotol Vista and along the flanks of Tornillo Creek east of Dugout Wells and consist mostly of bolson deposits. They were originally identified as 'older gravels' by Maxwell et al. (1967) and consist of proximal alluvial fan facies which overlie the Delaho and Banta Shut-In formations (Turner et al.2011). Primarily these contain larger sand and gravel clasts eroded relatively recently from the volcanic and plutonic rocks of the Chisos Mountains. However, they also contain scree from Paleozoic and Late Cretaceous strata exposed along the margins of the ancient bolson. The fingers and Estufa Canyon formations represent the youngest deposits within the Delaho and Estufa bolsons and have yet to produce fossils.

Pleistocene terrace deposits and grottos

Thin alluvial gravels, sands, silts, caliche-cemented silts, small dune fields harboring a variety of localized cut-and-fill structures and small head-cutting drainages harboring a variety of finely to poorly sorted rock types. These thin deposits form desert pavement atop alluvial terrace remnants where aeolian erosion and sheet-wash have often removed finer sediments (Turner et al. 2011). Fossils from the Pleistocene of BIBE are almost unknown at present however mammoth teeth have been found within a caliche deposit in BIBE near Grapevine Spring which may represent the former location of a Pleistocene ciénega during the most recent glacial age (see Maxwell et al. 1967, p. 154 for a photo of the in-situ teeth).

Numerous cliffside grottos can be also found throughout BIBE. Of interest is the discovery within one of these near Mule Ears Peaks of remains pertaining to California condors which no longer live in the Big Bend region. Whether these remains are truly fossils or not is debatable. However, they are estimated to be thousands of years old (Wetmore and Friedmann 1933).

Fossil taxonomic lists: methods

'Taxonomy' is the scientific study of naming, defining, and classifying groups of biological organisms based on shared or differing morphological characteristics. The following taxonomic lists were compiled from hundreds of reliable sources. These included peer-reviewed scientific reports, graduate-level academic studies (e.g., Ph.D. dissertations and Master's Theses), field trip guidebooks, scientific abstracts, as well as verifiable first-hand accounts (current research) reported to the author by qualified researchers. In the interest of compiling a comprehensive taxonomic catalog of fossils from Big Bend National Park (and immediate surrounds), all reported taxa are included. This distinction is important because, in some cases, a species reported decades ago may have more recently been taxonomically re-classified differently as something else. As a result, some older taxa may no longer be valid and/or a few may be recorded twice as the result of different taxonomic interpretations. In other cases, taxa may be listed multiple times with varying degrees of certainty (e.g., sometimes with a question mark or designated as a possible new species – see below). These are all included in the present report as they may represent more than one species. This circumstance serves to illustrate our constantly changing understanding of how species relate to one another.

The taxonomic lists presented here are organized alphabetically within classes of the Linnaean taxonomic classification system. Their common names are also provided as well. This serves to simplify the identification and listing of each species (from the perspective of interpretation) and allows for the convenient addition of future data within each table. This simplified method was chosen because taxonomic groupings at family-level (and below) often complicate matters to the point of utter confusion for non-scientists – especially as classification systems and taxonomic relationships are revised when new information comes to light.

Furthermore, additional taxa have been added to the original catalog produced by Wick and Corrick (2015) given that new discoveries have occurred since that time. For example, new taxonomic information was included by the author as late as September 2021 as the result of his ongoing (preliminary) research involving boney fishes from the Aguja Formation. However, although the present catalog is an exhaustive listing of taxa, it likely does not include absolutely every fossil species known from BIBE. Certainly, some discoveries have yet to be formally recorded (for example, the author and his colleagues have several works in progress), or some species may have been presented in older, more obscure, and/or unpublished contexts such as field trip guides and/or scientific abstracts and academic poster sessions. As such, some species have likely been missed during the literature survey. However, there are around 1400 different fossil species listed in this catalog alone.

These lists also embrace the 'morphotype concept' of taxonomy and is used so that scientists can communicate with each other more effectively. For example, different types of plant fossils from a single taxon are often named differently because that plant species may be expressed in the paleontological record by multiple fossil morphotypes (such as fossil wood, leaf impressions, and/or pollen). From this example, unless all three types

of plant fossils are found in close association, each type of fossil cannot be conclusively determined to pertain to the same plant species. Hence, each form is given its own name until a direct association can be confirmed. As such, a single plant species may unknowingly be represented here by more than one morphotype (and scientific name). Also included in these lists are non-body fossils (such as crustacean burrows and dinosaur eggshell fragments) produced by a living organism. These are also classified and named using the morphotype concept since they do not represent the actual fossilized remains of a particular animal, but only the preserved evidence of its lifeway.

Also included are the formations in which the fossils occur as well as the original (or significant) publications in which they were reported. Because commonly encountered species (e.g., various sharks among others) are mentioned in numerous reports, it is simply impractical to include every reference for many of these commonly reported species. It is, therefore, up to the reader to use the listed sources as springboards for further research. Problematic taxa and /or references indicated by an asterisk are discussed at the bottom of each list.

Finally, the reader needs to be aware that the author of the present work did not make any of the taxonomic interpretations for a particular species listed herein unless (as in a few cases) he actually authored one of the referenced papers. Among the names of the species listed herein, the reader will sometimes see various abbreviations associated with them. The applications of abbreviations such as these are standard practice among taxonomists (e.g., see Bengston 1988) and were assigned by the various authors of the referenced works and serve to indicate that they had some doubt regarding their taxonomic assignment of a particular species. This doubt may have resulted from a specimen being broken or incomplete, being obscured by rock, or the fact that it exhibits some morphological variation compared to others of its kind. For example, the use of "cf." before a species name indicates that a particular author felt that a particular specimen "compared favorably" enough to the listed species to suggests that it likely pertains to it. On the other hand, the term "aff." suggests that although a specimen has "affinities" to particular taxon, it is different enough that it may, in fact, represent a different, closely related species. Question marks are also sometimes used immediately before a specie's name to indicate even more doubt. In any case, a number of specimens listed here represent new genera and/or species that were deemed by the various authors of the referenced works as potentially being new (or potentially new) to science (e.g., those designated with n. gen and/or n. sp. in the taxonomic tables). These species are indicated immediately after their listed names in the following manner: 1) formally published new species (scientifically valid holotypes) are designated by a black dot; 2) specimens that are likely new to science (but have yet to be formally named) are designated by a cross; and 3) specimens that have been named but not published in a formal context (e.g., an unpublished Ph.D. dissertation) are designated by an open triangle. A legend to this effect is present at the bottom of each table. It is worth noting that among the many species new and potentially new to science listed here, only 44 are presently considered to be scientifically valid species (black dots). The remainder (open triangles and crosses) are not considered scientifically valid at the present time. Their inclusion in this publication was done out of thoroughness and their listings herein are not an attempt to formally validate them.

Discussion

Fossil plants (Table 1)

Since 1907, when Johan Udden first reported the occurrence of fossil wood in what would become Big Bend National Park, over 300 fossil plant taxa have been described including flowering plants (dicots), palms (monocots), conifers, tree ferns, leaf impressions, algae, palynomorphs and tree resin (amber). Because of the changing environment over time, fossil plant remains range from marine, coastal, and inland varieties spanning a diverse range of paleohabitats. Numerous type specimens (nine) have been formally described with several others having been recognized but not yet reported. Two-thirds of the fossil plant species reported from BIBE pertain to palynomorphs (e.g., pollen, spores, fungi, etc.).

Although fragmentary fossil wood specimens are observed within many continental strata in BIBE, they are uncommon or absent in most locations. However, a few horizons produce spectacular fossil logs, sometimes by the dozens (Lehman et al. 2018). The fossils within these assemblages normally occur as prone trunk segments up to several meters in length and up to three meters in diameter. In some areas, dozens of fossil trunks can be observed holding up small ridges within mudstone-dominated flats or protruding from fluvial sandstone horizons. In rare occurrences, stumps are preserved intact in their original positions of growth with root buttresses splayed from their bases. Several sites of this type have multiple individuals of the same species or a combination of species forming true fossilized paleo-forests (e.g., Lehman and Wheeler 2001; Lehman and Shiller 2020).

The degree of preservation involving fossil woods from BIBE ranges from those having experienced near-complete permineralization (i.e., exhibiting few visible diagnostic attributes) to those that preserve very detailed morphological features such as growth rings and cellular structure such as compression wood, parenchyma, and cross-field pitting (e.g., Wheeler and Lehman 2000, 2005). It is the latter type which is most useful from a diagnostic standpoint. This has resulted in the diagnosis of several new fossil species and provided insights into tree growth rates, sizes, and their preferred environments. Other specimens of fossilized wood are interesting from additional perspectives. In some cases, fossil woods are almost completely carbonized suggesting the occurrence of an-

Table 1. Fossil plants.

CLASSIFICATION	TAXON	FORMATIONS												REFERENCES
		GR	TC	DC	SE	DR	BO	PN	AG	JV	BP	HH	CN	
CYANOPHYTA														
blue-green algae	**Stromatolites**	X		X	X									Tarasconi 2000
ULVOPHYCEAE														
calcareous algae	***Cylindroporella* sp.**	X		X	X									Tarasconi 2000
	***Heteroporella* sp.**			X										Tarasconi 2000
	Permocalculus irenae	X		X										Tarasconi 2000
	***Salpingoporella* sp.**				X									Tarasconi 2000
	***Terquemella* sp.**				X									Tarasconi 2000
BRYOPSIDOPHYCEAE														
calcareous algae	***Boueina* sp.**		X											Tarasconi 2000
CHAROPHYTA														
algae (oogonia)	**?Charophytes Indet.**									X	X			Schiebout 1970; Coulson 1998
PHAEOPHYCEAE														
brown algae	**Fucales indet.**					X	X							Eley 1938
	***Halymenites* sp.**								X					Udden 1907; Eley 1938
PTERIDOPSIDA														
tree ferns	***Tempskya* sp.**										X			Chang 1973
CONIFEROPHYTA														
GYMNOSPERM TREES	***Abeitoxylon maxwellii* Δ**										X			Chang 1973; *Abbott 1985
	Araucariaceae indet.								X	X	X			Wheeler and Lehman 2005
	***Araucarioxylon maxwellii* Δ**										X			*Abbott 1985
	***Araucarioxylon* sp.**										X			Chang 1973
	***Brachyphyllum* sp.**								X					Baghai 1998
	Coniferophyta indet.											X		Maxwell et al. 1967
	***Glyptostrobus* sp.**								X					Baghai 1998
	Podocarpaceae indet.								X	X				Wheeler and Lehman 2005
	***Sequoia* sp.**								X					Baghai 1998
	?*Sequoia reichenbachia*								X					Dorf 1939
	***Thuyoxylon maxwellii* Δ**										X			Chang 1973; *Abbott 1985
	***Tornilloxylon maxwellii* Δ**										X			Chang 1973; *Abbott 1985
MONOCOTYLEDONEAE														
PALM TREES	***Sabal bigbendense* •**								X					Manchester et. al 2010
	Sabal bracknellense								X					Manchester et. al. 2010
	***Sabalites ungeri* (leaf impression)**								X					Dorf 1939
DICOTYLEDONEAE														
ANGIOSPERM TREES	***Acalyphoxylon maxwellii* Δ**										X			Chang 1973; *Abbott 1985
	***Agujoxylon olacaceoides* •**								X					Lehman and Wheeler 2001
	***Baasoxylon parenchymatosum* •**								X	X				Wheeler and Lehman 2000
	Baileyan Big Bend wood type I (scrambling vine)								X					Wheeler and Lehman 2000
	***Bombacoxylon langstoni* •**								X					Wheeler and Lehman 2000
	***Canarioxylon maxwellii* Δ**										X			Chang 1973; *Abbott 1985
	***Chimarrhioxylon maxwellii* Δ**										X			Chang 1973; *Abbott 1985
	***Cissus* sp.**								X					Baghai 1998
	***Crataveoxylon maxwellii* Δ**										X			Chang 1973; *Abbott 1985
	cf. *Cunonioxylon* sp.										X			Wheeler and Lehman 2009
	***Dialyantheroxylon maxwellii* Δ**										X			Chang 1973; *Abbott 1985
	Dicotyledoneae indet.											X		Maxwell et al. 1967
	Ericales indet.								X					Wheeler and Lehman 2009
	***Gassonoxylon araliosum* •**								X	X				Wheeler and Lehman 2000
	***Hasseltioxylon maxwellii* Δ**										X			Chang 1973; *Abbott 1985
	***Javelinoxylon multiporosum* •**									X				Wheeler et al. 1994
	Metcalfeoxylon kirtlandense								X					Lehman and Wheeler 2001; Lehman and Shiller 2020
	***Pachirioxylon maxwellii* Δ**										X			Chang 1973; *Abbott 1985
	***Pageoxylon cretaceum* •**								X					Wheeler and Lehman 2000
	***Paraphyllanthoxylon abbottii* •**										X			Wheeler 1991; Adams 2014
	cf. *Paraphyllanthoxylon anazasii*								X	X				Wheeler and Lehman 2000
	Platanoid wood type I (scrambling vine)								X					Wheeler and Lehman 2000
	Platanoid wood type II (scrambling vine)								X					Wheeler and Lehman 2000
	***Platanoxylon* sp.**										X			Chang 1973
	cf. *Platinus haydenii*										X			Wheeler 1991
	***Preplatanoxylon maxwellii* Δ**										X			*Abbott 1985
	***Pycnanthoxylon maxwellii* Δ**										X			Chang 1973; *Abbott 1985
	***Sabinoxylon wicki* •**									X				Wheeler and Lehman 2009
	***Sloaneoxylon maxwellii* Δ**										X			Chang 1973; *Abbott 1985
	***Vitexoxylon maxwellii* Δ**										X			Chang 1973; *Abbott 1985
FOSSIL LEAVES														
VARIOUS TAXA	***Ampelopis acerifolia***												X	*Lawson 1972
	Carbonized leaf impressions								X					Montogomery and Clark 2016
	Cheirolepidaceae								X					Baghai 1998
	Chloranthaceae								X					Baghai 1998
	Ficus* cf. *F. tennesseensis												X	*Lawson 1972

CLASSIFICATION	TAXON	FORMATIONS												REFERENCES
		GR	TC	DC	SE	DR	BO	PN	AG	JV	BP	HH	CN	
FOSSIL LEAVES (continued)														
	"Hamamelid-like"								X					Baghai 1998
	Laurus socialis												X	*Lawson 1972
	Monocotyledonae indet.									X				Lehman and Langston unpublished
VARIOUS TAXA	***Paracredneria* sp.**								X					Baghai 1998
	cf. *Persea*								X					Baghai 1998
	Platanacea								X					Baghai 1998
	Platanus raynoldsi												X	*Lawson 1972
	Podocarpaceae								X					Baghai 1998
	Rhizophoracea								X					Baghai 1998
	Taxodiaceae								X					Baghai 1998
	***Typha* sp.**												X	*Lawson 1972
	Dicot and fern leaf impressions in volcanic ash - multiple taxa under study								X					Wick in prep.
MISCELLANEOUS														
	Fossilized tree resin (amber)								X					Udden 1907; Maxwell et al. 1967
	Indeterminate fossil wood												X	Maxwell et al. 1967
PALYNOMORPHS														
SPORES, POLLEN, FUNGI, ETC.	***Alnipollenites trina***												X	*Lawson 1972
	Alnipollenites verus												X	*Lawson 1972
	Alsophiliidites kerquelensis												X	*Lawson 1972
	***Apiculatisporites* sp.**								X					Baghai 1996
	Appendicisporites prolematicus								X					Baghai 1996
	***Appendicisporites* sp.**								X					Baghai 1996
	Appendicisporites tricornitatus								X					Baghai 1996
	***Apteodinium* sp.**							X						Baghai 1996
	Arecipites microreticulatus								X					Baghai 1996
	***Arecipites* sp.**								X					Record 1988; Baghai 1996
	***Baltisphaeridium* sp.**							X	X					Baghai 1996
	Betulaceae indet.								X					Baghai 1996
	Betulaceoipollenites infrequens												X	*Lawson 1972
	Bombacacopites nacimientoensis												X	*Lawson 1972
	***Caligodinium* sp.**							X	X					Baghai 1996
	***Callialasporites* sp.**								X					Baghai 1996
	Camarozonsporites rudis								X					Baghai 1996
	***Camarozonsporites* sp.**							X	X					Baghai 1996
	***Canningia* sp.**								X					Baghai 1996
	***Cannosphaeropsis* sp.**								X					Baghai 1996
	Caryapollenites simplex								X					Baghai 1996
	***Caryapollenites* sp.**								X					Baghai 1996
	***Casaurinidites* sp.**								X					Baghai 1996
	***Ceratosporites* sp.**								X					Baghai 1996
	Cerodinium diebelii							X	X					Baghai 1996
	***Chatangiella* sp.**								X					Baghai 1996
	***Cicatricosisporites* sp.**								X					Baghai 1996
	Cicatricosporites dorogensis												X	*Lawson 1972
	***Cingulatisporites* sp.**								X					Baghai 1996
	Circulina parva							X	X					Baghai 1996
	Classopollis classoides								X					Baghai 1996
	Cleistosphaeridium polypes							X						Baghai 1996
	Complexipollis abditus								X					Baghai 1996
	***Complexipollis* sp.**								X					Baghai 1996
	Concavisporites* cf. *arugulatus								X					Baghai 1996
	***Cordosphaeridium* sp.**								X					Baghai 1996
	***Corsinipollenites* sp.**								X					Baghai 1996
	Cupuliferoipollenites pusillus								X					Baghai 1996
	***Cupuliferoipollenites* sp.**								X					Baghai 1996
	Cyathidites australis								X					Baghai 1996
	Cyathidites foveolatus								X					Baghai 1996
	Cyathidites minor								X					Baghai 1996
	***Cyathidites* sp.**								X					Baghai 1994; Baghai 1996
	Cycadopites carpentieri								X					Baghai 1996
	Cycadopites pollicularis												X	*Lawson 1972
	Cycadopites scabratus							X	X				X	*Lawson 1972; Baghai 1996
	***Cycadopites* sp.**							X	X					Baghai 1994; Baghai 1996
	***Cyclopsiella* sp.**							X	X					Baghai 1996
	Cyrilla minima												X	*Lawson 1972
	Cyrillaceaepollenites exactus								X					Baghai 1996
	Deflandrea cooksoniae								X					Baghai 1996
	Deflandrea obscura							X	X					Baghai 1996
	Deflandrea oebisfeldensis								X					Baghai 1996
	***Deflanrdea* sp.**							X	X					Baghai 1996
	Deltoidospora diaphana								X					Baghai 1996
	Deltoidospora mesozoica								X					Baghai 1996

CLASSIFICATION	TAXON	FORMATIONS												REFERENCES
		GR	TC	DC	SE	DR	BO	PN	AG	JV	BP	HH	CN	
PALYNOMORPHS (continued)														
SPORES, POLLEN, FUNGI, ETC.	***Deltoidospora minor***								X					Baghai 1996
	***Deltoidospora* sp.**								X					Baghai 1996
	cf. *Didymoporisporonites* sp.								X					Baghai 1996
	***Dinogymnium* sp.**							X	X					Baghai 1996
	Echinatisporites longechinus								X					Baghai 1996
	***Echinatisporites* sp.**							X	X					Baghai 1996
	Engelhardtia microfoveolate												X	*Lawson 1972
	Equisetosporites multicostatus								X					Baghai 1996
	Exesipollenites tumulus								X					Baghai 1996
	Faguspollenites granulatus												X	Lawson 1972
	cf. *Foveodiporites* sp.								X					Baghai 1996
	Gleicheniidites senonicus								X				X	*Lawson 1972; Baghai 1996
	Gleicheniidites senonicus								X					Baghai 1996
	***Gleicheniidites* sp.**								X					Baghai 1994, 1996
	Gnetaceapollenites eocenipites								X					Baghai 1996
	***Granulatisporites* sp.**								X					Baghai 1994, 1996
	***Gymnodinium* sp.**								X					Baghai 1996
	***Hymenozonotriletes* sp.**								X					Baghai 1996
	***Hyphites* sp.**								X					Baghai 1996
	***hypoxylonites* sp.**								X					Baghai 1996
	***Hystrichosphaera* sp.**								X					Baghai 1996
	***Hystrichosphaeridium* sp.**								X					Baghai 1996
	Hystrichosphaeridium tubiferum								X					Baghai 1996
	***Inapertisporites* sp.**							X	X					Baghai 1996
	Inaperturepollenites magnus								X					Baghai 1996
	***Inaperturepollenites* sp.**							X	X					Baghai 1994, 1996
	Inaperturopollenites dubius												X	*Lawson 1972
	Interpollis supplingensis								X					Baghai 1996
	Intertrilites scrobiculatus												X	*Lawson 1972
	***Intratrioporopollenites* sp.**								X					Baghai 1996
	Kuylisporites scutatus								X					Baghai 1996
	***Kuylisporites* sp.**								X					Baghai 1996
	Lacrimasporites levis												X	*Lawson 1972
	Laevigatosporites haardti												X	*Lawson 1972
	Laevigatosporites ovatus								X				X	*Lawson 1972; Baghai 1996
	Laevigatosporites percrassus												X	*Lawson 1972
	***Laevigatosporites* sp.**								X					Baghai 1996
	***Leiotriletes* sp.**								X					Baghai 1996
	***Leptodinium* sp.**								X					Baghai 1996
	Lilacidites dividuus								X					Baghai 1996
	Lilacidites leei								X					Baghai 1996
	***Lilacidites* sp.**							X	X					Baghai 1996
	Lilacidites variegatus								X					Baghai 1996
	Liliacidites* cf. *L. complexus							X	X					Baghai 1996
	***Liliacidites* sp.**												X	*Lawson 1972
	Lusatisporis indistincta								X					Baghai 1996
	***Lusatisporis* sp.**								X					Baghai 1996
	***Lycopodiumsporites* sp.**								X					Baghai 1996
	***Lygodiumsporites* sp.**								X					Baghai 1996
	Margocolporites cribellatus								X					Baghai 1996
	***Margocolporites* sp.**								X					Baghai 1996
	Matonisporites* cf. *M. phelbopteroides								X					Baghai 1996
	***Michrystridium* sp.**								X					Baghai 1996
	Microretiulatasporites* cf. *M. uniformis								X					Baghai 1996
	***Microretiulatasporites* sp.**								X					Baghai 1996
	***Microthyrites* sp.**								X					Baghai 1996
	Momipites* cf. *M. coryloides								X					Baghai 1996
	Momipites* cf. *M. tenuipolis								X					Baghai 1996
	Momipites* cf. *M. wyomingensis								X					Baghai 1996
	Momipites coryloides												X	*Lawson 1972
	***Momipites* sp.**							X	X					Baghai 1994, 1996
	Monocolpopollenites* cf. *M. magnus								X					Baghai 1996
	***Monocolpopollenites* sp.**								X					Baghai 1996
	Monoporisporites stoverii												X	*Lawson 1972
	Monosulcites* cf. *M. glottus								X					Baghai 1996
	Monosulcites perispinosis								X					Baghai 1996
	***Monosulcites* sp.**								X				X	*Lawson 1972; Baghai 1996
	***Multilinaenites* sp.**								X					Baghai 1996
	***Multiporopollenites* sp.**								X					Baghai 1996
	***Neoraistrickia* sp.**								X					Baghai 1996
	Nyssapollenites analepticus								X					Baghai 1996
	Nyssoidites larsoni												X	*Lawson 1972
	Osmundacidites* cf. *O. wellmanii								X					Baghai 1996
	***Osmundacidites* sp.**								X					Baghai 1996

CLASSIFICATION	TAXON	FORMATIONS												REFERENCES
		GR	TC	DC	SE	DR	BO	PN	AG	JV	BP	HH	CN	
PALYNOMORPHS (continued)														
SPORES, POLLEN, FUNGI, ETC.	***Osmundacidites wellmanii***								X					Baghai 1996
	Ovoidites ligneolus								X					Baghai 1996
	Palaeohystrichophora infusorioides								X					Baghai 1996
	***Palaeohystrichophora* sp.**								X					Baghai 1996
	***Paleostomocystis* sp.**								X					Baghai 1996
	Palmaepollenites tranquilis								X					Baghai 1996
	Palmaepollenites* cf. *P. tranquillis								X					Baghai 1996
	***Palmaepollenites* sp.**							X	X					Baghai 1996
	Parvisacctes radiatus								X					Baghai 1996
	***Parvisacctes* sp.**								X					Baghai 1996
	***Pediastrum* sp.**								X					Baghai 1996
	***Peregrinipollis* sp.**								X					Baghai 1996
	Phelodinium magnifica								X					Baghai 1996
	Pinus haploxylon												X	*Lawson 1972
	***Pinuspollenites* sp.**								X					Baghai 1996
	***Planctonites* sp.**								X					Baghai 1996
	Plicapollis retusus								X					Baghai 1996
	***Plicapollis* sp.**								X					Baghai 1994, 1996
	Plicatopollis* cf. *C. plicata								X					Baghai 1996
	***Pluricellaesporites* sp.**								X					Baghai 1996
	***Podocarpidites* sp.**								X					Baghai 1996
	***Polyadosporites* sp.**								X					Baghai 1996
	Polycingulatisporites reduncus								X					Baghai 1996
	***Portalites* sp.**								X					Baghai 1996
	Proteacidites marginus								X					Baghai 1996
	Proteacidites molis								X					Baghai 1996
	Proteacidites retusus								X					Baghai 1996
	***Proteacidites* sp.**								X					Baghai 1996
	Proteacidites thalmanni								X					Baghai 1996
	***Pseudolasopollis* sp.**								X					Baghai 1996
	Pseudolasopollis ventosa								X					Baghai 1996
	***Psilatricolporites* sp.**								X					Baghai 1996
	***Psilatriletes* sp.**								X					Baghai 1996
	Punctatosporites major								X					Baghai 1996
	***Punctatosporites* sp.**												X	*Lawson 1972
	Rectosulcites latus							X	X					Baghai 1996
	***Reticulatosporites* sp.**								X				X	*Lawson 1972; Baghai 1996
	Retipollenites* cf. *R. confusus								X					Baghai 1996
	***Retipollenites* sp.**							X	X					Baghai 1996
	Retitricolpites florentinus								X					Baghai 1996
	Retitriletes muricatus								X					Baghai 1996
	***Retitriletes* sp.**								X					Baghai 1996
	***Retricolpites* sp.**								X					Baghai 1996
	Rhiopites globosus												X	*Lawson 1972
	Rhoipites* cf. *R. cryptoporus								X					Baghai 1996
	***Rhoipites* sp.**								X					Baghai 1996
	Rugulatisporites quintus												X	*Lawson 1972
	Sabalpollenites* cf. *convexus								X					Baghai 1996
	***Scabritricolpites* sp.**								X					Baghai 1996
	Schizaeoisporites eocaenicus								X					Baghai 1996
	***Schizoporis* sp.**												X	*Lawson 1972
	Schizosporis parvus								X					Baghai 1996
	***Schizosporis* sp.**								X					Baghai 1996
	***Seductisporites* sp.**								X					Baghai 1996
	***Septohyphites* sp.**								X					Baghai 1996
	Sphagnumsporites antiquasporites								X					Baghai 1996
	***Sphagnumsporites* sp.**								X					Baghai 1996
	Spinidinium densispenatum							X	X					Baghai 1996
	Spinidinium microceratum							X						Baghai 1996
	***Spinidinium* sp.**							X	X					Baghai 1996
	***Staphlosporonites* sp.**								X					Baghai 1996
	Stereisporites* cf. *S. crassus								X					Baghai 1996
	Stereisporites psilatus												X	*Lawson 1972
	***Stereisporites* sp.**							X	X					Baghai 1996
	***Striadiporites* sp.**								X					Baghai 1996
	***Subtilisphaera* sp.**							X	X					Baghai 1996
	***Subtrudopollis* sp.**								X					Baghai 1996
	***Syncolporopollenites* sp.**								X					Baghai 1996
	Taurocusporites* cf. *T. segmentatus								X					Baghai 1996
	***Taurocusporites* sp.**								X					Baghai 1996
	Taxodiaceaepollenites hiatus							X	X				X	*Lawson 1972; Baghai 1996
	***Tetracellites* sp.**								X					Baghai 1996
	Tetracolporopollenites manifestus												X	*Lawson 1972
	***?Tetradites* sp.**								X					Record 1988

CLASSIFICATION	TAXON	FORMATIONS												REFERENCES
		GR	TC	DC	SE	DR	BO	PN	AG	JV	BP	HH	CN	
PALYNOMORPHS (continued)														
SPORES, POLLEN, FUNGI, ETC.	***?Tilia* sp.**								X					Record 1988
	Todisporites minor								X					Baghai 1996
	Triatriopollenites* cf. *T. pseudogranulatus								X					Baghai 1996
	Triatriopollenites* cf. *T. pseudovestibulum								X					Baghai 1996
	Triatripollenites rurensis								X					Baghai 1996
	***Triatripollenites* sp.**								X					Baghai 1996
	Tricolpites* cf. *T. reticulatus								X					Baghai 1996
	Tricolpites parvistriatus												X	*Lawson 1972
	***Tricolpites* sp.**								X				X	*Lawson 1972; Baghai 1996
	Tricolpopollenites levitas								X					Baghai 1996
	Tricolpopollenites microhenrici								X					Baghai 1996
	Tricolpopollenites micropunctatus								X					Baghai 1996
	***Tricolpopollenites* sp.**								X					Baghai 1996
	Tricolporites rhomboides								X					Baghai 1996
	***Tricolporites* sp.**								X					Record 1988; Baghai 1996
	Tricolporopollenites kruschii								X					Baghai 1996
	Tricolporopollenites* cf. *T. desultorius								X					Baghai 1996
	***Tricolporopollenites* sp.**								X					Baghai 1996
	Tricolporopollenites triangulus								X					Baghai 1996
	Triplanosporites pseudosinosus												X	*Lawson 1972
	Triplanosporites sinosus												X	*Lawson 1972
	Triporoletes novmexicanus								X					Baghai 1996
	Triporopollenites bituitus								X					Baghai 1996
	Triporopollenites coryloides							X	X					Baghai 1996
	Triporopollenites robustus								X					Baghai 1996
	Triporopollenites rugatus												X	*Lawson 1972
	***Triporopollenites* sp.**							X	X					Baghai 1996
	***Trithyrodinium* sp.**							X	X					Baghai 1996
	***Trivestibulopollenites* sp.**								X					Baghai 1996
	***Trudopollis* sp.**								X					Baghai 1996
	Ulmoideipites krempii								X					Baghai 1996
	***Undulatisporites* sp.**								X					Baghai 1996
	***Verrucatosporites* sp.**								X					Baghai 1996
	***Verrucingulatisporites* sp.**								X					Baghai 1996
	***Verrutriporites* sp.**								X					Baghai 1996
	Vitipites affluens								X					Baghai 1996
	***Vitipites* sp.**								X					Baghai 1994, 1996
	***Wilsonipites* sp.**							X	X					Baghai 1996
	Zlivisporis novamexicanum								X					Baghai 1996
	***Zlivisporis* sp.**								X					Baghai 1996
	***Zygnema* sp.**								X					Baghai 1996
	HOLOTYPE = •													
	UNPUBLISHED NEW TAXON = Δ													
	UNNAMED NEW TAXON = o													
		Glen Rose Limestone	**Telephone Canyon Formation**	**Del Carmine Formation**	**Santa Elena Limestone**	**Del Rio Clay**	**Boquillas Formation**	**Pen Formation**	**Aguja Formation**	**Javelina Formation**	**Black Peaks Formation (K/Pg undifferentiated)**	**Hannold Hill Formation**	**Canoe Formation**	
			Lower Cretaceous					**Upper Cretaceous**				**Cenozoic**		
		FORMATIONS												
MISCELLANEOUS	**Unidentified log fragments**	**Chisos Formation (Eocene)**												Maxwell et al. 1967

* Only those formations listed in this table have produced plant fossils in BIBE.
* As it relates to Lawson (1972), the "Tornillo Formation" section containing botanicals and palynomorphs is now recognized as the lower Canoe Formation (Turner et al. 2011; T. Lehman, pers. comm.).
* M.L. Abbot passed away prior to formal submission of her unpublished (1985) manuscript (now accessioned at BIBE). Oddly, Abbott's report contains a number of new taxa (14), all with the specific epithet *maxwellii*. It is not known if all were to be named in honor of Ross A. Maxwell or if the epithet was simply a placekeeper for different specific names to be added later. Additionally, a later review of Abbott's work was conducted by E. Wheeler and T. Lehman during the course of their research on fossil woods from the park. Their findings suggest that Abbott's specimens are, in fact, different morphotypes of the same wood taxon (*Paraphyllanthoxylon*) which casts doubt on the validity of the "holotypes" presented by Abbott. However, Wheeler recognized the contributions made by Abbot and named *Paraphylanthoxylon abbotti* in her honor (Wheeler 1991). A posthumous synthesis of Abbot's work (Abbot 1986) was presented by D. Rohr (Ed.).

cient forest fires. In others, insect (?termite) borings and frass have also been preserved (Rohr et al. 1986).

Fossil wood is widespread in BIBE and many specimens are situated near roads, trails or camping areas. From the public's perspective, they are also some of the most recognizable types of fossils in BIBE and as a result, are often reported to park management by visitors. Because they are somewhat obvious and popular, "petrified" woods also

remain one of the most easily vandalized fossil types in many NPS fossil-parks which has led to the loss of valuable scientific information (Wick and Corrick 2015).

Invertebrate fossils (Table 2)

Over 500 fossil invertebrate taxa have been reported from BIBE including sponges, corals, bivalves, gastropods, ammonites, nautiloids and crustaceans, as well as a host of foraminifera. Invertebrates have been observed in many formations within BIBE from marine, brackish and freshwater facies. Five, scientifically valid type specimens have been described from BIBE and several 'new' taxa have yet to be formally reported.

Invertebrate fossils are regularly discovered in marine and brackish water facies within BIBE. Because of their abundance, form, and common occurrence along the modern shores of North America, invertebrate fossils are very popular as they are easily recognizable to park visitors of all ages. Fresh water taxa are much less common than their saltwater counterparts however they are occasionally discovered in lacustrine and fluvial deposits within some continental strata in the park. Many invertebrate fossils are preserved as steinkerns which represent the fossilized fill of a hollow organic structure (such as a mollusk shell) that formed when mud or sediment consolidated within the structure and the structure itself disintegrated or dissolved. Many invertebrate fossils are found in Lower Cretaceous, marine carbonate rocks along the fault-scarps which flank the northeastern and southwestern margins of the park. Upper Cretaceous forms are commonly preserved along with the remains of vertebrate taxa (such as sharks and mosasaurs) in near-shore marine mudstones and marls of the Boquillas and Pen formations surrounding the Chisos Mountains and exposed just west of the park. Some invertebrates from BIBE are particularly useful as stratigraphic index fossils. These include the ammonite *Allocrioceras hazzardi* (Young) and the bivalve *Inoceramus undulatoplicatus* (Roemer) both from the shallow marine, Boquillas Formation (e.g., Maxwell et al. 1967).

The preservation of invertebrate fossils varies by formation and facies. Lower Cretaceous, marine carbonate rocks often preserve invertebrate fossils such as bivalves and gastropods, but these are often entombed in dense carbonate matrix and are very difficult to extract without damage. Microinvertebrates are also difficult to separate from these rocks and require laboratory preparation (thin section samples) to study the fossils within. Upper Cretaceous strata have produced well preserved, intact invertebrate specimens (e.g., ammonites and bivalves) which occur as steinkerns in carbonate facies or within concretionary horizons. Some are difficult to remove from bedrock while others can be quarried easily. Other bottom-dwelling invertebrates often occur in marine mudstones and shales as isolated individuals or in loose, congregated groups such as the oyster *Flemingostrea pratti* (Stephenson) and sea urchin *Hemisaster* (Desor). Occurrences of this type are often observed in horizons within marine or brackish water facies which may contain dozens of individuals which inhabited muddy estuarial bottoms. Some fossils, such as the oyster *Crassostrea cusetta* (Sohl and Kauffman) are often found in dense groups (formerly bioherms). Many individuals exhibit obvious warping of their shells as the result of a congested colonial lifeway. Trace fossils (e.g., burrow structures) are also routinely observed in various marine strata.

Vertebrate fossils (Table 3)

Over 250 vertebrate fossil taxa have been reported from strata within BIBE with 30 type specimens (holotypes) having been so far described. Numerous other specimens have been identified as pertaining to unique species but have not yet been formally described or named. The fossil taxa recovered from BIBE involve a variety of animals from marine, brackish, and freshwater habitats as well as many others from inland terrestrial environs. Although the park has good exposures of marine strata representing open marine environs, marine vertebrates are not well represented in the park. For example, marine rocks of the Boquillas Formation have been more productive just outside of BIBE where this formation is better exposed and more accessible; local private collectors have discovered some outstanding vertebrate specimens from these strata (e.g., Bell et al. 2013). Correspondingly well-preserved specimens pertaining to these same marine species are likely present within the park as well but have yet to be found.

Vertebrate fossils are more numerous (but still uncommon) throughout the Late Cretaceous, paralic and terrestrial strata within the park with some Late Cretaceous formations being more productive than others. However, sharks, fish, amphibians, reptiles, and mammals are well-represented in the BIBE fossil record. Most of these fossils are commonly observed as isolated fragmentary bones, many of which show some degree of damage or reworking as the result of pre-burial transport. Furthermore, those formations that more frequently produce vertebrates (e.g., the Aguja and Javelina Formations) are apparently devoid of them in many stratigraphic exposures and horizons while other outcrops are locally productive. In uncommon cases, numerous bones pertaining to a single individual have been found in close association or (more rarely) in articulation (e.g., Lehman and Wick 2010; Tykoski and Fiorillo 2016). However, complete skeletons are unheard of in BIBE. This circumstance has vexed many of us who have spent decades searching for good specimens in the park. However, it is very likely that deposition rates did not favor the rapid burial of carcasses here.

Although complete fossilized bones are infrequently encountered in Late Cretaceous strata, conspicuous vertebrate fossils are less common in Tertiary strata of BIBE. Although some larger, associated specimens have been discovered (e.g., Wilson 1967) most Tertiary fossil taxa have been diagnosed from small bone fragments or

Table 2. Invertebrate fossils.

CLASS	TAXON	FORMATIONS												REFERENCES
		GR	TC	DC	SP	SE	DR	BU	BO	PN	AG	JV	BP	
PROTOZOA														
single-celled org.	***Spironema* sp.**										X			Udden 1907
FORAMINIFERA														
	Ammobaculites cuyleri						X							Mauldin 1985
	Ammobaculites dentonensis						X							Mauldin 1985
	Ammobaculites fragmentarium								X					Bostik 1960
	Ammobaculites subcretacea						X		X					Huffman 1960; Mauldin 1985
	Anomalina plummerae						X							Mauldin 1985
	Archaeoglobigerina blowi								X	X				Graham 1995; Ashmore 2003
	Archaeoglobigerina bosquensis								X	X				Graham 1995; Ashmore 2003
	Archaeoglobigerina cretacea								X	X				Graham 1995
	Bolivina textularoides						X							Mauldin 1985
	Bolivinita planata								X					Bostik 1960
	Bolivinitella eleyi								X					Bostik 1960
	Brachycythere sphenoides								X					Bostik 1960
	Bulimina nannina						X							Mauldin 1985
	Buliminella carseyae								X					Bostik 1960
	Buliminella cushman								X					Bostik 1960
	***Charentia* sp.**				X									Tarasconi 2000
	Chrysalogonium* cf. *C. texanum								X					Bostik 1960
	Citharina complanata						X							Mauldin 1985
	Coskinolinoides texanus	X	X	X										Tarasconi 2000
	Costallagerina thompsoni								X	X				Graham 1995
	Costellagerina bulbosa								X	X				Graham 1995
	Costellagerina phlegeri								X	X				Graham 1995
	***Costellagerina smithi* •**									X				Graham 1995
	Cribratina texana						X							Tarasconi 2000
	Cuneolina* cf. *pavonia	X	X	X	X	X	X							Tarasconi 2000
	Cythereis bicornis								X					Bostik 1960
	Cythereis* cf. *C. austinensis								X					Bostik 1960
	Cythereis dallasensis								X					Bostik 1960
	Cytherella austinensis								X					Bostik 1960
PLANKTONIC CREATURES	***Dentalina communis***						X							Mauldin 1985
	Dentalina crypta						X							Mauldin 1985
	Dentalina debilis						X							Mauldin 1985
	Dentalina gracilis								X					Bostik 1960
	Dentalina intrasegma								X					Bostik 1960
	Dentalinopsis excavata						X							Mauldin 1985
	Dentalinopsis tricarinatum						X							Mauldin 1985
	Dentelina soluta						X							Mauldin 1985
	Dentilina hammensis						X							Mauldin 1985
	Dicarinella algeriana							X						Tiedemann 2010
	Dicarinella asymetrica								X	X				Graham 1995
	Dicarinella concavata								X	X				Graham 1995; Ashmore 2003
	***Dicarinella daileyi* •**									X				Graham 1995
	Dicarinella difformis								X	X				Graham 1995
	Dicarinella indica								X	X				Graham 1995
	Dictyoconus walnutensis	X	X	X										Tarasconi 2000
	Discorbis minima						X							Mauldin 1985
	Discorbis minutissima						X							Mauldin 1985
	Dorothia* cf. *D. alexanderi								X					Bostik 1960
	Dorothia* cf. *D. bulletta								X					Bostik 1960
	Dorothia stephensoni								X	X				Bostik 1960; Ashmore 2003
	Ellipsoidella gracillima								X					Bostik 1960
	Eouvigerina plummerae								X					Bostik 1960
	Favusella washitensis	X	X		X	X		X						Tarasconi 2000; Tiedemann 2010
	Flabellammina clava								X					Bostik 1960
	Frondicularia cordata								X					Bostik 1960
	Gaudryina austinana								X	X				Bostik 1960; Ashmore 2003
	Gaudryina rudita								X	X				Bostik 1960; Ashmore 2003
	Globigerina cretacea								X					Huffman 1960
	Globigerina rugosa								X					Huffman 1960; Bostik 1960
	Globigerina saratogaensis								X					Bostik 1960
	***Globigerina* sp.**									X				Udden 1907
	Globigerina voluta								X					Huffman 1960
	***Globigerinella aissan*a**								X	X				Bostik 1960; Ashmore 2003
	Globigerinelloides asperus								X	X				Graham 1995
	Globigerinelloides bentonensis							X						Tiedemann 2010
	Globigerellinoides caseyi							X						Tiedemann 2010

CLASS	TAXON	FORMATIONS												REFERENCES
		GR	TC	DC	SP	SE	DR	BU	BO	PN	AG	JV	BP	
FORAMINIFERA (continued)														
	Globigerinelloides multispina									X				Graham 1995
	Globiginerelloides prairiehillensis									X				Graham 1995
	Globoratalites umbilicatus								X					Bostik 1960
	Globorotalia arca								X					Huffman 1960
	Globorotalia cushmani								X					Bostik 1960
	Globorotalia membranacea								X					Huffman 1960
	***Globorotalia* sp.**						X							Mauldin 1985
	Globotruncana arca								X					Bostik 1960
	Globotruncana bulloides									X				Graham 1995
	Globotruncana canaliculata								X					Bostik 1960
	Globotruncana contusa								X					Bostik 1960
	Globotruncana cretacea								X					Huffman 1960
	Globotruncana fornicata								X	X				Bostik 1960; Graham 1995
	Globotruncana lapparenti									X				Graham 1995
	Globotruncana marginata								X					Huffman 1960; Bostik 1960
	Globotruncana membanacea								X					Huffman 1960
	Globulina exerta						X							Mauldin 1985
	Globulina lacrima								X					Bostik 1960
	Guembelitria graysonensis						X							Mauldin 1985
	Guembelitria harrisi						X							Mauldin 1985
	Gumbelina globocarinata								X					Bostik 1960
	Gumbelina moremani								X					Huffman 1960; Bostik 1960
	Gumbelina nuttalli								X					Huffman 1960
	Gumbelina plummerae								X					Bostik 1960
	Gumbelina pseudotessera								X					Huffman 1960; Bostik 1960
	Gumbelina reussi								X					Huffman 1960; Bostik 1960
	Gumbelina striata								X					Bostik 1960
	Gyroidina depressa								X	X				Bostik 1960; Ashmore 2003
	Gyroidina girardana								X					Bostik 1960
	Gyroidina globosa								X	X				Bostik 1960; Ashmore 2003
	Haplofragmoides concava						X							Mauldin 1985
	Haplostiche texana						X							Maxwell et al. 1967
PLANKTONIC CREATURES	***Hastigerinella alexanderi***								X					Bostik 1960
	Hastigerinella moremani								X					Bostik 1960; Huffman 1960
	Hastigerinella simplex								X					Huffman 1960
	Hastigerinella watersi								X					Bostik 1960
	Hastingerinoides alexanderi								X	X				Graham 1995
	Hastingerinoides watersi								X	X				Graham 1995
	Hedbergella delrioensis							X						Tiedemann 2010
	Hedbergella planispira						X	X						Mauldin 1985; Tiedemann 2010
	Hedbergella simplex							X						Tiedemann 2010
	***Hedbergella* sp.**	X	X		X	X		X						Tarasconi 2000; Tiedemann 2010
	Heterohelix* cf. *moremani	X			X	X		X						Tarasconi 2000
	Heterohelix globulosa								X	X				Graham 1995; Fry 2015
	Heterohelix moremani						X		X					Mauldin 1985; Fry 2015
	Heterohelix pulchra									X				Graham 1995
	Heterohelix reussi								X	X				Ashmore 2003; Graham 1995
	Heterohelix semicostata									X				Graham 1995
	Heterohelix striata									X				Graham 1995
	Kyphopyxa christneri								X	X				Bostik 1960; Ashmore 2003
	Lagena apiculata						X							Mauldin 1985
	Lagena hispida						X							Mauldin 1985
	Lagena striatifera						X							Mauldin 1985
	Lagena sulcata						X							Mauldin 1985
	Lenticulina gaultina						X							Mauldin 1985
	Lenticulina rotulata								X	X				Bostik 1960; Ashmore 2003
	***Lenticulina* sp.**	X			X	X		X						Tarasconi 2000
	Lingulina lamellata						X							Mauldin 1985
	Lingulina nodosaria						X							Mauldin 1985
	***Lingulina* sp.**								X					Huffman 1960
	Loxostumum cushmani								X					Bostik 1960
	Marginotruncana angusticarenata								X	X				Graham 1995
	***Marginotruncana bigbendensi*s**									X				Graham 1995
	***Marginotruncana coronat*a**								X	X				Graham 1995; Ashmore 2003
	***Marginotruncana marginat*a**								X	X				Graham 1995; Ashmore 2003
	***Marginotruncana pseudolinneian*a**								X	X				Graham 1995
	Marginotruncana renzi								X	X				Graham 1995
	Marginotruncana undulata								X	X				Graham 1995
	Marginulina austinana								X	X				Bostik 1960; Ashmore 2003
	Marginulina directa								X					Bostik 1960
	Marssonella oxycona								X	X				Bostik 1960; Ashmore 2003

CLASS	TAXON	FORMATIONS												REFERENCES
		GR	TC	DC	SP	SE	DR	BU	BO	PN	AG	JV	BP	
FORAMINIFERA (continued)														
	Neobulimina canadensis								X					Huffman 1960; Bostik 1960
	Neobulimina irregularis								X					Huffman 1960; Bostik 1960
	Neobulimina minima						X							Mauldin 1985
	Neoflabellina cushmani								X	X				Bostik 1960; Ashmore 2003
	Neoflabellina hebronensis								X					Bostik 1960
	Neoflabellina suturalis								X					Bostik 1960
	Nezzezata conica					X								Tarasconi 2000
	Nezzezata simplex					X								Tarasconi 2000
	Nodosaria affinis								X	X				Bostik 1960; Ashmore 2003
	Nodosaria barkeri						X							Mauldin 1985
	Nodosaria brandi						X							Mauldin 1985
	Nodosaria distans								X					Bostik 1960
	Nodosaria obscura						X							Mauldin 1985
	Nodosaria scotti						X							Mauldin 1985
	***Nodosaria* sp.**								X					Bostik 1960
	Nodosaria tappanae						X							Mauldin 1985
	***Opthalmidium* sp.**	X		X		X								Tarasconi 2000
	Orbitolina texana	X												Maxwell et al. 1967
	Ovalviolina* cf. *maccognoae					X								Tarasconi 2000
	Palmula pilulata								X	X				Bostik 1960; Ashmore 2003
	Paracypris angusta								X					Bostik 1960
	Parathalmanniella appeninnica							X						Tiedemann 2010
	Patellina subcretacea						X							Mauldin 1985
	***Peneroplis* sp.**			X										Tarasconi 2000
	***Planomalina* sp.**					X								Tarasconi 2000; Tiedemann 2010
	Planularia* cf. *P. dissona								X					Bostik 1960
	Planulina arimensis								X					Bostik 1960
	Planulina austinana								X	X				Bostik 1960; Ashmore 2003
	Planulina eaglefordensis								X					Huffman 1960; Bostik 1960
	Planulina kansasensis								X					Bostik 1960
	Pleurostomella austiniana								X					Bostik 1960
	Pleurostomella watersi								X					Bostik 1960
PLANKTONIC CREATURES	***Praeglobotruncana delrioensis***							X						Tiedemann 2010
	Praeglobotruncana stephani							X						Tiedemann 2010
	***Praeglobotruncana* sp.**							X						Tiedemann 2010
	Pseudofrondicularia undulosa								X	X				Bostik 1960; Ashmore 2003
	Pseudoguembelina pessagnoi •									X				Graham 1995
	Pseudoguembelina halesi •								X	X				Graham 1995
	Pseudotextularia elongata								X	X				Graham 1995
	Pterygocythere* cf. *P. saratogana								X					Bostik 1960
	Pyrulina cylindroides						X							Mauldin 1985
	Quinqueloculina aeschria						X							Mauldin 1985
	Rectogumbelina texana								X					Bostik 1960
	Reophax difflugiformis						X							Mauldin 1985
	***Reophax* sp.**					X								Tarasconi 2000
	Robulus munsteri								X					Huffman 1960; Bostik 1960
	Robulus taylorensis								X					Bostik 1960
	Rosita fornicata									X				Ashmore 2003
	Rotilapora montsavensis							X						Tiedemann 2010
	***Rotalipora* sp.**					X			X					Bell 1995; Tarasconi 2000
	Saracenaria triangularis								X					Bostik 1960
	Schackoina multispinata								X	X				Graham 1995
	***Scherochorella* sp.**				X									Tarasconi 2000
	Sculptobaculites goodlandensis	X	X	X	X									Tarasconi 2000
	***Shakoina* sp.**							X						Tiedemann 2010
	***Siderolites* sp.**								X					Bostik 1960
	Sigalia alpina									X				Graham 1995
	Sigalia deflaensis									X				Graham 1995
	Spirillina minima						X							Mauldin 1985
	Spiroplectammina laevis								X					Bostik 1960
	Spiroplectammina lalickeri								X					Bostik 1960
	Spiroplectammina longa						X							Mauldin 1985
	Spiroplectammina nuda						X							Mauldin 1985
	Textularia rioensis						X							Mauldin 1985
	***Textularia* sp.**									X				Udden 1907
	Thalmaninnella brotzeni							X						Tiedemann 2010
	***Thomasinella* sp.**						X							Tarasconi 2000
	***Ticinella* sp.**				X									Tarasconi 2000
	Valvulinaria loetterei						X							Mauldin 1985
	Ventilabrella austiniana								X	X				Bostik 1960; Graham 1995
	Ventilabrella* cf. *V. browni									X				Graham 1995

CLASS	TAXON	FORMATIONS												REFERENCES
		GR	TC	DC	SP	SE	DR	BU	BO	PN	AG	JV	BP	
FORAMINIFERA (continued)														
PLANKTONIC CREATURES	***Ventilabrella glabrata***									X				Graham 1995
	Virgulina tegulata								X					Huffman 1960; Bostik 1960
	Vitriwebbina biosculata								X					Bostik 1960
	Washitella typica						X							Mauldin 1985
	Whiteinella aprica								X	X				Graham 1995
	Whiteinella archaeocretacea								X	X				Graham 1995
SPONGIAE														
sponges	***Cliona* sp.**								X	X	X			Lehman 1985; Cooper et al. 2017
	***Myliusia* sp.**								X					Cooper et al. 2017
ARTICULATA														
brachiopods	***Kingena wacoensis***							X						Eley 1938
	Terabratulina brewsterensis								X	X				Eley 1938; Lehman 1985
	***Terabratulina* sp.**								X					Eley 1938
STENOLAEMATA														
bryozoans	**Cyclostomata indet.**						X							Tarasconi 2000
POLYCHAETA														
annelid worms	***Hamulus onyx***									X				Eley 1938; Lehman 1985
	Serpula* cf. *S. adnata										X			Lehman 1985
	Serpula cretacea									X	X			Eley 1938; Lehman 1985
ANTHOZOA														
stoney corals	**Faviidae indet.**								X					Eley 1938
ECHINOIDEA														
SEA URCHINS	**Echinoidia indet.**				X									Tarasconi 2000
	Enallaster calvini						X	X						Maxwell et al. 1967
	Enallaster inflatus						X							Eley 1938
	Enallaster mexicanus				X									Maxwell et al. 1967
	***Enallaster* sp.**		X											Maxwell et al. 1967
	Enallaster texana				X									Maxwell et al. 1967
	Hemiaster calvini						X							Eley 1938
	***Hemiaster* sp.**								X					Maxwell et al. 1967
	Hemiaster texanus									X				Lehman 1985
	Hemiasteridae indet.				X									Tarasconi 2000
	***Heteraster* sp.**				X			X						Tarasconi 2000; Maxwell et al. 1967
	Heteraster texana						X							Eley 1938
	Heterohelix globulosa								X					Fry 2015
	Heterohelix moremani													Fry 2015
	***Heterohelyx* sp.**							X						Tarasconi 2000
	Holectypus limitus						X							Eley 1938
	***Holectypus* sp.**		X											Maxwell et al. 1967
	Leiotomaster bosei								X					Eley 1938
	***Macraster* sp.**								X					Eley 1938
	***Phymosoma* sp.**		X											Maxwell et al. 1967
	***Pseudodiadema* sp.**								X					Eley 1938
CRINOIDA	***Saccocoma* sp.**							X						Tarasconi 2000
BIVALVIA														
CLAMS, OYSTERS, MUSSELS	***Amphidonte* sp.**	X					X							Tarasconi 2000
	Anomia* cf. *A. mexicana										X			Lehman 1985
	Anomia* cf. *A. argentaria										X			Eley 1938
	Anomia* cf. *A. tellinoides										X			Eley 1938
	***Aphrodina* sp.**										X			Eley 1938
	Aphrodina tippana									X	X			Eley 1938; Lehman 1985
	Arcidae indet.				X									Tarasconi 2000
	***Arcopagella* sp.**										X			Eley 1938
	Astartidae indet.				X									Tarasconi 2000
	Bivalvia indet.					X								Maxwell et al. 1967
	***Brachiodontes* sp.**										X			Lehman 1985
	Brachymeris alta										X			Eley 1938
	***Callista* sp.**										X			Eley 1938
	Camptonectes burlingtonensis										X			Udden 1907
	***Camptonectes* sp.**										X			Lehman 1985
	Caprinidae indet.					X								Tarasconi 2000
	Cardium carolinensis										X			?Udden 1907; Eley 1938
	Cardium congestum										X			Udden 1907
	Cardium longstreeti									X	X			Eley 1938
	***Cardium* sp.**		X	X	X						X			Eley 1938; Maxwell et al. 1967
	Cardium subcongesta				X									Maxwell et al. 1967
	Cardium vaughni										X			Eley 1938
	Chondrodontidae indet.					X								Tarasconi 2000
	Cladoceramus undulotplicatus								X					Stevens et al. 1995; Ashmore 2003; Cooper et al. 2017
	Cladoceramus undulatoplicatus michaeli								X					Cooper et al. 2017

CLASS	TAXON	FORMATIONS												REFERENCES
		GR	TC	DC	SP	SE	DR	BU	BO	PN	AG	JV	BP	
BIVALVIA (Continued)														
CLAMS, OYSTERS, MUSSELS	***Corbicula cytheriformis***										X			Udden 1907
	***Corbicula* sp.**										X			Udden 1907
	***Corbula* sp.**									X				Lehman 1985
	***Cordiceramus* sp.**									X				Ashmore 2003
	Crassatella* cf. *C. vadosa										X			Lehman 1985
	Crassatella* cf. *C. obliquata										X			Udden 1907
	Crassostrea cusseta										X			Lehman 1985
	Crassostrea trigonalis										X			Lehman 1985
	Cremnoceramus crassus crassus								X					Cooper et al. 2017
	Cremnoceramus deformis erectus								X					Cooper et al. 2017
	Cremnoceramus walterdorfensis								X					Cooper et al. 2017
	Cyclorisma carolinensis									X				Eley 1938
	***Cyclorisma* sp.**								X					Eley 1938
	Cymbophora berryi									X	X			Lehman 1985
	Cymbophora scabellum										X			Lehman 1985
	***Cymbophora* sp.**										X			Eley 1938
	Cymbophora trigonalis										X			Eley 1938
	Cymella bella										X			Lehman 1985
	Cyprimera depressa									X				Eley 1938; Lehman 1985
	Cyprimeria gabbi									X	X			Eley 1938; Maxwell et al. 1967
	Cyprimeria roddai									X				Lehman 1985
	***Cyprimeria* sp.**		X							X				Maxwell et al. 1967
	Cyprimeria texana				X									Maxwell et al. 1967
	***Cyprina* sp.**										X			Udden 1907
	Dianchora* cf. *austinensis								X					Eley 1938
	Didymotis costatus								X					Cooper et al. 2017
	Dreissena tippana										X			Eley 1938
	Durania austinensis								X					Eley 1938; Maxwell et al. 1967; Cooper et al. 2017
	***Durania* sp.**								X					Maxwell et al. 1967
	Durania terlinguae								X	X	X			Eley 1938; Maxwell et al. 1967
	Eoradiolites* cf. *E. davidsoni			X										Maxwell et al. 1967
	Eoradiolites* cf. *E. quadratus					X								Maxwell et al. 1967
	***Etea* sp.**									X				Lehman 1985
	Ethmocardium* cf. *E. welleri										X			Lehman 1985
	Exogyra arietina						X							Eley 1938; Maxwell et al. 1967
	Exogyra cancellata									X				Eley 1938
	Exogyra cartledgei						X							Eley 1938; Maxwell et al. 1967
	Exogyra clarki							X						Maxwell et al. 1967
	Exogyra costata									X				Eley 1938
	Exogyra costata spinosa									X				Eley 1938
	Exogyra laeviuscula									X				Lehman 1985
	Exogyra ponderosa ponderosa									X	X			Lehman 1985
	Exogyra ponderosa whitneyi									X				Eley 1938
	Exogyra ponderosa erraticostata									X				Lehman 1985
	Exogyra ponderosa upatoiensis									X				Lehman 1985
	Exogyra quitmanensis	X												Maxwell et al. 1967
	***Exogyra* sp.**									X				Maxwell et al. 1967
	Exogyra texana	X	X	X	X									Maxwell et al. 1967
	Exogyra whitneyi						X							Eley 1938; Maxwell et al. 1967
	Flemingostrea pratti										X			Lehman 1985
	Flemingostrea subspatulata										X			Lehman 1985
	***Flemingostrea subspatulata* n. subsp. +**										X			Lehman 1985
	***Gastrochaena* sp.**										X			Lehman 1985
	***Granocardium* sp.**										X			Lehman 1985
	Gryphaea* cf. *G. navia				X									Maxwell et al. 1967
	Gryphaea corrugata							X						Eley 1938
	Gryphaea graysonana						X	X						Maxwell et al. 1967
	Gryphaea mucronata		X				X	X						Eley 1938; Maxwell et al. 1967
	***Gryphaea* sp.**		X	X	X	X		X						Maxwell et al. 1967
	Haploscapha grandis								X					Maxwell et al. 1967
	***Homomya* sp.**				X									Maxwell et al. 1967
	Homomya washita							X						Eley 1938
	Ilmatogyra africana						X							Tarasconi 2000
	Inoceramus anomalus								X					Cooper et al. 2017
	Inoceramus annulatus								X					Udden 1907; Eley 1938
	Inoceramus arvanus								X					Cooper et al. 2017
	Inoceramus barabini									X				Lehman 1985
	Inoceramus biconstrictus										X			Eley 1938
	Inoceramus* cf. *I. concentricus								X					Eley 1938
	Inoceramus* cf. *I. subquadratus								X					Maxwell et al. 1967
	Inoceramus cumminsi										X			Lehman 1985; Eley 1938

CLASS	TAXON	FORMATIONS												REFERENCES
		GR	TC	DC	SP	SE	DR	BU	BO	PN	AG	JV	BP	
BIVALVIA (Continued)														
CLAMS, OYSTERS, MUSSELS	***Inoceramus dakotensis***								X					Cooper et al. 2017
	Inoceramus digitatus								X					Eley 1939
	Inoceramus exogyroides								X					Udden 1907
	Inoceramus ginterensis								X					Cooper et al. 2017
	Inoceramus* (*Haploscapha*) *grandis								X					Udden 1907; Eley 1938
	Inoceramus howelli								X					Cooper et al. 2017
	Inoceramus labiatus							X	X					Eley 1938; Maxwell et al. 1967
	Inoceramus oblongus									X				Lehman 1985
	Inoceramus perplexus								X					Cooper et al. 2017
	Inoceramus pertenuis										X			Eley 1938
	Inoceramus pictus								X					Cooper et al. 2017
	Inoceramus platinus									X				Lehman 1985
	Inoceramus prefragilis								X					Cooper et al. 2017
	Inoceramus problematicus								X		X			Eley 1938
	Inoceramus rutherfordi								X					Cooper et al. 2017
	***Inoceramus* sp.**								X	X	X			Udden 1907; Eley 1938; Maxwell et al. 1967
	Inoceramus umbonatus								X					Udden 1907
	Inoceramus undabundus								X					Cooper et al. 2017
	Inoceramus undulatoplicatus								X					Eley 1938; Maxwell et al. 1967; Bell et al. 2013
	***Inoperna* sp.**	X												Maxwell et al. 1967
	Isocardia medialis							X						Eley 1938
	***Leda* sp.**										X			Udden 1907
	Leptosolen* cf. *L. quadrilaterus										X			Lehman 1985
	Lima reticulata										X			Eley 1938; Lehman 1985
	Lima coahuilensis										X			Lehman 1985
	Lima shumardi							X						Eley 1938
	***Lima* sp.**										X			Udden 1907
	Lima wacoensis						X	X						Eley 1938; Maxwell et al. 1967
	***Linearea* sp.**									X	X			Lehman 1985
	Lingula* cf. *L. rauliniana										X			Udden 1907
	Lingula subspatulata										X			Eley 1938
	Liopistha bella										X			Eley 1938
	***Lopha* sp.**									X				Lehman 1985
	Lophia subovata				X									Maxwell et al. 1967
	Lucina linearia									X				Lehman 1985
	***Lucina* sp.**									X				Lehman 1985
	Lucinidae indet.				X									Tarasconi 2000
	***Lucinoma* sp.**									X				Lehman 1985
	Lycettia tippanus										X			Lehman 1985
	Mactra texana										X			Udden 1907
	Magadiceramus complicatus								X					Cooper et al. 2017
	Magadiceramus crenelatus								X					Cooper et al. 2017
	Magadiceramus subquadratus								X					Ashmore 2003
	Monopleuridae indet.					X								Tarasconi 2000
	Mytiloides goppelnensis								X					Cooper et al. 2017
	Mytiloides herbichi								X					Cooper et al. 2017
	Mytiloides mytiloidiformis								X					Cooper et al. 2017
	Mytiloides puebloensis								X					Cooper et al. 2017
	Mytiloides ratonensis								X					Cooper et al. 2017
	Mytiloides scupini								X					Cooper et al. 2017
	Mytiloides striatoconcentricus								X					Cooper et al. 2017
	***Mytilus* sp.**								X					Udden 1907; Eley 1938
	Neithia irregularis		X											Maxwell et al. 1967
	***Neithia* sp.**				X									Maxwell et al. 1967
	Nemodon eufaulensis										X			Lehman 1985
	Nicaisolopha lugubris								X					Cooper et al. 2017
	***Nucula* sp.**									X	X			Eley 1938; Lehman 1985
	Nuculidae indet.				X									Tarasconi 2000
	Ostrea beloiti								X					Cooper et al. 2017
	Ostrea congesta								X	X				Eley 1938; Maxwell et al. 1967
	Ostrea contracta										X			Udden 1907
	Ostrea cretacea										X			Eley 1938
	Ostrea elegantula										X			Udden 1907
	Ostrea falcata									X				Eley 1938
	Ostrea glabra										X			Udden 1907; Eley 1938
	Ostrea Johnsoni										X			Eley 1938
	Ostrea larva nasuta									X				Eley 1938
	Ostrea plumosa								X		X			Eley 1938
	Ostrea pratti									X	X			Eley 1938
	Ostrea satellites								X					Eley 1938
	Ostrea* cf. *O. veleniana										X			Udden 1907

CLASS	TAXON	FORMATIONS												REFERENCES
		GR	TC	DC	SP	SE	DR	BU	BO	PN	AG	JV	BP	
BIVALVIA (Continued)														
CLAMS, OYSTERS, MUSSELS	***Ostrea subspatulata***									X	X			Eley 1938
	Ostrea tecticostata										X			Udden 1907
	***Paranomia* sp.**								X					Eley 1938
	Pecinidae indet.				X		X							Tarasconi 2000
	Pecten cliffwoodensis										X			Eley 1938
	Pecten roemeri							X						Eley 1938; Maxwell et al. 1967
	Pecten subalpinus						X							Eley 1938
	Pecten texanus							X						Eley 1938
	***Pedalion* sp.**									X				Eley 1938
	Pholadomya* cf. *P. coahuilensis										X			Lehman 1985
	Pholadomya sanctisabae			X	X									Maxwell et al. 1967
	***Pholadomya* sp.**		X											Maxwell et al. 1967
	Pholadomyidae indet.				X									Tarasconi 2000
	Platyceramus americanus								X					Cooper et al. 2017
	Platyceramus* cf. *mantelli								X					Cooper et al. 2017
	Platyceramus platinus								X					Stevens et al. 1995; Ashmore 2003
	***Platyceramus* sp.**								X					Cooper et al. 2017
	Pleuromyidae indet.				X									Tarasconi 2000
	Porocystis globularis	X												Maxwell et al. 1967
	Protocardia multistriata				X									Tarasconi 2000
	Protocardia texana			X	X									Maxwell et al. 1967; Tarasconi 2000
	***Protocardium* sp.**		X	X										Maxwell et al. 1967
	Pseudoperna congesta									X				Lehman 1985; Ashmore 2003
	***Pseudoperna* n. sp. +**										X			Lehman 1985
	***Pseudoperna* sp.**								X					Cooper et al. 2017
	***Pteria* sp.**										X			Eley 1938; Cooper et al. 2017
	Pycnodontae aucella									X				Lehman 1985
	***Pycnodontae* sp.**	X	X	X	X	X	X							Tarasconi 2000
	Radiolites austinensis									X				Udden 1907
	***Radiolites* sp.**			X										Maxwell et al. 1967
	Radiolitidae indet.					X				X				Udden 1907; Tarasconi 2000
	Sphenoceramus digitatus								X					Ashmore 2003
	***Sphenoceramus* sp.**									X				Ashmore 2003
	Spondylus* cf. *S. guadalupae									X				Lehman 1985
	***Spondylus* sp.**								X					Eley 1938; Cooper et al. 2017
	Striarca poguei									X				Eley 1938
	Tapes chihuahuaensis		X		X									Maxwell et al. 1967
	***Tapes* sp.**			X										Maxwell et al. 1967
	Tellenia elliptica										X			Eley 1938
	Tellenia simplex										X			Eley 1938
	***Tellina* sp.**									X	X			Lehman 1985
	Teredo irregularis										X			Eley 1938
	***Teredo* sp.**								X					Eley 1938
	***Teredolites* sp.**									X	X			Lehman 1985
	Thracia gracilis										X			Udden 1907
	***Thracia* sp.**										X			Udden 1907
	Trapezium truncatum									X				Eley 1938
	Trigonia bartrami									X				Eley 1938
	***Trigonia* sp.**		X		X			X		X				Maxwell et al. 1967
	***Unio* sp.**										X	X	X	Lehman 1985; Schiebout 1970
	***Venericardia* sp.**										X			Lehman 1985
	Veneridae indet.				X									Tarasconi 2000
	Veniella carolinensis									X				Eley 1938
	Veniella conradi									X				Udden 1907; Eley 1938; Lehman 1985
	Veniella mullinensis									X				Eley 1938; Lehman 1985
GASTROPODA														
SNAILS, WHELKS	***Amauropsis* sp.**		X											Maxwell et al. 1967
	Anchura kiowana										X			Eley 1938
	***Anchura* sp.**										X			Eley 1938
	Aporrhais* cf. *A. subfusiformis				X									Maxwell et al. 1967
	Aporrhais tarrantensis		X	X										Maxwell et al. 1967
	Buccinopsis greenensis										X			Lehman 1985
	Buccinopsis globosa										X			Lehman 1985
	Buccinopsis parryi										X			Udden 1907
	Campeloma vetulum										X			Lehman 1985
	***Cerithidea* indet.**								X					*Cooper et al. current research
	***Cerithium* sp.**									X				Lehman 1985
	certhiid gastropods								X					Cooper et al. 2017
	***Cithara* sp.**										X			Eley 1938
	Gastropoda indet. (fresh water)											X	X	*Coulson 1998; Schiebout 1970
	Gastropoda indet. (marine)	X		X	X	X								Maxwell et al. 1967; Tarasconi 2000;
	Goniobasis tenera											X		*Coulson 1998

CLASS	TAXON	FORMATIONS												REFERENCES
		GR	TC	DC	SP	SE	DR	BU	BO	PN	AG	JV	BP	
GASTROPODA (Continued)														
SNAILS, WHELKS	***Gyrodes americanus***										X			Lehman 1985
	***Gyrodes* sp.**		X		X						X			Udden 1907; Eley 1938; Maxwell et al. 1967
	Gyrodes supraplicatus									X	X			Eley 1938; Lehman 1985
	Liopeplum thoracium									X				Eley 1938
	***Longoconcha* sp.**										X			Lehman 1985
	Lunatia carolinensis										X			Eley 1938
	Lunatia halli									X	X			Eley 1938
	Lunatia pedernalis						X							Eley 1938
	***Lunatia* sp.**										X			Eley 1938
	Margarita ornata										X			Eley 1938
	Melanatria vanusta										X			Eley 1938; Lehman 1985
	Morea reticulata tenuis										X			Eley 1938
	***Morea* sp.**										X			Lehman 1985
	***Natica* sp.**										X			Udden 1907
	***Nerinea* sp.**		X											Maxwell et al. 1967
	Perissolax dubia										X			Eley 1938
	Pugnellus abnormalis										X			Lehman 1985
	***Pugnellus* sp.**										X			Eley 1938
	Pyrifusus* cf. *P. bairdi										X			Lehman 1985
	***Pyrifusus* sp.**										X			Eley 1938; Lehman 1985
	Rostellites* cf. *R. biconicus										X			Eley 1938
	Rostellites texana										X			Udden 1907
	***Scurria* sp.**										X			Udden 1907
	Seminola globosa										X			Eley 1938
	Seminola greenensis										X			Eley 1938
	Stantonella interrupta										X			Lehman 1985
	Surcula stringosa										X			Eley 1938
	Trachytrition ?holmdelense										X			Eley 1938
	Turritella ola										X			Eley 1938
	Turritella quadrilira									X				Eley 1938; Maxwell et al. 1967
	Turritella quadrilirata									X				Lehman 1985
	***Turritella* sp.**		X	X	X		X	X		X				Maxwell et al. 1967
	Turritella trilira									X	X			Eley 1938; Lehman 1985
	Tylostoma hilli							X						Eley 1938
	***Tylostoma* sp.**		X	X				X		X	X			Maxwell et al. 1967; Eley 1938
	Viviparus retusus											X		*Coulson 1998
	Viviparus trochiformis											X		*Coulson 1998
	Viviparus* cf. *V. raynoldsanus										X			Udden 1907
	Voluta parvula										X			Eley 1938
	Volutaderma ovata									X				Eley 1938
	***Volutaderma* sp.**										X			Eley 1938
	Volutamorpha bella										X			Eley 1938
	Volutamorpha* cf. *V. raynoldsanus										X	X		Lehman 1985
	Volutamorpha conradi									X	X			Eley 1938
	***Volutamorpha* sp.**									X	X			Eley 1938
	Volutilithes cancellatus										X			Eley 1938
SCAPHOPODA														
tusk shells	***Dentalium gracile***										X			Udden 1907
CEPHALOPODA														
AMMONITES, NAUTILOIDS	***Acanthoceras bellense***								X					Cooper et al. 2017
	Acanthoceras amphibolum								X					White 2019
	Allocrioceras annulatum								X					Cooper et al. 2017
	Allocrioceras hazzardi								X					Maxwell et al. 1967; Cooper et al. 2017; White 2019
	***Allocrioceras* sp.**								X					*Cooper et al. current research
	Baculites asperiformis									X				Udden 1907; Lehman 1985
	Baculites* cf. *B. codyensis								X					Cooper et al. 2017
	Baculites haresi										X			Waggoner 2006
	Baculites ovatus								X	X	X			Eley 1938
	***Baculites* sp.**								X	X	X			Maxwell et al. 1967; Lehman 1985; Cooper et al. 2017
	***Belemnoidea* indet.**								X					*Cooper et al. current research
	***Budaiceras* sp.**							X						Eley 1938; Maxwell et al. 1967
	***Calycoceras* sp.**								X					Cooper et al. 2017
	***Coilopceras* sp.**								X					Maxwell et al. 1967; Bell et al. 2013
	Coilopceras springeri								X					Bell et al. 2013
	Collignoniceras woolgari								X					Bell 1995; Cooper et al. 2017
	***Craginites* sp.**				X									Maxwell et al. 1967
	Crioceras* cf. *latus								X					Udden 1907; Eley 1938
	***Cymatoceras* sp.**								X					Eley 1938
	Delawarella delawarenisis									X				Maxwell et al. 1967

CLASS	TAXON	FORMATIONS												REFERENCES
		GR	TC	DC	SP	SE	DR	BU	BO	PN	AG	JV	BP	
CEPHALOPODA (Continued)														
	Delawarella sabinalensis									X				Lehman 1985
	***Delawarella* sp.**									X				Maxwell et al. 1967
	***Desmoceras* sp.**				X									Maxwell et al. 1967
	Diploceras* cf. *D. cristatum				X									Tarasconi 2000
	Douvilleiceras* cf. *D. mammilatum	X												Maxwell et al. 1967
	***Egonoceras* sp.**		X											Maxwell et al. 1967
	Euhystrichoceras adkinsi								X					Cooper et al. 2017
	Euomphaloceras septemseriatum								X					Cooper et al. 2017
	Eupachydiscus* cf. *E. isculensis								X					Cooper et al. 2017
	Eutrephoceras dekayi									X	X			Udden 1907; Eley 1938; Lehman 1985
	Eutrephoceras* cf. *perlatum								X					Cooper et al. 2017
	***Eutrephoceras* sp.**								X					Maxwell et al. 1967
	***Forresteria* sp.**								X					Cooper et al. 2017
	***Gauthiericeras* sp.**								X					Cooper et al. 2017
	Glyptoxoceras ellisoni									X				Lehman 1985
	Hamites simplex								X					Cooper et al. 2017
	***Hypoturrilites* sp.**						X							Tarasconi 2000
	***Hoplitoplacenticeras* n. sp. +**										X			Waggoner 2006
	Idiohamites fremonti				X									Maxwell et. al. 1967
	***Mantelliceras* sp.**								X					Eley 1938
	Menabites delawarensis									X				Waggoner 2006
	***Menabites* sp.**								X					Cooper et al. 2017
	Metengonoceras* cf. *M. ambiguum		X											Maxwell et al. 1967
	Moremanoceras bravoense								X					Cooper et al. 2017
	Mortoniceras delawarensis									X				Eley 1938
	***Mortoniceras* sp.**				X				X					Eley 1938; Maxwell et al. 1967
	Oxytropidoceras bravoensis				X									Maxwell et al. 1967
	Oxytropidoceras geniculatum				X									Maxwell et al. 1967
	Pachydiscus paulsoni										X			Waggoner 2006
	Peroniceras* cf. *P. tridorsatum								X					Cooper et al. 2017
	***Peroniceras* sp.**								X					Maxwell et al. 1967; Ashmore 2003
AMMONITES, NAUTILOIDS	***Pervinquieria* sp.**				X									Maxwell et al. 1967
	Placenticeras placenta									X	X			Eley 1938; Maxwell et al. 1967
	Placenticeras intercalare									X	X			Waggoner 2006
	Placenticeras meeki									X	X			Maxwell et al. 1967; Lehman 1985
	***Placenticeras* sp.**									X	X			Eley 1938; Maxwell et al. 1967
	Placenticeras syrtale									X	X			Lehman 1985; Waggoner 2006
	Placenticeras whitfieldi									X				Udden 1907; Eley 1938
	Plesiotexanites americanus								X					Cooper et al. 2017
	Plesiotexanites shiloensis								X					Cooper et al. 2017
	Prionocycloceras hazzardi								X					Cooper et al. 2017
	Prionocyclus hyatti								X					Cooper et al. 2017; Bell et al. 2013
	***Prohysteroceras* sp.**				X									Maxwell et al. 1967
	Protexanites bourgeoisianus								X					Cooper et al. 2017
	Pseudocalycoceras angolaense								X					Cooper et al. 2017
	***Pseudocalycoceras* sp.**								X					Cooper et al. 2017
	***Pseudoschloenbachia* sp.**									X				Lehman 1985
	Scaphites hippocrepis									X				Waggoner 2006
	Scaphites semicostatus								X					Cooper et al. 2017
	***?Scaphites* sp.**						X		X	X				Lehman 1985; Tarasconi 2000
	Schloenbachia conensis									X				Udden 1907
	Schloenbachia leonensis									X				Udden 1907
	Scipinoceras* cf. *S. gracilis								X					Maxwell et al. 1967
	Spinaptychus sternbergi									X				Maxwell et al. 1967
	***Stantoceras* sp.**								X					Cooper et al. 2017
	Stoliczkaia adkinsi						X	X						Eley 1938
	***Stoliczkaia* sp.**						X							Maxwell et al. 1967
	Submortoniceras belli									X				Lehman 1985
	Submortoniceras chicoense									X				Lehman 1985
	***Submortoniceras mariscalense* •**									X				Young 1963; Lehman 1985
	Submortoniceras vanuxemi									X				Lehman 1985
	Tarrantoceras sellardsi								X					Cooper et al. 2017
	Texanites* cf. *T. quinquenodosus								X					Cooper et al. 2017
	Texanites* cf. *T. texanus								X	X				Maxwell et al. 1967
	Texanites* cf. *T. stangeri								X					Cooper et al. 2017
	***Texanites* sp.**								X					Maxwell et al. 1967
	Texanites twiningi									X				Lehman 1985
	Texasia dentatocarinata									X				Lehman 1985
	Turrilites acutus								X					Cooper et al. 2017
	Yezoites kieslingswaldensis								X					*Cooper et al. current research
	***Yezoites* sp.**								X					Cooper et al. 2017

CLASS	TAXON	FORMATIONS												REFERENCES
		GR	TC	DC	SP	SE	DR	BU	BO	PN	AG	JV	BP	
CRUSTACEA														
crabs	***?Avitelmessus* sp.**										X			Lehman 1985
fecal pellets	**Arthropoda indet.**											X		*Coulson 1998
OSTRACODA														
seed shrimp	**Ostracoda indet.**			X										Tarasconi 2000
MISCELLANEOUS														
	The following have been reported in BIBE (Eley 1938) from undivided Lower Cretaceous strata he called "Devil's River Limestone".													
	***Alectryonia* sp. (Bivalvia)**			?X										Eley 1938
	***Crassatollina* sp. (Bivalvia)**													Eley 1938
	***Gryphaea marcoi* (Bivalvia)**													Eley 1938
	***Gryphaea washitaensis* (Bivalvia)**													Eley 1938
	***Kingena wacoensis* (Articulata)**													Eley 1938
	***Lunatia* sp. (Gastropoda)**													Eley 1938
	***Nerina* sp. (Gastropoda)**													Eley 1938
	***Toucasia patagiata* (Maxillopoda)**													Eley 1938
TRACE FOSSILS														
	***Chondrites* burrows (marine)**								X					Sanders 1988: White 2019
	***Fodichnia* burrows (marine)**									X				Mosely 1992
	***Gastrochaenolites* burrows (marine)**								X					Sanders 1988
	***Gyrolithes* burrows (marine)**									X				Mosely 1992
	***Ophiomorpha* burrows (marine)**										X			Lehman 1985; Wick and Corrick 2015
	***Planolites* burrows (marine)**								X					Sanders 1988
	***Rhizocorallium* burrows (marine)**								X					Sanders 1988
	***Thalassinoides* burrows (marine)**								X					Sanders 1988
	?Crustacean burrows indet. (fresh water)											X	X	*Coulson 1998
	Clinoid sponge borings (on marine oysters)										X			Lehman 1985
	Lithophagid borings (on marine oysters)										X			Lehman 1985; Wick and Corrick 2015
	Termite borings and frass												X	Rohr et al. 1986
		GR	TC	DC	SP	SE	DR	BU	BO	PN	AG	JV	BP	
	HOLOTYPE = •	Glen Rose Limestone	Telephone Canyon Formation	Del Carmen Limestone	Sue Peaks Formation	Santa Elena Limestone	Del Rio Clay	Buda Limestone	Boquillas Formation	Pen Formation	Aguja Formation	Javelina Formation	Black Peaks Formation	
	UNPUBLISHED NEW TAXON = Δ													
	UNNAMED NEW TAXON = +													
			LOWER CRETACEOUS						**UPPER CRETACEOUS**					
CLASS	**TAXON**						**FORMATIONS**							**REFERENCES**
GRAPTOLITES							**Maravillas Formation (Ordivician)**							
colonial animals	**Graptolithina indet.**	X												Maxwell et al. 1967
CONODONTS							**Maravillas Formation (Ordivician)**							
eel-like chordates	***Amorphagnathus ordovicicus***	X												Turner et al. 2011
	***Belodina* sp.**	X												Turner et al. 2011
	Oistodus venustus	X												Turner et al. 2011
	Panderodus gracilis	X												Turner et al. 2011
	Panderodus unicostatus	X												Turner et al. 2011
	Protopanderodus insculptus	X												Turner et al. 2011
	Periodon aculeatus	X												Turner et al. 2011
	Phragmodus undatus	X												Turner et al. 2011
GASTROPODA							**Canoe Formation (Eocene)**							
snail	***Helix* sp.**	X												Maxwell et al. 1967

* Cooper et. al. (current research) indicates taxa collected by Roger Cooper and colleagues, currently residing in the collections of the Texas Memorial Museum (copies of this record on file at BBNP). Please note that 'current research' may ultimately result in taxonomic revision.
* Coulson (1998) reports these taxa from the Javelina Fm. although this part of the section is now recognized as being in the Cretaceous (lower) portion of the Black Peaks Fm. (Lehman and Coulson 2002).

isolated teeth (e.g., Stevens et al. 1969; Schiebout 1974; Standhardt 1986).

Vertebrate microfossils are also common within both Cretaceous and Tertiary strata of BIBE although finding especially productive sites is remarkably challenging. Furthermore, although some microvertebrate specimens can be surface picked in the field, much of the microfossil material so far reported from the park has been collected via screen-washing or acidization of bulk matrix and collected microscopically (sometimes over years) in the laboratory – a laborious process. In any case, the critical importance of vertebrate microfossil sites cannot be overstated. Microfossils representing multiple, coexisting species from a single locality almost always tell scientists much more about an ancient ecosystem than do large, isolated bones or partial skeletons of a single animal. For example, just a handful of highly productive sites within the Aguja Formation have produced thousands of microvertebrate fossil specimens

Table 3. Vertebrate fossils.

CLASS	TAXON	COMMON NAME	FORMATIONS											REFERENCES
			BO	PN	AG	JV	KBP	PgBP	HH	CN	CH	DE	BS	
CHONDRICHTHEYS														
CARTILAGINOUS FISHES	***Anomotodon augustidens***	Shark			X									Lehman 1985
	Brachyrhyzodus wichitaensis	Guitarfish			X									Schubert et al. 2017
	Cantioscyllium* aff. *C. myersi	Shark			X									Schubert et al. 2017
	Chiloscyllium* aff. *C. greeni	Shark			X									Schubert et al. 2017
	Chondrichthyes indet.	Shark	X	X	X									Maxwell et al. 1967; Schubert et al. 2017
	***Columbusia* sp.**	Carpet Shark			X									Schubert et al. 2017
	Cretalamna appendiculata	Shark		X										Standhardt in Langston et al. 1989
	Cretalamna* cf. *C. sarcoportheta	Shark			X									Schubert et al. 2017
	Cretorectolobus olsoni	Shark		X	X									Standhardt 1986; Lehman 1985
	***Dasyatidea* indet.**	Stingray			X									Sankey 1998; Sankey 2010
	***Dasyatus* sp.**	Stingray						X						Standhardt 1986
	***Hybodus* sp.**	Shark			X									Sankey 1998
	Hybodontidae indet.	Shark			X									Lehman et al. 2019
	Igdabatis* cf. *I. indicus	Stingray			X									Schubert et al. 2017
	Ischyriza avonicola	Sawfish			X									Sankey 1998; Montgomery and Clark 2016
	Ischyrhyza* cf. *I. avonicola	Sawfish			X									Schubert et al. 2017
	Ischyriza mira	Sawfish		X	X									Lehman 1985; Schubert et al. 2017
	Lamna appendiculata	Shark			X									Applegate 1972
	Lamna texana	Shark			X									Udden 1907*
	Lamna* cf. *L. elegans	Shark			X									Udden 1907*
	Lissodus selachos	Shark		X	X									Standhardt 1986; Sankey 1998
	Lonchidion selachos	Shark			X									Schubert et al. 2017
	***Meristodon* sp.**	Shark			X									Schubert et al. 2017
	?*Myledaphus bipartitus*	Skate			X									Standhardt 1986; Montgomery and Clark 2016
	***Myliobatus* sp.**	Eagle Ray							X					Standhardt in Langston et al. 1989
	***Myliobatiformes* indet.**	Eagle Ray			X									Schubert et al. 2017
	***Odontaspis* sp.**	Sand Shark			X									Standhardt 1986
	Onchopristis dunklei	Sawfish			X									Sankey 1998; Montgomery and Clark 2016
	***Onchopristis* sp.**	Sawfish			X									Davies 1983
	Protoplatyrhina renae	Guitarfish			X									Schubert et al. 2017
	Ptychodus mortoni	Shark	X											Eley 1938
	Ptychotrygon agujaensis •	Skate			X									McNulty and Slaughter 1972; Schubert et al. 2017
	Ptychotrygon* cf. *P. cuspidata	Skate			X									Schubert et al. 2017
	Ptychotrygon triangularis	Skate			X									Schubert et al. 2017
	***Ptychotrygon* sp.**	Skate		X	X									Standhardt 1986; Schubert et al. 2017
	***Rhinobatos* sp.**	Guitarfish			X									Schubert et al. 2017
	Rhombodus levis	Eagle Ray			X									Schubert et al. 2017
	***Rhombodus* sp.**	Eagle Ray						X						Standhardt 1986
	Scapanorynchus raphiodon	Shark			X									Applegate 1972
	Scapanorynchus texanus	Shark			X									Lehman 1985; Sankey 1998; Schubert et al. 2017
	Serratolamna* cf. *S. caraibaea	Shark			X									Schubert et al. 2017
	Squalicorax kaupi	Shark		X	X									Lehman 1985; Schubert et al. 2017
	Squalicorax* aff. *S. yangaensis	Shark			X									Schubert et al. 2017
	Squalicoraz* aff. *S. lindstromi	Shark			X									Schubert et al. 2017
	***Squatina* sp.**	Shark			X									Schubert et al. 2017
	Squatirhina americana	Carpet Shark			X									Sankey 1998; Montgomery and Clark 2016
	Texatrygon* cf. *T. copei	Skate			X									Schubert et al. 2017
CHONDRICHTHEYS MISC.														
coprolites (fossil dung)	**Chondrichthyes indet.**	Shark			X									Wick and Corrick 2015
OSTEICHTHYES														
	Acanthomorpha indet.	Boney Fish			X									Wick in review
	***Albula* sp.**	Boney Fish			X									Schubert et al. 2017; Wick current research 2021
	Amia uintaensis	Bowfin Fish			X									Lehman 1985
	Amiinae indet.	Bowfin Fish			X									Wick in review
	Amiidea indet.	Bowfin Fish			X									Lehman 1985; Standhardt 1986; Rowe et al. 1992
Boney FISHES	**cf. *Anomoeodus* sp.**	Boney Fish			X									Wick in review
	***Atractosteus* sp.**	Gar			X									Standhardt 1986; 1995
	cf. ?*Coriops* sp.	Boney Fish			X									Wick current research 2021
	***Cylindracanthus* sp.**	Boney Fish			X									Montgomery and Clark 2016
	Ellimmichthyiformes indet.	Boney Fish			X									Wick in review
	aff. *Enchodus* sp.	Boney Fish			X									Wick in review
	?*Enchodus* sp.	Boney Fish			X									Schubert et al. 2017
	Eotexachara malateres •	Boney Fish			X									Wick 2021c
	cf. Gonoryhnchiformes indet.	Boney Fish			X									Wick in review
	Hiodontidae indet.	Boney Fish			X									Wick in review
	Laminospondylus transversus	Boney Fish	X											*Cooper et al. current research

CLASS	TAXON	COMMON NAME	FORMATIONS											REFERENCES
			BO	PN	AG	JV	KBP	PgBP	HH	CN	CH	DE	BS	
OSTEICHTHYES (Continued)														
Boney FISHES	**?*Lepidotes* sp.**	Boney Fish			X									Schubert et al. 2017
	Lepisosteus occidentalis	Gar			X									Sankey 1998
	Lepisostidae indet.	Gar		X	X	X	X	X	X					Davies 1983; Standhardt 1986; Rowe et al. 1992
	Melvius thomasi	Bowfin Fish			X									Boreske 1974; Standhardt 1986; Rowe et al. 1992
	***Melvius* sp.**	Bowfin Fish			X									Lehman et al. 2019
	cf. *Melvius* sp.	Bowfin Fish			X									Wick in review
	cf. *Micropycnodon* sp.	Boney Fish			X									Wick in review
	Ostariophysi indet.	Boney Fish			X									Wick in review
	Osteichthyes indet.	Indet.	X		X	X								Standhardt 1986; Schubert et al. 2017
	cf. *Wilsonichthys* sp.	Boney Fish			X									Wick in review
	Paralbula casei	Boney Fish			X									Schubert et al. 2017
	Paralbula* cf. *P. casei	Boney Fish			X									Wick in review
	***Paralbula* sp.**	Boney Fish			X									Montgomery and Clark 2016
	***Primuluchara laramidensis* •**	Boney Fish			X									Wick 2021c
	***Phyllodonitdae* indet.**	Bonefish			X									Sankey 1998; Rowe et al. 1992
	Semionotifomes	Boney Fish			X									Wick, current research 2021
	?*Stephanodus* sp.	Boney Fish			X									Schubert et al. 2017
	Teleostei indet.	Indet.			X	X	X							Lehman 1985; Standhardt 1986
	cf. *Xiphactinus* sp.	Boney Fish		X										Lehman current research
AMPHIBIA														
FROGS, TOADS, SLAMANDERS	***Albanerpeton* cf. *galaktion***	Salamander			X									Wick 2021a
	Albanerpeton gracile	Salamander			X									Wick 2021a
	Albanerpeton nexousum	Salamander			X									Standhardt 1986; Wick 2021
	***Albanerpeton* sp.**	Salamander			X									Rowe et al. 1992; Sankey 1998
	Anura indet. (multiple species)	Frog			X			X						Standhardt 1986; Rowe et al. 1992; Wick 2021b
	Bufo* cf. *B. marinus	True Toad											X	Stevens 1977; Stevens and Stevens 1989
	Habrosaurus dilatus	Salamander				X								Standhardt 1986
	Opisthotriton kayi	Salamander				X								Standhardt 1986
	***Scapherpeton* sp.**	Salamander			X									Sankey 1998; Montgomery and Clark 2016
	Scapherpeton tectum	Salamander			X									Standhardt 1986
REPTILIA														
TURTLES, LIZARDS, CROCODYLIANS, PTEROSAURS, DINOSAURS	***Adocus* sp.**	Turtle			X									Lehman 1985
	***Agujaceratops mariscalensis* •**	Dinosaur			X									Lucas et al. 2006
	***Agujaceratops mavericus* •**	Dinosaur			X									Lehman et al. 2017
	Alamosaurus sanjuanensis	Dinosaur				X	X							Lehman and Coulson 2002; Tykoski and Fiorillo 2016
	***Alamosaurus* ?n. sp.**	Dinosaur					X							Fronimos 2010
	***Allognathosuchus* sp.**	Alligator-Like						X	X					Schiebout 1973; Hartnell 1980
	Anguidae indet.	Lizard			X									Sankey 1998
	***Angulomasticator daviesi* •**	Dinosaur			X									Wagner and Lehman 2009
	Ankylosauridae indet.	Dinosaur			X									Standhardt 1986; Rowe et al. 1992
	Anomalepididae indet.	Snake						X						Standhardt 1986
	***Apsgnathus triptodon* •**	Lizard			X									Nydam et al. 2013
	***Aspideretes* sp.**	Turtle			X	X								Lehman 1985; Rowe et al. 1992
	Baena* cf. *B. nodosa	Turtle			X									Lehman 1985
	***Baena* sp.**	Turtle			X	X								Lehman 1985; Rowe et al. 1992
	***Basilemys* sp.**	Turtle			X									Lehman et al. 2019
	cf. *Basilemys* sp.	Turtle			X	X								Davies 1983; Lehman 1985
	***Borealosuchus* sp.**	Crocodylian						X						Brochu 2000
	Bothriagenys mysterion	Lizard			X									Wick and Shiller 2020
	***Bothriagenys flectomendax* •**	Lizard			X									Wick and Shiller 2020
	cf. *Bothriagenys* sp.	Lizard			X									Wick and Shiller 2020
	cf. *Brachychampsa* sp.	Alligator-Like			X	X	X	X						Standhardt 1986
	***Bravoceratops polyphemus* •**	Dinosaur				X								Wick and Lehman 2013
	***Bothremys* sp.**	Turtle			X									Anglen 2001
	Caenagnathidae indet.	Dinosaur			X									Longrich et al. 2010
	***Catactegenys solaster* •**	Lizard			X									Nydam et al. 2013; Wick and Shiller 2020
	Ceratopsidae indet.	Dinosaur			X									Rowe et al. 1992; Lehman et al. 2019; Strain 1940
	***Chamops* sp.**	Lizard			X									Sankey 1998; 2008
	Chamopsiidae indet.	Lizard			X									Wick and Shiller 2020
	aff. Chamopsiidae	Lizard			X									Wick and Shiller 2020
	Champsosauridae indet.	Crocodile-Like						X						Standhardt in Langston et al. 1989
	Chasmosaurus mariscalensis	Dinosaur			X									Lehman 1982, 1989a; Forster et al. 1993*
	Chelonia indet.	Turtle			X				X					Hartnell 1980; Rowe et al. 1992
	***Chupacabrachelys complexus* •**	Turtle			X									Lehman and Wick 2010
	?*Claosaurus* sp.	Dinosaur			X									Udden 1907*
	Clidastes liodontus	Mosasaur		X										Bell et al. 2013
	***Clidastes* sp.**	Mosasaur		X										Bell et al. 2013
	Compsemys victa	Turtle			X									Standhardt 1986
	aff. *Coniophis* sp.	Snake			X									Wick and Shiller 2020
	Crocodylia indet.	Crocodylian			X					X				Maxwell et al. 1967; Sankey 1998

CLASS	TAXON	COMMON NAME	FORMATIONS											REFERENCES
			BO	PN	AG	JV	KBP	PgBP	HH	CN	CH	DE	BS	
REPTILIA (Continued)														
	?*Crotalus* sp.	Snake											X	Stevens et al. 1969; Stevens 1977
	***Ctenosaura* or *Sauromalus* sp.**	Lizard										X		Stevens 1977; Steven and Stevens 1989
	***Deinosuchus riograndensis* •**	Crocodylian			X									Colbert and Bird 1954; Anglen and Lehman 2000
	cf. *Deinosuchus* sp.	Crocodylian			X									Lehman et al. 2019
	Denazinemys	Turtle			X									Lucas and Sullivan 2006
	cf. *Denazinemys* sp.	Turtle			X									Lehman et al. 2019
	Dermatemydidae indet.	Turtle						X						Schiebout 1973
	Diplocynodon* cf. *D. stuckeri	Alligator-Like						X						Schiebout 1973
	Dipsosaurus* cf. *D. dorsalis	Lizard										X		Stevens et al. 1969; Steven and Stevens 1989
	cf. *Dromaeosaurus*	Dinosaur			X									Rowe et al. 1992
	Dromaeosauridae indet.	Dinosaur			X									Lehman et al. 2019
	***Dryadissector shilleri* •**	Lizard			X									Wick et al. 2015; Wick and Shiller 2020
	?*Dryptosaurus*	Dinosaur			X									Udden 1907*
	Dunnophis* cf. *D. microechinis	Snake						X						Standhardt 1986
	***Ectenosaurus* n. sp. +**	Mosasaur												Bell et al. 2013
	cf. *Edmontonia* sp.	Dinosaur			X									Sankey 2010; A.M.N.H. collections records.
	cf. *Edmontosaurus* sp.	Dinosaur				X								Lawson 1972; Davies 1983
	cf. *Euoplocephalus* sp.	Dinosaur			X									Standhardt 1986
	?*Geochelone* sp.	Tortoise										X		Stevens 1977; Steven and Stevens 1989
	Glyptosaurus* cf. *G. sylvestris	Lizard						X						Standhardt 1986
	Glyptosaurinae indet.	Lizard			X									Sankey 1998, 2008
	Goniopholis* cf. *G. kirtlandicus	Crocodile			X									Lehman 1985
	***Goniophoididae* n. gen. n. sp. +**	Crocodile			X									Lehman et al. 2019
	***Goniopholididae* indet.**	Crocodile			X									Rowe et al. 1992
	***Gopherus* sp.**	Tortoise											X	Stevens et al. 1969; Steven and Stevens 1989
	?*Gryposaurus alsatei*	Dinosaur				X								Lehman et al. 2016
	?*Gryposaurus* n. sp. o Δ	Dinosaur			X									Wagner and Lehman 2001
	Hadrosauridae indet.	Dinosaur			X									Strain 1940; Davies and Lehman 1989
	Hadrosauridae n. gen. n. sp. +	Dinosaur				X								Lehman et al. 2019
	***Heloderma texana* •**	Lizard										X		Stevens et al. 1969; Stevens 1977
	cf. *Helopanoplia* sp.	Turtle			X									Sankey 2006, 2010
	***Hoplochelys* sp.**	Turtle						X						Standhardt in Langston et al. 1989; Sankey 2010
	***Hydrargysaurus gladius* •**	Lizard			X									Wick and Shiller 2020
	Hypsilophodontidae indet.	Dinosaur			X									Davies 1983
	***Hypostylos lehmani* •**	Lizard			X									Wick and Shiller 2020
	Kritosaurus* cf. *K. navajovius	Dinosaur			X	X								Davies 1983
	***Kritosaurus* sp.**	Dinosaur				X								Lehman et al. 2016
	***Lambeosaurinae* indet.**	Dinosaur			X									Davies 1983
	cf. *Leidyosuchus* sp.	Alligator-Like			X	X	X	X						Standhardt in Langston et al. 1989
	Leptorhynchos gaddisi	dinosaur			X									Longrich et al. 2013
	Mosasauridae indet.	Mosasaur	X	X	X									Maxwell et al. 1967; Shubert 2013
	Mosasauroidea indet.	Mosasaur	X											Bell et al. 2013
	Necrosauridae indet.	Lizard			X									Rowe et al. 1992; Miller 1997
	***Nodosauridae* n. gen. n. sp. +**	Dinosaur			X	X								Longrich et al. 2010
	Odaxosaurus piger	Lizard			X									Miller 1997; Nydam et al. 2013
	***Odaxosaurus* sp.**	Lizard			X									Rowe et al. 1992; Miller 1997
	Ornithomimidae n. gen. n. sp. +	Dinosaur			X									Lehman et al. 2019
	Ornithomimidae indet.	Dinosaur			X									Longrich et al. 2010
	cf. *Paleosaniwa canadensis*	Lizard			X									Miller 1997
	cf. *Parasaniwa wyomingensis*	Lizard			X									Nydam et al. 2013
	cf. *Parasaniwa* sp.	Lizard			X									Miller 1997
	***Panoplosaurus* sp.**	Dinosaur			X									Coombs 1978
	Paronychodon lacustris	Dinosaur			X									Standhardt 1986; Sankey 2005
	cf. *Paronychodon*	Dinosaur			X									Wick et al. 2015
	***Peneteius* sp.**	Lizard			X									Nydam et al. 2007; Sankey 1998, 2008
	***Phylodactylus* sp.**	Gekko			X									Montgomery and Clark 2016
	Platecarpus planifrons	Mosasaur	X											Bell et al. 2013
	Platecarpus* cf. *P. planifrons	Mosasaur	X											Bell et al. 2013
	Plioplatecarinae indet.	Mosasaur			X									Bell et al. 2013
	Pristichampsus* cf. *P. vorax	Crocodile							X					Langston et al. 1989 (appendix)
	***Provaranosaurus* sp.**	Lizard						X						Maxwell et al. 1967; Standhardt 1986
	***Proxestops* sp.**	Lizard			X									Rowe et al. 1992
	?*Proxestops* sp.	Lizard			X									Montgomery and Clark 2016
	***Pterosauria* n. gen n. sp. +**	Pterosaur				X								Lehman and Busbey 2007
	***Quetzalcoatlus northropi* •**	Pterosaur				X								Lawson 1975; Langston 1981
	***Quetzalcoatlus* sp.**	Pterosaur				X								Langston 1986; Kellner and Langston 1996
	***Restes* sp.**	Lizard			X									Rowe et al. 1992
	Richardoestesia* cf. *R. gilmorei	Dinosaur			X									Sankey 2001
	cf. *Richardoestesia*	Dinosaur			X									Rowe et al. 1992; Wick et al. 2015
	Russellosaurinae indet.	Mosasaur	X											Bell et al. 2013

TURTLES, LIZARDS, CROCODYLIANS, PTEROSAURS, DINOSAURS

CLASS	TAXON	COMMON NAME	FORMATIONS											REFERENCES
			BO	PN	AG	JV	KBP	PgBP	HH	CN	CH	DE	BS	
REPTILIA (Continued)														
TURTLES, LIZARDS, CROCODYLIANS, PTEROSAURS, DINOSAURS	***Richardoestesia isoceles*** •	Dinosaur			X									Sankey 2001
	***Sauriscus* sp.**	Lizard			X									Rowe et al. 1992
	***Saurolophinae* indet.**	Dinosaur				X								Lehman et al. 2016
	Saurornitholestes langstoni	Dinosaur			X									Sankey 2001
	cf. *Saurornitholestes*	Dinosaur			X									Rowe et al. 1992; Wick et. al 2015
	***Saurornitholestes* indet.**	Dinosaur			X									Sankey 2010
	Serpentes indet.	Snake			X									Rowe et al. 1992; Nydam et al. 2013
	cf. *Socognathus* sp.	Lizard			X									Wick and Shiller 2020
	cf. *Stegoceras* sp.	Dinosaur			X									Lehman 1985
	?*Stegoceras* sp.	Dinosaur			X									Lehman 2010
	Teiidae indet.	Lizard			X									Rowe et al. 1992; Sankey 1998, 2008
	Terlinguachelys fischbecki •	Sea Turtle			X									Lehman and Tomlinson 2004
	Texacephale langstoni •	Dinosaur			X									Longrich et al. 2010
	Therapoda indet.	Dinosaur			X									Wick et al. 2015
	Thescelus* cf. *T. insiliens	Turtle			X									Lehman 1985
	***Thescelus* sp.**	Turtle			X									Lawson 1972
	Titanosauridae indet.	Dinosaur				X								Wick and Lehman 2014
	Torosaurus utahensis	Dinosaur				X								Lawson 1976; Hunt and Lehman 2008
	Trionychidae indet.	Turtle			X									Sankey 1998; Lehman et al. 2019
	***Troodon* sp.**	Dinosaur			X	X								Standhardt 1986; Sankey 1998
	cf. *Troodon*	Dinosaur			X									Rowe et al. 1992
	Tyannosauridae indet.	Dinosaur			X	X	X							Lehman 1985; Sankey 2010; Wick et al. 2015
	Tyrannosaurinae indet.	Dinosaur			X									Lehman and Wick 2012
	Tyrannosaurus rex	Dinosaur												Lawson 1976
	?*Tyrannosaurus* cf. *T. rex*	Dinosaur				X								Wick 2014
	***Tyrannosaurus vannus* Δ**	Dinosaur				X								Lawson 1972
	Tylosaurus kansasensis	Mosasaur	X											Bell et al. 2013
	Tylosaurus nepaeolicus	Mosasaur	X											Bell et al. 2013
	***Tylosaurus* sp.**	Mosasaur	X	X										Bell et al. 2013
	***Tylosaurus* indet.**	Mosasaur	X											Bell et al. 2013
	Varanoidea indet.	Lizard			X									Nydam et al. 2013; Wick and Shiller 2020
	Xenosauridae indet.	Lizard			X									Rowe et al. 1992; Nydam et al. 2013
REPTILIA misc.														
eggshell fragments	**?*Continuoolithus***	unknown			X									Montgomery and Clark 2016
	Ornithischia indet.	Dinosaur			X									Welsh and Sankey 2008
	Saurischia indet.	Dinosaur			X									Welsh and Sankey 2008
	Reptilia indet.	Indet.				X								Lehman and Langston unpublished
coprolite	**Dinosauria indet.**	Dinosaur			X									Baghai-Riding and DiBenedetto 2001
coprolites	**Reptilia indet.**	Indet.			X	X								Coulson 1998; Montgomery and Clark 2016
feeding traces (bite marks)	**Crocodylia indet.**	Crocodile			X									Schwimmer 2002; Lehman and Wick 2010
	Tyrannosauridea indet.	Dinosaur			X	X								Montgomery and Clark 2016
skin impressions	**?*Gryposaurus alsatei*** •	Dinosaur				X								Lehman et al. 2016
AVES														
birds	**cf. Aves indet.**	Bird			X	X								Sankey 2005; Wick et al. 2015
MAMMALIA														
PRIMITIVE AND ADVNCED MAMMALS	***Albertatherium primus***	Marsupial			X									Brink 2015; 2016
	Alphadon* cf. *A. marshi	Marsupial			X	X								Standhardt 1986
	Alphadon halleyi	Marsupial			X									Brink 2015; 2016
	Alphadon* cf. *A. halleyi	Marsupial			X									Sankey 1998
	Alphadon* cf. *A. sahnii	Marsupial			X									Sankey 1998
	Alphadon* cf. *A. wilsoni	Marsupial			X									Rowe et al. 1992
	***Alphadon* n. sp. +**	Marsupial			X									Rowe et al. 1992
	***Alphadon* sp.**	Marsupial			X									Sankey 2001; Montgomery and Clark 2016
	Alphadon perexiguus •	Marsupial			X									Cifelli 1994
	***Aquascalientia* sp.**	Camelid										X		Stevens 1977; Stevens and Stevens 1989
	***Aquiladelphis* sp.**	Marsupial			X									Brink 2015, 2016
	Archaeolagus buangulus	Rabbit										X		Stevens et al. 1969
	Archaeolagus* cf. *A. acaricolus	Rabbit										X		Stevens et al. 1969
	Arctocyonides* cf. *A. ferox	Carnivore						X						Schiebout 1974
	Baioconodon	Condylarth						X						Standhardt 1995
	Barylambda jackwilsoni	Pantodont						X						Schiebout 1974
	***Barylambda* sp.**	Pantodont							X					Hartnell 1980
	Bomburia prisca	Condylarth						X						Standhardt 1995
	?*Brachyerix hibbardi*	Hedgehog										X		Stevens 1977
	Buisnictis chisoensis •	Skunk											X	Stevens et al. 1969; Stevens and Stevens 1989
	Caenolambda jepseni	Pantodont						X						Hartnell 1980
	Caenolambda pattersoni	Pantodont						X						Hartnell 1980
	***Caenolambda* sp.**	Pantodont						X						Schiebout 1974
	Canidae indet.	Carnivore										X		Stevens et al. 1969; Stevens 1977
	Carsioptychus coarctatus	Condylarth						X						Standhardt 1986, 1995
	Cedaromys* cf. *C. hutchisoni	Multituberculate			X									Brink 2015, 2016

CLASS	TAXON	COMMON NAME	FORMATIONS											REFERENCES
			BO	PN	AG	JV	KBP	PgBP	HH	CN	CH	DE	BS	
MAMMALIA (Continued)														
PRIMITIVE AND ADVNCED MAMMALS	***Chiromyoides caesor***	Primate						X						Schiebout 1974
	Chriacus baldwini	Racoon-Like						X						Schiebout 1974
	***Cimexomys* sp.**	Multituberculate			X									Sankey 2001
	***Cimolomyidae* n. gen. n. sp. +**	Multituberculate			X									Standhardt 1986
	Cimolodon* cf. *electus	Multituberculate			X									Rowe et al. 1992
	***Cimolodon* sp.**	Multituberculate			X									Brink 2015, 2016
	cf. *Cimolodon* sp.	Multituberculate			X									Rowe et al. 1992
	Cimolomys clarki	Multituberculate			X									Rowe et al. 1992
	***Cimolomys* sp.**	Multituberculate			X									Sankey 2001
	***Citellus* n. sp. +**	Ground squirrel											X	Stevens 1977; Stevens and Stevens 1989
	***Coryphodon* sp.**	Pantodont							X					Maxwell et al. 1967; Hartnell 1980
	Dakotamys shakespeari	Multituberculate			X									Brink 2015, 2016
	***Delahomeryx browni* •**	Deer-Like										X		Stevens et al. 1969; Stevens and Stevens 1989
	?*Deuterogonodon* sp.	Carnivore						X						Schiebout 1974
	Ectocion* cf. *E. montanensis	Condylarth						X						Schiebout 1974
	Ectypodus musculus	Multituberculate						X						Schiebout 1974
	Ellipsodon priscus	Condylarth						X						Standhardt 1986
	***Eoalphadon* n. sp. +**	Marsupial			X									Brink 2015, 2016
	Eoconodon coryphaeus	Condylarth						X						Standhardt 1986
	***Eoconodon* sp.**	Condylarth						X						Standhardt 1986
	Epicyon haydeni	Carnivore											X	Stevens and Stevens 2003
	Epihippis gracilis	Primitive Horse									X			Runkel 1988
	Eucosmodontidae indet.	Multituberculate			X									Standhardt 1986
	cf. *Eucyon* sp.	Fox-Like											X	Stevens and Stevens 2003
	?Ferugliotheriidae	?Multituberculate			X									Brink 2015, 2016
	***Gallolestes agujaensis* •**	Eutherian			X									Cifelli 1994
	***Gallolestes* sp.**	Eutherian												Rowe et al. 1992
	?*Gallolestes* n. sp. +	Eutherian			X									Brink 2015, 2016
	***Gelestops* sp.**	Shrew-Like				X								Standhardt 1986, 1995
	***Gregorymys riograndensis* •**	Gopher										X		Stevens 1977
	Haplaletes disceptatrix	Condylarth						X						Schiebout 1974
	Haploconus inopinatus	Condylarth						X						Standhardt 1986, 1995
	Helohyus lentus	Pig-Like								X				Maxwell et al. 1967
	***Hemiauchenia* sp.**	Camel-Like											X	Stevens et al. 1969; Stevens 1977
	Heteromyidae indet.	Kangaroo Rat										X	X	Stevens et al. 1969; Stevens 1977
	Hyopsodus* cf. *H. paulus	Weasel-Like								X				Runkel 1988
	Hyopsodus* cf. *H. wortmani	Weasel-Like							X					Hartnell 1980
	Hyopsodus miticulus	Weasel-Like							X					Hartnell 1980
	***Hyopsodus* sp.**	Weasel-Like								X				Runkel 1988
	***Hypolagus* n. sp. +**	Rabbit											X	Stevens 1977; Stevens and Stevens 1989
	***Hypsiops leptoscelos* •**	Oreodont										X		Stevens et al. 1969
	Hypsiops* cf. *H. luskensis	Oreodont										X		Maxwell et al. 1967
	Hyrachyus* cf. *H. modestus	Tapir-Like								X				Maxwell et al. 1967
	***Hyrachyus* sp.**	Tapir-Like										X		Stevens et al. 1969; Stevens and Stevens 1989
	Hyracotherium angustidens	Horse-Like						X	X					Scheibout 1974
	Hyracotherium vasacciense	Horse-Like							X					Maxwell et al. 1967; Hartnell 1980
	cf. *Isectolophus*	Tapir-Like								X				Runkel 1988
	?*Janumys* sp.	Multituberculate			X									Brink 2015, 2016
	***Jepsenella* n. sp. +**	Elephant shrew-like						X						Schiebout 1974
	***Lambdotherium* sp.**	Brontothere							X					Maxwell et al. 1967
	Lambertocyon eximius	Conylarth						X						Schiebout 1974; Gingerich 1979
	Leptocyon* cf. *L. vafer	Carnivore											X	Stevens et al. 1969; Stevens and Stevens 1989
	Leptoreodon edwardsi	Deer-LIke								X				Runkel 1988
	Leptoreodon pusillis	Deer-Like								X				Runkel 1988
	cf. *Loxolophus* sp.	Primitive Omnivore						X						Langston et al. 1989 (appendix)
	Mammalia n. sp.	"Tribotheria"												Rowe et al. 1992
	***Martes* sp.**	Marten-Like											X	Stevens and Stevens 2003
	?*Megatylopus* sp.	Large Camelid											X	Stevens 1977; Stevens and Stevens 1989
	***Meniscoessus* n. sp. +**	Multituberculate			X									Rowe et al. 1992
	***Meniscoessus* sp.**	Multituberculate			X	X								Standhardt 1986; Brink 2015, 2016
	Menodus bakeri	Brontothere									X			Wilson 1977
	Merychyus* cf. *M. calaminthus	Oreodont										X		Stevens 1977; Stevens and Stevens 1989
	***Mesodma* sp.**	Multituberculate			X									Sankey 2001
	Mesdoma thompsoni	Multituberculate						X						Standhardt 1986
	Mesocyon venator	Canid										X		Stevens et al. 1969; Stevens and Stevens 1989
	***Mesodma* sp.**	Multituberculate			X									Sankey and Gose 2001; Montgomery and Clark 2016

CLASS	TAXON	COMMON NAME	FORMATIONS											REFERENCES
			BO	PN	AG	JV	KBP	PgBP	HH	CN	CH	DE	BS	
MAMMALIA (Continued)														
	Metamynodon mckinneyi	Rhinoceros-Like								X				Runkel 1988
	?*Michenia australis*	Camel-Lke										X		Stevens et al. 1969; Stevens 1977
	Mimetodon silberlingi	Multituberculate						X						Schiebout 1974
	***Mioclaenidea* n. gen. n. sp. +**	Condylarth						X						Standhardt 1995
	Mixodectes malaris	Rodent-Like						X						Standhardt 1986
	?*Mookomys* sp.	Rodent										X		Stevens et al. 1969
	***Moschoedestes delahoensis* •**	Rhinoceros										X		Stevens et al. 1969
	Multituberculata n. gen. n. sp. +	Multituberculate			X									Rowe et al. 1992
	Nannodectes* cf. *gidleyi	Primate-Like						X						Schiebout 1974; Gingerich 1976
	Nanotragulus ordinatus	musk-deer										X		Stevens 1977; Steven and Stevens 1989
	Navajovius kohlhaasae	Primate						X						Schiebout 1974
	cf. *Neohipparion*	Horse-Like											X	Stevens et al. 1969; Steven and Stevens 1989
	Neoplagiaulax douglassi	Multituberculate						X						Hartnell 1980
	Neoplagiaulacidae	Multituberculate			X									Rowe et al. 1992
	cf. *Nimravides catocopis*	Felid											X	Stevens and Stevens 2003
	?*Nothocyon* cf. *N. annectens*	carnivore										X		Stevens et al. 1969
	Omomyidae indet.	Primate								X				Runkel 1988
	Oxydactylus* cf. *gibbi	Camel-Like										X		Maxwell et al. 1967
	Palaechthon* cf. *woodi	primate						X						Standhardt 1986
	?*Palaeictops* sp.	"Hedge-rat"						X						Schiebout 1974
	***Paleomolops langstoni* •**	Trituberculate			X									Cifelli 1994
	Paleotomus senior	Carnivore						X						Standhardt 1986
	Paracimexomys* cf. *P. perplexus	Multituberculate			X									Brink 2015, 2016
	***Paracimexomys* sp.**	Multituberculate												Brink 2015, 2016
	cf. *Paracimexomys*	Multituberculate			X									Sankey 2001
	***Paracimexomys* ?n. gen. n. sp. +**	Multituberculate			X									Brink 2015, 2016
	***Paracimexomys* indet.**	Multituberculate			X									Brink 2015, 2016
	Paramys excavatus	Rodent							X					Hartnell 1980
	?*Paranyctoides* sp.	Eutherian			X									Brink 2015, 2016
	Parectypodus sinclairi	Multituberculate						X						Schiebout 1974; Standhardt 1986
	Parectypodus sloani	Multituberculate						X						Schiebout 1974
	?*Paroligobunis* sp.	Weasel-Like										X		Stevens et al. 1969
	Pediomys* cf. *krejcii	Marsupialk			X									Rowe et al. 1992
	?*Peratherium* sp.	Marsupial						X				X		Standhardt 1986; Stevens 1977
	Periptychus carinidens	Condylarth						X						Maxwell et al. 1967; Standhardt 1986
	Periptychus superstes	Condylarth						X						Maxwell et al. 1967
	Phenacocoelus leptoscelos	Oreodont										X		Stevens et al. 1969; Steven and Stevens 1989
	Phenacodus bisonensis	Condylarth						X						Schiebout 1974; Standhardt 1986
	Phenacodus* cf. *P. matthewi	Condylarth						X						Hartnell 1980
	Phenacodus grangeri	Condylarth						X						Hartnell 1980
	Phenacodus primaevis	Condylarth						X	X					Schiebout 1974; Maxwell et al. 1967
	Phenacolemur* cf. *P. praecox	Primate							X					Hartnell 1980
	Phenacolemur frugivoris	Primate						X						Schiebout 1974; Hartnell 1980
	Plesiadapsis gidleyi	Primate-Like						X						Hartnell 1980
	***Pliohippus* or *Astrohippus* sp.**	Horse-Like											X	Stevens 1977; Steven and Stevens 1989
	***Priscocamelus wilsoni* •**	Camel-Like										X		Stevens et al. 1969; Steven and Stevens 1989
	Prolapsus sibilatoris	Large rodent								X				Runkel 1988
	Prolapsus junctionis	Large Rodent								X				Runkel 1988
	Promioclaenus acolytus	Condylarth						X						Schiebout 1974; Hartnell 1980
	***Promioclaenus* sp.**	Condylarth						X						Standhardt 1986
	***Prothryptacodon* sp.**	Condylarth						X						Standhardt 1986
	***Protictis* n. sp. +**	Weasel-Like						X						Standhardt 1986
	Protoreodon pumilis	Oreodont								X	X			Runkel 1988
	Protoselene opisthacus	Condylarth						X						Schiebout 1974
	cf. *Pseudaelurus* sp.	Felid											X	Stevens and Stevens 2003
	Psittacotherium multifragum	Taeniodont						X						Maxwell et al. 1967; Schoch 1981
	Ptilodontoidea indet.	Multituberculate			X									Standhardt 1986
	Ptilodus douglassi	Multituberculate						X						Maxwell et al. 1967
	Ptilodus mediaevus	Multituberculate						X						Schiebout 1974
	***Ptilodus* n. sp. +**	Multituberculate						X						Standhardt 1986
	***Ptilodus* sp.**	Multituberculate						X						Standhardt 1986
	Similisciurus maxwelli	Squirrel-Like										X		Stevens 1977
	Spalacolestinae indet.	Symmetrodont			X									Brink 2015, 2016
	?Stagnodontidae indet.	Marsupial			X									Brink 2015, 2016
	***Stenomylus* sp.**	Camelid										X		Stevens 1977; Steven and Stevens 1989
	Stenomylus* cf. *S. crassipes	Camelid										X		Maxwell et al. 1967
	Stygimys vastus	Multituberculate						X						Standhardt 1986
	Symmetrodontoides foxi	Symmetrodont			X									Brink 2015, 2016
	Tetraclaenodon puercensis	Condylarth						X						Maxwell et al. 1967
	Titanoides zeuxis	Pantodont						X						Schiebout 1974

PRIMITIVE AND ADVNCED MAMMALS

CLASS	TAXON	COMMON NAME	FORMATIONS											REFERENCES
			BO	PN	AG	JV	KBP	PgBP	HH	CN	CH	DE	BS	
MAMMALIA (Continued)														
PRIMITIVE AND ADVNCED MAMMALS	***Tricentes truncatus***	Condylarth						X	X					Hartnell 1980
	cf. *Triplopus*	Rhinoceros-Like									X			Wilson and Schiebout 1984; Runkel 1988
	Turgidodon* cf. *T. lillegraveni	Marsupial			X									Cifelli 1994
	***Turgidodon* n. sp. +**	Marsupial			X									Rowe et al. 1992
	?*Turgidodon* n. sp. +	Marsupial			X									Brink 2015; 2016
	Uintacyon scotti	Marten-Like									X			Maxwell et al. 1967
	?*Varalphadon* sp.	Marsupial			X									Brink 2015; 2016
	***Viridomys* n. sp. +**	Multituberculate						X						Standhardt 1986
	***Vulpes* sp.**	Canid											X	Stevens and Stevens 2003
	?*Zanycteris* sp.	Early Primate						X						Schiebout 1974
	HOLOTYPE = •													
	UNPUBLISHED NEW TAXON = Δ													
	UNNAMED NEW TAXON = +													
			Boquillas Formation	**Pen Formatrion**	**Aguja Formation**	**Javelina Formation**	**Cretaceous (K) Black Peaks Formation**	**Paleogene Black Peaks Formation**	**Hannold Hill Formation**	**Canoe Formation**	**Chisos Formation**	**Delaho Formation**	**Banta Shut-in Formation**	
			UPPER CRETACEOUS (K)					**PALEOGENE (Pg)**				**NEOGENE**		
			FORMATIONS											
MISCELLANEOUS	**THE FOLLOWING VERTEBRATE TAXA HAVE ALSO BEEN FOUND IN BIBE:**													
	Coprolites (fossil dung)	indet.	**Paleocene Black Peaks Formation**											Schiebout 1970
	Elephantidae indet.	Mammoth	**Pleistocene caliche-silt deposit (cienega lake)**											Eley 1938; Maxwell et al. 1967
	Osteichthyes indet.	Fish	**Sue Peaks Formation (Lower Cretaceous - marine)**											Tarasconi 2000
	Gymmogyps califwnianus	Condor	**Holocene deposits in cliffside grottos**											Wetmore and Friedmann 1933

* "*Lambdotherium*" originally identified in Maxwell 1967, p. 104. This specimen was later re-identified in 1975 as cf. *Phenacodus primaevus* or *grangeri* by J. A. Wilson as noted on the specimen card in the collections of the vert. paleo lab at U. T. Austin (specimen # TMM 40181-1). Verified on-site by S. Wick, 5-30-2012.
* Cooper et al. (current research) indicates taxa collected by Roger Cooper and colleagues, currently residing in the collections of the Texas Memorial Museum (copies of this record on file at BBNP). Please note that 'current research' may ultimately result in taxonomic revision.
* Udden 1907. Udden's identification of fossil taxa from Big Bend National Park (e.g. *Cloasaurus*) was based upon the information available at the time. Some of these may no longer be considered taxonomically valid or are in error based on continuing research but are herein included as they are contained iwithin a relevant paleontological report. Furthermore, in some cases, Udden does not specify exact provenience for all specimens reported. It is therefore possible that some taxa identified in his report wer found outside of today's Big Bend National Park in nearby areas.
* *Chasmosaurus marsicalensis* renamed *Agujaceratops mariscalensis* (see entry above).

(including several new species) and contributed immeasurably to our understanding of Late Cretaceous terrestrial ecosystem of southern North America (e.g., Standhardt 1986; Rowe et al. 1992; Sankey 2008, 2010; Nydam et al. 2013; Wick et al. 2015; Wick and Shiller 2020; Wick 2021a, b, c).

Another significant circumstance is that BIBE sits apart geographically from other regions in North America that have produced fossils of similar age and type (e.g., Late Cretaceous vertebrate fossil-bearing locations in northern Mexico, New Mexico, Montana, and southern Canada among others). This allows for the study of vertebrate faunas from an interregional standpoint to better define endemic faunal regions, taphonomic relationships, continental paleoenvironmental regimes, as well as evolutionary processes unique to one region versus another (sensu Lehman 1997, 2001).

Acknowledgements

The author is indebted to their colleagues at the Division of Science and Resource Management at Big Bend National Park (especially D. Corrick) for their friendship and support regarding this project as well as the earlier, more comprehensive inventory completed in 2015 – like this account, that work was also a labor of love. I thank M. Brown and J.C. Sagebiel of the Texas Vertebrate Paleontology Laboratory at the Jackson School Museum of Earth Sciences at The University of Texas at Austin for their longtime support of the author's paleontological endeavors and curation of many of the specimens reported herein. T. Lehman and T. Shiller II have provided very useful stratigraphic interpretations and entertaining insights over many paleontological excursions throughout the Big Bend of West Texas. J. Wick is offered an especially kind word of appreciation for supporting the paleontological and geological adventures of the author. The author thanks T. Shiller II and T. Adams for critical reviews that improved the manuscript.

After acceptance of the current work, the author was made aware of the recent discovery of the new pterosaur *Javelinadactylus sagebieli* n. gen. n. sp. from the Javelina Formation in Big Bend National Park (Campos 2021).

References

Abbot ML (1985) Petrified wood from the Paleocene, Black Peaks Formation, Big Bend National Park, Texas. Unpublished manuscript, Big Bend National Park archives, 61 pp.

Abbot ML (1986) Petrified wood from the Paleocene Black Peaks Formation, Big Bend National Park, Texas, Rohr DM (Ed.). In: Pausé PH, Spears RG (Eds) Geology of the Big Bend Area and Solitario dome, Texas. West Texas Geological Society 1986 Field Trip Guidebook, 86–82: 141–142.

Adams AL (2014) Stratigraphy and paleontology of Upper Cretaceous strata on the western Rosillos Mountains Ranch, Brewster County, Texas. Master's Thesis, Texas Christian University, Fort Worth, Texas. https://repository.tcu.edu/handle/116099117/6041

Adkins WS (1933) Mesozoic system in Texas. In: Sellards EH, Adkins WS, Plummer F (Eds) The geology of Texas, vol. 1, University of Texas Bulletin 3232, 240–518.

Anglen J, Lehman TM (2000) Habitat of the giant crocodilian *Deinosuchus*, Aguja Formation (Upper Cretaceous) Big Bend National Park, Texas. Journal of Vertebrate Paleontology 20(3): 26A.

Anglen J (2001) A vertebrate bone-bed in the Aguja Formation (Upper Cretaceous) Big Bend National Park, Texas. Master's Thesis, Texas Tech University, Lubbock, Texas, 91 pp.

Applegate SP (1972) A revision of the higher taxa of orectolobids. Marine Biological Association of India Publication 14: 743–751.

Ashmore RA (2003) Foraminiferal biostratigraphy and petrography of the lower Pen Formation (Upper Cretaceous) Big Bend region, Trans-Pecos Texas. Master's Thesis, Texas Tech University, Lubbock, Texas.

Baghai NL (1994) Classification and analysis of palynomorphs of the Aguja Formation (Campanian) Big Bend National Park, Brewster County, Texas. Gulf Coast Association of Geological Societies, Transactions 44: 63–70.

Baghai NL (1996) An analysis of palynomorphs from Upper Cretaceous sedimentary rocks with emphasis on the Aguja Formation, Big Bend National Park, Brewster County, Texas. Ph.D. Dissertation, The University of Texas at Austin, Austin, Texas.

Baghai NL (1998) Reconstructing paleoecology and paleoclimatology from Campanian plant megafossils and dispersed cuticles, Big Bend National Park, Texas. In: Hunter RA (Ed.) Tate '98 – Life in the Cretaceous. Tate Geological Museum Guidebook no. 3, Field Conference, June 5 – June 7, 1998, 35–44.

Baghai-Riding NL, DiBenedetto JN (2001) An unusual dinosaur coprolite from the Campanian Aguja Formation, Texas. Transactions of the Gulf Coast Association of Geological Societies 51: 9–20.

Baker CL, Bowman WF (1917) Geologic exploration of the southeastern Front Range Of Trans-Pecos Texas. University of Texas Bulletin 1753, 172 pp.

Beatty HL (1992) Fluvial sedimentology and sandstone petrography of the Hannold Hill Formation (Eocene) Big Bend, Texas. Texas Tech University, Master's Thesis, Texas Tech University, Lubbock, Texas.

Befus KS, Hanson RE, Lehman TM, Griffin WR (2008) Cretaceous basaltic phreatomagmatic volcanism in West Texas: Maar complex at Pena Mountain, Big Bend National Park, Texas. Journal of Volcanology and Geothermal Research 173: 245–264. https://doi.org/10.1016/j.jvolgeores.2008.01.021

Bell Jr GL (1995) Middle Turonian (Cretaceous) mosasauroids. National Park Service, Big Bend, Texas. Paleontological Research vol. 2, Technical Report NPS/NRPO/NRTR-93/11.

Bell Jr GL, Barnes KR, Polcyn MJ (2013) Late Cretaceous mosasauroids (Reptilia, Squamata) of the Big Bend region in Texas, USA. Earth and Environmental Science Transactions of the Royal Society of Edinburgh 103: 1–11. https://doi.org/10.1017/S1755691013000406

Bengston P (1988) Open Nomenclature. Palaeontology 31: 223–227.

Bird RT (1985) Bones for Barnum Brown. Texas Christian University Press, Fort Worth, 226 pp.

Blakey RC, Ranney WD (2018) Ancient Landscapes of Western North America: a Geologic History with Paleogeographic Maps. Springer, Cham, Switzerland, 228 pp. https://doi.org/10.1007/978-3-319-59636-5

Boreske J (1974) A review of the North American fossil amiid fishes. Museum of Comparative Zoology Bulletin 146: 1–87.

Bostik WC (1960) Micropaleontology of the upper Eagle Ford and lower Austin groups, Big Bend National Park, Texas. M.A. thesis, Texas Technical College, Lubbock, Texas.

Brink AA (2015) An early Campanian mammalian fauna from the Big Bend Region off Texas. Society of Vertebrate Paleontology Annual Meeting October 2015, Program and Abstracts 96.

Brink AA (2016) An early Campanian (Late Cretaceous) mammalian fauna from the lower shale member of the Aguja Formation in the Big Bend region of Texas. Ph.D. Dissertation, Texas Tech University, Lubbock, Texas. https://ttu-ir.tdl.org/handle/2346/73722?show=fullandlocale-attribute=es

Brochu CA (2000) *Borealosuchus* (Crocodylia) from the Paleocene of Big Bend National Park, Texas. Journal of Paleontology 74: 181–187. https://doi.org/10.1666/0022-3360(2000)074<0181:BCFTPO>2.0.CO;2

Busbey AB III, Lehman TM [Eds] (1989) Vertebrate Paleontology, Biostratigraphy and Depositional Environments, Latest Cretaceous and Tertiary, Big Bend Area, Texas. Guidebook field trip nos. 1a, b, c. Society of Vertebrate Paleontology 49th annual meeting, Austin, Texas, 90 pp.

Busbey III AB (1989) Santa Elena Canyon. In: Busbey III AB, Lehman TM (Eds) Vertebrate paleontology, biostratigraphy and depositional environments, latest Cretaceous and Tertiary, Big Bend area, Texas. Guidebook field trip nos. 1a, b, c. Society of Vertebrate Paleontology 49th annual meeting, Austin, Texas, 27–27.

Campos HBN (2021) A new azhdarchoid pterosaur from the Late Cretaceous Javelina Formation of Texas. Biologia. https://doi.org/10.1007/s11756-021-00841-7

Chang SW (1973) Petrified wood from the Paleocene, Black Peaks Formation, Big Bend National Park, Texas. Master's Thesis, Sul Ross State University, Alpine, Texas.

Cifelli RL (1994) Therian mammals of the Terlingua local fauna (Judithian) Aguja Formation, Big Bend of the Rio Grande, Texas. University of WyomIng Contributions to Geology 30: 117–136.

Colbert RH, Bird RT (1954) A gigantic crocodile from the Upper Cretaceous beds of Texas. American Museum of Natural History Novitates 1688.

Coombs WP (1978) The families of the ornithischian dinosaur order Ankylosauria. Paleontology 21: 143–170.

Cooper DS, Cooper RW, Stevens JB, Stevens MS, Cobban WA, Walaszczyk I (2017) The Boquillas Formation of the Big Bend National Park, Texas, USA, a reference Cenomanian through Santonian (Upper Cretaceous) carbonate succession at the southern end of the Western Interior Seaway. Acta Geologica Polonica 67: 547–565. https://doi.org/10.1515/agp-2017-0033

Coulson AB (1998) Sedimentology and taphonomy of a juvenile *Alamosaurus* site in the Javelina Formation (Upper Cretaceous) Big

Bend National Park, Texas. Master's Thesis, Texas Tech University, Lubbock, Texas.

Davies K (1983) Hadrosaurian dinosaurs of Big Bend National Park, Brewster Co., Texas. Master's Thesis, The University of Texas at Austin, Austin, Texas.

Davies KL, Lehman TM (1989) The WPA quarries. In: Busbey III AB, Lehman TM (Eds) Vertebrate paleontology, biostratigraphy and depositional environments, latest Cretaceous and Tertiary, Big Bend Area, Texas. Guidebook field trip nos. 1a, b, c. Society of Vertebrate Paleontology 49th annual meeting, Austin, Texas, 32–42.

Dorf E (1939) Fossil Plants from the Upper Cretaceous Aguja Formation of Texas. American Museum Novitates 1015: 1–9.

Eley HM (1938) The Invertebrate Paleontology of the Big Bend Park, Marathon, Texas. Master's Thesis, The University of Oklahoma, Norman, Oklahoma.

Folk RL, McBride EF (1978) Origin of the Caballos Novaculite. In: Mazzullo SJ (Ed.) Tectonics and Paleozoic facies of the Marathon geosyncline, West Texas: Permian Basin Section, SEPM, Publication 78-17: 101–130.

Forster CA, Sereno PC, Evans TW, Rowe T (1993) A complete skull of *Chasmosaurus mariscalensis* (Dinosauria: Ceratopsidae) from the Aguja Formation (late Campanian) of west Texas. Journal of Vertebrate Paleontology 13: 161–170. https://doi.org/10.1080/02724634.1993.10011498

Fronimos JA (2010) Skeletal morphology and pneumaticity of the Late Cretaceous titanosaur *Alamosaurus sanjuanensis*, Big Bend National Park, Texas. Master's Thesis, Texas Tech University, Lubbock, Texas.

Fry KO (2015) Lithofacies, biostratigraphy, chemostratigraphy, and stratal architecture of the Boquillas Formation and Eagle Ford Group: a comparison of outcrop and core data from Big Bend National Park to Maverick Basin, southwest Texas, USA. Master's Thesis, The University of Texas at Austin, Austin Texas.

Gingerich PD (1976) Cranial anatomy and evolution of early Tertiary Plesiadapidae (Mammalia, Primates). University of Michigan Museum of Paleontology Papers on Paleontology 15: 1–141.

Gingerich PD (1979) *Lambertocvon eximius* a new arctocyonid (Mammalia, Condylarthra) from the Late Paleocene of western North America. Journal of Paleontology 53: 524–529.

Hartnell JA (1980) The vertebrate paleontology, depositional environment, and sandstone provenance of early Eocene rocks on Tornillo Flat, Big Bend National Park, Brewster County, Texas. Master's Thesis, Louisiana State University, Baton Rouge, Louisiana.

Henry CD, Price JG, Miser DE (1989) Geology and Tertiary igneous activity of the Hen Egg Mountain and Christmas Mountains quadrangles, Big Bend Region, Trans-Pecos Texas. University of Texas at AustIn, Bureau of Economic Geology, Report of Investigations 183, 105 pp. https://doi.org/10.23867/RI0183D

Hill RT, Vaughn TW (1898) Geology of the Edwards Plateau and Rio Grande Plain adjacent to Austin and San Antonio, Texas, with reference to the occurrences of underground waters. Eighteenth annual report of the Director of the U. S. Geological Survey for the year 1896–1897, Part II: 193–321.

Hill RT (1891) The Comanche series of the Texas-Arkansas region. Bulletin of the Geological Society of America 2: 503–528. https://doi.org/10.1130/GSAB-2-503

Huffman ME (1960) Micropaleontology of the lower portion of the Boquillas Formation Near Hot Springs, Big Bend National Park, Brewster County, Texas. Master's Thesis, Texas Technical College, Lubbock, Texas.

Hunt RK, Lehman TM (2008) Attributes of the ceratopsian dinosaur *Torosaurus*, and new material from the Javelina Formation (Maastrichtian) of Texas. Journal of Paleontology 82: 1127–1138. https://doi.org/10.1666/06-107.1

Kellner AWA, Langston Jr W (1996) Cranial remains of *Quetzalcoatlus* (Pterosauria, Azhdarchidae) from Late Cretaceous sediments of Big Bend National Park, Texas. Journal of Vertebrate Paleontology 16: 222–231. https://doi.org/10.1080/02724634.1996.10011310

King PB (1937) Geology of the Marathon Region, Texas. U.S. Geological Survey Professional Paper 187, 148 pp. https://doi.org/10.3133/pp187

Langston Jr W (1981) Pterosaurs. Scientific American 244: 122–136. https://doi.org/10.1038/scientificamerican0281-122

Langston Jr W (1986) Rebuilding the world's biggest flying creature: the second coming of *Quetzalcoatlus northropi*. In: Pausé PH, Spears RG (Eds) Geology of the Big Bend Area and Solitario dome, Texas. West Texas Geological Society 1986 Field Trip guidebook 86–82: 125–128.

Langston Jr W, Standhardt B, Stevens M (1989) Fossil vertebrate collecting in the Big Bend – history and retrospective. In: Busbey III AB, Lehman TM (Eds) Vertebrate Paleontology, Biostratigraphy and Depositional Environments, Latest Cretaceous and Tertiary, Big Bend Area, Texas. Guidebook field trip nos. 1a, b, c. Society of Vertebrate Paleontology 49th annual meeting, Austin, Texas, 11–21.

Lawson DA (1972) Paleoecology of the Tornillo Formation, Big Bend National Park, Brewster County, Texas. Master's Thesis, The University of Texas at Austin, Austin, Texas.

Lawson D A (1975) Pterosaur from the Latest Cretaceous of West Texas: Discovery of the largest flying creature. Science 87: 947–948. https://doi.org/10.1126/science.187.4180.947

Lawson DA (1976) *Tyrannosaurus* and *Torosaurus*, Maastrichtian dinosaurs from Trans-Pecos Texas. Journal of Paleontology 50: 158–164.

Lehman TM (1982) A ceratopsian bone bed from the Aguja Formation (Upper Cretaceous) Big Bend National Park, Texas. Master's Thesis, The University of Texas at Austin, Austin, Texas.

Lehman TM (1985) Sedimentology, stratigraphy, and paleontology of Upper Cretaceous (Campanian Maastrichtian) sedimentary rocks in Trans-Pecos Texas. Ph.D. dissertation, University of Texas at Austin, Austin, Texas.

Lehman TM (1986) Late Cretaceous sedimentation in Trans-Pecos Texas. In Pausé PH, Spears RG (Eds) Geology of the Big Bend Area and Solitario Dome, Texas. West Texas Geological Society 1986 Field Trip Guidebook 86–82: 105–100.

Lehman TM (1989a) *Chasmosaurus mariscalensis*, sp. nov., a new ceratopsian dinosaur from Texas. Journal of Vertebrate Paleontology 9: 137–162. https://doi.org/10.1080/02724634.1989.10011749

Lehman TM (1989b) Hot Springs. In: Busbey III AB, Lehman TM (Eds) Vertebrate paleontology, biostratigraphy and depositional environments, latest Cretaceous and Tertiary, Big Bend Area, Texas. Guidebook field trip nos. 1a, b, c. Society of Vertebrate Paleontology 49th annual meeting, Austin, Texas, 30–31.

Lehman TM (1997) Late Campanian dinosaur biogeography in the Western Interior of North America. Dinofest International, Philadelphia, The Academy of Natural Sciences, 223–240.

Lehman TM (2001) Late Cretaceous dinosaur provinciality. In: Tanke DH, Carpenter K (Eds) Mesozoic Vertebrate Life. Indiana University Press, 310–328.

Lehman TM (2010) Pachycephalosauridae from the San Carlos and Aguja Formations (Upper Cretaceous) of west Texas, and observations of the frontoparietal dome. Journal of Vertebrate Paleontology 30: 786–798. https://doi.org/10.1080/02724631003763532

Lehman TM, Busbey III AB (2007) Big Bend Field Trip Guidebook. Society of Vertebrate Paleontology, 67th Annual Meeting, Austin, Texas, 69 pp.

Lehman TM, Coulson AB (2002) A juvenile specimen of the sauropod dinosaur *Alamosaurus sanjuanensis* from the Upper Cretaceous of Big Bend National Park, Texas. Journal of Paleontology 76: 156–172. https://doi.org/10.1666/0022-3360(2002)076%3C0156:AJSOTS%3E2.0.CO;2

Lehman TM, Langston Jr W (1996) Habitat and behavior of *Quetzalcoatlus*: paleoenvironmental reconstruction of the Javelina Formation (Upper Cretaceous) Big Bend National Park, Texas. Journal of Vertebrate Paleontology, Abstracts of Papers 16(Sup. 3): 48A. https://doi.org/10.1080/02724634.1996.10011371

Lehman TM, Shiller II TA (2020) An angiosperm woodland in the Javelina Formation (Upper Cretaceous), Big Bend National Park, Texas, U.S.A. Cretaceous Research 115: 104569. https://doi.org/10.1016/j.cretres.2020.104569

Lehman TM, Tomlinson SL (2004) *TerlInguachelys fischbecki*, a new genus and species of sea turtle (Chelonoiodea; Protostegidae) from the Upper Cretaceous of Texas. Journal of Paleontology 78: 1163–1178. https://doi.org/10.1666/0022-3360(2004)078%3C1163:TFANGA%3E2.0.CO;2

Lehman TM, Wheeler EA (2001) A fossil dicotyledonous woodland forest from the Upper Cretaceous of Big Bend National Park, Texas. Palaios 16: 102–108. https://doi.org/10.1669/0883-1351(2001)016%3C0102:AFDWFF%3E2.0.CO;2

Lehman TM, Wick SL (2010) *Chupacabrachelys complexus*, n. gen. n. sp. (Testudines: Bothremydidae) from the Aguja Formation (Campanian) of west Texas. Journal of Vertebrate Paleontology 30: 1709–1725. https://doi.org/10.1080/02724634.2010.520782

Lehman TM, Wick SL (2012) Tyrannosaurian dinosaurs from the Aguja Formation (Upper Cretaceous) of Big Bend National Park, Texas. Proceedings of the Royal Society of Edinburgh 103: 471–485. https://doi.org/10.1017/S1755691013000261

Lehman TM, McDowell F, Connelly J (2006) First isotopic (U-Pb) age for the Late Cretaceous *Alamosaurus* vertebrate fauna of West Texas, and its significance as a link between two faunal provinces. Journal of Vertebrate Paleontology 26: 922–928. https://doi.org/10.1671/0272-4634(2006)26[922:FIUAFT]2.0.CO;2

Lehman TM, Wick SL, Wagner JR (2016) Hadrosaurian dinosaurs from the Maastrichtian Javelina Formation, Big Bend National Park, Texas. Journal of Paleontology 90: 333–356. https://doi.org/10.1017/jpa.2016.48

Lehman TM, Wick SL, Barnes KR (2017) New specimens of horned dinosaurs from the Aguja Formation of West Texas, and a revision of *Agujaceratops*. Journal of Systematic Palaeontology 15: 641–674. https://doi.org/10.1080/14772019.2016.1210683

Lehman TM, Wick SL, Beatty HL, Straight WH, Wagner JR (2018) Stratigraphy and depositional history of the Tornillo Group (Upper Cretaceous–Eocene) of West Texas. Geosphere 14: 2206–2244. https://doi.org/10.1130/GES01641.1

Lehman TM, Wick SL, Brink AA, Shiller II TA (2019) Stratigraphy and vertebrate fauna of the lower shale member of the Aguja Formation (early Campanian) in West Texas. Cretaceous Research 99: 291–314. https://doi.org/10.1016/j.cretres.2019.02.028

Linnert C, Robinson SA, Lees JA, Brown PR, Pérez-Rodríguez I, Petrizzo MR, Falzoni F, Littler K, Antonío Arz A, Russell EE (2014) Evidence for global cooling in the Late Cretaceous. Nature Communications 5: e4194. https://doi.org/10.1038/ncomms5194

Longrich N, Sankey JT, Tanke D (2010) *Texacephale langstoni*, a new genus of pachycephalosaurid (Dinosauria: Ornithischia) from the upper Campanian Aguja Formation, southern Texas, USA. Cretaceous Research 31: 274–284. https://doi.org/10.1016/j.cretres.2009.12.002

Longrich NR, Barnes K, Clark S, Millar L (2013) Caenagnathidae from the Upper Campanian Aguja Formation of West Texas, and a Revision of the Caenagnathinae. Bulletin of the Peabody Museum of Natural History 54: 23–49. https://doi.org/10.3374/014.054.0102

Lucas SG, Sullivan RM, Hunt AP (2006) Re-evaluation of *Pentaceratops* and *Chasmosaurus* (Orithischia, Ceratopsidae) in the Upper Cretaceous of the Western Interior. New Mexico Museum of Natural History and Science Bulletin 35: 367–370.

Manchester SR, Lehman TM, Wheeler EA (2010) Fossil palms (Arecacea, Coryphoideae) associated with juvenile herbivorous dinosaurs in the Upper Cretaceous Aguja Formation, Big Bend National Park, Texas. International Journal of Plant Sciences 171: 679–689. https://doi.org/10.1086/653688

Mauldin RA (1985) Foraminiferal biostratigraphy, paleoecology, and correlation of the Del Rio Clay (Cenomanian) from Big Bend National Park, Brewster County, Texas, to the Cerro Muleros area, Dona Ana County, New Mexico. Master's Thesis, The University of Texas at El Paso, El Paso Texas.

Maxwell RA, Lonsdale JT, Hazzard RT, Wilson JA (1967) Geology of Big Bend National Park, Brewster County, Texas. University of Texas Bureau of Economic Geology Publication 6711, 320 pp.

McNulty CL, Slaughter BH (1972) The Cretaceous selachian genus *Ptychotrygon* Jaekel 1894. Ecologae Geologicae Helvetiae 65: 647–655.

Miller MS (1997) Squamates of the Campanian Terlingua Local Fauna, Brewster County, Texas. Master's Thesis, The University of Texas at Austin, Austin, Texas.

Mosley JL (1992) The paleoecology and biostratigraphy of the McKinney Springs Tongue of the Pen Formation (Late Cretaceous) Big Bend National Park, Texas. Master's Thesis, Texas Tech University, Lubbock Texas.

Montgomery H, Clark S (2016) Paleoecology of the Gaddis site in the Upper Cretaceous Aguja Formation, Terlingua, Texas. Palaios 31: 1–11. https://doi.org/10.2110/palo.2015.099

Nydam RL, Rowe TB, Cifelli RL (2013) Lizards and snakes of the Terlingua Local fauna (late Campanian) Aguja Formation, Texas, with comments on the distribution of paracontemporaneous squamates throughout the Western Interior of North America. Journal of Vertebrate Paleontology 33: 1081–1099. https://doi.org/10.1080/02724634.2013.760467

Page WR, Turner KJ, Bohannon RG (2008) Tectonic history of Big Bend National Park. In: Gray JE, Page WR (Eds) Geological, Geochemical, and Geophysical Studies by the U.S. Geological Survey in Big Bend National Park, Texas. U.S. Geological Survey Circular, 1327, 5–13. https://doi.org/10.3133/cir1327

Record RS (1988) Paleoenvironmental analysis of coastal marsh deposits in the Aguja Formation, Late Cretaceous, Trans-Pecos Texas. Master's Thesis, Texas Tech University, Lubbock, Texas.

Rigsby CA (1986) The Big Yellow Sandstone: a sandy braided stream. In: Pausé PH, Spears RG (Eds) Geology of the Big Bend Area and Solitario Dome, Texas. West Texas Geological Society 1986 Field Trip Guidebook 86-82: 111–115.

Rohr DM, Boucot AJ, Miller J, Abbot M (1986) Oldest evidence of wood damage by termites from the Upper Cretaceous of Big Bend National Park, Texas. In: Pausé PH, Spears RG (Eds) Geology of the Big Bend Area and Solitario dome, Texas. West Texas Geological Society 1986 Field Trip guidebook, 86-82, 139–140.

Rowe T, Cifelli RL, Lehman TM, Weil A (1992) The Campanian Terlingua local fauna, with a summary of other vertebrates from the Aguja Formation, Trans-Pecos Texas. Journal of Vertebrate Paleontology 12: 472–493. https://doi.org/10.1080/02724634.1992.10011475

Runkel AC (1988) Stratigraphy, sedimentology, and vertebrate paleontology of Eocene rocks, Big Bend region, Texas. Ph.D. Dissertation, University of Texas at Austin, Austin, Texas.

Sanders RB (1988) Sedimentology and isotope geochemistry of the Upper Cretaceous Ernst Member of the Boquillas Formation, Big Bend National Park, Texas. Master's Thesis, Texas Tech University, Lubbock, Texas.

Sankey JT (1998) Vertebrate paleontology and magnetostratigraphy of the upper Aguja Formation (Late Campanian) Talley Mountain area, Big Bend National Park, Texas. Ph.D. dissertation, Louisiana State University, Baton Rouge, Louisiana.

Sankey JT (2001) Late Campanian southern dinosaurs, Aguja Formation, Big Bend, Texas. Journal of Paleontology 75: 208–215. https://doi.org/10.1666/0022-3360(2001)075%3C0208:LCSDAF%3E2.0.CO;2

Sankey JT (2005) Late Cretaceous vertebrate paleoecology of Big Bend National Park, Texas. In: Braman DR, Therrien F, Koppelhus EB, Taylor W (Eds) Dinosaur Park Symposium, Royal Tyrrell Museum Special Publication, 98–106.

Sankey JT (2006) Turtles of the upper Aguja Formation (Late Campanian) Big Bend National Park, Texas. In: Lucas, SG, Sullivan RM (Eds) Late Cretaceous vertebrates from the Western Interior. New Mexico Museum of Natural History Bulletin 35: 235–243.

Sankey JT (2008) Vertebrate paleoecology from microsites, upper Aguja Formation (Late Cretaceous) Big Bend National Park, Texas. In: Sankey JT, Baszio S (Eds) The Unique Role of Vertebrate Microfossil Assemblages. In: Paleoecology and Paleobiology. Indiana University Press, Bloomington, 61–77.

Sankey JT (2010) Faunal composition and significance of high-diversity, mixed bonebeds containing *Agujaceratops mariscalensis* and other dinosaurs, Aguja Formation (Upper Cretaceous) Big Bend, Texas. In: Ryan MJ, Chinnery-Allgier BJ, Eberth DA (Eds) New Perspectives on Horned Dinosaurs, Indiana University Press, Bloomington, 520–537.

Sankey JT, Gose W (2001) Late Cretaceous mammals and magnetostratigraphy, Big Bend, Texas. Occasional Papers of the Museum of Natural Science, Louisiana State University 77: 1–16. https://doi.org/10.31390/opmns.077

Schiebout JA (1970) Sedimentology of Paleocene Black Peaks Formation, western Tornillo Flat, Big Bend National Park, Texas. Master's Thesis, The University of Texas at Austin, Austin, Texas.

Schiebout JA (1973) Vertebrate paleontology and paleoecology of Paleocene Black Peaks Formation, Big Bend National Park, Texas. Ph.D. dissertation, University of Texas at Austin, Austin, Texas.

Schiebout JA (1974) Vertebrate paleontology and paleoecology of Paleocene Black Peaks Formation, Big Bend National Park, Texas. Texas Memorial Museum Bulletin 24, 88 pp.

Schubert JA, Wick SL, Lehman TM (2017) An Upper Cretaceous (middle Campanian) marine chondrichthyan and osteichthyan fauna from the Rattlesnake Mountain sandstone member of the Aguja Formation in West Texas. Cretaceous Research 69: 6–33. https://doi.org/10.1016/j.cretres.2016.08.008

Schwimmer DR (2002) King of the Crocodylians: The Paleobiology of *Deinosuchus*. Indiana University Press, Bloomington, Indiana, 220 pp.

Standhardt BR (1986) Vertebrate paleontology of the Cretaceous/Tertiary transition of Big Bend National Park, Texas. Ph.D. Dissertation, Louisiana State University, Baton Rouge, Louisiana.

Standhardt BR (1989) [In: Langston Jr W, Standhardt B, Stevens M]Fossil Vertebrate Collecting in the Big Bend (appendix). In: Busbey III AB, Lehman TM (Eds) Vertebrate Paleontology, Biostratigraphy and Depositional Environments, Latest Cretaceous and Tertiary, Big Bend Area, Texas. Guidebook field trip nos. 1a, b, c. Society of Vertebrate Paleontology 49th annual meeting, Austin, Texas, 11–18.

Standhardt BR (1995) Early Paleocene (Puercan) vertebrates of the Dogie locality, Big Bend National Park, Texas. In: Santucci VL, McClelland L (Eds) National Park Service paleontological research vol. 2, Technical Report NPS/ NRPO/NRTR-93/11.

Stevens JB, Stevens MS (1985) Basin and range deformation and depositional timing, Trans-Pecos Texas. In: Dickerson PW, Muehlberger WR (Eds) Structure and tectonics of Trans-Pecos Texas. Field Conference Guidebook, West Texas Geological Society Publication 85-81: 157–164.

Stevens JB, Ashmore RA, Doornbos LC, Reed DA, Stevens MS (1995) Faunal change in cyclic deposits of the Late Coniacian-Early Santonian, Terlingua Group, Big Bend National Park, Trans-Pecos, Texas. Geological Society of America abstracts with programs 27(6): A176.

Stevens MS (1977) Further study of Castolon Local Fauna (early Miocene) Big Bend National Park, Texas. Texas Memorial Museum, Pearce-Sellards Series 28, 70 pp.

Stevens MS, Stevens JB (1989) Neogene – Quaternary deposits and vertebrate faunas, Trans-Pecos, Texas. In: Busbey III AB, Lehman TM (Eds) Vertebrate Paleontology, Biostratigraphy and Depositional Environments, Latest Cretaceous and Tertiary, Big Bend Area, Texas. Guidebook field trip nos. 1a, b, c, Society of Vertebrate Paleontology 49th annual meeting, Austin, Texas, 67–90.

Stevens MS, Stevens JB (2003) Carnivora (Mammalia, Felidae, Canidae, and Mustelidae) from the earliest Hemphillian Screw Bean Local Fauna, Big Bend National Park, Brewster County, Texas. In: Flynn LJ (Ed.) Vertebrate Fossils and their Context. American Museum of Natural History Bulletin 279: 177–211. https://doi.org/10.1206/0003-0090(2003)279%3C0177:C%3E2.0.CO;2

Stevens MS, Stevens JB, Dawson MR (1969) New early Miocene formation and vertebrate local fauna, Big Bend National Park, Brewster County, Texas. The University of Texas at Austin, Texas Memorial Museum Pearce-Sellards Series 15, 53 pp.

Strain WS (1940) Report on works progress administration paleontological project sponsored by the Texas College of Mines and Met-

allurgy. W.P.A. progress report for W.P.10106/0.P. 465-66-3-374. Unpublished, Big Bend National Park archives, 21 pp.

Tarasconi M (2000) Palaeoecology and facies development of the mid-Cretaceous (Comanchean) of Big Bend National Park, Texas, U.S.A. Ph.D. dissertation, University of Erlangen, Nuremburg, Germany.

Tiedemann NS (2010) The sequence stratigraphy of the Commanchean – Gulfian interval, Big Bend National Park, West Texas. Master's Thesis. Ball State University, Muncie, Indiana.

Turner KJ, Berry ME, Page WR, Lehman TM, Bohannon RG, Scott RB, Miggins DP, Budahn JR, Cooper RW, Drenth BJ, Anderson ED (2011) Geologic map of Big Bend National Park, Texas. U.S. Geological Survey Scientific Investigations, Map 3142, scale 1:75,000, pamphlet, 84 pp. https://pubs.usgs.gov/sim/3142/

Tykoski RS, Fiorillo AR (2016) An articulated cervical series of *Alamosaurus sanjuanensis* Gilmore, 1922 (Dinosauria, Sauropoda) from Texas: new perspective on the relationships of North America's last giant sauropod. Journal of Systematic Palaeontology 15: 339–364. https://doi.org/10.1080/14772019.2016.1183150

Udden JA (1907) A sketch of the geology of the Chisos country, Brewster County, Texas. University of Texas Bureau of Economic Geology Bulletin 93, 101 pp.

Udden JA, Baker CL, Böse E (1916) Review of the geology of Texas. University of Texas Bulletin 44, 164 pp.

Upchurch P, Barrett PM, Dodson P (2004) Sauropoda. In: Weishample DB, Dodson P, Osmólska H (Eds) The Dinosauria (2nd edn.). University of California Press, Berkley, 259–322. https://doi.org/10.1525/california/9780520242098.003.0015

Vaughan TW (1900) Reconnaissance in the Rio Grande coal fields of Texas. U.S. Geological Survey Bulletin 164, 100 pp.

Waggoner KJ (2006) Sutural form and shell morphology of *Placenticeras*, and systematic descriptions of Late Cretaceous ammonites from the Big Bend region. Ph.D. dissertation, Texas Tech University, Lubbock, Texas.

Wagner JR, Lehman TM (2001) A new species of *Kritosaurus* from the Cretaceous of Big Bend National Park, Brewster County, Texas. Journal of Vertebrate Paleontology 21: 110–111A.

Wagner JR, Lehman TM (2009) An enigmatic new lambeosaurine hadrosaur (Reptilia: Dinosauria) from the upper shale member of the Campanian Aguja Formation of Trans-Pecos Texas. Journal of Vertebrate Paleontology 29: 605–611. https://doi.org/10.1671/039.029.0208

Welsh E, Sankey JT (2008) First dinosaur eggshells from Texas: Aguja Formation (late Campanian) Big Bend National Park. In: Sankey JT, Baszio S (Eds) The unique role of vertebrate microfossil assemblages in paleoecology and paleobiology. Indiana University Press, Bloomington, 166–177.

Wetmore A, Friedmann H (1933) The California condor in Texas. The Condor 35: 37–38. https://doi.org/10.2307/1363436

Wheeler EA, Lehman TM (2000) Late Cretaceous woody dicots from the Aguja and Javelina Formations, Big Bend National Park, Texas, USA. International Association of Wood Anatomists Journal 21: 83–120. https://doi.org/10.1163/22941932-90000239

Wheeler EA, Lehman TM (2005) Upper Cretaceous – Paleocene conifer woods from Big Bend National Park, Texas. Palaeogeography, Palaeoclimatology, Palaeoecology 226: 233–258. https://doi.org/10.1016/j.palaeo.2005.05.014

Wheeler EA, Lehman TM (2009) New late Cretaceous and Paleocene dicot woods of Big Bend National Park, Texas, and review of Cretaceous wood characteristics. IAWA Journal 30: 293–318. https://doi.org/10.1163/22941932-90000220

Wheeler EA, Lehman TM, Gasson PE (1994) *Javelinoxylon*, an Upper Cretaceous dicotyledonous tree from Big Bend National Park, Texas, with presumed malvalean affinities. American Journal of Botany 81: 703–710. https://doi.org/10.1002/j.1537-2197.1994.tb15504.x

Wheeler EA (1991) Paleocene dicotyledonous trees from Big Bend National Park, Texas: variability in wood types common in the Late Cretaceous and Early Tertiary, and ecological inferences. American Journal of Botany 78: 658–671. https://doi.org/10.2307/2445087

White RA (2019) Stratigraphy of the Ernst Member of the Upper Cretaceous Boquillas Formation, Black Gap Wildlife Management Area, Brewster County, Texas. Master's Thesis, Texas Christian University, Fort Worth, Texas.

Wick SL (2014) New evidence for the occurrence of *Tyrannosaurus* in West Texas, and discussion of Maastrichtian tyrannosaurid dinosaurs from Big Bend National Park. Cretaceous Research 50: 52–58. https://doi.org/10.1016/j.cretres.2014.03.010

Wick SL (2021a) Albanerpetontids (Lissamphibia, Albanerpetontidae) from the Aguja Formation (early Campanian) and first report of *Albanerpeton galaktion* in West Texas. Canadian Journal of Earth Sciences 58(2): 141–149. https://doi.org/10.1139/cjes-2020-0071

Wick SL (2021b) Fossil frogs from the early Campanian of West Texas with comments on Late Cretaceous anuran diversity in southern Laramidia. Palaeobiodiversity and Palaeoenvironments. https://doi.org/10.1007/s12549-021-00481-4

Wick SL (2021c) New early Campanian characiform fishes (Otophysi: Characiformes) from West Texas support a South American origin for known North American characiforms from North America. Cretaceous Research 128: 104993. https://doi.org/10.1016/j.cretres.2021.104993

Wick SL, Corrick DW (2015) Paleontological Inventory of Big Bend National Park, Texas: the place, the people, and the fossils. Big Bernd National Park Division of Science and Resource Management internal technical document, unpublished, 200 pp.

Wick SL, Lehman TM (2014) A complete titanosaur femur from West Texas with comments regarding hindlimb posture. Cretaceous Research 49: 39–44. https://doi.org/10.1016/j.cretres.2014.02.003

Wick SL, Shiller II TA (2020) New taxa among a remarkably diverse assemblage of fossil squamates from the Aguja Formation (Lower Campanian) of West Texas. Cretaceous Research 114: 104516. https://doi.org/10.1016/j.cretres.2020.104516

Wick SL, Lehman TM (2013) A new ceratopsian dinosaur from the Javelina Formation (Maastrichtian) of West Texas, and implications for chasmosaurine phylogeny. The Science of Nature 100: 667–682. https://doi.org/10.1007/s00114-013-1063-0

Wick SL, Lehman TM, Brink AA (2015) A theropod tooth assemblage from the lower Aguja Formation (early Campanian) of West Texas, and the roles of small theropod and varanoid lizard mesopredators in a tropical predator guild. Palaeogeography, Palaeoclimatology, Palaeoecology 418: 229–244. https://doi.org/10.1016/j.palaeo.2014.11.018

Wilson JA, Runkel AC (1989) Field guide to the Paleogene stratigraphy and vertebrate paleontology of the Big Bend region. In: Busbey III AB, Lehman TM (Eds) Vertebrate Paleontology, Biostratigraphy and Depositional Environments, Latest Cretaceous and Tertiary, Big Bend Area, Texas. Guidebook field trip nos. 1a, b, c. Society of Vertebrate Paleontology 49th annual meeting, Austin, Texas, 47–59.

Wilson JA, Schiebout JA (1984) Early Tertiary vertebrate faunas, Trans-Pecos Texas: Ceratomorpha less Amynodontidae. Pearce-Sellards Series 39, 47 pp.

Wilson JA (1967) Early Tertiary mammals. In: Maxwell RA, Lonsdale JT, Hazzard RT, Wilson JA (Eds) Geology of Big Bend National Park, Brewster County, Texas. University of Texas Bureau of Economic geology Publication 6711: 157–169.

Wilson JA (1977) Early Tertiary vertebrate faunas, Big Bend area, Trans-Pecos, Texas: Brontotheriidae. Pearce-Sellards Series 25, 15 pp.

Woodward HN, Lehman TM (2009) Bone histology and microanatomy of *Alamosaurus sanjuanensis* (Sauropoda: Titanosauria) from the Maastrichtian of Big Bend National Park, Texas. Journal of Vertebrate Paleontology 29: 807–821. https://doi.org/10.1671/039.029.0310

Woodward HN (2005) Bone histology of the titanosaurid sauropod *Alamosaurus sanjuanensis* from the Javelina Formation, Texas. Journal of Vertebrate Paleontology 25(3): 132A.

Young K (1963) Upper Cretaceous ammonites from the Gulf Coast of the United States. University of Texas at Austin, Bureau of Economic Geology Series, University of Texas publication 6304.

Zitteliana 95, 2021, 135–145 | DOI 10.3897/zitteliana.95.63317

SNSB Bayerische Staatssammlung für Paläontologie und Geologie

ZITTELIANA
An International Journal of Paleontology and Geobiology

In search for the unlikely: Leaf-mining caterpillars (Gracillariidae, Lepidoptera) from Upper Cretaceous and Eocene ambers

Thilo C. Fischer[1]

1 *Bavarian State Collection of Zoology, Münchhausenstraße 21, 81247 München, Germany*

http://zoobank.org/F0DEFCBA-9EAF-43EE-93C2-AD1D6E88BD5B

Corresponding author: Thilo C. Fischer (thilo.fischer@4gene.de)

Academic editor: Alexander Nützel ♦ **Received** 20 January 2021 ♦ **Accepted** 14 July 2021 ♦ **Published** 8 December 2021

Abstract

Fossil leaf-mining caterpillars from amber are firstly described as the new species *Phyllocnistis cretacea* from Upper Cretaceous Myanmar amber and *Phyllonorycter inopinata* from Eocene Baltic amber. Both show typical traits of leaf-miners, and specifically, of later instars of caterpillars of their respective genera. The findings give further evidence for these being quite old and conservative genera of Gracillariidae. These are basal Ditrysia which retained the larval feeding and mining live mode. The findings also represent direct fossil evidence of individual stages of hypermetamorphosis known from extant Gracillariidae. The finds from the Upper Cretaceous and their putative identifications give direct evidence for a minimal geological age for the genus *Phyllocnistis* (Phyllocnistinae) and, by indirect conclusion based on their divergence, also for the genus *Phyllonorycter* in a sister clade (Lithocolletinae). It also predates mining habit closer to the time of radiation of their angiospermous host plants.

Keywords

Baltic amber, hypermetamorphosis, larval feeding, Myanmar amber, pupation

Introduction

Lepidoptera are exceedingly rare in the fossil record (Grimaldi and Engel 2005; Sohn et al. 2012, 2013). They are also rare in ambers which allow for a preservation of their delicate morphological structures which are needed for identification. As a working hypothesis for further studies in fossil Lepidoptera it was assumed that the larval stages of Lepidoptera, caterpillars, allow identification and geological dating of taxa not yet found as imaginal stages in ambers. This would be due to their different feeding and live mode, habitat, taphonomy but also their smaller size in comparison to the average size of ambers. Specimens not completely included in ambers are mostly destroyed by oxidation, breakage, abrasion, or other erosive processes. There is an obvious bias towards smaller inclusions (specimens), resulting for example for a strong overrepresentation of micro- versus macrolepidopteran inclusions. Focussing efforts with sample acquisition on larval stages of Lepidoptera from amber, a first member of Geometridae from Baltic amber has been identified from such a caterpillar (Fischer et al. 2019). Leaf-mining caterpillars are quite small larval stages being internal feeders restricted in body size by their well-protected mode of living within leaves. Taphonomy of such internal feeders, this is inclusion of such larvae outside their habitat by liquid resin, seems a quite unlikely event. However, several taxa leaving their mines for pupation are known, e.g., *Anarsioses aberrans*, being set apart from *Phyllonorycter* as a new genus for this behaviour and differences in male genitalia (Davis 2019). Despite of long-term scientific studies in Baltic amber since the 19th century such inclusions of leaf-mining caterpillars had to date not been identified.

Leaf-mining Lepidoptera are of interest for several reasons. From the scientific point of view, they represent a primitive feeding and live mode found in many basal Lepidoptera families, which has been retained in a number of basal Ditrysia (a more derived group of Lepidopterans with respect to female genital organs) (Scoble 2002). Gracillariidae are a prominent family of ditrysian leaf-miners (Men-

Copyright *Thilo C. Fischer.* This is an open access article distributed under the terms of the Creative Commons Attribution License (CC BY 4.0), which permits unrestricted use, distribution, and reproduction in any medium, provided the original author and source are credited.

PENSOFT®

ken et al. 2009) and are exceedingly diverse (Nieukerken et al. 2011) with 101 genera and 1866 species. Economically, leaf-miners can become important pests of crop plants, especially for crops kept in monocultures.

Within the family Gracillariidae Stainton, 1854 the three subfamilies Gracillariinae, Lithocolletinae, and Phyllocnistinae had been recognized (e.g., Parenti 2000). A most recent molecular phylogenetic analysis, however, revises this to eight subfamilies (Kawahara et al. 2017). Imagos of putative Gracillariidae have been described from Baltic amber as *Gracillariites lithuanicus* and *G. mixtus* (Kozlov 1987). Palaeontological evidence for such caterpillars comes only from their leaf mines rarely preserved in some fossil leaves, mostly from the Neogene and Paleogene. However, oldest Lithocolletinae mines are from the Cretaceous (cf. *Cameraria* cf. *aceriella* Clemens, 1859 (Proc. Acad. Nat. Sci. Phil. 325) from the Dakota Formation (late Albian, Early Cretaceous) of Central Kansas; cf. *Phyllonorycter oliveirae* Martins-Neto, 1989 from the Ora Formation (Turonian, Late Cretaceous of Negev Desert [lithocolletiform mines]) (Krassilov and Shuklina 2008) (overview in Sohn et al. 2012, 2013). Mines of Phyllocnistinae had been dated to 99 +/- 10 m.y. (Wahlberg et al. 2013). The dating of the divergence of this sister subfamily to Lithocolletinae with the genus *Phyllonorycter* was used as a calibration point for a combined molecular phylogenetic and host plant correlation study for the genus *Phyllonorycter*. The conclusion on the sister genus dated the origin of *Phyllonorycter* to the Palaeocene (62.3 m.y.) (Lopez-Vaamonde et al. 2006; also compare Wahlberg et al. 2013).

Here, caterpillars from Upper Cretaceous Myanmar amber and Eocene Baltic amber are identified as leaf miners by typical characters (small and flat body, legs and prolegs reduced, prognathous with modified mouthparts). Caterpillars from both ambers can also be identified as putative members of the genera *Phyllonorycter* and *Phyllocnistis* and are described as new species. Their taphonomy and paleoecology is discussed.

Material and methods

Authentication of the amber inclusions is ensured by purchase from trusted salespersons and an amber inclusion collector known by long-term relations. The ambers are kept at constant temperature in plastic clip bags within metal boxes, excluding excess oxygen and light. The holotypes will be deposited at the SNSB, Bavarian State Collection of Zoology, Munich with the number SNSB-ZSM-LEP amb003 and -004. Due to the presence of pyrite the inclusions cannot be studied by micro-computer-tomography. Photographs were taken by Artur Michalski with an imaging system composed of a digital photocamera Canon EOS 4000D on a stereobinocular microscope Nikon SMZ 800, SMZ 1500 (fusion), and PLAN APO lens. For illumination, a Fiber Optical Illuminator with halogen lights was used. Image stacks were generated using COMBINE ZM software.

Results

Eocene Caterpillar from Baltic Amber

The caterpillar (Fig. 1) is a single finding, being the only specimen of its type among 1152 Lepidopteran fossils from Baltic amber in the studied collection, and of 138 caterpillars among these.

The fossil caterpillar from Baltic amber shows characteristics of leaf-mining caterpillars in being flat, small, prognathous with modified mouthparts pointing forwards, and in having reduced legs and prolegs strongly reduced or absent. Hence, it is compared to caterpillars of Lepidopteran families with leaf mining larvae, namely Acrolepiidae, Adelidae, Acanthopteroctetidae, Argyresthiidae, Bucculatricidae, Carposinidae, Choreutidae, Coleophoridae, Cosmopterygidae, Douglasiidae, Elachistidae, Eriocraniidae, Gelechiidae, Glyphipterygidae, Gracillariidae, Heliodinidae, Heliozelidae, Heterobathmiidae, Incurvariidae, Lyonetiidae, Momphidae, Nepticulidae, Palaephatidae, Prodoxidae, Pterophoridae, Pyralidae, Roeslerstammiidae, Ochsenheimeriinae, Oecophoridae, Opostegidae, Scythrididae, Tischeriidae, Tortricidae, and Yponomeutidae (Lepiforum by Csóka 2003; Hering 1951; Connor and Taverner 1997; Kristensen 1999; Pitkin et al. 2019; Ellis 2020), but also to leaf-mining families of the orders Diptera (Agromyzidae), Coleoptera (Buprestidae, Curculionidae), and Hymenoptera (Tenthredinidae) (Grimaldi and Engel 2005). Most differ in one or more of the traits body size or outlines, presence of urogomphi (Coleoptera), form of thoracic and abdominal segments, presence, or form of lateral bulges of segments, head shape, shape of last segment, and presence and kind of setae. Summarizing, the most similar caterpillars are found within Gracillariidae, especially with respect to the presence of prolegs only at A3 to A5, which is found in many Gracillariidae (pers. comm. H. Vargas 2021).

Among Gracillariidae *Phyllocnistis* (Phyllocnistinae) is close to the phenotype of the fossil caterpillar but differs in having a conical last segment and a broader thorax (Hering 1951: fig. 28; Pitkin et al. 2019 (e.g., *Phyllocnistis unipunctella*), Global Taxonomic Database of Gracillariidae, e.g., *Phyllocnistis hemera*). Phenotypes most similar or almost identical to the fossil are found from subfamily Lithocolletinae (Csóka 2003; Pitkin et al. 2019). There are twelve extant genera of Lithocolletinae, among these *Cameraria* and *Phyllonorycter* (De Prins and De Prins 2006–2021). *Cameraria* is widely known by *C. ohridella*, a prominent species as a pest of chestnut (Parenti 2000). Both genera have larvae most like the Baltic amber caterpillar, especially with respect to the triangular form of larval head (e.g., *Phyllonorycter leucographella* (Sterling and Parsons 2012)), but *C. ohridella* larvae differ in the form of the lateral bulges and the outline of the body. Most alike are larvae of *Phyllonorycter* species. Like in many Gracillariidae genera, the first larval instars (Fig. 2) are apodal and their mouthparts are modified (Parenti 2000).

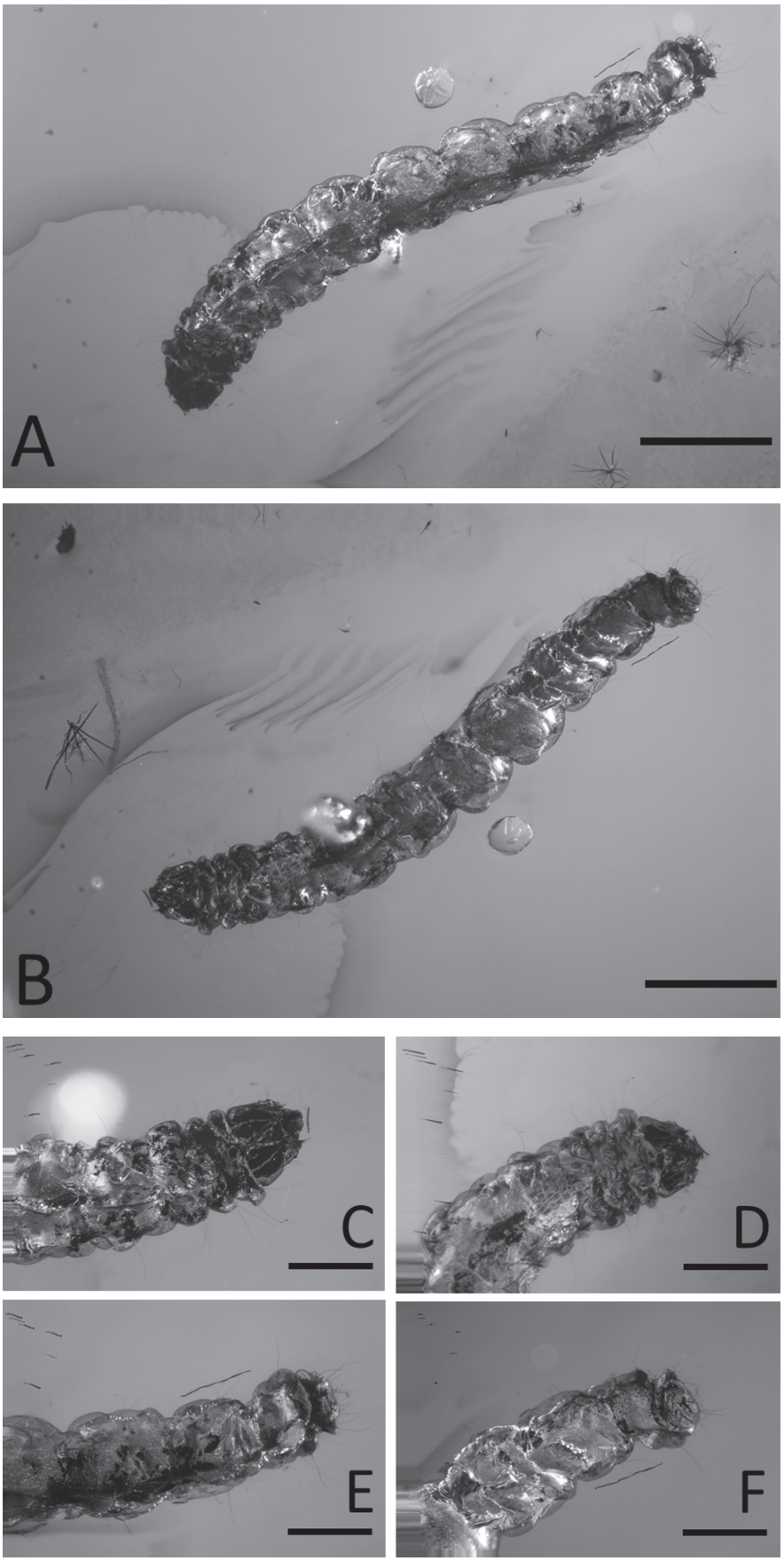

Figure 1. Holotype of *Phyllonorycter inopinata*, **A**: larva, dorsal view, **B**: ventral view, **C**: head and thoracic segments, dorsal view, **D**: ventral view, **E**: terminal segments, dorsal view, **F**: terminal segments, dorsal view. Scale bar 1 mm.

In advanced stages the larva develops thoracic legs and abdominal prolegs.

Some fossil insect taxa from Baltic amber are hard to be distinguished from their extant counterparts, e.g., *Lasius schiefferdeckeri* from extant *Lasius alienus* (or *niger* var. *alienus*) (Wilson 1955). Also, the *Phyllonorycter* caterpillar described here strongly resembles some extant species like *P. platani*. However, it is common practice not to affiliate such findings to extant species due to the lack of chance to check for internal morphologic characters or to use sequence-based approaches. Preservation of amber inclusions also may have an influence on interpretation of morphologic characters. The fossil from the Eocene of Baltic amber is consequently described as a new species of *Phyllonorycter*.

Systematic palaeontology*

Order Lepidoptera Linnaeus, 1758
Clade Ditrysia Börner, 1925
Superfamily Gracillarioidea Stainton, 1854
Family Gracillariidae Stainton, 1854
Genus *Phyllonorycter* Hübner, 1822

Phyllonorycter inopinata nov. spec.

http://zoobank.org/F0DEFCBA-9EAF-43EE-93C2-AD1D6E88BD5B

Etymology. The species name "*inopinata*" "surprising" refers to the seemingly unlikely find of a leaf mining caterpillar preserved in amber.

Holotypus. Specimen ex coll. Fischer no. 8182, Fig. 1

Locus typicus. Amber mine of Yantarni, RUS

Stratum typicum. "Blaue Erde" (Upper Eocene to Lower Oligocene)

Repository. Bavarian State Collection of Zoology, Munich, Germany; accession number SNSB-ZSM-LEP amb003.

Description of holotype. The caterpillar is 5 mm long and subcylindrical, maximum width 0.73 mm (in A4). The head is 0.36 mm long and 0.5 mm broad, depressed, triangular, and prognathous. Mandibles and antennae are developed. The legs are small (0,15–0.2 mm long). The thorax (T1 to T3) is 0.45 mm long and 0.63 mm broad. The longest abdominal segment is 0.61 mm (A4), the shortest abdominal segment is 0.3 mm (A9). Prolegs at abdominal segments A3 to A5 are small. There are three setae in lateral positions on either side of each segment, these are maximal 0.2 mm in length and could not be exactly positioned. The terminal segment is 0.21 mm long and 0.43 mm broad.

Diagnosis. A differential diagnosis to other *Phyllonorycter* species is currently impossible. The holotype is the only known specimen of the new species *P. inopinata*. Consequently, there is no information on variability and differences between subsequent instars. A comparison to similar extant species like *P. leucographella* or *P. platani* suffers from the same insecurities. Future findings from Baltic amber may enable a differential diagnosis.

Cretaceous Caterpillars from Myanmar Amber

Caterpillars are rare in Myanmar amber. Only six specimens among 287 Lepidopteran inclusions from Myanmar amber are present in the studied collection, three of which are studied here.

The possibility that the larvae from Myanmar amber are non-lepidopteran was considered but can be ruled out, most obviously for the holotype of the new species with its clearly visible spinneret. Most similar in general resemblance are Buprestidae larvae (Coleoptera) which also occur in Myanmar amber (own observation). However, these have a different body outline with even thicker head and thorax, and they lack setae.

Genus *Phyllocnistis* Zeller, 1848

Species *Phyllocnistis cretacea* nov. spec.

http://zoobank.org/F0DEFCBA-9EAF-43EE-93C2-AD1D6E88BD5B

Etymology. The species name "*cretacea*" refers to the Cretaceous age of the species.

Holotypus. Specimen ex coll. Fischer no. 7513, Fig. 3.

Locus typicus. Sediments of Hukawng Valley (Myanmar).

Stratum typicum. Earliest Cenomanian, determined 99 m.y. (Cruickshank and Ko 2003; Shi et al. 2012).

Repository. Bavarian State Collection of Zoology, Munich, Germany; accession number SNSB-ZSM-LEP amb004.

Description of holotype. The caterpillar is 7 mm long and flat, maximum width 1.18 mm (in T2). The thorax (T1 to T3) is 1.06 mm long. Dorsal prothoracic plates of roughly triangular form are present (figuring alike in Hering (1951: fig. 85a). The broadest segment of the abdomen is A6 with 0.88 mm, the abdomen is 5.78 mm long. The head is 0.53 mm long and 0.75 mm broad, depressed, triangular, and prognathous. Mandibles are developed, antennae are minuscule. The spinneret is well-developed and 0.05 mm long. Legs and prolegs are not developed. The longest abdominal segment is 0.68 mm (A3), the shortest abdominal segment is 0.38 mm (A9).

There are each two lateral bulges (dorsal and ventral ones) on either side of all abdominal segments, each bulge carries a prominent seta; these setae are maximal 0.2 mm in length and bent backwards. The terminal segment is 0.28 mm long and 0.5 mm broad.

There are several syninclusions preserved in the same amber: Coleoptera (5 taxa), Hymenoptera (a wasp), Psocoptera, trichomes, a 4 mm wood fragment, arthropod feces, undefinable plant, and chitin detritus.

Description of paratype I. The caterpillar (coll. Fischer no. 7790) is 6.5 mm long and subcylindrical, maximum width 1.02 mm (in T3) (Fig. 4). The thorax (T1 to T3) is 1.25 mm long. The broadest segment of the abdomen is A4 with 0.88 mm, the abdomen is 4.41 mm long. The head is 0.39 mm long and 0.65 mm broad, depressed, triangular,

* Systematics according to van Nieukerken et al. (2011)

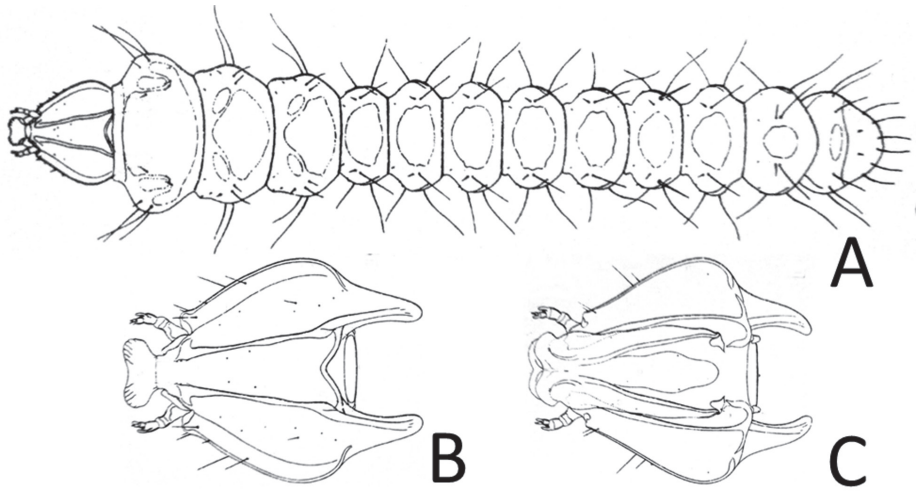

Figure 2. (changed after Parenti, 2000): First type larva (mandibles not drawn) of *Phyllonorycter platani*, **A**: larva, dorsal view, **B**: head-capsule, dorsal view, **C**: head-capsule ventral.

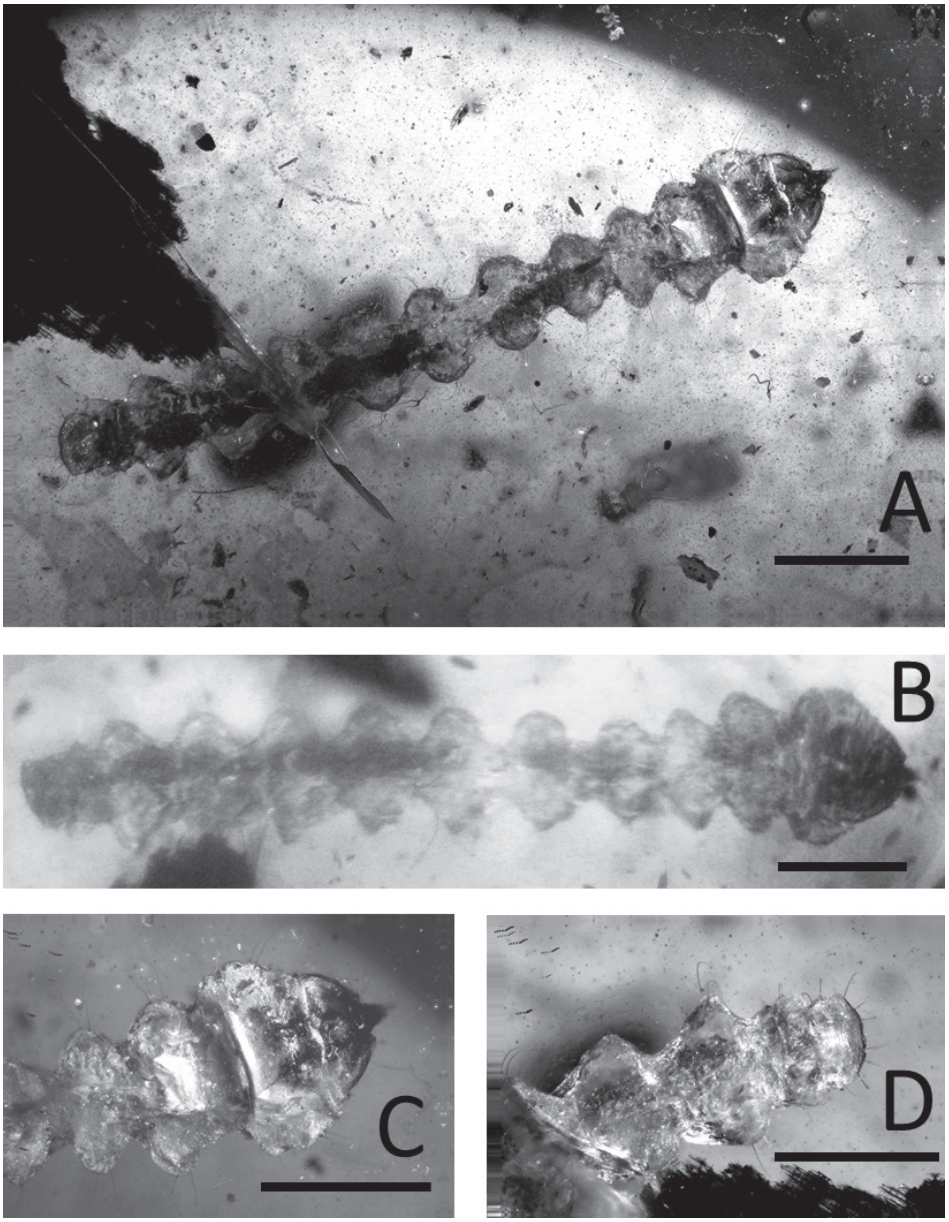

Figure 3. Holotype of *Phyllocnistis cretacea*, **A**: larva, dorsal view, **B**: ventral view (inclusion deeper within the amber), **C**: head in detail, dorsal view, **D**: terminal segments in detail, dorsal view. Scale bar: 1 mm.

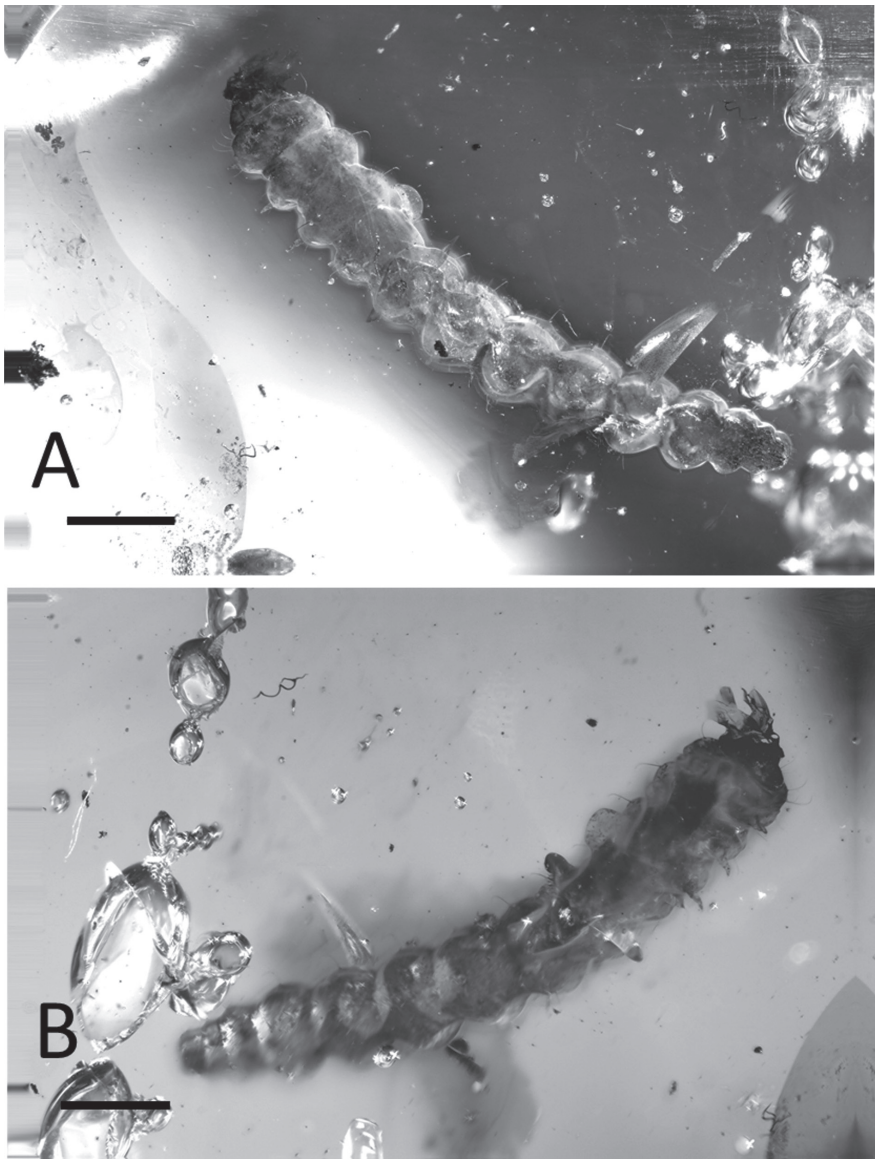

Figure 4. Paratype I of *Phyllocnistis cretacea*, **A**: larva, dorsal view, **B**: ventral view, length of caterpillar 6.5 mm. Scale bar: 1 mm.

and prognathous. Mandibles and antennae are developed. A visible leg is 0.26 mm long. The longest abdominal segment is 0.77 mm (A4), the shortest abdominal segment is 0.26 mm (A9). There are no prolegs. There are each two lateral bulges (dorsal and ventral) on either side of all abdominal segments. There are at least two setae in lateral positions on either side of each segment, these are maximal 0.16 mm in length. The terminal segment is 0.3 mm long and 0.32 mm broad.

Remark: The paratype is non-compressed, but part of the head is not well preserved. Dorsal prothoracic plates may be present, impressions with similar form are visible. A spinneret is not visible, but the head is partly hidden by some chitinous membrane.

Description of paratype II. The caterpillar (coll. Fischer no. 7512) is 4 mm long and subcylindrical, maximum width 0.83 mm (in T1) (Fig. 5). The thorax (T1 to T3) is 1.2 mm long. The broadest segment of the abdomen is A3 with 0.7 mm, the abdomen is 2.93 mm long. The head is partly retracted in the thoracic segment T1, 0.69 mm long (visible through T1) and 0.56 mm broad, depressed, triangular, and prognathous. Head and thorax are significantly thicker than abdomen in general outline. Mandibles and antennae are developed but tiny. There are no legs and prolegs. The abdomen is 2.93 mm in length, the longest abdominal segment is 0.39 mm (A5), the shortest abdominal segment is 0.17 mm (A10). There are each two lateral bulges (dorsal and ventral) on either side of all abdominal segments. The terminal segment is 0.17 mm long and 0.3 mm broad. There are no setae visible.

Remark. There are feces preserved which were produced by the caterpillar. Some trichomes are also preserved in the amber.

Diagnosis of *Phyllocnistis cretacea*. Subcylindrical caterpillars, up to 7 mm long (in known specimens and instars), head depressed, triangular and prognathous, head partly retracted or retractable in thorax, mandibles developed, minuscule antennae present, spinneret at least in late instars present, thorax with T1 having the largest diameter of all segments, tiny legs may be devel-

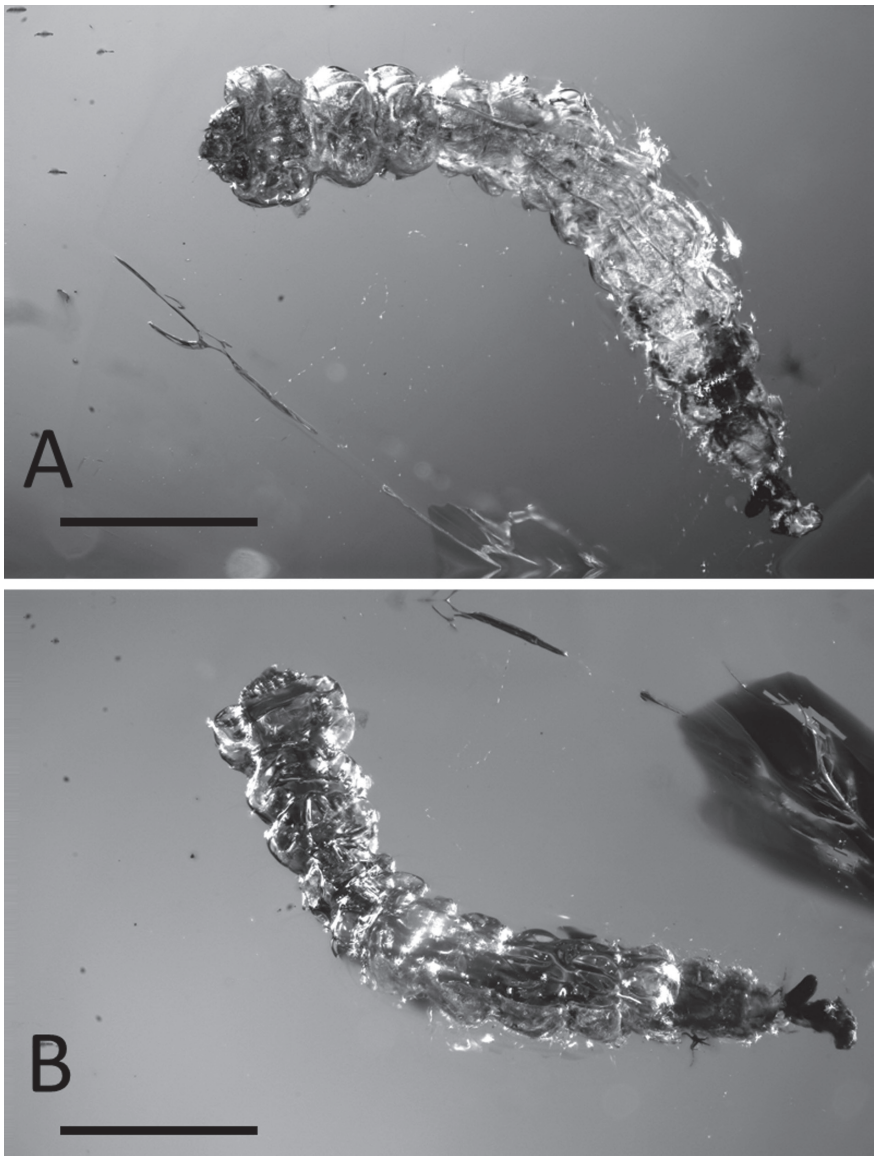

Figure 5. Paratype II of *Phyllocnistis cretacea*, **A**: larva, dorsal view, **B**: ventral view, length of caterpillar 4 mm. Scale bar: 1 mm.

oped, each segments with two lateral bulges (dorsal and ventral) on either side of all abdominal segments, setae can be present, spinneret and dorsal prothoracic plates of roughly triangular form may be developed, there are no prolegs.

Remarks. Among Lepidoptera, an affiliation to *Phyllocnistis* is affirmed by typical traits of the genus, such as having a triangular prognathous head, and lateral bulges of segments. However, the lack of prolegs casts some doubt on the identification. Most likely, at least the holotype and paratype I, but possibly also paratype II, represent late or last instars and prolegs would be expected on A3, A4 and A5 (Potts and Peterson 1960; Fracker 2015). However, the prolegs may be too tiny to be detectable with respect to the preservation state. It is assumed here that reduction of proleg development for some larval stages could occur at species level as reduction of legs and prolegs is common in mining Lepidoptera (Hering, 1951). Future finds of such caterpillars hopefully will allow to differentiate larval stages or related species.

Discussion

Leaf mining habit and identification

The prognathous mouthparts of the caterpillars are the most evident character for feeding by mining. The function of such mouthparts can be illustrated by a microscopic video (https://www.youtube.com/watch?v=LqL6LKEg-05k&feature=youtu.be). The characteristic lateral bulges present at every segment are especially well developed in many species of the leaf-mining genus *Phyllonorycter*, but also in some quite unrelated miners like leaf-mining Buprestidae (Coleoptera) larvae (Csóka 2003: 168; Grimaldi and Engel 2005). They may be due to convergent evolution with maximisation of body mass keeping good lateral flexibility of the abdomen. Other traits characteristic for miners (flat, small, legs and prolegs reduced) are also present in the studied amber inclusions. However, the caterpillars are relatively large for miners, are only subcylindrical and have somewhat developed legs. In *Phyllonorycter* prolegs

are present in the final instars (Scoble 2002: 116). Prolegs are absent in early instars of Gracillariidae (Scoble 2002: 116). The change from small apodal and flat early instars is described for later instars of Lithocolletinae (and other Gracillariidae) and termed hypermetamorphosis, and there may be even more stages like in *Marmara arbutiella* (Wagner et al. 2000). The fossil *Phyllonorycter* caterpillar described here may represent the third to fifth instar, referring to description of extant larval development in Lithocolletinae (Fracker 1915; Davis and Robinson 1998; Parenti 2000). Fracker (1915) mentions the character "prolegs at A3 to A5" (not A6) as a distinctive feature of later instars of (extant) Gracillariidae in general. The presence of mandibles (also in the *Phyllocnistis* caterpillars from Myanmar amber) argues against interpretation as last instars.

The phenotype of the specimen from Baltic amber allows a putative identification as *Phyllonorycter* (Gracillariidae) as described above. The finding is a direct evidence for the genus, subfamily and family and validates the evidence for the presence of the taxa by fossil mines (citations given in Introduction).

The specimens from Myanmar amber are similar regarding general phenotype but differ in a thicker thorax and a partly retracted or retractable head. This phenotype is found in extant *Phyllocnistis* (Gracillariidae) and some of the larval stages of *Spinivalva gaucha*, a neotropical Gracillariinae taxon (Brito et al. 2013). *Dendrorycter marmaroides* Kumata 1978 is similar with respect to the presence of two lateral bulges (dorsal and ventral), but these are pointing backwards. *Phyllocnistis* has a small spinneret (Cerdeña et al. 2020; pers. comm. H. Vargas 2021), in contrast in the Cretaceous holotype the spinneret is well developed. The interpretation of a size reduction of the spinneret as the derived state with the extant genus seems to be realistic.

Gracillariidae are basal Ditrysia which retained the primitive larval feeding and live mode by mining found in many basal Lepidoptera except the most basal families like detrivorous Micropterigidae (Menken et al. 2009). Exclusively internal feeding gives protection from predators, weather, desiccation, UV-radiation, and assures a reliable food supply. Leaf mining puts a constraint on body size of the larva and often goes along with monophagy and host dependence (Connor and Taverner 1997; Csóka 2003). However, in Gracillariidae hypermetamorphosis occurs in late larval instars and may be accompanied by a switch to external feeding, change of mine and leaf (Hering 1951), or may allow external pupation (Parenti 2000). Gracillariidae are mainly hosted by Eurosids I (Menken et al. 2009), a broad group of angiosperm families. Nevertheless, monophagy is realized by numerous species of *Phyllonorycter* which use specific plant genera or species as hosts (e.g., Pitkin et al. 2019).

Eocene *Phyllonorycter inopinata* caterpillar from Baltic Amber

Extant *Phyllonorycter* species mine on oaks and beech (*Quercus, Fagus,* Fagaceae), birch (*Betula*), hornbeams (*Carpinus, Ostrya*), alder (*Alnus*, all Betulaceae), hazel (*Corylus*, Corylaceae), hawthorne (*Crataegus*), apple (*Malus*), pear (*Pyrus*), quince and medlar (*Cydonia / Chaenomeles*), snowy Mespilus (*Mespilus*), wild service tree (*Amelanchier*) and rowan (*Sorbus*), cherry, plum and blackthorn (*Prunus*), pyracanth (*Pyracantha*), cotoneaster (Cotoneaster) (all Rosaceae), willow (*Salix*), poplar (*Populus*) (both Salicaceae), honeysuckles (*Lonicera, Leycesteria*), snowberry (*Symphoricarpus*), arrowwood (*Viburnum*, all Caprifoliaceae), sycamore (*Acer*, Aceraceae), plane (*Platanus*, Platanaceae), elm tree (*Ulmus*, Ulmaceae), cowberry (*Vaccinium*, Ericaceae), broom (*Cytisus*, *Genista*), greenweed (*Chamaecytisus*), laburnum (*Laburnum*) and gorse (*Ulex*, all Fabaceae) and various clovers and beans (*Trifolium*, *Vicia* and other herbaceous Fabaceae), scabious (*Scabiosa*, Dipsacaceae, herbaceous), and especially stressed plants (Csóka 2003; Pitkin et al. 2019). Most important host for *Phyllonorycter* seem oaks, Betulaceae, Rosaceae and Salicaceae. Arborescent plants are preferred rather than herbaceous ones, and only dicotyledonous plants in general.

Among the group of extant *Phyllonorycter* host genera, there is fossil evidence from Baltic amber for the presence of *Quercus*, *Fagus* (Fagaceae, but also other genera are known), *Alnus*, *Betula*, *Carpinus* (Betulaceae), *Corylus* (Corylaceae), Rosaceae indet., "*Populitis*", *Salix* (Salicaceae), *Acer* (Aceraceae), *Ulmus* (Ulmaceae), and Ericaceae indet.

Oaks must have been widely distributed in Baltic amber forest, as stellate trichomes of oaks are by far the most abundant plant remains in Baltic amber, occurring in about every second piece. Male oak inflorescences are also well known, and many species of *Quercus* have been described from Baltic amber (Spahr 1993; Gröhn and Kobbert 2017). Hence, oaks seem possible hosts for *Phyllonorycter* in the Baltic amber forest.

However, the climate in Eocene Baltic amber has been tropical (e.g., Grimaldi and Engel 2005). This contrasts with extant *Phyllonorycter* hosts described mostly from temperate regions, but many plant genera are known from Baltic amber which nowadays do occur in subtropical climates (e.g., Magnoliaceae, Dilleniaceae (Spahr 1993)). Hence, there is uncertainty in considerations on putative host plants for the fossil miner.

Pupation of *Phyllonorycter* is reported to normally occur within their blotch mines (Davis and Robinson 1998), giving a possible explanation for the rarity of the find of a later instar caterpillar in a fossil resin like Baltic amber (and Myanmar amber, see below). However, the closely related taxon *Anarsioses aberrans* exits the mine for pupation and has been differentiated from its former affiliation *Phyllonorycter aberrans* (Braun) for this behaviour and some differences in male genitalia (the latter without fossilization potential) (Davis 2019).

The descriptions of *Gracillariites lithuanicus* and *G. mixtus* (Kozlov 1987) are scarce, and the imagos seem to be too undersized to become correlated with the caterpillar taxon *Phyllonorycter inopinata*.

Upper Cretaceous caterpillar *Phyllocnistis cretacea* from Myanmar Amber

The origin of *Phyllonorycter* had been dated back at least to the Palaeocene (62.3 m.y.) by molecular phylogenetic analysis using mines of the sister taxon *Phyllocnistis* for calibration of divergence (Lopez-Vaamonde et al. 2006). The findings from Myanmar amber which is dated to 99 m.y. (Shi et al. 2012) and the putative identification as *Phyllocnistis* predate the occurrence of the genus and place its origin closer to the radiation of their angiospermous host plants.

Little is known about the flora and putative host plants from the biotope in which Myanmar amber originated. The origin of the resin is suggested to be the Cupressaceae conifer *Metasequoia* (Grimaldi et al. 2002) or an araucarian pine (Poinar et al. 2007). The environment was reported to be tropical (Grimaldi et al. 2002); botanical fossils are found but have remained mostly unstudied.

Mode of living and taphonomy

An interesting question is the evolution of hypermetamorphosis of late stages in larval development of Gracillariidae and its relation to larval size and internal versus external feeding, change of mine and host leaf, and the place of pupation.

Leaf miners seem to have little potential in fossilization as caterpillars would have to leave or get exposed from their mines to become embedded in resin for subsequent fossilization. Up to now only mines in fossil leaves had been known.

The fossil caterpillars described here possibly either have left their mines for external feeding or, more likely with respect to their prognathous mouthparts and the well-developed spinneret, for outside pupation. For extant Gracillariidae both, pupation inside the mine or derived structures (ptychonomes) or outside of the mine, is known (Parenti 2000). Alternatively, the caterpillars preserved in amber were driven out of their mines by resin flow, drying of the leaf or some other mechanical force breaking the mine. From the collection under study there is an inclusion in Baltic amber of an early instar of a Psychidae – Typhoniinae larva obviously driven out from its still intact case by resin flow and found close to this case (not shown). This finding demonstrates that this embedding effect may occur as early instar Psychidae larvae (to the best of the author's knowledge) do not leave their cases.

The presence of a well-developed spinneret and the presence of legs seem to strengthen the hypothesis that caterpillars left their mines for pupation. External feeding usually is accompanied with hypognathous (pointing downwards) mouthparts, sitting on a leaf or other plant organ, and feeding below it and at an edge. External feeding seems unlikely for the caterpillars described here due to their prognathous mouthparts in combination with a well-developed spinneret. Hering (1951) states that prognathous Gracillariidae larvae die when they are removed from their mines. Given this interpretation, a driving force for hypermetamorphosis with late development of legs (and prolegs in *P. inopinata*) could be the ability to search for better places for pupation. For sure, this conclusion is hypothetical and needs confirmation by other further findings or support from other lines of evidence.

Conclusions

The finding from the Upper Cretaceous gives direct evidence of leaf-mining caterpillars, beyond their known fossil mines. Minimal geological ages for the proposed identifications *Phyllonorycter* and *Phyllocnistis* could be concluded, with the insecurities discussed. Both findings confirm the conservative character of the leaf-mining habit for well-known extant leaf-miner taxa. There is now some more evidence for the hypothesis that evolution of hypermetamorphosis in Gracillariidae might have been driven by facilitating pupation outside the leaf mine.

Acknowledgments

A. Michalski (Wrocław, Poland) is acknowledged for providing photographs of the inclusions. N. Wielsch (Jena) kindly supported me by providing literature. C. Giacoma (Dipartimento di Scienze della vita e Biologia dei Sistemi, Università degli Studi di Torino) is gratefully acknowledged for the permission to reproduce a figure of a publication of U. Parenti. Axel Hausmann (Bavarian State Collection of Zoology, Munich) and Marc Epstein (Plant Pest Diagnostics Branch, California Department of Food & Agriculture) kindly helped by commenting and correcting a draft of the manuscript, by making scientific contacts, and by correcting English language. Two reviewers contributed with corrections and helpful comments, this is gratefully acknowledged.

Mandatory statement

The author has no funding to report. The author has declared that no competing interests exist.

References

Börner C (1925) Lepidoptera, Schmetterlinge. In: Brohmer P, ed. Fauna von Deutschland. Ein Bestimmungsbuch unserer heimischen Tierwelt. Quelle und Meyer, Leipzig, 358–387.

Brito R, Gonçalves GL, Vargas HA, Moreira GRP (2013) A new Brazilian *Passiflora* leafminer: *Spinivalva gaucha*, gen.n., sp.n. (Lepidoptera, Gracillariidae, Gracillariinae) the first gracillariid without a sap-feeding instar. Zookeys 291, 1–26. https://doi.org/10.3897/zookeys.291.4910

Cerdeña J, Farfán J, Vargas HA, Brito R, Gonçalves GL, Lazo A, Moreira GRP (2020) *Phyllocnistis furcata* sp. nov.: a new species of leaf-miner associated with *Baccharis* (Asteraceae) from South-

ern Peru (Lepidoptera, Gracillariidae). ZooKeys 996: 121–145. https://doi.org/10.3897/zookeys.996.53958

Connor EF, Taverner MP (1997) The Evolution and Adaptive Significance of the Leaf-Mining Habit. Oikos 79(1): 6–25. https://doi.org/10.2307/3546085

Cruickshank RD, Ko K (2003) Geology of an amber locality in the Hukawng valley, northern Myanmar. Journal of Asian Earth Sciences 21 (5), 441–455. https://doi.org/10.1016/S1367-9120(02)00044-5

Csóka G (2003) Leaf Mines and Leaf Miners. Forest Research Institute, Agroinform Kiadó és Nyomda Kft., Budapest, 192 pp.

Davis DR (2019) *Anarsioses*, a new generic name for *Phyllonorycter aberrans* (Braun) (Lepidoptera: Gracillariidae). Zootaxa 4701 (6): 574–580. https://doi.org/10.11646/zootaxa.4701.6.6

Davis DR, Robinson GS (1998) The Tinoidea and Gracillarioidea. In: Kristensen NP, (Ed.) Lepidoptera, Moths and Butterflies, Volume 1: Evolution, Systematics and Biogeography, Handbook of Zoology, Vol. IV Arthropoda, Insecta, Part 35. Walter de Gruyter, Berlin, New York, 91–118. https://doi.org/10.1515/9783110804744

De Prins J, De Prins W (2006–2021) Global Taxonomic Database of Gracillariidae (Lepidoptera). World Wide Web electronic publication. https://doi.org/10.1163/9789004475397

De Prins J, De Prins W (2006–2021) Global Taxonomic Database of Gracillariidae (Lepidoptera). http://www.gracillariidae.net/species/show/2311, online resource, last assessed 13. May 2020 (*Phyllocnistis hemera* Brito and Fochezato, 2017, Brazil).

Ellis WN (2020) Leafminers and plant galls of Europe. https://bladmineerders.nl/, Online resource, last assessed 6. June 2020.

Fischer TC, Michalski A, Hausmann A (2019) Geometrid caterpillar in Eocene Baltic amber (Lepidoptera, Geometridae). Scientific Reports 9: 17201. https://doi.org/10.1038/s41598-019-53734-w

Fracker SB (1915) The classification of lepidopterous larvae. Illinois biological monographs II, 1. University of Illinois, Urbana, 153 pp. https://doi.org/10.5962/bhl.title.10246

Grimaldi D, Engel MS (2005) Evolution of the Insects. Cambridge University Press, Cambridge, New York, 755 pp.

Grimaldi DA, Engel MS, Nascimbene PC (2002) Fossiliferous Cretaceous amber from Myanmar (Burma): Its rediscovery, biotic diversity, and paleontological significance. American Museum Novitates 3361: 1–71. https://doi.org/10.1206/0003-0082(2002)361<0001:fcafmb>2.0.co;2

Gröhn C, Kobbert MJ (2017) Pflanzen - seit der Saurierzeit eingeschlossen in Bernstein. Wachholtz Mumann Publishers, Kiel, Hamburg, 235 pp.

Hering M (1951) Biology of the Leaf Miners. Uitgeverij. Dr. W. Junk, s'-Gravenhage, 420 pp. https://doi.org/10.1007/978-94-015-7196-8

Hübner J (1822) Systematisches-alphabetisches Verzeichniss aller bisher bey den Fürbildungen zur Sammlung europäischer Schmetterlinge angegebenen Gattungsbennungen; mit Vorbemerkung auch augsburgischer Gattungen. Augsburg, Verfasser, H342, 1–81. https://doi.org/10.5962/bhl.title.48605

Kawahara AY, Plotkin D, Ohshima I, Lopez-Vaamonde C, Houlihan PR, Breinholt JW, Kawakita A, Xiao L, Regier JC, Davis DR, Kumata T, Sohn J-C, De Prins J, Mitter C (2017) A molecular phylogeny and revised higher-level classification for the leaf-mining moth family Gracillariidae and its implications for larval host-use evolution, Systematic Entomology 42: 60–81. https://doi.org/10.1111/syen.12210

Kozlov MV (1987) New moth-like Lepidoptera from the Baltic amber, Paleontological Journal 4: 59–67.

Krassilov V, Shuklina S (2008) Arthropod trace diversity on fossil leaves from the mid-Cretaceous of Negev, Israel. Alavesia, 2, 239–245.

Kristensen NP (Ed.) (1999) Lepidoptera, Moths and Butterflies, Volume 1: Evolution, Systematics and Biogeography, Handbook of Zoology, Vol. IV Arthropoda, Insecta, Part 35. Walter de Gruyter, Berlin, New York. https://doi.org/10.1515/9783110804744.toc

Kumata T (1978) A new stem-miner of alder in Japan, with a review of the larval transformation in the Gracillariidae (Lepidoptera). Insecta Matsumurana, New Series 13: 1–27.

Linnæus C (1758) Systema naturæ per regna tria naturæ, secundum classes, ordines, genera, species, cum characteribus, differentiis, synonymis, locis. Tomus I. Editio decima, reformata. Holmiæ: Salvius. https://doi.org/10.5962/bhl.title.542

Lopez-Vaamonde C, Wikström N, Labandeira C, Godfray HCJ, Goodman SJ, Cook JM (2006) Fossil-calibrated molecular phylogenies reveal that leaf-mining moths radiated millions of years after their host plants. Journal of Evolutionary Biology 19: 1314–1326. https://doi.org/10.1111/j.1420-9101.2005.01070.x

Martins-Neto RG (1989) Novos insetos Terciários do Estado de São Paulo. Revista Brasileira de Geociências, 19(3), 375–386. https://doi.org/10.25249/0375-7536.1989375386

Menken SBJ, Boomsma JJ, Nieukerken EJ (2009) Large-scale evolutionary patterns of host plant associations in the Lepidoptera. Evolution 64-4: 1098–1119. https://doi.org/10.1111/j.1558-5646.2009.00889.x

Nieukerken van, EJ et al. (50 authors) (2011) Order Lepidoptera Linnaeus, 1758, In: Zhang Z-Q (Ed.) Animal Biodiversity: An outline of higher classification and survey of taxonomic richness. Zootaxa 3148: 212–221. https://doi.org/10.11646/zootaxa.3148.1.41

Parenti U (2000) A Guide to the Microlepidoptera of Europe. Guide I. Museo Regionale di Scienze Naturali Torino, Torino, 426 pp.

Pitkin B, Ellis W, Plant C, Edmunds R (2019, update). The leaf and stem mines of flies and other insects (Coleoptera, Diptera, Hymenoptera and Lepidoptera). http://www.ukflymines.co.uk/

Poinar GO, Lambert JB, Wu Y (2007) Araucarian source of fossiliferous Burmese amber: spectroscopic and anatomical evidence. Journal of the Botanical Research Institute of Texas 1: 449–455.

Potts RWL, Peterson A (1960) Larvae of Insects. An Introduction to Nearctic Species. Part I Lepidoptera and Plant Infesting Hymenoptera. Ohio State University, Columbus, Ohio, 315 pp. https://doi.org/10.2307/2421868

Scoble MJ (2002) The Lepidoptera – Form, Function and Diversity. The Natural History Museum / Oxford University Press, Oxford, 404 pp.

Shi G, Grimaldi DA, Harlow GE, Wang J, Wang J, Yang M, Lei W, Li Q, Li X (2012) Age constraint on Burmese amber based on U-Pb dating of zircons. Cretaceous Research 37: 155–163. https://doi.org/10.1016/j.cretres.2012.03.014

Sohn J-C, Labandeira C, Davis D, Mitter C (2012) An annotated catalogue of fossil and subfossil Lepidoptera (Insecta: Holometabola) of the world. Zootaxa 3286: 1–132. https://doi.org/10.11646/zootaxa.3286.1.1

Sohn J-C, Lamas G (2013) Corrections, additions, and nomenclatural notes to the recently published World catalogue of fossil and subfossil Lepidoptera. Zootaxa 3599 (4): 395–399. https://doi.org/10.11646/zootaxa.3599.4.8

Spahr U (1993) Systematischer Katalog und Bibliographie der Bernstein- und Kopalflora. Stuttgarter Beiträge zur Naturkunde, Serie B (Geologie und Paläontologie) 195: 1–99.

Stainton HT (1854) Lepidoptera: Tineina. In: Tibbats H, ed. Insecta Britannica. Vol. 3. London: Lovell Reeve, 313 pp. https://doi.org/10.5962/bhl.title.67721

Sterling P, Parsons M (2012) Field Guide to the Micromoths of Great Britain and Ireland. British Wildlife Publishing Ltd, The Old Dairy, Milton on Stour, Gillingham, Dorset, 416 pp.

Wagner DL, Loose JL, Fitzgerald TD, Benedictis JA, Davis DR (2000) A hidden past: the hypermetamorphic development of *Marmara arbutiella* (Lepidoptera: Gracillariidae). Annals of the Entomological Society of America 93: 59–64. https://doi.org/10.1603/0013-8746(2000)093[0059:AHPTHD]2.0.CO;2

Wahlberg N, Wheat CW, Peňa C (2013) Timing and Patterns in the Taxonomic Diversification of Lepidoptera (Butterflies and Moths). PLoS ONE 8(11): e80875. https://doi.org/10.1371/journal.pone.0080875

Wilson EO (1955) A monographic revision of the ant genus *Lasius*. Bulletin of the Museum Comparative Zoology 113: 1–201. https://doi.org/10.1086/401086

Zeller PC (1848) Die Gattungen der mit Augendeckeln versehenen blattminirenden Schaben. Linnaea Entomologica. Zeitschrift herausgegeben von dem Entomologischen Vereine in Stettin 3: 248–344.